THE SCATTERING OF SOUND WAVES IN TWO-DIMENSIONAL DUCTS WITH DISCONTINUITIES IN HEIGHT AND MATERIAL PROPERTY

A thesis submitted for the degree of Doctor of Philosophy

by

Daniel Paul Warren

Department of Mathematical Sciences, Brunel University

December 1999

Abstract

Eigen-mode matching techniques offer a versatile approach for solving acoustic scattering problems in ducts. However, until recently, these techniques have been restricted to problems in which the boundary conditions contain at most one derivative, that is, Neumann, Dirichlet or Robin's conditions. Here a method is developed to solve scattering problems in ducts that are discontinuous in height and have at least one surface described by a high order boundary condition. Attention is focussed on the membrane condition, but the method can be extended to elastic plates and other higher order conditions. An original orthogonality condition is derived and used to solve two problems. Limiting cases of the results are compared with some special cases solveable by standard Fourier techniques and (for the case of no height discontinuity) the Wiener-Hopf technique.

Contents

List of Tables

List of Figures

Declaration

No portion of the work referred to in this thesis has been submitted in support of an application for another degree or qualification of this or any other university or other institution of learning.

The work in Chapters 3 and 4 has been submitted for publication as joint work with Dr. J.B. Lawrie in a paper entitled "Acoustic scatterring in wave-guides of discontinuous geometry and material property" to *Wave Motion.*

Acknowledgements

I would like to thank the Department of Mathematical Sciences, Brunel University for their support and funding throughout the duration of my study.

A special thank you to Dr. Jane Lawrie who supervised my work and gave me the drive and enthuasiasm to see it to its conclusion, despite my other varied commitments throughout.. I would also like to pay tribute to the memory of Prof. Gerry Wickham, who saw potential in my final year project and convinced me that a PhD was a good idea.

I would especially like to thank my parents for all the concern they have shown in the tough times and for helping me celebrate the successes, my brother who has doubled as the greatest friend I could have and my grandparents for their continued support. I have found new friends and cemented old friendships through the course of my study - all are dear to me and I hope will continue to be for sometime to come.

Most importantly though, I would like to thank Aimee, my wife. I can't find the words to say how much she has done and how very special she is to me. Her devotion has been unceasing and her support has been boundless. Without her, the document you are about to read would probably not have been written.

Chapter 1

Introduction

For many years, structural acoustics has provided challenging and interesting problems for researchers in the fields of engineering and applied mathematics alike. The significant and continued interest in the subject is often motivated by the requirement to design and construct objects in which structural vibration and the noise associated with it is to be minimised. Such noise is generated by a variety of mechanisms but typically involves the scattering of waves at a discontinuity in either the material properties or the geometry of the object. For this reason it is important to understand the scattering characteristics of all the key features of a given structure. In fact, in the high frequency limit, the geometric theory of diffraction (Keller, 1962) enables the total sound field at any point in space to be calculated as the sum of all the scattered wave contributions. This alone justifies the study of a range of problems all of which are canonical to diffraction theory.

Problems that involve a change in the material properties of an otherwise planar structure may be amenable to solution by the Wiener-Hopf technique. This technique, described in great detail by Noble (1958), has proved to be a powerful and flexible tool, enabling the analytic solution of a variety of complicated problems involving the scattering of sound waves at an edge or sharp discontiuity. Cannell (1975) uses the Wiener-Hopf technique to solve a problem where a plane acoustic field is incident from an angle, upon a lightly loaded elastic half-plane in a uniform acoustic medium. As mentioned above, work in this field is often motivated by the desire to limit structure borne sound, and this work in particular is related to the problems of noise generated by jet aircraft. In this first paper an exact solution to the general problem, valid for arbitrary values of fluid and plate parameters is given using the Wiener-Hopf method, in terms of a contour integral. In a later paper (Cannell 1976), a similar problem is considered where the half-plane is heavily loaded and freely attached to a baffle.

Brazier-Smith (1987) considers a problem of a more complex geometry. In this paper two co-planar semi-infinite plates of differing thickness which are joined along one edge are considered. An incident wave is incident normally on the join. The join is considered to take one of three forms, either free-free (that being, the plates are not attached in any

way), hinged (implying zero displacement but varying gradient on either side of the join) or welded (allowing gradient and displacement to vary in a continuous manner over the join). The three possible edge conditions produce distinct solutions when solved using the Wiener-Hopf technique. The solutions found in all three cases can be used to consider both the heavy and light fluid loaded cases, by simply adjusting the parameters of the problem accordingly. Norris & Wickham (1995) revisit the problem tackled by Brazier-Smith using a more elegant method. By employing a general procedure as opposed to the direct method used by Brazier-Smith, the factorization of the Wiener-Hopf kernel yields finite integral expressions for the reflected, transmitted and acoustically radiated fields. The final expression of these three elements also provides the opportunity to enforce the edge conditions rigorously.

Alternatively, where the change in material property occurs in a less abrupt or smooth manner to that described above, a solution may be sought by modelling the material parameters as functions of the spatial variables. Such an approach may enable the boundary-value problem to be recast as a difference equation, the solution to which provides valuable insight into the qualitative behaviour of the physical problem. This approach was originally formulated by Roseau (1976) and has subsequently been employed by Evans (1985), Fernyhough & Evans (1996) and Grant & Lawrie (1999).

For non-planar structures no standard solution method is available. One such class of problem involves two semi-infinite planar boundaries joined along their edges to form a wedge of arbitrary angle containing the propagating medium. When the boundaries comprise wave-bearing surfaces, the scattering problem is immensely difficult. The first major solution is due to Maliuzhinets (1958) who solved the scattering problem for the case in which the boundaries satisfy the Robin (impedance) condition. He employed the Sommerfeld integral representation of the fluid velocity potential to reduce the boundary-value problem to a system of difference equations, the solution to which he wrote in terms of a new special function which has since been termed the Maliuzhinets' function. The extension of this work to wedges whose boundaries comprise membranes or elastic plates posed a significant problem to the applied mathematics community.. Abrahams (1986, 1987) considered two such problems and, using the Kontorvich-Lebedev transform, obtained a solution for special wedge angles. It was, however, not until 1994 that Osipov posed an ansatz that would extend the work of Maliuzhinets to high order boundary conditions and arbitrary wedge angle. Independent work by Abrahams & Lawrie (1995) and Lawrie & Abrahams (1996) provided the first full analytic and numerical investigation of the reflection and transmission of membrane waves by a corner of arbitrary angle. This work was soon followed by an article by Osipov & Norris (1996) who, again independently, solved the same problem.

Corners comprise only part of any structure and their scattering effects cannot, therefore, usually be considered in isolation. For example, waveguides with one or more abrupt

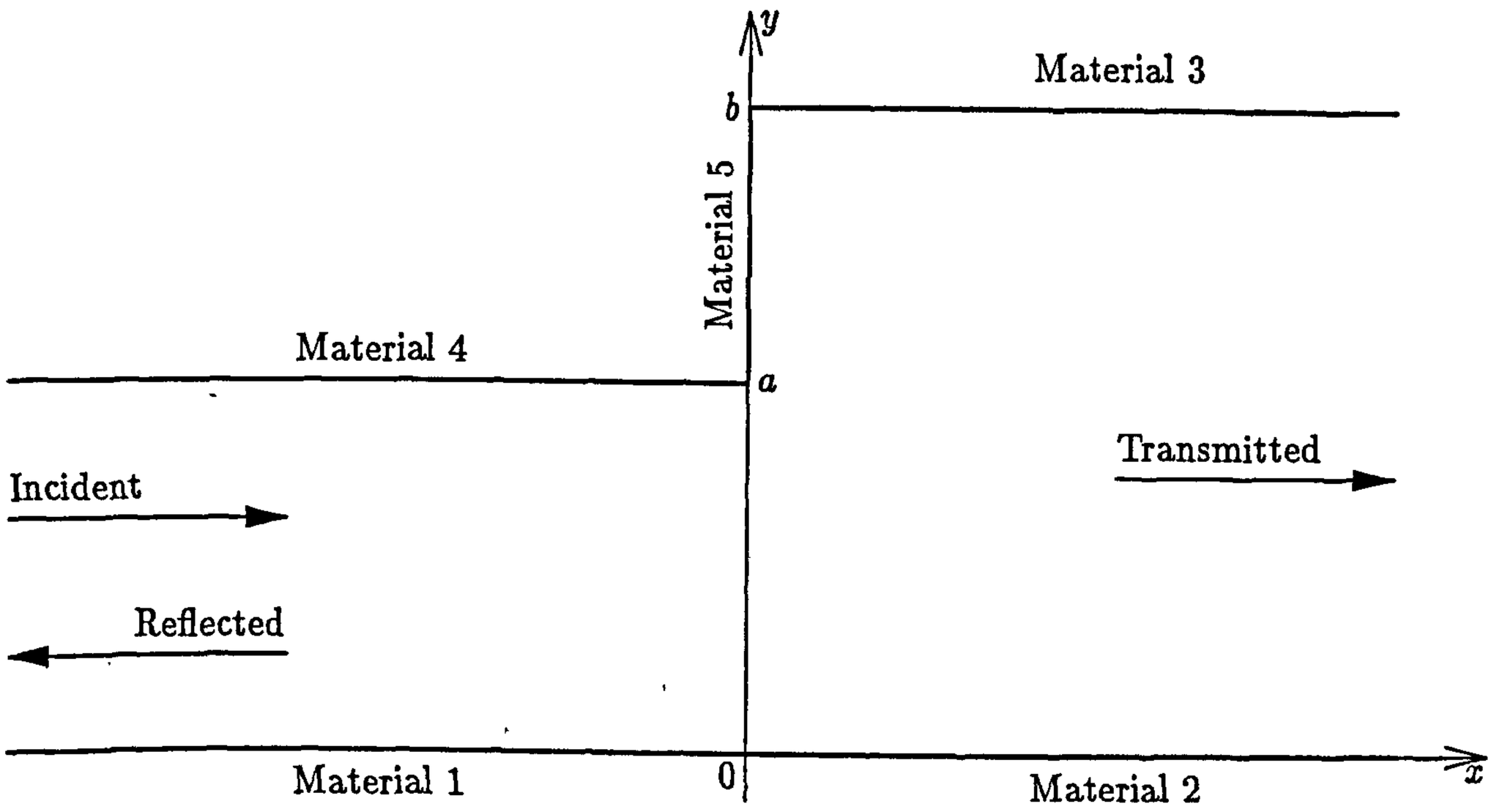

Figure 1.1: Physical configuration of the general problem considered in the thesis

changes in height contain at least two corners in their geometry. Further, a change in geometry of this type may co-incide with a change in material property (see figure 1.1). It is problems of this type that are to be considered in this thesis.

Chapter 2 commences with a review of some basic examples of this class of problem in which the boundary conditions are Neumann, Dirichlet or Robin's in type. Solution methods for waveguide problems with these types of boundaries are known and well understood. Section 2.1 comprises the solution to the problem where all boundary conditions are of Neumann type and so the surfaces of the duct are acoustically hard (this problem is henceforth referred to as *the hard/hard problem* in view of the nature of the duct walls on either side of the height discontinuity). The problem is solved using standard Fourier series methods and results are given for a number of cases. The solution to the hard/hard problem takes the form of an infinite system of algebraic equations, the convergence of the truncated system is found to be very slow. To rectify this problem, the system of equations is altered algebraically to create a further system, still appropriate for the problem at hand but solvable for a different set of variables. Once this new system is solved, the original variables (that are in fact, amplitudes of the acoustic modes) can be regained by simple substitutions. The algebraic alteration that occurs is analysed in section 2.2, to investigate why it is required and what makes the new system more convergent (and thus solvable).

Section 2.3 comprises an over view of the Sturm-Liouville theory. This theory is a generalization of the Fourier series method used in section 2.1, for considering ducts with impedance (Robin's) boundary conditions at the surfaces. By employing this technique, it is possible to tackle the problem where all surfaces are acoustically rigid, apart from that

located at $y = b$, $x > 0$ which is an impedance boundary condition (here after referred to as *the hard/impedance problem*). This problem is solved in section 2.4 and results are given. Also discussed in section 2.4 is the problem where all surfaces are acoustically rigid apart from that occupying the region $y = b$, $x > 0$ which is of Dirichlet type (this problem hereafter referred to as *the hard/soft problem*). The Dirichlet boundary condition, and indeed, the Neumann condition as tackled in sections 2.1, are special cases of the Robin's condition.

In section 2.5, Sturm-Liouville theory is applied again, this time to a problem where all surfaces are acoustically rigid apart from that occupying the region $y = b$, $x > 0$ which is now a membrane (hereafter, *the hard/membrane problem*). On this occassion the method is found to fail due to the higher order of the membrane boundary condition and so, for the solution of this problem a new method is required. It is problems of this type that have provoked such concentrated efforts to find solutions in the past. However, by applying a technique similar to that used in the preliminary stages of the derivation of the Sturm-Liouville theory, an orthogonality condition that allows the hard/membrane problem to be completed is found. The analysis that brings about the discovery of this orthogonality condition is included in section 2.6, and the reader is referred to Lawrie & Abrahams (1999) for further details

It is worth noting at this point that the three problems solved so far (those being the hard/hard, hard/impedance and hard/soft problems) provide a useful insight into more complicated problems of this class. Not only is this analysis a good template to follow for the techniques that will be employed when more complex problems are tackled, but also the programming for gaining numerical solutions to these problems is instructive. Further, and maybe most importantly, the results gained from these preliminary problems prove to be useful as a comparison with results gained in later chapters. The validation of results lends considerable weight to the techniques employed and conclusions drawn later in the thesis.

The orthogonality condition that is derived in section 2.6 is applied to solve the hard/membrane problem in chapter 3. However, as mentioned above, the case where there is no change in duct height (that is, where $a = b$) is amenable to solution using the Wiener-Hopf technique. The solution for this special case is presented in section 3.2 and provides a useful check for results produced by the methods employed in section 3.1. The two sets of results are compared in section 3.3. Also, by choosing the values of the parameters that define the behaviour of the membrane correctly, it can be made to behave in a very similar way to an acoustically soft surface, and so results from the system found in section 3.1 can be compared with those gained in section 2.4 for the hard/soft problem.

In chapter 4, the orthogonality condition of section 2.6 is applied again, this time to the problem where the surfaces occupying $y = a$, $x < 0$ and $y = b$, $x > 0$ are both membranes, whilst all other surfaces are acoustically rigid (*the membrane/membrane problem*). Again

the special case, where $a = b$ is considered using the Wiener-Hopf method in section 4.2 and a range of results are given in section 4.3.

Note that in all sections where results have been presented, the values selected for the parameters of the problem have been chosen arbitrarily. These values are not intended to replicate physical geometries or material behaviours, but to provide a benchmark for the accuracy and correctness of future work.

Chapter 2

Preliminary examples

Before going on to tackle examples of two-dimensional duct problems where the duct surfaces are described by higher-order boundary conditions, it is important to discuss the techniques available for problems of a simpler nature – not least because some of these problems provide useful checks for later analysis. In this chapter, combinations of Neumann, Dirichlet and Robin's boundary conditions are considered with a field equation of second-order. In all cases, the problems are concerned with the sound field in a waveguide comprising two, semi-infinite ducts, joined along a matching interface. The duct to the left of the matching interface is of height, a, whilst that to the right is of height b where $a \leq b$. The lower surfaces of the two ducts are alined and acoustically rigid whilst the upper surfaces are of Neumann, Dirichlet or Robin's type. Where the two ducts meet at the matching interface, the gap between their upper surfaces is closed by a rigid surface (see figure 2.1) and the region exterior to the ducts is *in vacuo.* The solution of such problems can be found using separation of variables to yield an eigenfunction expansion. For the first two problems, the resulting eigen-subsystem will be Sturm-Liouville in nature and so can be solved using well-known, simple orthogonality conditions leading to a system of well behaved linear algebraic equations. This system, though infinite, can be truncated to a level where sufficient accuracy of solutions is given.

Considered first, in Section 2.1, is the case where all surfaces are rigid, that is the surfaces perfectly reflect the sound field. This problem is amenable to solution by standard Fourier techniques. The convergence of the solution is discussed in Section 2.2. In Section 2.3, Sturm-Liouville theory is discussed in regard to a general example. The analysis discussed in Section 2.3 is then applied to the hard/impedance problem in Section 2.4. It should be noted that Dirichlet and Neumann conditions are special cases of the Robin's condition. The limitations of the Sturm-Liouville theory are demonstrated in Section 2.5, where a problem in which one duct surface is described by a high-order boundary condition is considered. A brief discussion of the differences between the problem of sections 2.4 and 2.5 is presented in Section 2.6, and a new orthogonality relation, appropriate to the non Sturm-Liouville eigen-subsystem of Section 2.5 is derived. The new orthogonality relation

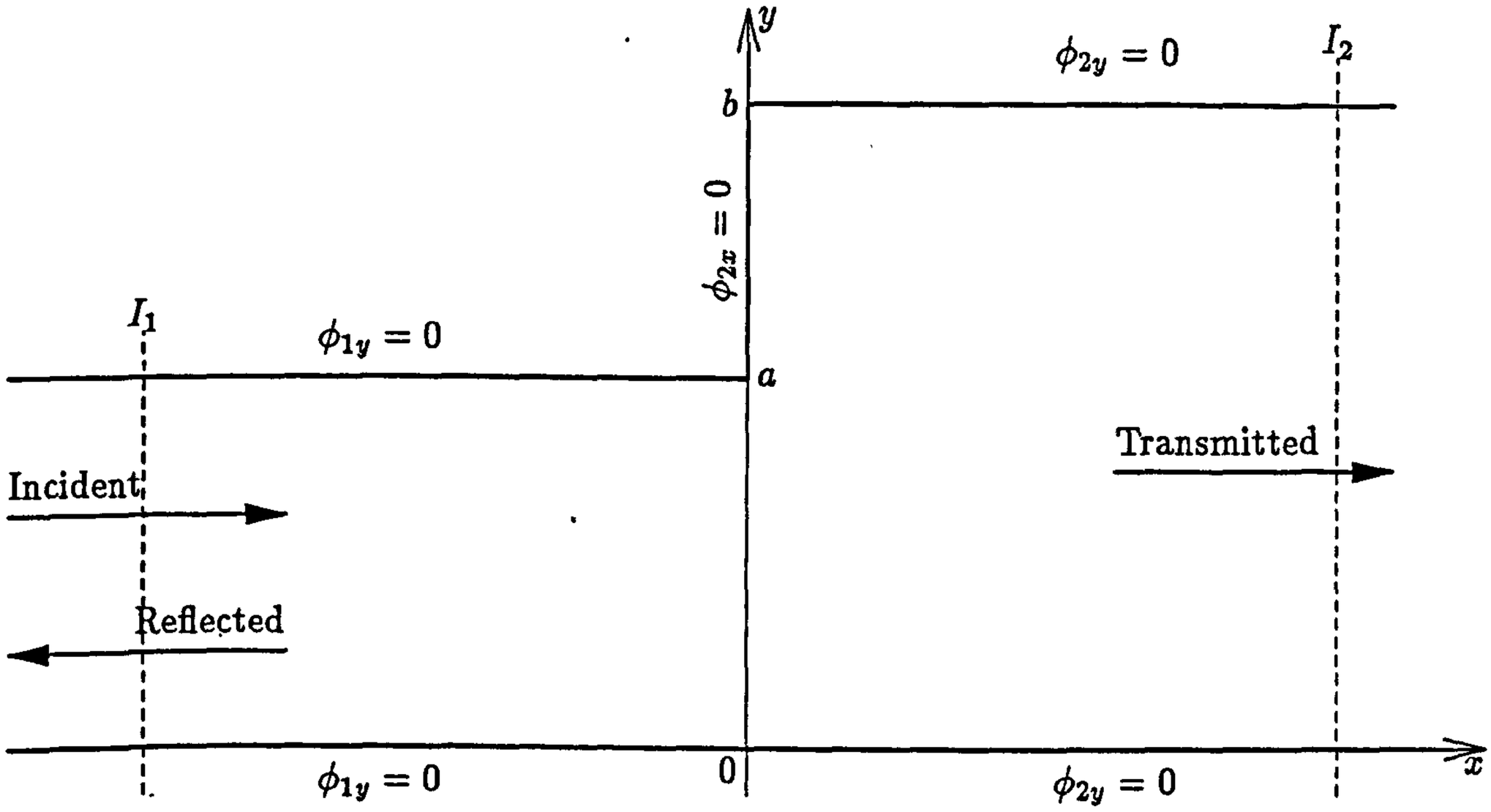

Figure 2.1: Physical configuration for the problem of Section 2.1

provides a valuable tool by which duct problems with membrane boundaries can be solved (see Chapters 3 and 4).

2.1 Acoustic reflection and transmission at the junction of two rigid ducts of differing height

The initial problem is to determine the sound field within two semi-infinite, two dimensional ducts which are joined along an interface at $\bar{x} = 0, 0 \leq \bar{y} \leq \bar{b}$. The first duct occupies the region $0 \leq \bar{y} \leq \bar{a}$, $\bar{x} < 0$ and the second, the region $0 \leq \bar{y} \leq \bar{b}$, $\bar{x} > 0$ with $\bar{b} \geq \bar{a} > 0$, where $(\bar{x}, \bar{y})$ are the usual Cartesian coordinates. The duct is assumed to be closed so that the vertical surface $\bar{x} = 0, \bar{a} < \bar{y} < \bar{b}$ forms part of its boundary. All surfaces are acoustically hard, see figure 2.1. The interior region of this structure is filled with a compressible fluid of sound speed $c = \omega/k$ and density ρ. A plain sound wave, of unit amplitude and harmonic time dependence with radian frequency ω, propagates along the duct in the positive x direction.

The boundary-value problem is described in terms of the fluid velocity potential $\bar{\Phi}(\bar{x}, \bar{y}, \bar{t})$ which satisfies the wave equation. The choice of forcing ensures that the velocity potential has harmonic time dependence and thus may be written in the form

$$\bar{\Phi}(\bar{x}, \bar{y}, \bar{t}) = \bar{\phi}_{tot}(\bar{x}, \bar{y}) e^{-i\omega\bar{t}}, \tag{2.1.1}$$

where $\bar{\phi}_{tot}(\bar{x}, \bar{y})$ satisfies Helmholtz' Equation as derived in many reference texts include Crighton *et al* (1992), that is

$$\left\{ \frac{\partial^2}{\partial \bar{x}^2} + \frac{\partial^2}{\partial \bar{y}^2} + k^2 \right\} \bar{\phi}_{tot}(\bar{x}, \bar{y}) = 0. \tag{2.1.2}$$

It is convenient to non-dimensionalize the problem with respect to a length scale k^{-1} and time scale ω^{-1}. An overbar has hitherto indicated a dimensional quantity and henceforth its un-barred counterpart is non-dimensional. Thus, the non-dimensionalised velocity potential, ϕ_{tot}, is given in terms of its dimensional counterpart as

$$\bar{\phi}_{tot}(\bar{x},\bar{y}) = \frac{\omega}{k^2}\phi_{tot}(x,y) \tag{2.1.3}$$

and the second derivatives with respect to $\bar{x}$ and $\bar{y}$ become

$$\frac{\partial^2}{\partial \bar{x}^2} = k^2\frac{\partial^2}{\partial x^2}, \quad \frac{\partial^2}{\partial \bar{y}^2} = k^2\frac{\partial^2}{\partial y^2}. \tag{2.1.4}$$

Hence, the governing equation, (2.1.2), now takes the form

$$\nabla^2\phi + \phi = 0. \tag{2.1.5}$$

The non-dimensional velocity field is expressed in terms of two potentials, $\phi_1(x,y)$ for $x < 0$ and $\phi_2(x,y)$ for $x > 0$, meeting at the matching interface $x = 0$, such that

$$\phi_{tot} = \begin{cases} \phi_1, & x < 0 \\ \phi_2, & x > 0 \end{cases}. \tag{2.1.6}$$

The boundary conditions imposed on $\phi_1(x,y)$ are

$$\frac{\partial \phi_1}{\partial y} = 0, \qquad y = 0, \tag{2.1.7}$$

$$\frac{\partial \phi_1}{\partial y} = 0, \qquad y = a \tag{2.1.8}$$

where $a = k\bar{a}$. Equations (2.1.7) and (2.1.8) state that the normal component of fluid velocity vanishes at the surfaces $y = 0$ and $y = a$, implying that these surfaces are rigid.

Similarly, for $x > 0$ the duct is comprised of rigid surfaces at $y = 0$ and $y = b$, so the boundary conditions imposed on ϕ_2 are

$$\frac{\partial \phi_2}{\partial y} = 0, \qquad y = 0, \tag{2.1.9}$$

$$\frac{\partial \phi_2}{\partial y} = 0, \qquad y = b \tag{2.1.10}$$

with $b = k\bar{b}$.

The fluid pressure and normal velocity are continuous across the matching interface whilst the surface $a < y \leq b$, $x = 0$ is rigid. These conditions are expressed in terms of the fluid velocity potential as

$$\phi_1 = \phi_2, \qquad x = 0, \qquad 0 \leq y \leq a \tag{2.1.11}$$

and

$$\frac{\partial \phi_2}{\partial x} = \begin{cases} \frac{\partial \phi_1}{\partial x}, & 0 \leq y \leq a, \quad x = 0 \\ 0, & a < y \leq b, \quad x = 0 \end{cases}. \tag{2.1.12}$$

As mentioned above, the acoustic field is forced by a plane wave, incident in the positive x direction. It is convenient to include this incident field in the expression for the potential ϕ_1, and so

$$\phi_1 = \phi_{inc} + \phi_{ref} \tag{2.1.13}$$

where, given the time dependence in equation (2.1.1), $\phi_{inc} = e^{ix}$. The reflected field, ϕ_{ref}, is comprised of an infinite sum of reflected duct modes, and so can be written in the form

$$\phi_{ref} = \sum_{n=0}^{\infty} A_n \phi_{1n}. \tag{2.1.14}$$

To determine the form of a single duct mode ϕ_{1n}, $n = 0, 1, 2, \ldots$, separation of variables is used. In the usual manner ϕ_{1n} is written as

$$\phi_{1n}(x, y) = X_1(x) Y_1(y) \tag{2.1.15}$$

where the subscript 1 indicates that these functions are components of the reflected field. Then, using (2.1.2)

$$\frac{X_1''}{X_1} = -\frac{Y_1''}{Y_1} - 1 = -\eta^2 \tag{2.1.16}$$

where the separation variable is chosen to ensure that X_1 is sinusoidal. Thus

$$X_1(x) = A_1 e^{i\eta x} + B_1 e^{-i\eta x} \tag{2.1.17}$$

$$Y_1(y) = C_1 \cosh(\tau y) + D_1 \sinh(\tau y) \tag{2.1.18}$$

where A_1, B_1, C_1 and D_1 are arbitrary constants and

$$\tau = (\eta^2 - 1)^{\frac{1}{2}}. \tag{2.1.19}$$

Since reflected waves propagate in the negative x direction then $A_1 = 0$ and since all duct surfaces are rigid, $D_1 = 0$ and $\tau = in\pi/a$. It follows that

$$\phi_{1n} = \cos\left(\frac{n\pi y}{a}\right) e^{-i\eta_n x} \tag{2.1.20}$$

where,

$$\eta_n = \left(1 - \frac{n^2\pi^2}{a^2}\right)^{\frac{1}{2}}, \tag{2.1.21}$$

and, for convenience the arbitrary constants are omitted. In the case where $n > \frac{a}{\pi}$, η_n is taken as the positive imaginary value given by (2.1.21). Thus, the potential ϕ_1 has the form

$$\phi_1 = e^{ix} + \frac{A_0 e^{-ix}}{2} + \sum_{n=1}^{\infty} A_n \cos\left(\frac{n\pi y}{a}\right) e^{-i\eta_n x} \tag{2.1.22}$$

where the coefficients, A_n, are the complex amplitudes of each duct mode, ϕ_{1n}. The term for $n = 0$ is taken outside of the summation the coefficient is chosen to be $A_0/2$ to be consistent with a standard Fourier cosine series.

The potential, ϕ_2, is made up purely of transmitted waves and so, in a similar manner,

$$\phi_{2n}(x,y) = X_2(x)Y_2(y). \tag{2.1.23}$$

Again, using (2.1.5)

$$\frac{X_2''}{X_2} = -\frac{Y_2''}{Y_2} - 1 = -\nu^2 \tag{2.1.24}$$

where, again the separation variable is chosen to ensure that X_2 is sinusoidal. So

$$X_2(x) = A_2 e^{i\nu x} + B_2 e^{-i\nu x} \tag{2.1.25}$$

$$Y_2(y) = C_2 \cosh(\gamma y) + D_2 \sinh(\gamma y) \tag{2.1.26}$$

where A_2, B_2, C_2 and D_2 are arbitrary constants and

$$\gamma = (\nu^2 - 1)^{\frac{1}{2}}. \tag{2.1.27}$$

The transmitted field will only propogate in the positive x direction, so $B_2 = 0$ and again, since all surfaces in this model are acoustically hard, $D_2 = 0$ and $\gamma = in\pi/b$. Thus,

$$\phi_{2n} = \cos\left(\frac{n\pi y}{b}\right) e^{i\nu_n x} \tag{2.1.28}$$

with

$$\nu_n = \left(1 - \frac{n^2\pi^2}{b^2}\right)^{\frac{1}{2}}, \tag{2.1.29}$$

and, as before, the arbitrary constants are omitted. It follows that

$$\phi_2 = \frac{B_0 e^{ix}}{2} + \sum_{n=1}^{\infty} B_n \cos\left(\frac{n\pi y}{b}\right) e^{i\nu_n x} \tag{2.1.30}$$

where the coefficients, B_n, are the complex amplitudes of each duct mode, ϕ_{2n}. In a similar way to that in (2.1.22), the $n = 0$ term is taken outside the summation term and expressed as $B_0/2$ to create a standard Fourier cosine series form.

Now that expressions for ϕ_1 and ϕ_2 as eigenfunction expansions have been found, it is possible to apply the matching conditions at the interface, $x = 0$. Continuity of fluid pressure is expressed in terms of ϕ_1 and ϕ_2 by equation (2.1.11). Hence

$$\frac{2 + A_0}{2} + \sum_{\ell=1}^{\infty} A_\ell \cos\left(\frac{\ell\pi y}{a}\right) = \frac{B_0}{2} + \sum_{m=1}^{\infty} B_m \cos\left(\frac{m\pi y}{b}\right), \quad 0 \le y \le a. \tag{2.1.31}$$

The expressions on each side of (2.1.31) are standard Fourier series and so the coefficients $A_\ell, \ell = 0, 1, 2, \ldots, \infty$ or $B_m, m = 0, 1, 2, \ldots, \infty$ can be expressed as an infinite sum of terms involving the other set of coefficients, by using the usual Fourier series formula. A second equation is found by considering the matching condition that implies continuity of fluid velocity, (2.1.12) and substituting the expressions for ϕ_1 and ϕ_2 into that, giving

$$\frac{B_0}{2} + \sum_{n=1}^{\infty} B_m \nu_n \cos\left(\frac{n\pi y}{b}\right) = \begin{cases} 1 - \dfrac{A_0}{2} - \displaystyle\sum_{\ell=1}^{\infty} A_\ell \eta_\ell \cos\left(\dfrac{\ell\pi y}{a}\right), & 0 \le y \le a \\ 0, & a < y \le b \end{cases}. \tag{2.1.32}$$

The form of (2.1.32) is such that the left hand side is a Fourier series and so B_m, $m = 0, 1, 2, \ldots, \infty$ can be expressed in terms of infinite sums of A_ℓ, $\ell = 0, 1, 2, \ldots, \infty$, but because of the piece-wise nature of the right hand side, the converse is not true. Thus, since this cannot be used to determine $A_\ell, \ell = 0, 1, 2, \ldots, \infty$, instead standard Fourier analysis must be applied to (2.1.31) to obtain these coefficients. So, using the usual technique for evaluating the coefficients of Fourier Series as detailed in Korner (1988) among others,

$$\begin{aligned} 2 + A_0 &= \frac{2}{a}\int_0^a \left\{\frac{B_0}{2} + \sum_{m=1}^{\infty} B_m \cos\left(\frac{m\pi y}{b}\right)\right\} dy \\ &= B_0 + \frac{2b}{\pi a}\sum_{m=1}^{\infty} \frac{B_m \sin\left(\frac{m\pi a}{b}\right)}{m} \end{aligned} \tag{2.1.33}$$

and

$$\begin{aligned} A_\ell &= \frac{2}{a}\int_0^a \left\{\frac{B_0}{2} + \sum_{m=1}^{\infty} B_m \cos\left(\frac{m\pi y}{b}\right)\right\} \cos\left(\frac{\ell\pi y}{a}\right) dy \\ &= \frac{2ab}{\pi}\sum_{m=1}^{\infty} \frac{B_m m(-1)^\ell}{m^2a^2 - \ell^2b^2} \sin\left(\frac{m\pi a}{b}\right). \end{aligned} \tag{2.1.34}$$

Similarly, when standard Fourier techniques are applied to (2.1.32) to find B_m, $m = 0, 1, 2, \ldots, \infty$ it is found that

$$\begin{aligned} B_0 &= \frac{2}{b}\int_0^a \left\{1 - \frac{A_0}{2} - \sum_{\ell=1}^{\infty} A_\ell \eta_\ell \cos\left(\frac{\ell\pi y}{a}\right)\right\} dy \\ &= \frac{2a}{b}\left[1 - \frac{A_0}{2}\right] \end{aligned} \tag{2.1.35}$$

and

$$\begin{aligned} B_n &= \frac{2}{b\nu_n}\int_0^a \left\{1 - \frac{A_0}{2} - \sum_{\ell=1}^{\infty} A_\ell \eta_\ell \cos\left(\frac{\ell\pi y}{a}\right)\right\} \cos\left(\frac{n\pi y}{b}\right) dy \\ &= \frac{2}{\pi n \nu_n} \sin\left(\frac{n\pi a}{b}\right)\left[1 - \frac{A_0}{2} - n^2a^2\sum_{\ell=1}^{\infty} \frac{\eta_\ell A_\ell (-1)^\ell}{n^2a^2 - \ell^2b^2}\right]. \end{aligned} \tag{2.1.36}$$

Now, having gained expressions for $A_\ell, \ell = 0, 1, 2, \ldots$ in terms of $B_m, m = 0, 1, 2, \ldots$ and vice versa, it is possible to combine these to form a system in either purely A_ℓ's or B_m's. Here a system in B_m is formed. First using (2.1.33) in (2.1.35) it is found that

$$B_0 = \frac{4a}{b+a} - \frac{2b}{\pi(b+a)}\sum_{m=1}^{\infty} \frac{B_m \sin\left(\frac{m\pi a}{b}\right)}{m}. \tag{2.1.37}$$

Similarly, by substituting (2.1.33) and (2.1.34) into (2.1.36) gives

$$B_n = \frac{2\sin(n\pi r)}{n\pi\nu_n}\left[2 - \frac{B_0}{2} - \frac{1}{\pi}\sum_{m=1}^{\infty} B_m \sin(m\pi r)\left\{\frac{1}{rm} + \sum_{\ell=1}^{\infty} \frac{2mn^2r^3\eta_\ell}{(m^2r^2 - \ell^2)(n^2r^2 - \ell^2)}\right\}\right], \tag{2.1.38}$$

where $r = \frac{a}{b}$.

The system that is formed by (2.1.37) and (2.1.38) is infinite and, because of the nature of the coefficients of $B_m, m = 0, 1, 2, \ldots$ in the summation terms, non-convergent. The cause of this non-convergence is discussed later in the chapter, but for the time being it is taken that convergence can be improved by a simple substitution of the form

$$B_n = \frac{2}{\pi n \nu_n} \sin(n\pi r)\, D_n. \tag{2.1.39}$$

Then

$$D_n = 1 - \frac{A_0}{2} - n^2 r^2 \sum_{\ell=1}^{\infty} \frac{\eta_\ell A_\ell (-1)^\ell}{n^2 r^2 - \ell^2}. \tag{2.1.40}$$

and (2.1.33) becomes

$$A_0 = \frac{2(r-1)}{r+1} + \frac{4}{\pi^2 r(r+1)} \sum_{m=1}^{\infty} \frac{\sin^2(m\pi r) D_m}{m^2 \nu_m}. \tag{2.1.41}$$

whilst (2.1.34) reduces to

$$A_\ell = \frac{4r(-1)^\ell}{\pi^2} \sum_{m=1}^{\infty} \frac{\sin^2(m\pi r) D_m}{(m^2 r^2 - \ell^2)\nu_m}. \tag{2.1.42}$$

Expressions (2.1.41) and (2.1.42) are now substituted into (2.1.40) to obtain

$$D_n = \frac{2b}{a+b} - \frac{4}{\pi^2} \sum_{m=1}^{\infty} \frac{\sin^2(m\pi r) D_m}{\nu_m} \left[\frac{1}{2r(r+1)m^2} + n^2 r^3 \sum_{\ell=1}^{\infty} \frac{\eta_\ell}{(m^2 r^2 - \ell^2)(n^2 r^2 - \ell^2)} \right], \tag{2.1.43}$$

which is solvable for D_n, $n = 1, 2, 3, \ldots, \infty$ and is convergent, albeit slowly. Once D_n, $n = 1, 2, 3, \ldots, \infty$ are evaluated, $B_n, n = 1, 2, 3, \ldots, \infty$ can be found directly via (2.1.39) and $A_\ell, \ell = 0, 1, 2, \ldots, \infty$ can also be found using (2.1.41) and (2.1.42), but B_0 in terms of D_n is, as yet, undefined. This gap can be filled by substituting for B_n in (2.1.37) to give

$$B_0 = \frac{4r}{r+1} - \frac{4}{\pi^2(r+1)} \sum_{m=1}^{\infty} \frac{\sin^2(m\pi r) D_m}{m^2 \mu_m} \tag{2.1.44}$$

and so by solving a truncated version of the system given by (2.1.43), all values of $A_\ell, \ell = 0, 1, 2, \ldots$ and $B_n, n = 0, 1, 2, \ldots$ can be found.

Whilst this new system in D_n is convergent the rate of convergence is poor. As a consequence, for results of high accuracy the number of terms required in the truncated system is large and so computation times are long. The aim is to be able to achieve highly accurate results with as little computational time as possible, so the convergence of the system in (2.1.43) needs to be further improved. This can be achieved by utilising the asymptotic properties of the term in the inner sum, that is

$$\sum_{\ell=1}^{\infty} \frac{\eta_\ell}{(m^2 r^2 - \ell^2)(n^2 r^2 - \ell^2)}. \tag{2.1.45}$$

The quantity η_ℓ is defined by

$$\begin{aligned} \eta_\ell &= \left(1 - \frac{\ell^2\pi^2}{a^2}\right)^{\frac{1}{2}} \\ &\sim \frac{i\ell\pi}{a}, \qquad \ell \to \infty, \end{aligned} \tag{2.1.46}$$

and so the inner sum can be rewritten as

$$\sum_{\ell=1}^{\infty} \frac{\eta_\ell}{(m^2r^2-\ell^2)(n^2r^2-\ell^2)} = \sum_{\ell=1}^{\infty} \frac{\eta_\ell - \frac{i\ell\pi}{a}}{(m^2r^2-\ell^2)(n^2r^2-\ell^2)} + \frac{i\pi}{a}\sum_{\ell=1}^{\infty} \frac{\ell}{(m^2r^2-\ell^2)(n^2r^2-\ell^2)}. \tag{2.1.47}$$

The second sum can be evaluated exactly and it transpires that

$$\begin{aligned} \sum_{\ell=1}^{\infty} \frac{\eta_\ell}{(m^2r^2-\ell^2)(n^2r^2-\ell^2)} &= \sum_{\ell=1}^{\infty} \frac{\eta_\ell - \frac{i\ell\pi}{a}}{(m^2r^2-\ell^2)(n^2r^2-\ell^2)} \\ &+ \frac{i\pi}{2ar^2(n^2-m^2)}\left[\frac{n-m}{rnm} + \pi\left\{\cot(\pi rm) - \cot(\pi rn)\right\} + 2\left\{\psi(rm) - \psi(rn)\right\}\right] \end{aligned} \tag{2.1.48}$$

where $\psi(z)$ is the Psi or Digamma function defined by

$$\psi(z) = \frac{d[\ln\{\Gamma(z)\}]}{dz} = \frac{\Gamma'(z)}{\Gamma(z)} \tag{2.1.49}$$

(see Abramowitz and Stegun (1964)) and $\Gamma(z)$ is the usual Gamma function. Expression (2.1.48) appears to have a singularity when $m = n$. However, on the application of L'Hôpital's Rule, it is found that (2.1.48) becomes

$$\sum_{\ell=1}^{\infty} \frac{\ell}{(m^2r^2-\ell^2)^2} = \frac{1}{4r^2m}\left[\frac{1}{rm^2} - \frac{r\pi^2}{\sin^2(mr\pi)} + 2r\psi'(rm)\right] \tag{2.1.50}$$

when $m = n$. Hence, with the singularity removed

$$\begin{aligned} D_n &= 1 - \frac{r-1}{r+1} - \frac{4}{\pi^2}\sum_{m=1}^{\infty} \frac{\sin^2(m\pi r)D_m}{\nu_m}\left[\frac{1}{2r(r+1)m^2}\right. \\ &\left. + \frac{in\pi}{2am(n+m)} + \frac{in^2r\pi F_{mn}}{2a(n+m)} + n^2r^3\sum_{\ell=1}^{\infty} \frac{\eta_\ell - \frac{i\ell\pi}{a}}{(m^2r^2-\ell^2)(n^2r^2-\ell^2)}\right] \end{aligned} \tag{2.1.51}$$

where

$$F_{mn} = \begin{cases} \frac{\pi}{n-m}\left\{\cot(\pi rm) - \cot(\pi rn)\right\} + \frac{2}{n-m}\left\{\psi(rm) - \psi(rn)\right\}, & n \neq m \\ \frac{-r\pi^2}{\sin^2(mr\pi)} + 2r\psi'(rm), & n = m \end{cases} \tag{2.1.52}$$

This system has a diagonally dominant matrix form and also offers rapid convergence under computation resulting in a high level of accuracy, gained using a relatively small number of terms. With computation time kept to a bare minimum, highly accurate results are readily available for analysis. The truncated system is solved using *Mathematica* and the values $D_m, m = 1, 2, 3, \ldots, t$, ($t$ being the number of terms in the truncated system) are

then used in the expressions derived above to give values for required A_ℓ, $\ell = 0, 1, 2, \ldots, t$ and B_m, $m = 0, 1, 2, \ldots, t$. The code for the *Mathematica* programme is given in Appendix A.1.

To check these results, a power balance is calculated. Since the surfaces of the duct are perfectly reflecting and the duct is closed then no power is lost from the system, and none is carried in the form of waves induced on the boundary surfaces. Thus, the power associated with the incident wave must balance the sum of that for the reflected and transmitted waves. The results gained from the solution of the system given in (2.1.51) should reflect this theory. First consider the dimensional equation for power, as derived in Auld (1990) and given by

$$\bar{P} = \frac{1}{2}\,\omega\rho\,\mathrm{Re}\left[\int_S i\bar{\phi}\left(\frac{\partial\bar{\phi}}{\partial\bar{n}}\right)^* d\bar{s}\right] \tag{2.1.53}$$

where '*' indicates the complex conjugate, S is an arbitrary cross-sectional surface of the duct and n is normal to that surface. This expression must be non-dimensionalised using the same basis as for the rest of the problem to provide a power equation that is suitable for application to this problem. As previously noted

$$\bar{\phi} = \frac{\omega}{k^2}\phi \tag{2.1.54}$$

and so

$$\left(\frac{\partial\bar{\phi}}{\partial n}\right)^* = \frac{\omega}{k}\left(\frac{\partial\phi}{\partial\bar{n}}\right)^*. \tag{2.1.55}$$

Further, using the dimensions of power

$$\bar{P} = Mk^{-2}\omega^3 P, \tag{2.1.56}$$

and similarly,

$$\rho = Mk^3. \tag{2.1.57}$$

Thus, the non-dimensional form of (2.1.53) is

$$P = \frac{1}{2}\,\mathrm{Re}\left[\int_s i\phi\left(\frac{\partial\phi}{\partial n}\right)^* ds\right]. \tag{2.1.58}$$

The system considered in this section has one source of power, that being the incident field, whilst power travels out of the system via the reflected field and the transmitted field, as shown in figure 2.1. A power balance is achieved if the total energy flux in the positive x direction crossing the surface I_1 is equal to that travelling in the positive x direction across I_2. Note that unit vector in the normal direction to I_1 and I_2 is x.

The incident field takes the form of a plane wave with unit amplitude and so, P_{in}, the power fed into the system per unit length in the z direction is given by

$$\begin{aligned} P_{in} &= \frac{1}{2}\,\mathrm{Re}\left[\int_0^a ie^{ix}\left(-ie^{-ix}\right)dy\right] \\ &= \frac{a}{2}. \end{aligned} \tag{2.1.59}$$

Power leaving the system will be either reflected, P_{ref}; that is moving in the opposite direction to the power into the system, the negative x direction, or it will be transmitted, P_{trans} which moves in the positive x direction and so leaves the system along the duct of width b. The reflected field is given as

$$\phi_{ref} = \frac{A_0 e^{-ix}}{2} + \sum_{\ell=1}^{\infty} A_\ell \cos\left(\frac{\ell\pi y}{a}\right) e^{-i\eta_\ell x} \tag{2.1.60}$$

and so

$$P_{ref} = \mathrm{Re}\left[\frac{i}{2}\int_0^a \left[\frac{A_0 e^{-ix}}{2} + \sum_{\ell=1}^{\infty} A_\ell \cos\left(\frac{\ell\pi y}{a}\right) e^{-i\eta_\ell x}\right] \times \left[\frac{iA_0^* e^{ix}}{2} + \sum_{m=1}^{\infty} i\eta_m A_m^* \cos\left(\frac{m\pi y}{a}\right) e^{i\eta_m x}\right] dy\right] \tag{2.1.61}$$

The integrand of (2.1.61) can be expanded to obtain

$$\begin{aligned} P_{ref} = \mathrm{Re}\Bigg[\frac{i}{2}\int_0^a \Bigg[&\frac{iA_0A_0^*}{4} + \frac{iA_0^* e^{ix}}{2}\sum_{\ell=1}^{\infty} A_\ell \cos\left(\frac{\ell\pi y}{a}\right) e^{-i\eta_\ell x} \\ &+ \frac{A_0 e^{-ix}}{2}\sum_{m=1}^{\infty} i\eta_m A_m^* \cos\left(\frac{m\pi y}{a}\right) e^{i\eta_m x} \\ &+ \sum_{\ell=1}^{\infty}\sum_{m=1}^{\infty} i\eta_m A_\ell A_m^* \cos\left(\frac{\ell\pi y}{a}\right)\cos\left(\frac{m\pi y}{a}\right) e^{i(\eta_m-\eta_\ell)x}\Bigg] dy\Bigg] . \end{aligned} \tag{2.1.62}$$

On the assumption that, for each term, the orders of summation and integration can be interchanged, it is clear that the second and third terms do not contribute to this integral. The first term is easily evaluated as

$$\begin{aligned} \frac{i}{2}\mathrm{Re}\left[\int_0^a \frac{A_0 e^{-ix}}{2}\left[\frac{iA_0^* e^{ix}}{2}\right] dy\right] &= -\frac{1}{2}\mathrm{Re}\left[\int_0^a \frac{A_0A_0^*}{4}\, dy\right] \\ &= \frac{-|A_0|^2 a}{8} \end{aligned} \tag{2.1.63}$$

The last term of (2.1.62) satisfies the standard orthogonality relation used in Fourier series methods for $\left\{\cos\left(\frac{\ell\pi y}{a}\right), \cos\left(\frac{m\pi y}{a}\right)\right\}$. Thus

$$\frac{i}{2}\int_0^a \sum_{\ell=1}^{\infty}\sum_{m=1}^{\infty} i\eta_m A_\ell A_m^* \cos\left(\frac{\ell\pi y}{a}\right)\cos\left(\frac{m\pi y}{a}\right) e^{i(\eta_m-\eta_\ell)x} dy = \begin{cases} 0, & m \neq \ell \\ -\frac{|A_\ell|^2\eta_\ell a}{4}, & m = \ell \end{cases} . \tag{2.1.64}$$

However, here the real part of (2.1.62) is sought. It is clear that (2.1.63) is purely real, but the polarity of (2.1.63) is dependent upon the value of η_ℓ. From (2.1.21) it can be seen that when $a > \ell\pi$, η_ℓ is real but when $a < \ell\pi$, η_ℓ is pure imaginary. Indeed in the case where $a < \pi$, (2.1.64) makes no contribution to P_{ref} since all terms are imaginary.

Upon reassembling the constituent parts of (2.1.62), P_{ref} can now be expressed as

$$P_{ref} = -\frac{|A_0|^2 a}{8} - \mathrm{Re}\left[\sum_{\ell=1}^{\infty}\frac{|A_\ell|^2\eta_\ell a}{4}\right], \tag{2.1.65}$$

where, as noted above, the infinite sum will be truncated or may not contribute at all, since not all terms will be real for any finite value of a. Since n (which here is in the direction of positive x) is in the opposite direction to the propogating reflected field, it is not surprising that P_{ref} is found to be negative in value. The energy flux in the positive x direction across I_1 on figure 2.1 is thus found to be

$$P_{inc} + P_{ref} = \frac{a}{2} - \frac{|A_0|^2 a}{8} - \mathrm{Re}\left[\sum_{\ell=1}^{\infty} \frac{|A_\ell|^2 \eta_\ell a}{4}\right]. \tag{2.1.66}$$

The transmitted field is given by

$$\phi_{trans} = \frac{B_0 e^{ix}}{2} + \sum_{n=1}^{\infty} B_n \cos\left(\frac{n\pi y}{b}\right) e^{i\nu_n x} \tag{2.1.67}$$

and so, following the above method, energy flux across I_2 on figure 2.1 is given as

$$P_{trans} = \frac{|B_0|^2 b}{8} + \mathrm{Re}\left[\sum_{n=1}^{\infty} \frac{|B_n|^2 \nu_n b}{4}\right]. \tag{2.1.68}$$

The power balance is now given by

$$P_{inc} + P_{ref} = P_{trans} \tag{2.1.69}$$

or equivalently

$$\frac{a}{2} - \frac{|A_0|^2 a}{8} - \mathrm{Re}\left[\sum_{\ell=1}^{\infty} \frac{|A_\ell|^2 \eta_\ell a}{4}\right] = \frac{|B_0|^2 b}{8} + \mathrm{Re}\left[\sum_{n=1}^{\infty} \frac{|B_n|^2 \nu_n b}{4}\right] \tag{2.1.70}$$

which can be rearranged to give

$$1 = \frac{|A_0|^2}{4} + \frac{|B_0|^2 b}{4a} + \mathrm{Re}\left[\sum_{\ell=1}^{\infty} \frac{|A_\ell|^2 \eta_\ell}{2} + \sum_{n=1}^{\infty} \frac{|B_n|^2 \nu_n b}{2a}\right]. \tag{2.1.71}$$

This expression may be used to check the validity of the results gained from the system given previously in this section.

2.1.1 Results

The results in this section comprise a selection of graphs and some tables. Successive transmitted modes are switched on by increasing b and the graphs show the effect this has on the fundamental and secondary reflected and transmitted modes. In each case a is fixed. Each graph is discussed individually, although in many cases, the explanation of the behaviour demonstrated is similar.

The tables of results are to demonstrate the continuing accuracy of the power balance calculations for a range of fixed a and varying b. As b is increased, the number of terms included in the power balance increases also, and this is considered in the analysis.

In the first three graphs, $a = 2.1$ and b is varied from 2.1 to 14.1. Figure 2.2 shows a graph of the modulus of the fundamental reflected coefficient and peaks can be seen

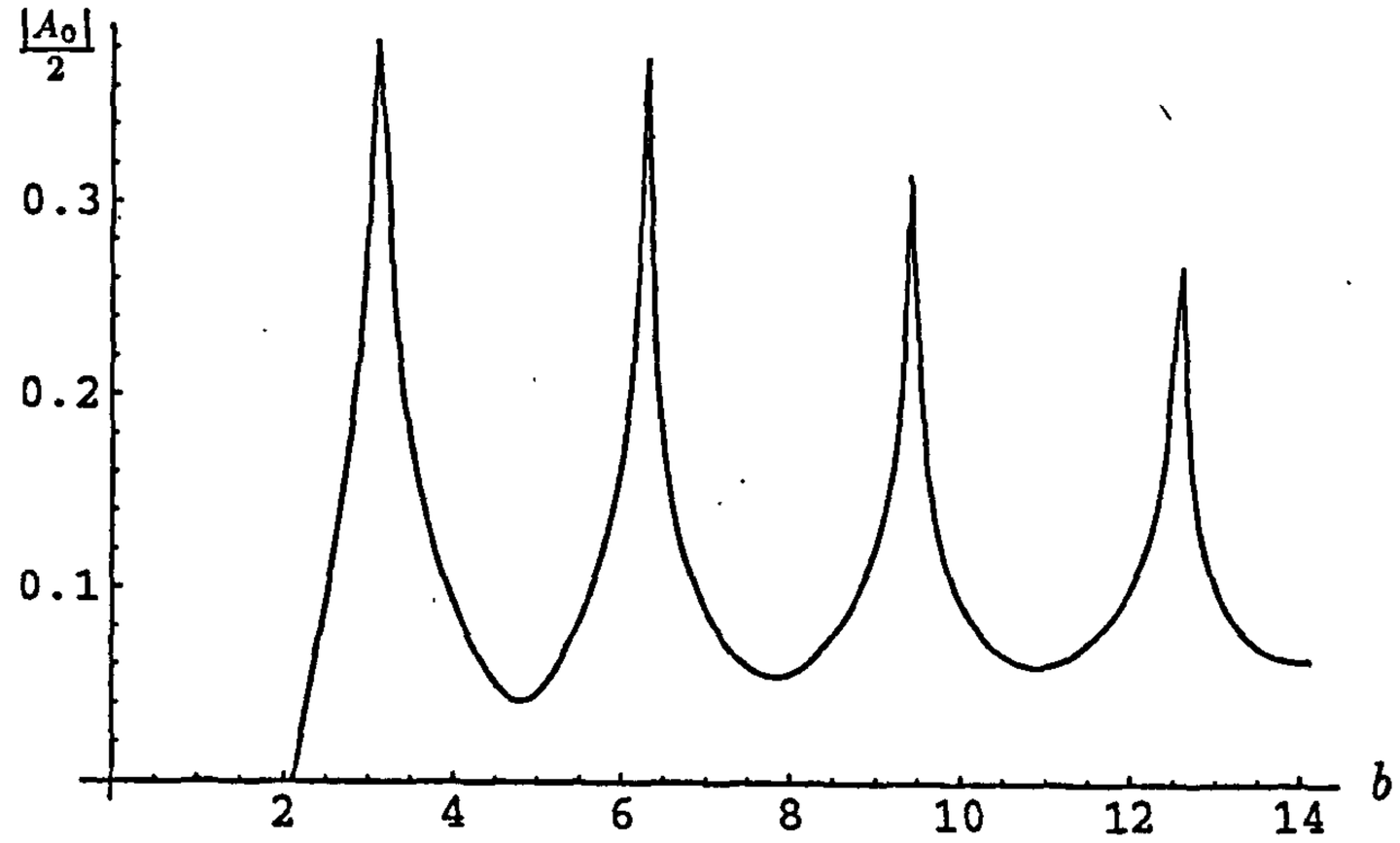

Figure 2.2: Plot of the modulus of the reflection coefficient of the fundamental mode for the hard/hard problem with $a = 2.1$.

occurring at regular intervals. These peaks are actually located at $n\pi$, $n = 1, 2, 3, \ldots$. The peaks occur as each new transmitted mode (with coefficient B_n, $n = 1, 2, 3, \ldots$) becomes significant to the total far field within the system. In figures 2.3 and 2.4, $|B_0|$ and $|B_1|$ are shown. It can be seen from these that the transmitted nodes fluctuate as b is increased.

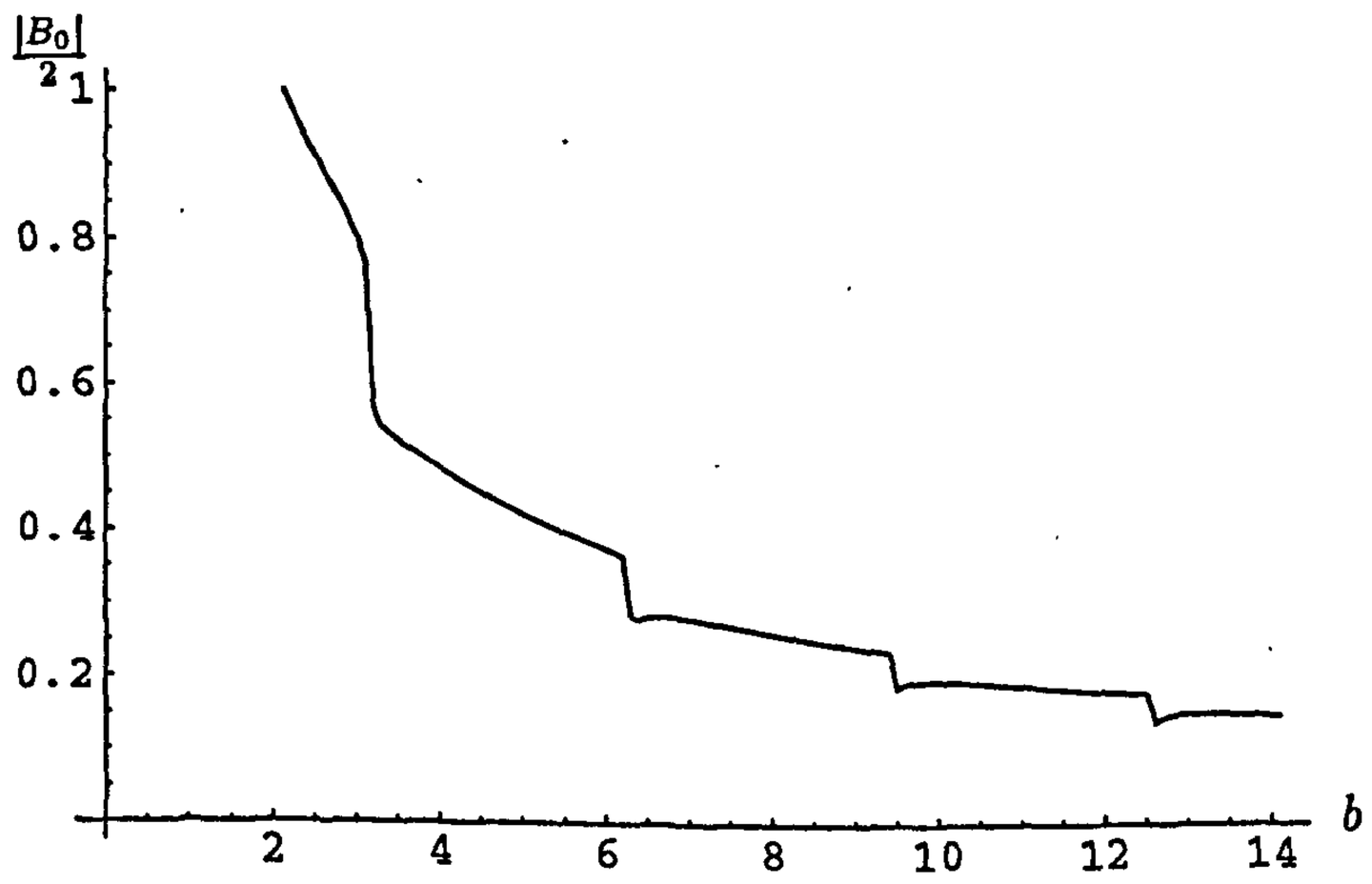

Figure 2.3: Plot of the modulus of the transmitted coefficient of the fundamental mode for the hard/hard problem with $a = 2.1$.

In the range $a \leq b \leq \pi$ it is clear from figures 2.2 and 2.3 that A_0 and B_0 have the greatest contribution to the total power of the system. Note also that at the point $a = b$,

$|A_0| = 0$ and $|B_0| = 1$. This is not a surprise since at the point $a = b$ the duct is of uniform height from $-\infty$ to ∞ and is perfectly transmitting, so any field introduced from one end will pass through to the other with no interaction, hence the primary transmitted field should equal the incident field exactly. From figure 2.4 the effect of B_1 can be seen to become significant at the point where $b = \pi$. For $b > \pi$, $|A_0|$ periodically peaks at $n\pi$, $n = 2,3,\ldots$, whilst both $|B_0|$ and $|B_1|$ show gradual decrease of value, with sharp downward steps at $n\pi$, $n = 2,3,\ldots$. These steps occur everytime a new transmitted mode becomes significant to the total power of the system. That is, B_2 is 'switched on' on at 2π, B_3 at 3π and so on.

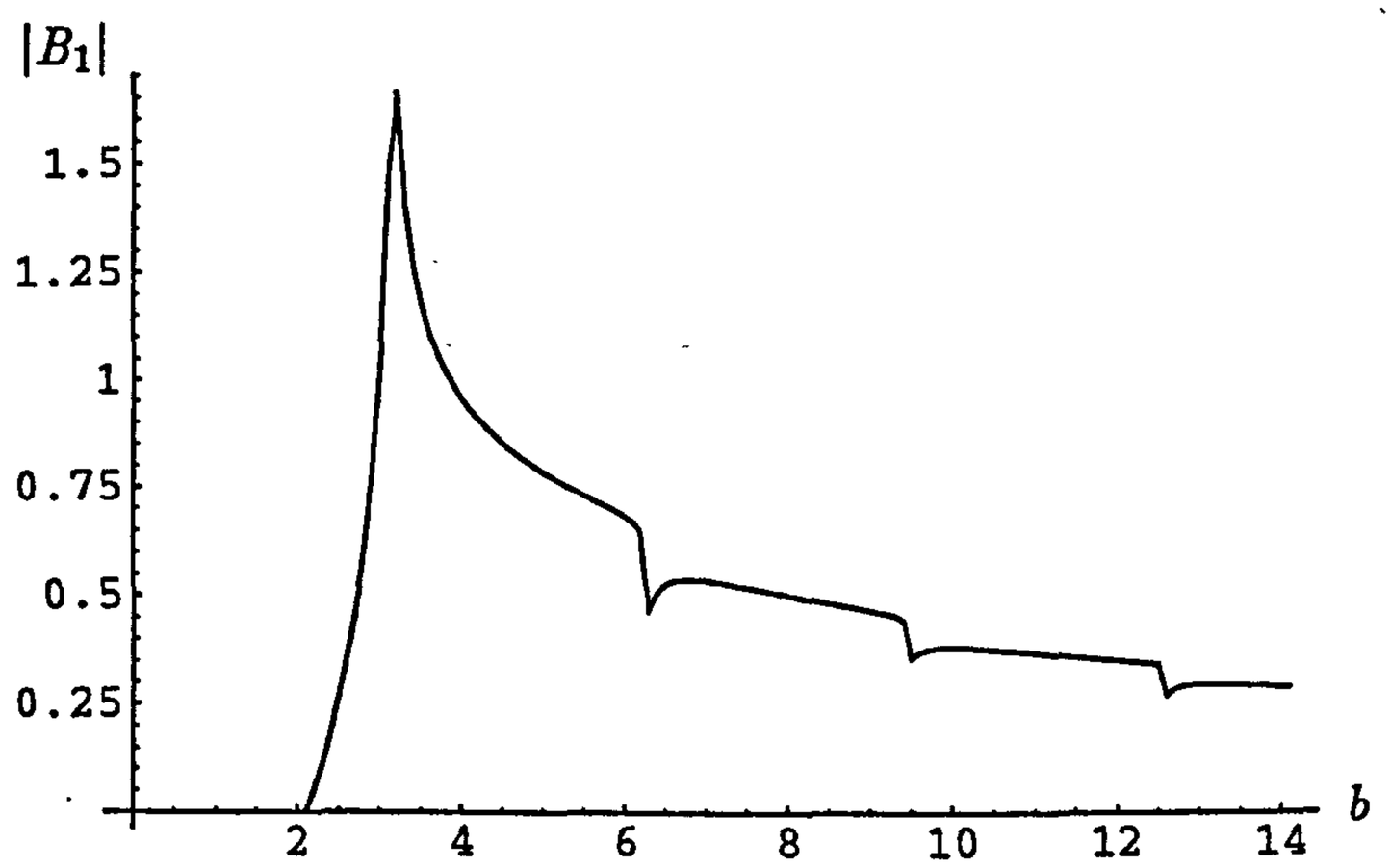

Figure 2.4: Plot of the modulus of the reflection coefficient of the secondary mode for the hard/hard problem with $a = 2.1$.

The next four graphs show similar data for the case where $a = 4.3$ Now, since $a > \pi$, there are two significant reflected modes from the outset, these being A_0 and A_1. These are shown in figures 2.5 and 2.6. Both show the same peak and trough behaviour as $|A_0|$ in figure 2.2.

Also, at $a = b$, $|A_0| = |A_1| = 0$, whilst it can be seen from figures 2.7 and 2.8 that B_0 is the only significant transmitted mode at this point. This is again because the duct takes the form of an infinite perfectly transmitting duct when $a = b$ and so the transmitted field is identical to the incident field, since there is no structural or geometrical discontinuities to affect it.

It can be seen that $|B_1|$ steadily increases in value until $b = 2\pi$. At this point, as mentioned previously, B_2 begins to contribute to the transmitted field and so from that point on, B_1 decreases in value.

In the following tables, a value for a is again set and b is increased. For each value of b, a power balance is calculated, as described in Section 2.1. Remember that as a

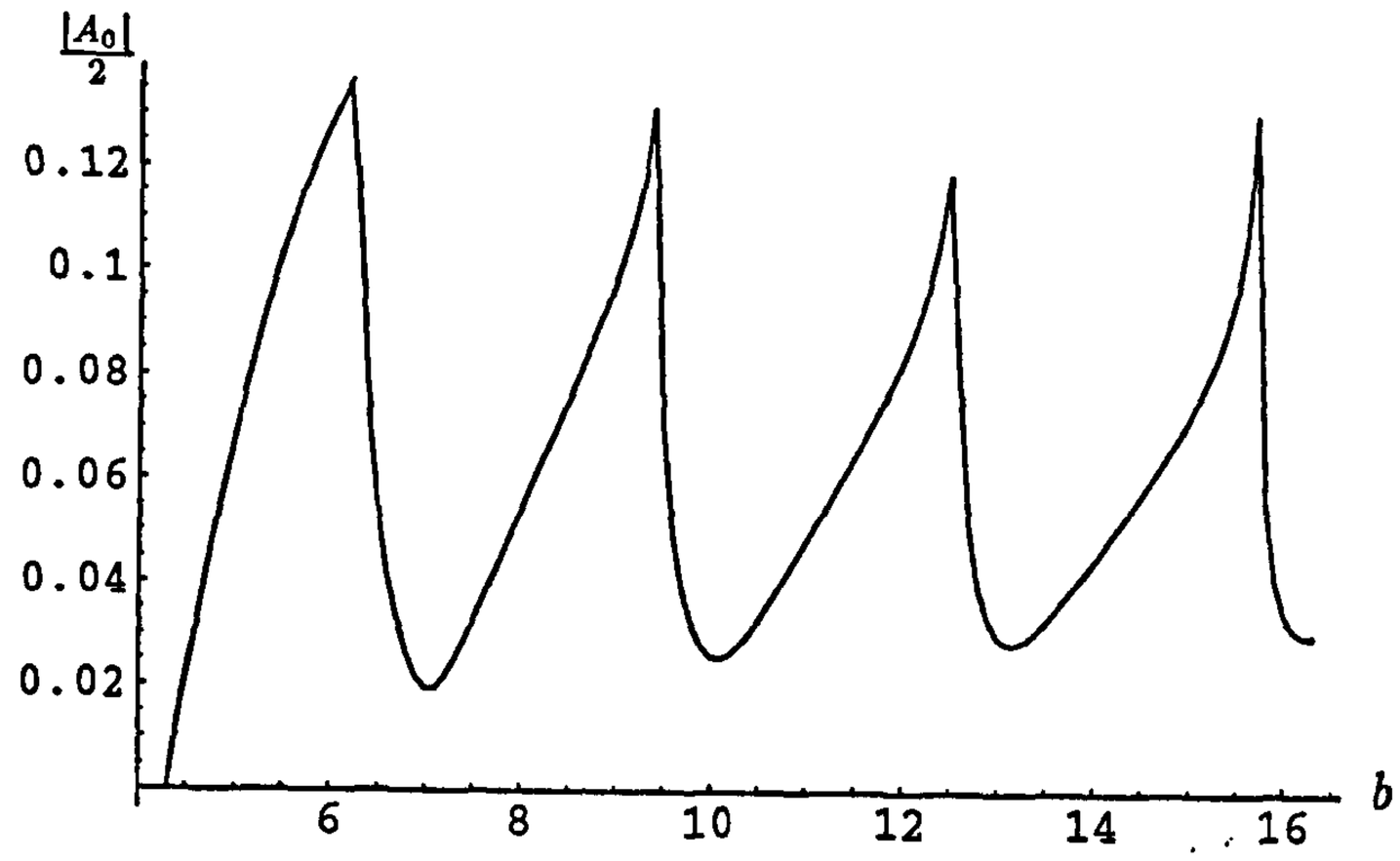

Figure 2.5: Plot of the modulus of the reflection coefficient of the fundamental mode for the hard/hard problem with $a = 4.3$.

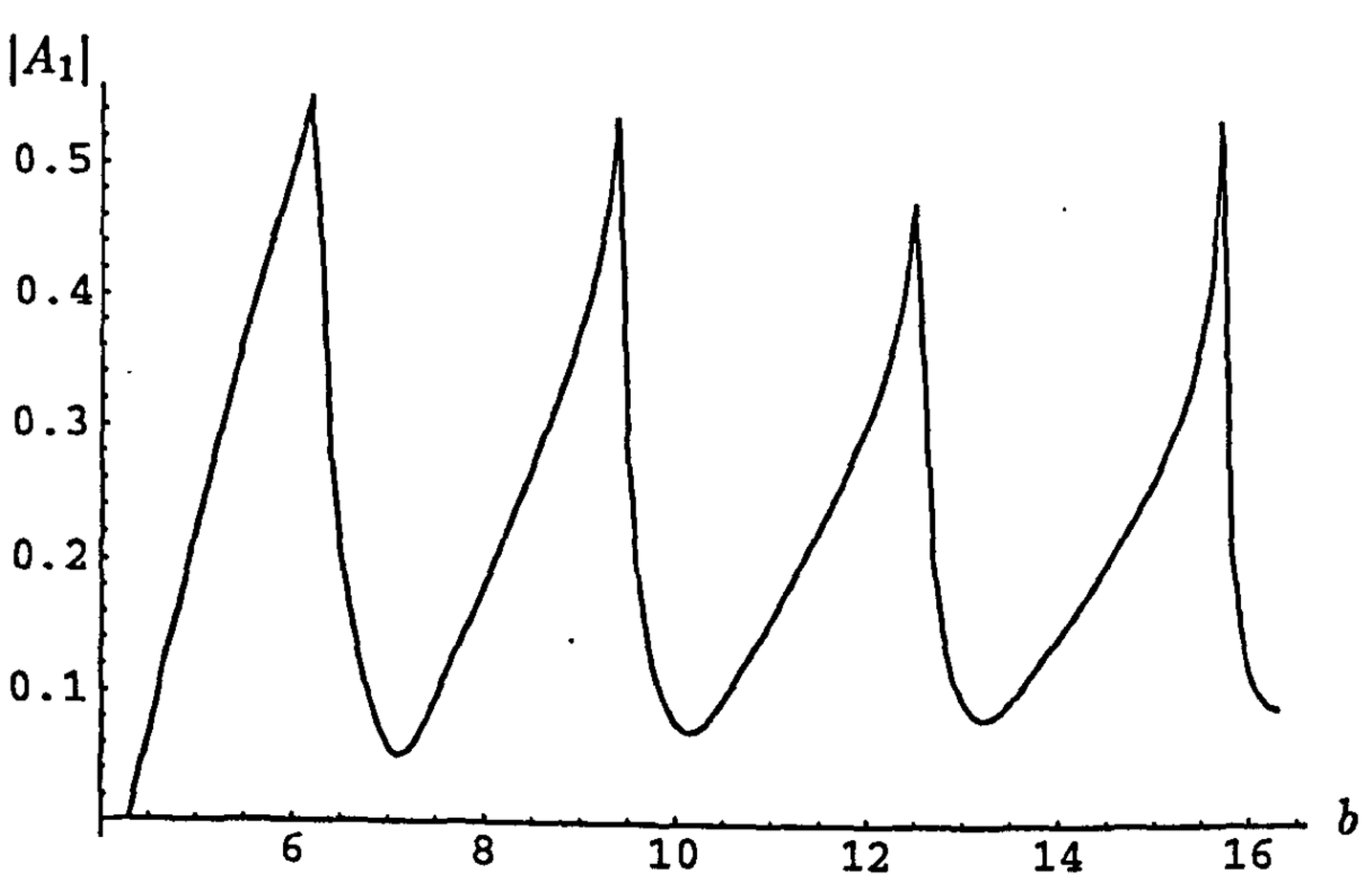

Figure 2.6: Plot of the modulus of the reflection coefficient of the secondary mode for the hard/hard problem with $a = 4.3$.

and b increase, more terms in the reflected and transmitted fields respectively must be considered, as described previously in the section (see (2.1.61) – (2.1.64) for explanation).

In table 2.1, $a = 0.8$. As mentioned previously, when $a < \pi$ only A_0 is significant in the power balance and so that is the only reflected mode inculded on the table. As b increases, the number of transmitted modes that are significant also increases, which is reflected in the table, showing a second, and then a third transmitted mode being included. Clearly, the accuracy of the results is borne out by the sum of the significant reflected and

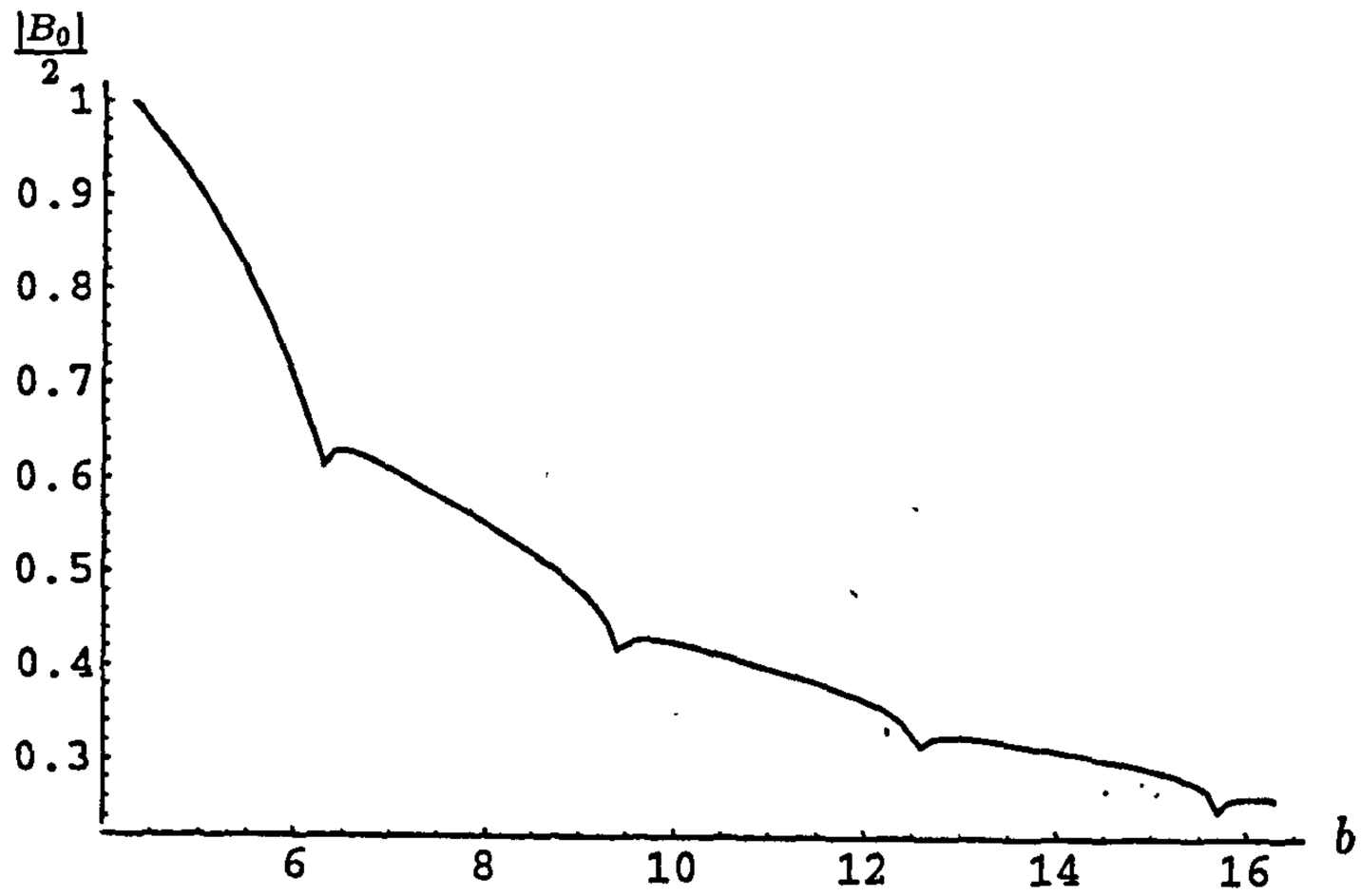

Figure 2.7: Plot of the modulus of the transmitted coefficient of the fundamental mode for the hard/hard problem with $a = 4.3$.

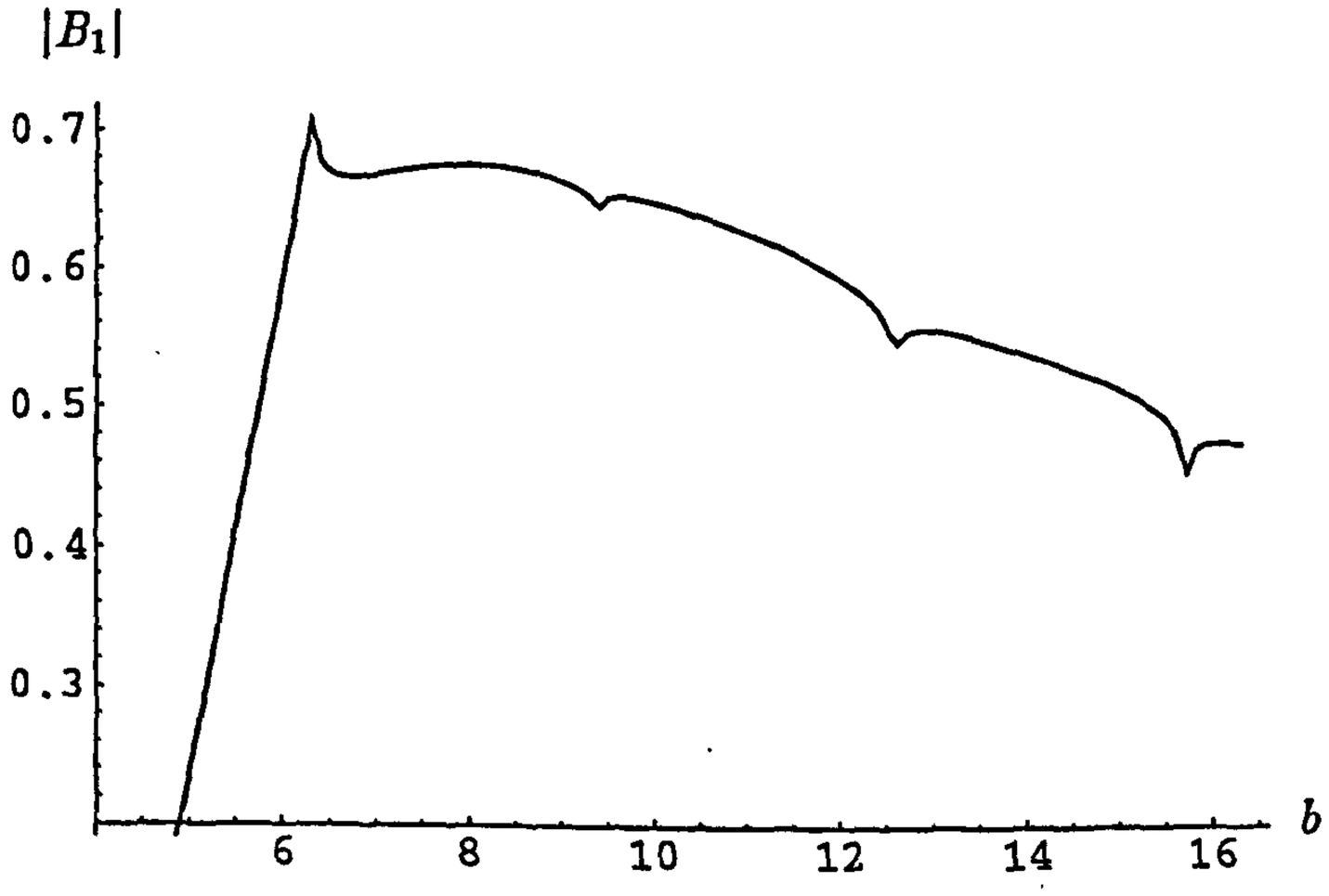

Figure 2.8: Plot of the modulus of the transmitted coefficient of the secondary mode for the hard/hard problem with $a = 4.3$.

transmitted terms always being close to 1, as prescribed by (2.1.71).

Table 2.2 again has a fixed at a value such that $a < \pi$. The same increase in the number of transmitted modes that are significant to the power balance is also seen, with the behaviour being that $n+1$ terms are significant for $b > n\pi$, $n = 0, 1, 2, \ldots$. Again the total of the transmitted and reflected power is equal to 1 in all cases.

In table 2.3, $\pi < a < 2\pi$ and so two reflected modes are now of importance (A_0 and A_1). With the increase of b still bringing more transmitted modes into the equation, again

b	$\frac{\lvert A_0\rvert^2}{4}$	$\frac{\lvert B_0\rvert^2 b}{4a}$	$\frac{\lvert B_1\rvert^2 \nu_1 b}{2a}$	$\frac{\lvert B_2\rvert^2 \nu_2 b}{2a}$	$\frac{\lvert B_3\rvert^2 \nu_3 b}{2a}$	Total
0.8		1				1
1.8	0.18277	0.81787				1.00064
2.8	0.53240	0.46851				1.00091
3.8	0.02089	0.24599	0.73340			1.00028
4.8	0.12630	0.26041	0.61434			1.00105
5.8	0.29748	0.22022	0.48230			1
6.8	0.02576	0.13348	0.28473	0.55662		1.00059
7.8	0.10606	0.15103	0.31592	0.42698		1
8.8	0.21947	0.14158	0.29246	0.34974		1.00325
9.8	0.02520	0.08810	0.18102	0.20568	0.49999	1
10.8	0.09459	0.10522	0.21497	0.23595	0.34927	1
11.8	0.17801	0.10288	0.20930	0.22450	0.28531	1

Table 2.1: The power balance for $a = 0.8$, b increasing

b	$\frac{\lvert A_0\rvert^2}{4}$	$\frac{\lvert B_0\rvert^2 b}{4a}$	$\frac{\lvert B_1\rvert^2 \nu_1 b}{2a}$	$\frac{\lvert B_2\rvert^2 \nu_2 b}{2a}$	$\frac{\lvert B_3\rvert^2 \nu_3 b}{2a}$	Total
2.3		1				1
3.3	0.04000	0.60051	0.35949			1
4.3	0.00450	0.48235	0.51315			1
5.3	0.00200	0.44380	0.55420			1
6.3	0.08018	0.32468	0.36763	0.22751		1
7.3	0.00428	0.28980	0.45595	0.24997		1
8.3	0.00258	0.27791	0.45840	0.26111		1
9.3	0.02089	0.27339	0.45422	0.25150		1
10.3	0.00467	0.20615	0.36445	0.25258	0.17215	1
11.3	0.00285	0.20175	0.36353	0.26541	0.16646	1
12.3	0.01058	0.19961	0.36186	0.26752	0.16043	1

Table 2.2: The power balance for $a = 2.3$, b increasing

the results can be seen to be accurate. Table 2.4 shows similarly accurate results.

One other characteristic of note, shown in all tables is for the case where $a = b$. As mentioned previously, this case is where the duct has no discontinuity in height, and also no discontiuity in material property, and so is just a duct that has no effect on the incident wave – it just passes straight through. This results in the only significant reflected and transmitted mode being B_0, which must carry exactly the power of the incident field.

2.2 Convergence in Section 2.1

In Section 2.1, what appears to be a solvable system, for $B_n, n = 0, 1, 2, \ldots$ is given in (2.1.38). However, when this system is truncated and a solution is sought computationally, it is found that the system does not converge. To overcome this problem, two methods of improving the convergence of the system are employed. In this section, the reasons for

b	$\frac{\lvert A_0\rvert^2}{4}$	$\frac{\lvert A_1\rvert^2\eta_1}{2}$	$\frac{\lvert B_0\rvert^2 b}{4a}$	$\frac{\lvert B_1\rvert^2\nu_1 b}{2a}$	$\frac{\lvert B_2\rvert^2\nu_2 b}{2a}$	$\frac{\lvert B_3\rvert^2\nu_3 b}{2a}$	$\frac{\lvert B_4\rvert^2\nu_4 b}{2a}$	Total
4.1			1					1
5.1	0.00791	0.03357	0.89440	0.06412				1
6.1	0.01453	0.08976	0.61209	0.28362				1
7.1	0.00067	0.00154	0.58849	0.36352	0.04578			1
8.1	0.00452	0.02006	0.54017	0.42272	0.01254			1
9.1	0.01035	0.05955	0.44657	0.45018	0.03336			1
10.1	0.00085	0.00217	0.40981	0.47978	0.04744	0.05996		1
11.1	0.00349	0.01519	0.38920	0.48843	0.07474	0.02896		1
12.1	0.00780	0.04247	0.34660	0.47143	0.11584	0.01586		1
13.1	0.00091	0.00252	0.31322	0.46029	0.15488	0.00459	0.06358	1
14.1	0.00291	0.01240	0.30423	0.45958	0.17288	0.01145	0.03656	1
15.1	0.00624	0.03256	0.28111	0.43988	0.19196	0.02839	0.01987	1

Table 2.3: The power balance for $a = 4.1$, b increasing

b	$\frac{\lvert A_0\rvert^2}{4}$	$\frac{\lvert A_1\rvert^2\eta_1}{2}$	$\frac{\lvert B_0\rvert^2 b}{4a}$	$\frac{\lvert B_1\rvert^2\nu_1 b}{2a}$	$\frac{\lvert B_2\rvert^2\nu_2 b}{2a}$	$\frac{\lvert B_3\rvert^2\nu_3 b}{2a}$	$\frac{\lvert B_4\rvert^2\nu_4 b}{2a}$	Total
5.8			1					1
6.8	0.00216	0.00554	0.84857	0.05705	0.08669			1
7.8	0.00069	0.00186	0.72276	0.16491	0.10978			1
8.8	0.00029	0.00065	0.66636	0.25106	0.08164			1
9.8	0.00159	0.00426	0.58274	0.32884	0.02772	0.05485		1
10.8	0.00061	0.00160	0.52711	0.38887	0.00481	0.07699		1
11.8	0.00037	0.00086	0.49397	0.42716	0.00068	0.07695		1
12.8	0.00158	0.00430	0.44681	0.44389	0.01372	0.04739	0.04231	1
13.8	0.00063	0.00163	0.41384	0.46064	0.03405	0.03487	0.05434	1
14.8	0.00041	0.00097	0.39251	0.47011	0.05624	0.02058	0.05918	1

Table 2.4: The power balance for $a = 5.8$, b increasing

the success of these methods, and the cause of the convergence problem are discussed.

Expressions (2.1.37) and (2.1.38) can be combined to obtain

$$B_n = \frac{2\sin(n\pi r)}{n\pi\nu_n}\left[G - \sum_{m=1}^{\infty} B_m b_{mn}\right], \quad n = 1, 2, 3, \ldots \tag{2.2.1}$$

where $r = \frac{b}{a}$, G is a forcing term given by

$$G = \frac{2b}{a+b} \tag{2.2.2}$$

and

$$b_{mn} = \frac{\sin(m\pi r)}{m\pi r(1+r)} + \frac{2mn^2r^3\sin(m\pi r)}{\pi}\sum_{\ell=1}^{\infty}\frac{\eta_\ell}{(m^2r^2-\ell^2)(n^2r^2-\ell^2)}. \tag{2.2.3}$$

Upon rearranging (2.2.1) it can be seen that

$$\frac{B_n n\pi\nu_n}{2\sin(n\pi r)} + \sum_{m=1}^{\infty} B_m b_{mn} = G, \quad n = 1, 2, 3, \ldots. \tag{2.2.4}$$

When rewritten in matrix form, this becomes

$$\begin{bmatrix} \frac{B_1\pi\nu_1}{2\sin(\pi r)} \\ \frac{2B_2\pi\nu_2}{2\sin(2\pi r)} \\ \frac{3B_3\pi\nu_3}{2\sin(3\pi r)} \\ \vdots \end{bmatrix} + \begin{bmatrix} b_{11} & b_{21} & b_{31} & \cdots \\ b_{12} & b_{22} & b_{32} & \cdots \\ b_{13} & b_{23} & b_{33} & \cdots \\ \vdots & \vdots & \vdots & \ddots \end{bmatrix} \begin{bmatrix} B_1 \\ B_2 \\ B_3 \\ \vdots \end{bmatrix} = \begin{bmatrix} G \\ G \\ G \\ \vdots \end{bmatrix} \tag{2.2.5}$$

which can be easily rearranged to give

$$\begin{bmatrix} b_{11} + \frac{\pi\nu_1}{2\sin(\pi r)} & b_{21} & b_{31} & \cdots \\ b_{12} & b_{22} + \frac{2\pi\nu_2}{2\sin(2\pi r)} & b_{32} & \cdots \\ b_{13} & b_{23} & b_{33} + \frac{3\pi\nu_3}{2\sin(3\pi r)} & \cdots \\ \vdots & \vdots & \vdots & \ddots \end{bmatrix} \begin{bmatrix} B_1 \\ B_2 \\ B_3 \\ \vdots \end{bmatrix} = \begin{bmatrix} G \\ G \\ G \\ \vdots \end{bmatrix}. \tag{2.2.6}$$

Since

$$\nu_n = \left(1 - \frac{n^2\pi^2}{b^2}\right)^{\frac{1}{2}}, \tag{2.2.7}$$

the terms on the diagonal of the matrix grow as $n \to \infty$ which implies that the system is non-convergent and so the matrix cannot be truncated. However, making the substitution

$$B_n = \frac{2}{\pi n \nu_n} \sin(n\pi r)\, D_n \tag{2.2.8}$$

a new system in D_n is found, that being (2.1.43). Now (2.2.1) assumes the form

$$\frac{2\sin(n\pi r)D_n}{n\pi\nu_n} = \frac{2\sin(n\pi r)}{n\pi\nu_n}\left[G - \sum_{m=1}^{\infty} \frac{2\sin(m\pi r)D_m}{m\pi\nu_m} b_{mn}\right] \tag{2.2.9}$$

which reduces to

$$D_n + \sum_{m=1}^{\infty} \frac{2\sin(m\pi r)D_m}{m\pi\nu_m} b_{mn} = G. \tag{2.2.10}$$

Upon writing this in matrix form, the following system is obtained

$$\begin{bmatrix} \frac{2\sin(\pi r)}{\pi\nu_1} b_{11} + 1 & \frac{2\sin(2\pi r)}{2\pi\nu_2} b_{21} & \frac{2\sin(3\pi r)}{3\pi\nu_3} b_{31} & \cdots \\ \frac{2\sin(\pi r)}{\pi\nu_1} b_{12} & \frac{2\sin(2\pi r)}{2\pi\nu_2} b_{22} + 1 & \frac{2\sin(3\pi r)}{3\pi\nu_3} b_{32} & \cdots \\ \frac{2\sin(\pi r)}{\pi\nu_1} b_{13} & \frac{2\sin(2\pi r)}{2\pi\nu_2} b_{23} & \frac{2\sin(3\pi r)}{3\pi\nu_3} b_{33} + 1 & \cdots \\ \vdots & \vdots & \vdots & \ddots \end{bmatrix} \begin{bmatrix} D_1 \\ D_2 \\ D_3 \\ \vdots \end{bmatrix} = \begin{bmatrix} G \\ G \\ G \\ \vdots \end{bmatrix} \tag{2.2.11}$$

The matrix coefficients display one of two types of behaviour. In the case where $m \neq n$ the coefficients tend towards zero as n or m tends to ∞. When $m = n$, the coefficients tend to 1. Thus, letting

$$\frac{2\sin(m\pi r)}{m\pi\nu_m} b_{mn} = d_{mn} \tag{2.2.12}$$

then

$$\begin{bmatrix} d_{11}+1 & d_{21} & d_{31} & \cdots & & & & \\ d_{12} & d_{22}+1 & d_{32} & \cdots & & & & \\ d_{13} & d_{23} & d_{33}+1 & \cdots & & & & \\ \vdots & \vdots & \vdots & \ddots & & & & \\ & & & & 1+\varepsilon_m & \varepsilon_{m+1} & \varepsilon_{m+2} & \cdots \\ & & & & \varepsilon_m & 1+\varepsilon_{m+1} & \varepsilon_{m+2} & \cdots \\ & & & & \varepsilon_m & \varepsilon_{m+1} & 1+\varepsilon_{m+2} & \cdots \\ & & & & \vdots & \vdots & \vdots & \ddots \end{bmatrix} \begin{bmatrix} D_1 \\ D_2 \\ D_3 \\ \vdots \\ D_m \\ D_{m+1} \\ D_{m+2} \\ \vdots \end{bmatrix} = \begin{bmatrix} G \\ G \\ G \\ \vdots \\ G \\ G \\ G \\ \vdots \end{bmatrix} \tag{2.2.13}$$

where $d_{mm} \sim \varepsilon_m \to 0$ as $m \to \infty$.

This system, although an improvement, is still not convergent. However, the right hand side of the equation is constant, unchanging with the value of m and it follows that the individual equations in the system as $m \to \infty$ simply reads as

$$D_m = G, \qquad m \gg 1. \tag{2.2.14}$$

This behaviour is sufficient to ensure that

$$B_n = \frac{2\sin(n\pi r)G}{n\pi\nu_n} \sim \frac{2}{n^2\pi^2}, \quad n \to \infty. \tag{2.2.15}$$

A further modification conducted in (2.1.47) – (2.1.52) gives rise to a convergent system by subtracting out the leading order term of the numerator in the sum in (2.1.45), this yielding

$$\eta_\ell \sim \frac{i\ell\pi}{a} - \frac{ia}{\ell\pi} + O\left(\frac{1}{\ell^3}\right) \tag{2.2.16}$$

and so for the expression summed over ℓ in (2.1.51), the behaviour is

$$\frac{\eta_\ell - \frac{i\ell\pi}{a}}{(m^2r^2-\ell^2)(n^2r^2-\ell^2)} = O\left(\frac{1}{\ell^5}\right), \tag{2.2.17}$$

which gives very rapid convergence. Thus, in this case, the convergence problem can be overcome.

2.3 Sturm-Liouville Theory

Section 2.1 deals with a boundary-value problem for which the solution is available by recourse to standard Fourier analysis. It is desirable, however, to consider a more general problem in which the upper duct surface for $x > 0$ satisfies the impedance (Robin's) condition. The solution method is, in fact, very similar, but separation of variables now yields an eigen-subsystem of Sturm-Liouville type. Before this problem is discussed in detail it is instructive to summarise here the salient features of Sturm-Liouville theory. The Strum-Liouville theory can be found in greater detail from a number of texts, for example Churchill & Brown (1982).

A simple generalised problem is considered, involving a duct occupying the region $a \leq y \leq b$ with the surfaces located at $y = a$ and $y = b$ having impedance (Robin's) boundary conditions. The boundary-value problem has a general second-order governing equation, that is

$$\phi_{xx} + \frac{r}{t}\phi_{yy} + \frac{r'}{t}\phi_y + \frac{s}{t}\phi = 0 \tag{2.3.1}$$

where $r(y), r'(y), s(y)$ and $t(y)$ are real-valued continuous functions of y, $r'(y)$ is the first derivative of $r(y)$ with respect to y, $r(y) > 0$ when $a < y < b$ and $t(y) \neq 0$ for all y. The two boundary conditions are

$$a_1\phi(x,a) + a_2\phi_y(x,a) = 0, \tag{2.3.2}$$

$$b_1\phi(x,b) + b_2\phi_y(x,b) = 0, \tag{2.3.3}$$

where a_1 and a_2 are constant and never both equal to zero and likewise with b_1 and b_2. The physical configuration for such a problem is shown in Figure 2.9

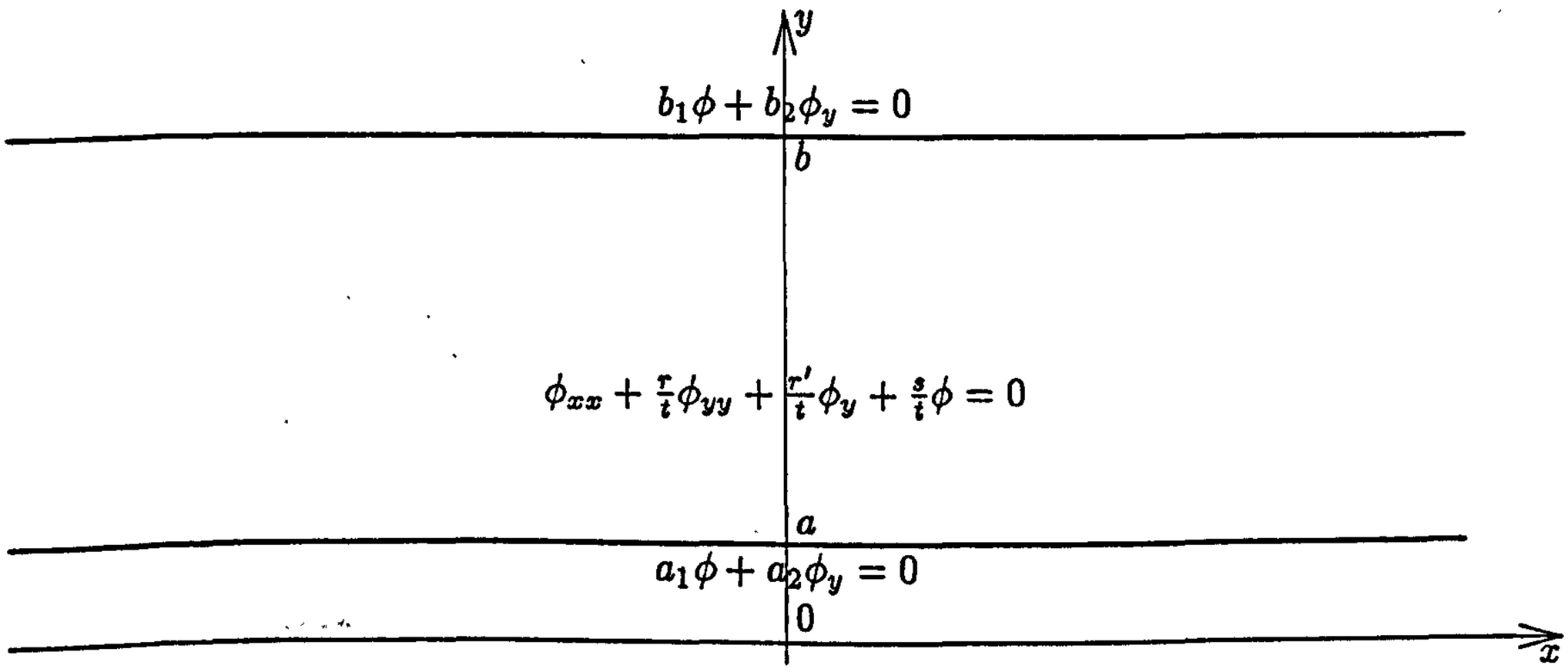

Figure 2.9: Physical configuration for the problem of Section 2.3

Separation of variables is used on the system and so, in the usual manner

$$\phi = X(x)Y(y). \tag{2.3.4}$$

When this is substituted into the governing equation (2.3.1) it can be seen that

$$X''Y + \frac{rY''X}{t} + \frac{r'Y'X}{t} + \frac{sXY}{t} = 0. \tag{2.3.5}$$

This can be rearranged and the separation variable, λ, introduced so that

$$\frac{r'Y' + rY''}{Yt} + \frac{s}{t} = \frac{X''}{X} = -\lambda. \tag{2.3.6}$$

When the terms involving the eigenfunction Y are considered alone, this can be rearranged to give

$$(rY')' + (s + \lambda t)Y = 0 \tag{2.3.7}$$

whilst the boundary conditions, expressed in terms of Y become

$$a_1 Y(a) + a_2 Y'(a) = 0, \tag{2.3.8}$$

$$b_1 Y(b) + b_2 Y'(b) = 0. \tag{2.3.9}$$

Take two distinct eigenvalues of this system, λ_m and λ_n and the eigenfunctions associated with these, Y_m and Y_n. Each pair must satisfy (2.3.7) and so

$$(rY_m')' + sY_m = -\lambda_m t Y_m, \tag{2.3.10}$$

$$(rY_n')' + sY_n = -\lambda_n t Y_n. \tag{2.3.11}$$

On multiplying (2.3.10) by Y_n and (2.3.11) by Y_m and subtracting one from the other, the resulting expression is

$$\begin{aligned}(\lambda_n - \lambda_m)\, t Y_m Y_n &= (rY_m')' Y_n - (rY_n')' Y_m \\ &= \frac{d}{dy}\left[r\left(Y_m' Y_n - Y_n' Y_m\right)\right]. \end{aligned} \tag{2.3.12}$$

Hence,

$$(\lambda_n - \lambda_m) \int_a^b t\, Y_m Y_n\, dy = [r(y)\Delta(y)]_a^b \tag{2.3.13}$$

where

$$\Delta(y) = \begin{vmatrix} Y_m' & Y_m \\ Y_n' & Y_n \end{vmatrix}. \tag{2.3.14}$$

However, since (2.3.8) must hold for both Y_m and Y_n then $\Delta(a) = 0$ and likewise, (2.3.9) implies that $\Delta(b) = 0$ also. Thus

$$(\lambda_n - \lambda_m) \int_a^b t\, Y_m Y_n\, dy = 0. \tag{2.3.15}$$

Since λ_m and λ_n are distinct, non-equal eigenvalues, then the orthogonality property which is sought is found to be

$$\int_a^b t Y_m Y_n\, dy = 0, \quad m \neq n. \tag{2.3.16}$$

A boundary-value problem of the form described by (2.3.7) – (2.3.9) may be referred to as being Sturm-Liouville in type and has associated with it an orthogonality relation given in (2.3.16).

As an illustration of the application of Sturm-Liouville theory, an example is considered. The boundary-value problem is such that the governing equation, given in general form by (2.3.7), reduces to

$$Y''(y) + \lambda Y(y) = 0, \tag{2.3.17}$$

whilst the boundary conditions are stated to be

$$Y'(0) = 0, \tag{2.3.18}$$

$$hY(a) + Y'(a) = 0, \tag{2.3.19}$$

where h is a positive constant. Thus, the boundary at $y = 0$ is of Neumann type whilst that at $y = a$ is an impedance (Robin's) condition. The problem as described in (2.3.17) - (2.3.19) has three possible distinguishing cases; those are the cases where $\lambda = 0$, $\lambda > 0$ and $\lambda < 0$; each will be considered.

In the case where $\lambda = 0$, the solution is found trivially to be that the eigenfunction $Y(y) \equiv 0$, and thus zero is not an eigenvalue.

When $\lambda > 0$, then it is taken that $\lambda = \alpha^2, \alpha > 0$ and so the general solution of the differential equation (2.3.17), taken with the first boundary condition, gives

$$Y(y) = A\cos(\alpha y). \tag{2.3.20}$$

When the second boundary condition is imposed, in order for A to be non-zero, α must be a root of

$$h\cos(\alpha a) - \alpha\sin(\alpha a) = 0, \tag{2.3.21}$$

which can be rearranged and expressed as

$$\tan(\alpha a) = \frac{h}{\alpha}. \tag{2.3.22}$$

It is clear that this has an infinite number of consecutive positive roots, and these roots are given in Abramowitz and Stegun (1964). The corresponding eigenvalues are given as $\lambda_n = \alpha_n^2, n = 0, 1, 2, \ldots$, and eigenfunctions of $Y_n(y) = \cos(\alpha_n y)$.

When $\lambda < 0$, then take $\lambda = -\beta^2, \beta > 0$. By following similar steps as for the case where $\lambda > 0$ it is easily shown that, for this case

$$Y(y) = B\cosh(\beta y) \tag{2.3.23}$$

and so to prevent B from being non-zero, β must satisfy the equation

$$\tanh(\beta a) = -\frac{h}{\beta}. \tag{2.3.24}$$

This equation has no real roots however, and so the complete solution of this Sturm-Liouville problem is

$$Y_n(y) = A_n\cos(\alpha_n y) \tag{2.3.25}$$

where $\alpha_n^2 = \lambda_n$ and $\alpha_n, n = 0, 1, 2, \ldots$ are the roots of (2.3.22).

Now consider the orthogonality relation, defined generally in (2.3.16). That is, in this case

$$\int_0^a \cos(\alpha_m y)\cos(\alpha_n y)dy = \begin{cases} 0, & m \neq n \\ C_n, & m = n \end{cases}. \tag{2.3.26}$$

In the case where $m = n$ then the integral becomes

$$\int_0^a \cos^2(\alpha_n y)dy = \frac{1}{2}\left[a + \frac{\sin(2\alpha_n a)}{2\alpha_n}\right]. \tag{2.3.27}$$

However, using (2.3.22), this can be rewritten as

$$\begin{aligned} \int_0^a \cos^2(\alpha_n y)dy &= \frac{ah + \sin^2(\alpha_n a)}{2h} \\ &= C_n. \end{aligned} \tag{2.3.28}$$

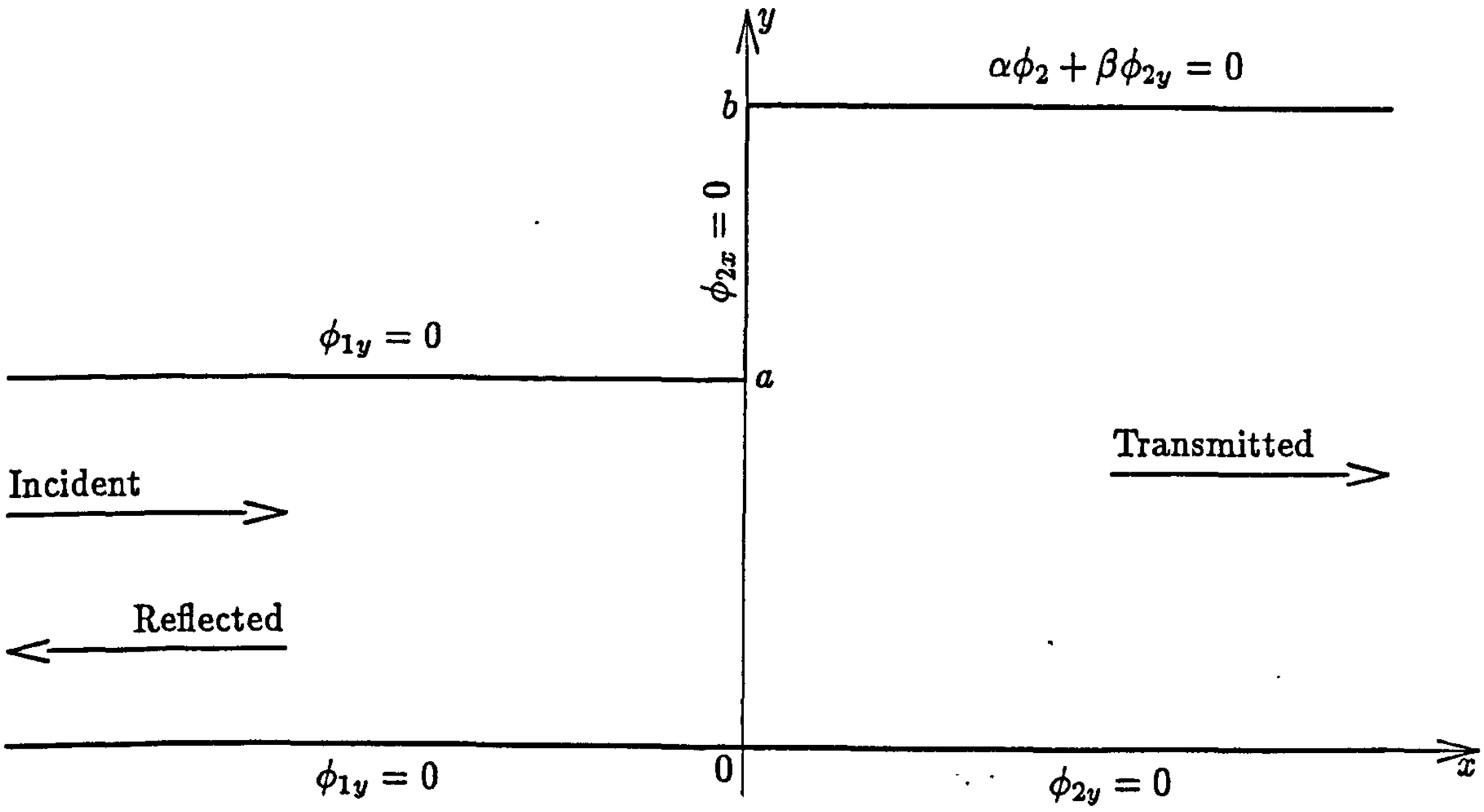

Figure 2.10: Physical configuration for the problem of Section 2.4

2.4 Reflection and transmission at the junction of two ducts of differing height and wall conditions

In this section, the theory of Section 2.3 is employed to solve a more general boundary-value problem. The geometric configuration of the problem is identical to that of the problem encountered in Section 2.1, in that it comprises two ducts of different heights, meeting at an interface, the first duct occupying the region $0 \leq \bar{y} \leq \bar{a}$, $\bar{x} < 0$ and the second, the region $0 \leq \bar{y} \leq \bar{b}$, $\bar{x} > 0$ with $\bar{b} \geq \bar{a} > 0$. Also the duct to the left of the matching interface, $\bar{x} = 0$ is acoustically rigid, but the upper surface of the duct to the right now has a boundary described by Robin's condition. The vertical surface between the ducts, $\bar{x} = 0$, $\bar{a} < \bar{y} \leq \bar{b}$ is acoustically hard as in the first case, see figure 2.10. All other conditions are as they were for the case in Section 2.1, as is the incident field.

The same notation and non-dimensionalisation as in Section 2.1 is used again here, and so the problem is reduced to solving Helmholtz' equation subject to specified boundary conditions. That is

$$\left(\nabla^2 + 1\right)\phi = 0, \qquad -\infty < x < \infty. \tag{2.4.1}$$

The boundary conditions on the duct on the left hand side of the matching interface are

$$\frac{\partial \phi_1}{\partial y} = 0, \qquad y = 0, \tag{2.4.2}$$

$$\frac{\partial \phi_1}{\partial y} = 0, \qquad y = a \tag{2.4.3}$$

and on the right hand side are

$$\frac{\partial \phi_2}{\partial y} = 0, \qquad y = 0, \tag{2.4.4}$$

$$\alpha\phi_2 + \beta\frac{\partial\phi_2}{\partial y} = 0, \qquad y = b. \tag{2.4.5}$$

The problem here is more general because of the nature of the upper boundary condition applied to the duct to the right of the interface, $x = 0$. By adjusting the values of α and β appropriately, the boundary condition becomes Neumann, Dirichlet or Robin's in form. For example, the problem considered in Section 2.1 is equivalent to the case where $\alpha = 0$ and $\beta > 0$.

Fluid pressure and normal velocity are again continuous across the matching interface and the surface $a < y \leq b, x = 0$ is rigid so that conditions (2.1.12) and (2.1.13) still hold, that is

$$\phi_1 = \phi_2, \qquad x = 0, \qquad 0 \leq y \leq a \tag{2.4.6}$$

and

$$\frac{\partial\phi_2}{\partial x} = \begin{cases} \frac{\partial\phi_1}{\partial x}, & 0 \leq y \leq a, \quad x = 0 \\ 0, & a < y \leq b, \quad x = 0 \end{cases} . \tag{2.4.7}$$

In this problem, as in Section 2.1, ϕ_1 comprises the incident wave and a reflected field, such that

$$\phi_1 = e^{ix} + \phi_{ref} \tag{2.4.8}$$

where ϕ_{ref} comprises an infinite sum of reflected duct modes. Thus

$$\phi_{ref} = \sum_{n=0}^{\infty} A_n\phi_{1n}, \tag{2.4.9}$$

where $\phi_{1n}, n = 0, 1, 2, \ldots$ is an eigenmode for the problem. Separation of variables is used and the separation variable, η, is chosen to make X_1 sinusoidal. Thus

$$X_1(x) = A_1e^{i\eta x} + B_1e^{-i\eta x} \tag{2.4.10}$$

$$Y_1(y) = C_1\cosh(py) + D_1\sinh(py) \tag{2.4.11}$$

where A_1, B_1, C_1 and D_1 are arbitrary constants and

$$p = (\eta^2 - 1)^{\frac{1}{2}}. \tag{2.4.12}$$

Since the reflected field will only be made up of waves travelling in the negative x direction, $A_1 = 0$ and since the lower surface of the duct on the left hand side of $x = 0$ is acoustically hard, $D_1 = 0$. Further, the acoustically hard property of the upper surface of this duct implies that $p_n = \frac{in\pi}{a}$ and hence the eigenmodes are given by

$$\phi_{1n} = \cos\left(\frac{n\pi y}{a}\right)e^{-i\eta_n x} \tag{2.4.13}$$

where, for convenience, the arbitrary constants are omitted and $\eta_n = (1 - \frac{n^2\pi^2}{a^2})^{1/2}$. It follows that

$$\phi_1 = e^{ix} + \frac{A_0}{2}e^{-ix} + \sum_{n=1}^{\infty} A_n\cos\left(\frac{n\pi y}{a}\right)e^{-i\eta_n x} \tag{2.4.14}$$

where the coefficients, A_n, are the complex amplitudes of each duct mode, ϕ_{1n}. Again here the $n = 0$ term is given coefficient $A_0/2$ to create a Fourier cosine series.

The potential, ϕ_2 is made up of purely transmitted waves and so using separation of variables as in Section 2.1

$$X_2(x) = A_2 e^{i\nu x} + B_2 e^{-i\nu x} \tag{2.4.15}$$

$$Y_2(y) = C_2 \cosh(qy) + D_2 \sinh(qy) \tag{2.4.16}$$

where A_2, B_2, C_2 and D_2 are arbitrary constants and

$$q = (\nu^2 - 1)^{\frac{1}{2}}. \tag{2.4.17}$$

Transmitted waves travel only in the positive x direction, so $B_2 = 0$ and since the lower surface of this duct is acoustically hard, $D_2 = 0$ also, so

$$\phi_{2n} = \cosh(q_n y) e^{i\nu_n x} \tag{2.4.18}$$

where, for convenience the arbitrary constants are omitted, $\nu_n = (q_n^2 + 1)^{1/2}$ and $q_n, n = 0, 1, 2, \ldots, \infty$ are the roots of the dispersion relation obtained on substituting (2.4.18) into (2.4.5), that is

$$\alpha \cosh(q_n b) + \beta q_n \sinh(q_n b) = 0 \tag{2.4.19}$$

and so

$$\phi_2 = \sum_{n=0}^{\infty} B_n \cosh(q_n y) e^{i\nu_n x} \tag{2.4.20}$$

where the coefficients, B_n are the complex amplitudes of each duct mode ϕ_{2n}.

Equations (2.4.14) and (2.4.20) are a Fourier cosine series and a Sturm-Liouville series representation for ϕ_1 and ϕ_2 repectively. The next step is again to substitute these into the conditions at the matching interface, $x = 0, 0 \le y \le b$. Continuity of fluid pressure is expressed by (2.4.6) and gives rise to

$$\frac{2 + A_0}{2} + \sum_{\ell=1}^{\infty} A_\ell \cos\left(\frac{\ell \pi y}{a}\right) = \sum_{m=0}^{\infty} B_m \cosh(q_m y), \quad 0 \le y \le a. \tag{2.4.21}$$

As before, the left hand side of this expression is a Fourier cosine series, so the standard techniques can be applied to find expressions for $A_\ell, \ell = 0, 1, 2, \ldots, \infty$. Thus, for $\ell = 0$

$$\begin{aligned} 2 + A_0 &= \frac{2}{a} \sum_{m=0}^{\infty} B_m \int_0^a \cosh(q_m y) dy \\ &= \frac{2}{a} \sum_{m=0}^{\infty} \frac{B_m \sinh(q_m y)}{q_m} \end{aligned} \tag{2.4.22}$$

and, for $\ell = 1, 2, 3, \ldots$

$$\begin{aligned} A_\ell &= \frac{2}{a} \sum_{m=0}^{\infty} B_m \int_0^a \cosh(q_m y) \cos\left(\frac{\ell \pi y}{a}\right) dy \\ &= \frac{2}{a} \sum_{m=0}^{\infty} B_m R_{\ell m} \end{aligned} \tag{2.4.23}$$

where

$$R_{\ell m} = \int_0^a \cosh(q_m y)\cos\left(\frac{\ell\pi y}{a}\right) dy = \frac{(-1)^\ell q_m \sinh(q_m a)}{q_m^2 + \frac{\ell^2\pi^2}{a^2}}. \tag{2.4.24}$$

These two expressions can be combined to give a single expression, that being

$$A_\ell = -2\delta_{0\ell} + \frac{2}{a}\sum_{m=0}^{\infty} B_m R_{\ell m}, \quad \ell = 0, 1, 2, \ldots, \infty \tag{2.4.25}$$

where $\delta_{\ell m}$ is the Kronecker delta, defined by

$$\delta_{\ell m} = \begin{cases} 1, & \ell = m \\ 0, & \ell \neq m \end{cases}. \tag{2.4.26}$$

The second matching condition, (2.4.7) states that normal fluid velocity is also continuous across the interface and so, applying the expressions gained for ϕ_1 and ϕ_2 yields

$$\sum_{n=0}^{\infty} B_n \nu_n \cosh(q_n y) = \begin{cases} \frac{2 - A_0}{2} - \sum_{\ell=1}^{\infty} A_\ell \eta_\ell \cos\left(\frac{\ell\pi y}{a}\right), & 0 \leq y \leq a \\ 0, & a < y \leq b \end{cases}. \tag{2.4.27}$$

Here, the left hand side is not a standard Fourier series and the right hand side is defined piecewise on $0 \leq y \leq b$. Thus, the standard Fourier series approach cannot be used to isolate either A_n or $B_n, n = 0, 1, 2, \ldots$. However, the Sturm Liouville theory is applicable and so multiplying (2.4.27) through by $\cosh(q_m y)$ and integrating from 0 to b gives

$$\sum_{n=0}^{\infty} B_n \nu_n \int_0^b \cosh(q_n y)\cosh(q_m y)\, dy = \frac{2 - A_0}{2}\int_0^a \cosh(q_m y)\, dy - \sum_{\ell=1}^{\infty} A_\ell \eta_\ell \int_0^a \cos\left(\frac{\ell\pi y}{a}\right)\cosh(q_m y)\, dy \tag{2.4.28}$$

From (2.3.22) the appropriate orthogonality relation (since, for this problem, $t(y) = 1$) is

$$\int_0^b \cosh(q_m y)\cosh(q_n y)\, dy = \begin{cases} C_n, & n = m \\ 0, & n \neq m \end{cases} \tag{2.4.29}$$

where

$$C_n = \frac{\sinh(2q_n b) + 2q_n b}{4q_n}. \tag{2.4.30}$$

On applying this result to (2.4.28), the coefficients $B_n, n = 0, 1, 2, \ldots$ are expressed in terms of A_ℓ by

$$\begin{aligned} B_n \nu_n C_n &= \frac{2 - A_0}{2}\int_0^a \cosh(q_n y)\, dy - \sum_{\ell=1}^{\infty} A_\ell \eta_\ell \int_0^a \cos\left(\frac{\ell\pi y}{a}\right)\cosh(q_n y)\, dy \\ &= \left(\frac{2 - A_0}{2}\right) R_{0n} - \sum_{\ell=1}^{\infty} A_\ell \eta_\ell R_{\ell n}. \end{aligned} \tag{2.4.31}$$

Now, having gained expressions for $A_\ell, \ell = 0, 1, 2, \ldots, \infty$ in terms of an infinite summation of $B_m, m = 0, 1, 2, \ldots \infty$ and vice versa, it is possible to combine these expressions to form an infinite system for either purely A_n or $B_n, n = 0, 1, 2, \ldots$. As in Section 2.1, a system for B_n is formed by substituting (2.4.25) into (2.4.31), that is

$$B_n = \frac{1}{\nu_n C_n}\left[2R_{0n} - \frac{R_{0n}}{a}\sum_{m=0}^{\infty} B_m R_{0m} - \frac{2}{a}\sum_{\ell=1}^{\infty}\sum_{m=0}^{\infty}\eta_\ell B_m R_{\ell m} R_{\ell n}\right] \tag{2.4.32}$$

This final solution throws up what appears to be a problem. The quantity $R_{\ell m}R_{\ell n}$ appears in the last term in the above expression and, from (2.4.24), it is clear that there is a singularity for the case $q_m^2 + \frac{\ell^2\pi^2}{a^2} = 0$ or $q_n^2 + \frac{\ell^2\pi^2}{a^2} = 0$. Consider simply $R_{\ell m}$ in the case where $q_m = \frac{i\ell\pi}{a}$. By applying L'Hopital's rule to $R_{\ell m}$ it can be seen that

$$\lim_{q_m \to \frac{i\ell\pi}{a}} R_{\ell m} = \frac{(-1)^\ell\left[\sinh(q_m a) + q_m a\cosh(q_m a)\right]}{2q_m}. \tag{2.4.33}$$

However, since $q_m = \frac{i\ell\pi}{a}$, then

$$\begin{aligned}\lim_{q_m \to \frac{i\ell\pi}{a}} R_{\ell m} &= \frac{(-1)^\ell\left[\sin(\ell\pi) + i\ell\pi\cos(\ell\pi)\right]}{\frac{2i\ell\pi}{a}} \\ &= \frac{a}{2}\end{aligned} \tag{2.4.34}$$

and so in this limit, $R_{\ell m}$ is defined by (2.4.34), likewise $R_{\ell n}$.

The *Mathematica* code used to calculate the numerical solutions given later in this section is given in Appendix A.2

As mentioned previously, the Robin's boundary condition given in (2.4.5) for the surface occupying the region $y = b, x > 0$, may have its behaviour altered by appropriate selection of α and β. Specifically, it can be made to behave as a Dirichlet boundary by taking $\beta = 0$ or as a Neumann condition by taking $\alpha = 0$. The second of these cases is in fact the problem where all surfaces are acoustically hard, which was examined in Section 2.1, and so requires no further consideration. The case where the upper boundary of the right hand duct assumes Dirichlet form is discussed as this particular problem will prove useful in later sections for comparison of results.

In this specific case ($\beta = 0$), condition (2.4.5) now becomes

$$\phi_2 = 0, \qquad y = b. \tag{2.4.35}$$

It follows that $q_n, n = 0, 1, 2, \ldots$ are now the roots of

$$\cosh(q_n b) = 0 \tag{2.4.36}$$

and so are simply found to be $q_n = \frac{i(2n+1)\pi}{2b}, n = 0, 1, 2, \ldots$. Thus, for this specific case

$$\phi_2 = \sum_{n=0}^{\infty} B_n \cos\left[\frac{(2n+1)\pi y}{2b}\right] e^{i\nu_n x} \tag{2.4.37}$$

where

$$\nu_n = \left(1 - \frac{(2n+1)^2\pi^2}{4b^2}\right)^{\frac{1}{2}} \tag{2.4.38}$$

The method from here on in follows the same format as for the general condition, except that now, $R_{\ell m}$ and C_n have the forms

$$R_{\ell m} = \frac{2b(-1)^\ell \sin\left[\frac{(2n+1)\pi a}{2b}\right]}{(2n+1)\left[1 - \frac{4\ell^2 b^2}{(2n+1)^2 a^2}\right]} \tag{2.4.39}$$

and

$$C_n = \frac{b}{2}\left[\frac{(-1)^n b}{\pi(2n+1)} + 1\right]. \tag{2.4.40}$$

When these new definitions are applied to (2.4.32), the appropriate system for this special case is obtained. Numerical solution is straightforward and highly accurate results are found with rapid computation. There is no problem with convergence in this case.

2.4.1 Results

The first two graphs show the effect that varying the value of α and β has on the moduli of the fundamental reflected and transmitted modes. In figure 2.11 the fundamental reflected mode is shown for $\alpha/\beta = 0.1, 1$ and 10. It can be seen that in the case where $\alpha/\beta = 0.1$ the graph follows a very similar pattern to that of the graphs showing fundamental reflected modes in Section 2.1, that is starting very close to zero and have peak values at $b \approx n\pi$, $n = 1, 2, 3, \ldots$. This is because β is much larger than α and so the boundary condition (2.4.5) is behaving in a similar way to

$$\frac{\partial \phi_2}{\partial y} = 0, \tag{2.4.41}$$

as was the case in Section 2.1.

As the value of α/β increases, the peaks on the graph move to the right. This shifting is caused by the roots of (2.4.5) moving due to the change from β being greater than α, to the case where $\beta \approx \alpha$ and on to where α is much greater than β. Now, in this case, (2.4.5) is behaving more and more like

$$\phi_2 = 0, \quad y = b, \tag{2.4.42}$$

and hence the roots of (2.4.5) are now located at $y \approx \frac{(2n+1)\pi}{2b}$, $n = 1, 2, 3, \ldots$.

In a very similar way, the characteristic troughs in the graphs showing fundamental transmitted modes, move from occurring at $b \approx n\pi$, $n = 1, 2, 3, \ldots$ when $\beta \gg \alpha$ to $b \approx \frac{(2n+1)\pi}{2}$, $n = 1, 2, 3, \ldots$ when $\beta \ll \alpha$.

Figures 2.13 and 2.14 show very similar characteristics, with their peaks and troughs respectively moving to the right of the graph as α/β increases.

This movement of the peaks on the graph for the modulus of the fundamental reflected mode and of the troughs on the graph for the modulus of the fundamental transmitted

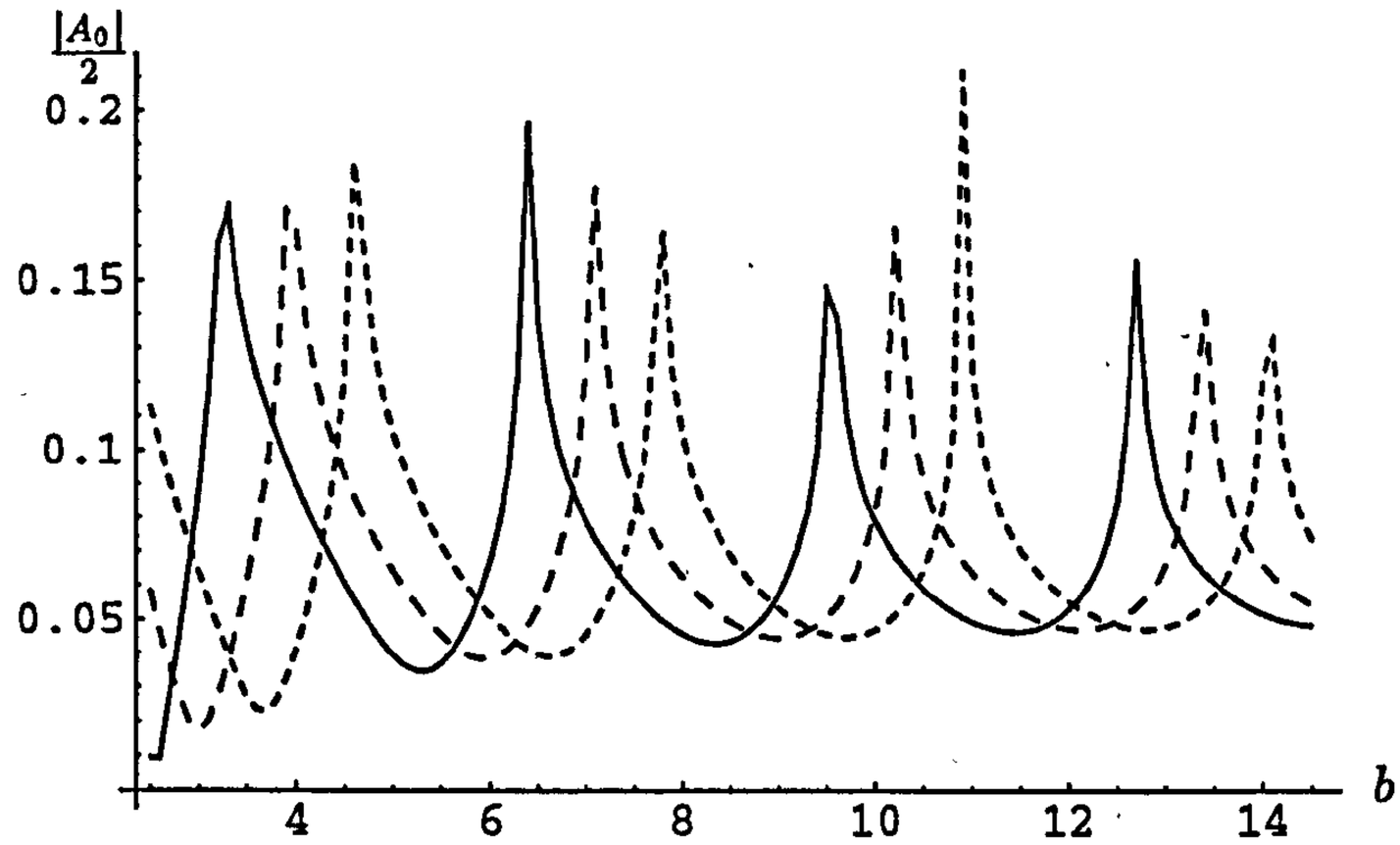

Figure 2.11: Plot of the modulus of the reflection coefficient of the fundamental mode for the hard/impedance problem with $a = 2.5$ and varying b. The case where $\alpha/\beta = 10$ is the thin dotted line, $\alpha/\beta = 1$ is the thick dotted line and $\alpha/\beta = 0.1$ is the solid line.

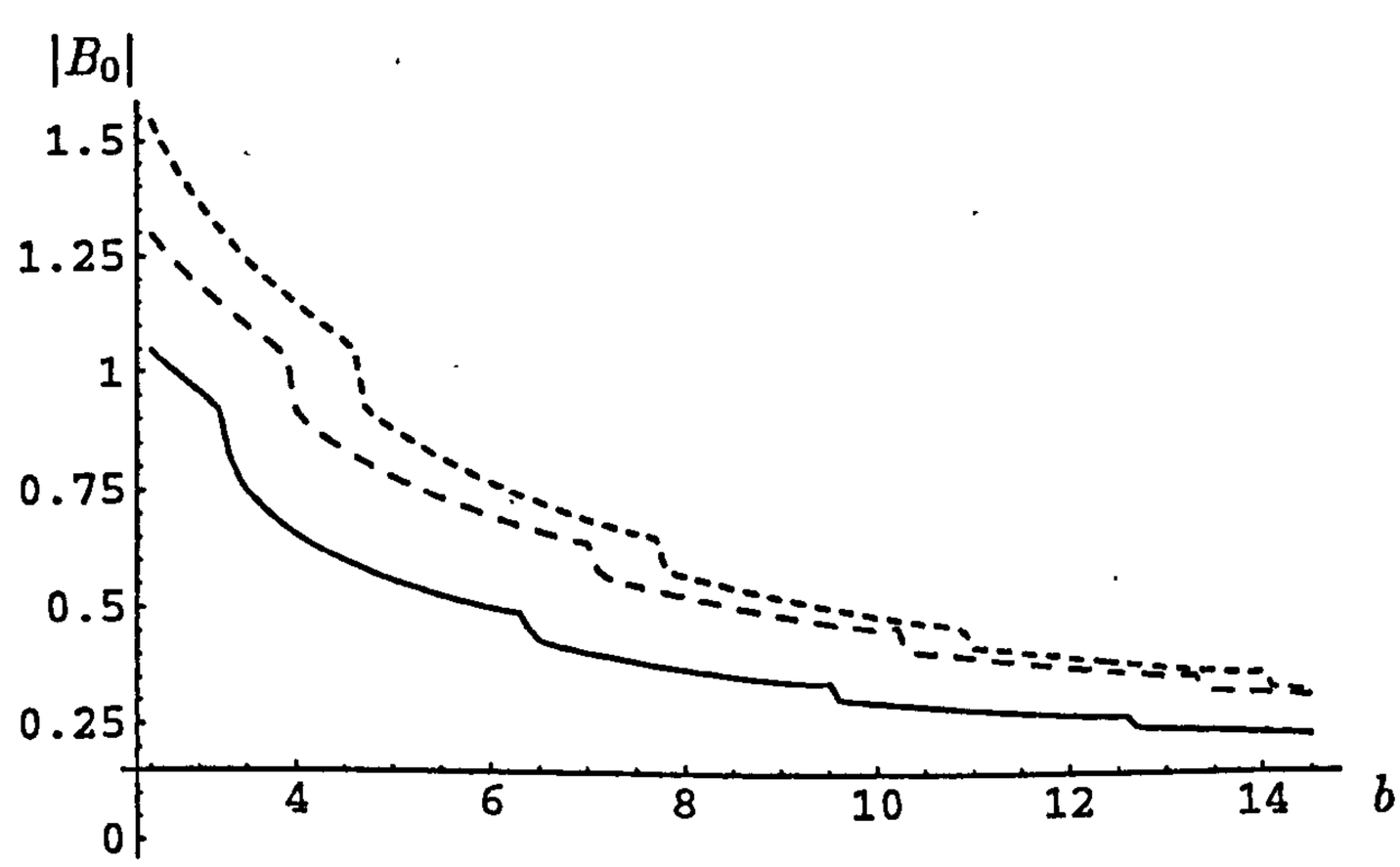

Figure 2.12: Plot of the modulus of the transmitted coefficient of the fundamental mode for the hard/impedance problem with $a = 2.5$ and varying b. The case where $\alpha/\beta = 10$ is the thin dotted line, $\alpha/\beta = 1$ is the thick dotted line and $\alpha/\beta = 0.1$ is the solid line.

mode can be easily explained. At the end of Section 2.1, analysis was conducted of the total power in the system. This analysis took the form of a power balance, where it was stated and confirmed that the total power introduced to the duct had to be equal to the total of that reflected and transmitted. It was further shown that although the reflected and transmitted power took the form of infinite sums, many of the terms in these sums

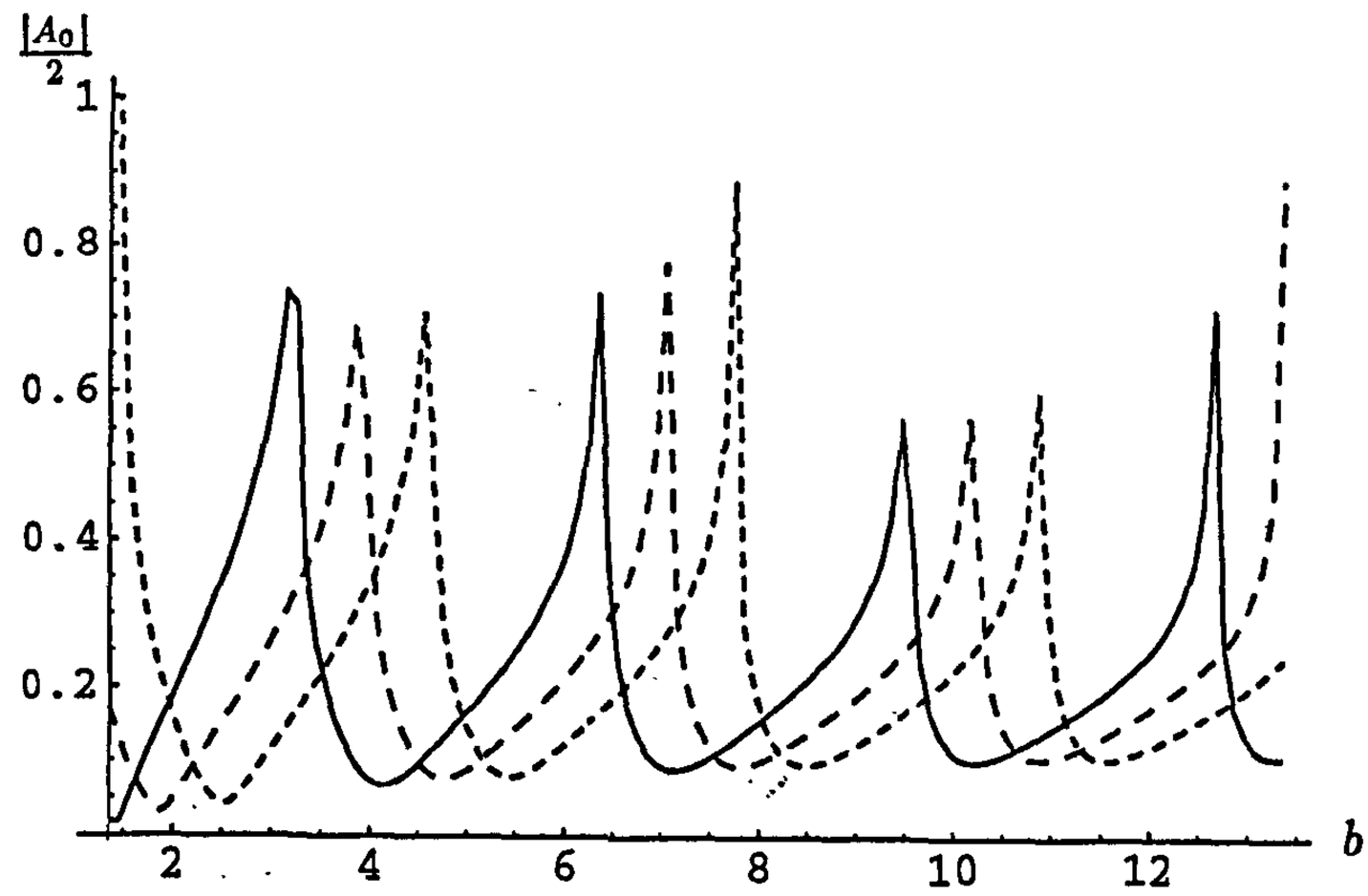

Figure 2.13: Plot of the modulus of the reflection coefficient of the fundamental mode for the hard/impedance problem with $a = 1.35$ and varying b. The case where $\alpha/\beta = 10$ is the thin dotted line, $\alpha/\beta = 1$ is the thick dotted line and $\alpha/\beta = 0.1$ is the solid line.

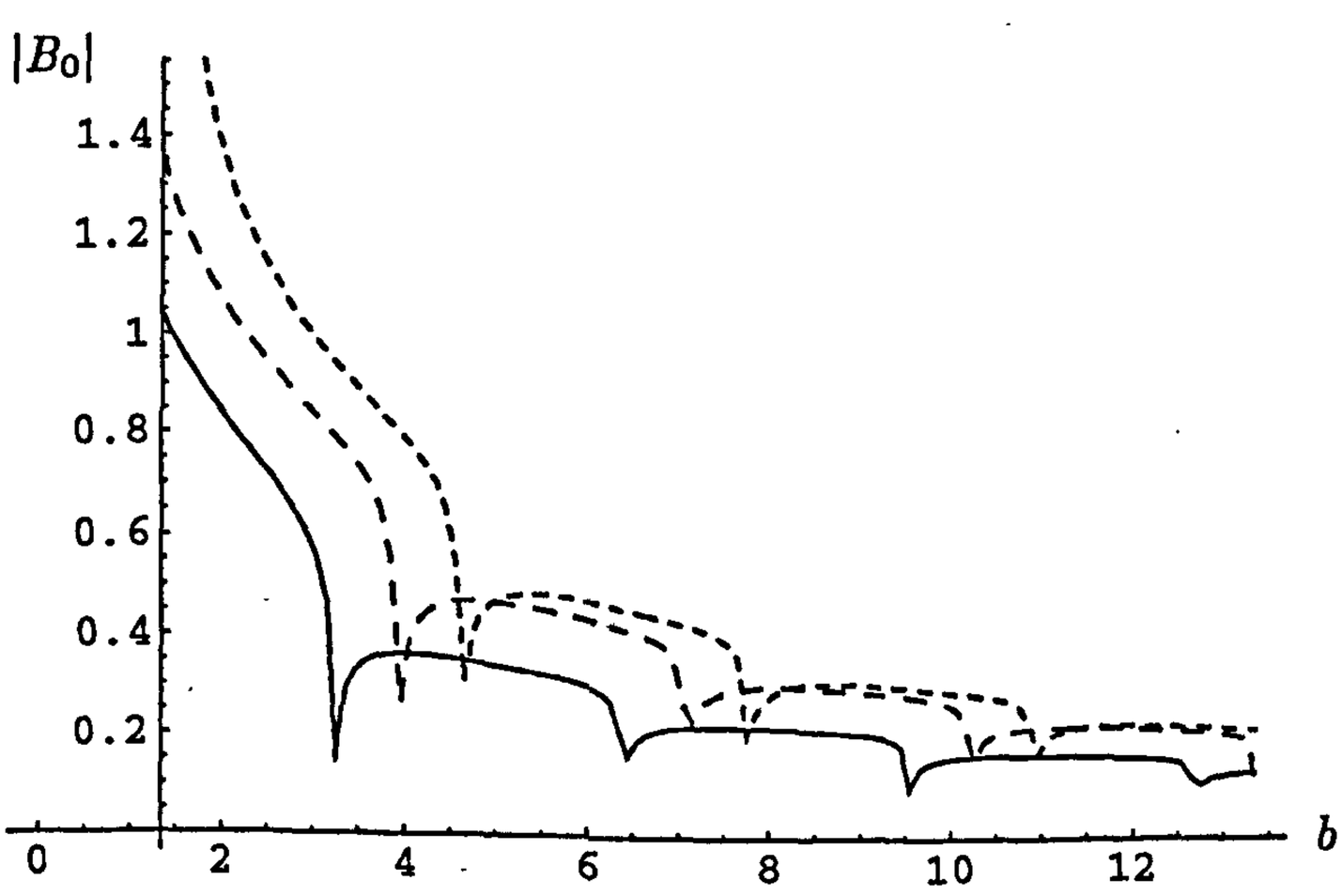

Figure 2.14: Plot of the modulus of the transmitted coefficient of the fundamental mode for the hard/impedance problem with $a = 1.35$ and varying b. The case where $\alpha/\beta = 10$ is the thin dotted line, $\alpha/\beta = 1$ is the thick dotted line and $\alpha/\beta = 0.1$ is the solid line..

had no effect in the far field. Only those eigenmodes associated with real positive roots of the dispersion relationship are significant as was explained in section 2.1. It was also noted that as the value of a (or b, dependent upon which amplitude is being considered) increases, more roots became real and 'turn on' new modes in the far field.

The same principles apply here: as the value of b increases, so the number of roots

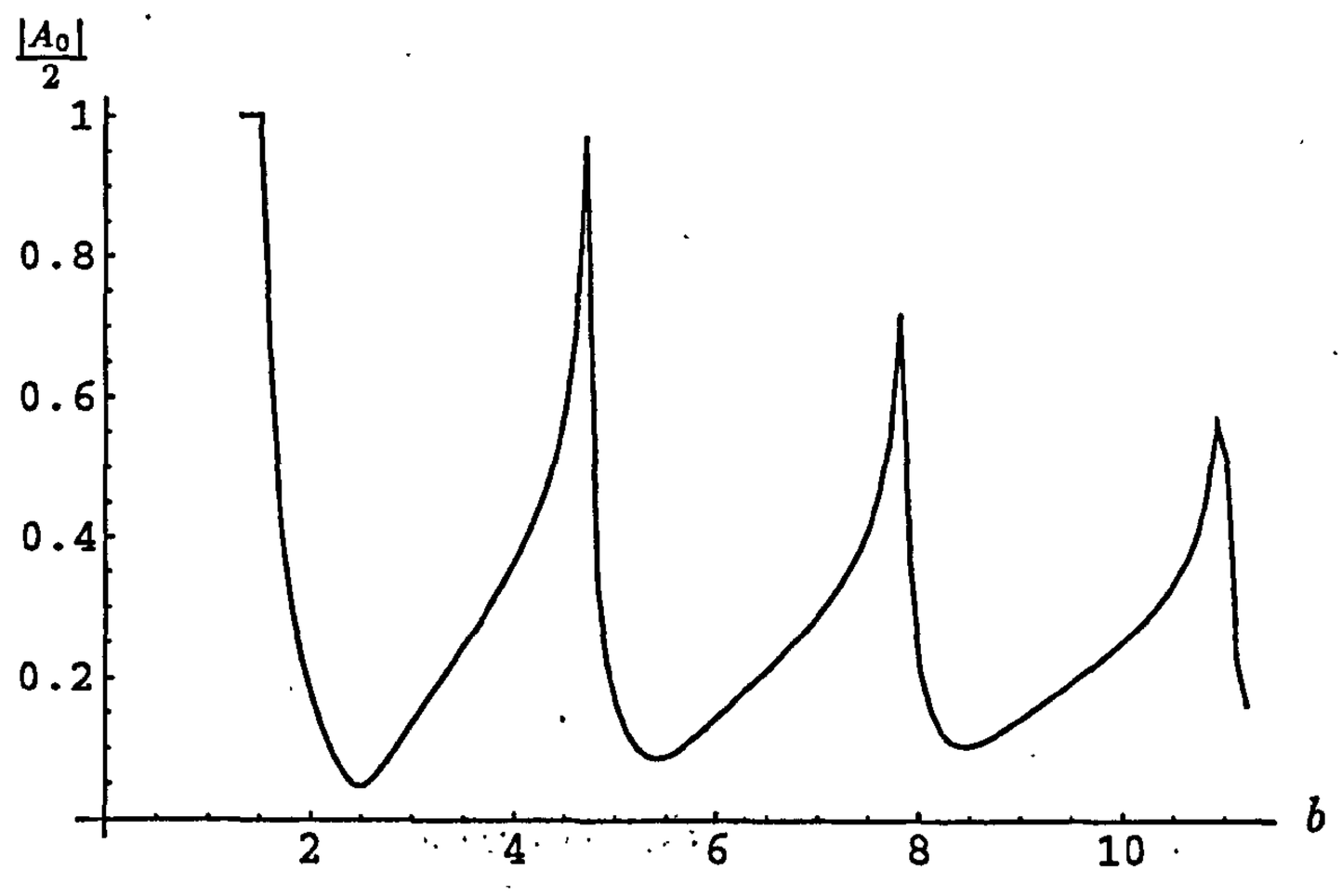

Figure 2.15: Plot of the modulus of the reflection coefficient of the fundamental mode for the hard/soft problem with $a = 1.211$ and varying b.

of (2.4.19) that are real (and thus the number of transmitted modes that are significant) increases. However, for this problem, the location of the roots depends upon the ratio of α to β. When $\beta \gg \alpha$, the problem is very similar to that considered in Section 2.1 and so the peaks on the graph of the fundamental reflected mode and the troughs on the graph of the fundamental transmitted mode occur very close to where they were located in that initial problem. As β becomes closer in value to α the peaks and troughs move across the graph. Once $\alpha \ll \beta$ the location of the peaks and troughs tends towards $\frac{(2n+1)\pi}{2}$, $n = 1, 2, 3, \ldots$.

The remaining four graphs show results for the case where $\beta = 0$, that is the special case described in (2.4.35) – (2.4.40). As stated, the roots of the boundary condition given in (2.4.36) are $q_n = \frac{i(2n+1)\pi}{2b}, n = 0, 1, 2, \ldots$. It is easy to see from the graphs that new transmitted modes are turned on when $b = \frac{(2n+1)\pi}{2}$, $n = 1, 2, 3, \ldots$.

These last four graphs will be used later in sections 3.3 and 4.3 for comparison with results from subsequent problems.

2.5 The failure of the Sturm-Liouville theory for problems of ducts with a membrane surface

In this section, the techniques applied to the two problems tackled so far will be used in an attempt to solve a problem of identical geometry but where one surface is modelled by a boundary condition that contains second-order derivatives. As in the cases of the previous problems, the duct occupying the region $0 \leq \bar{y} \leq \bar{a}$, $\bar{x} < 0$ and $0 \leq \bar{y} \leq \bar{b}$, $\bar{x} > 0$ with $\bar{b} \geq \bar{a} > 0$, where $(\bar{x}, \bar{y})$ are the usual cartesian coordinates is closed so that the

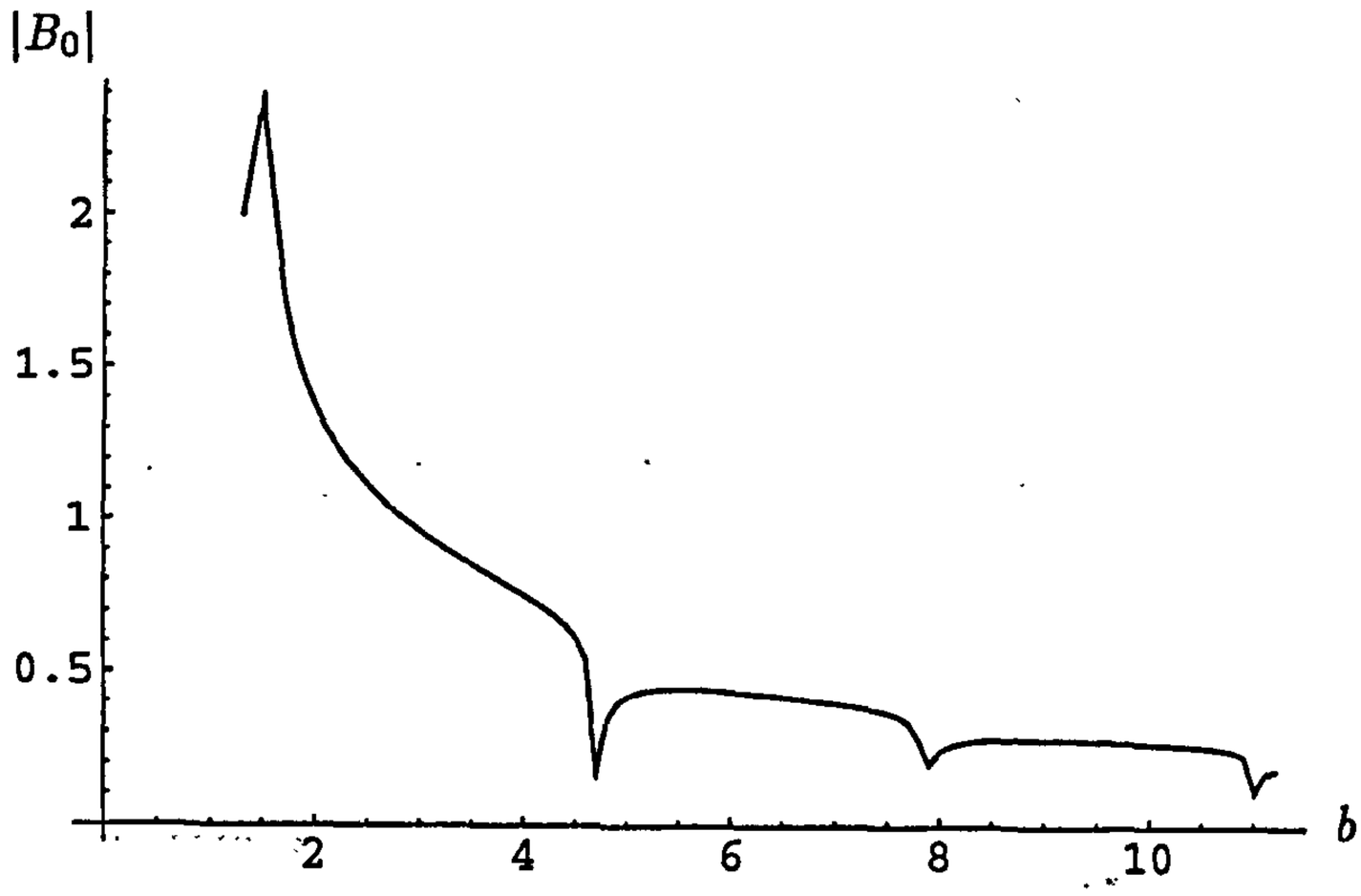

Figure 2.16: Plot of the modulus of the transmitted coefficient of the fundamental mode for the hard/soft problem with $a = 1.211$ and varying b.

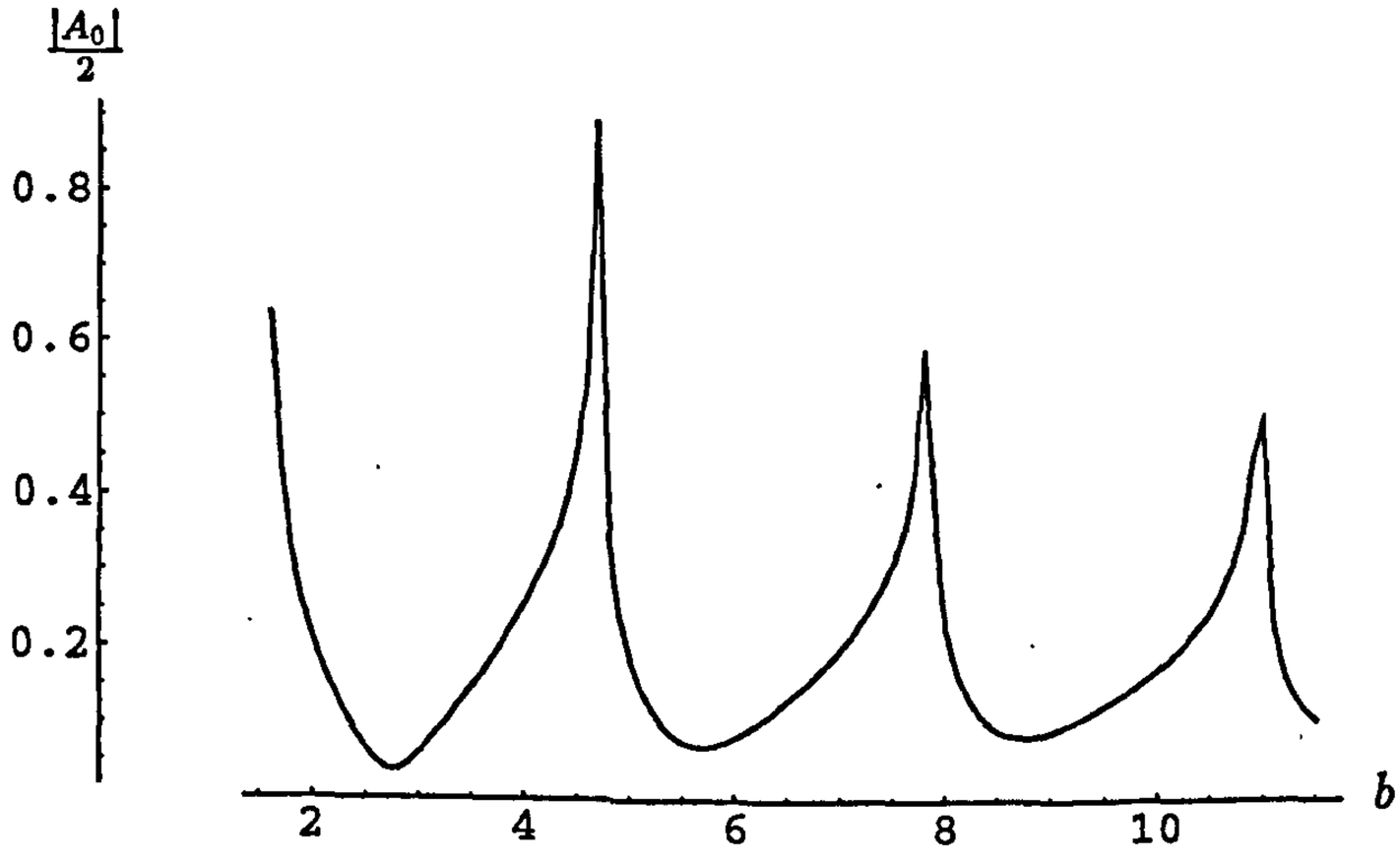

Figure 2.17: Plot of the modulus of the reflection coefficient of the fundamental mode for the hard/soft problem with $a = 1.51$ and varying b.

vertical surface $\bar{x} = 0$, $\bar{a} < \bar{y} < \bar{b}$ forms part of its boundary. The surface $\bar{y} = \bar{b}$, $\bar{x} > 0$ is now occupied by a membrane, of tension T and mass per unit area ρ_m, whilst every other surface is acoustically hard, see figure 2.19.

The interior region of this structure is filled with a compressible fluid of sound speed $c = \omega/k$ and density ρ, whilst the region exterior to the duct is *in vacuo*. A plain sound wave, of unit amplitude and harmonic time dependence with radian frequency ω, propagates along the duct in the positive $\bar{x}$ direction. The dimensional boundary-value

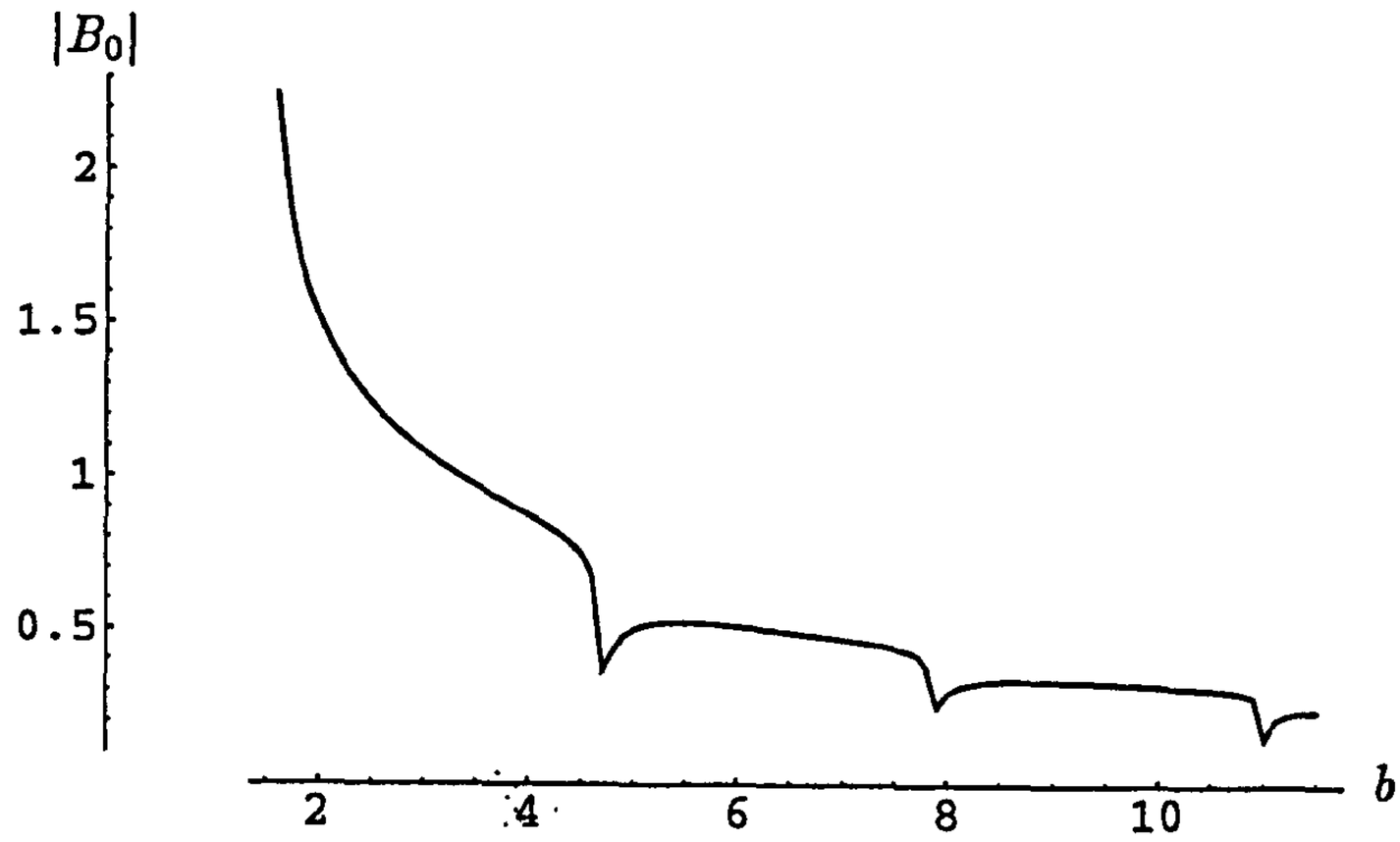

Figure 2.18: Plot of the modulus of the transmitted coefficient of the fundamental mode for the hard/soft problem with $a = 1.51$ and varying b.

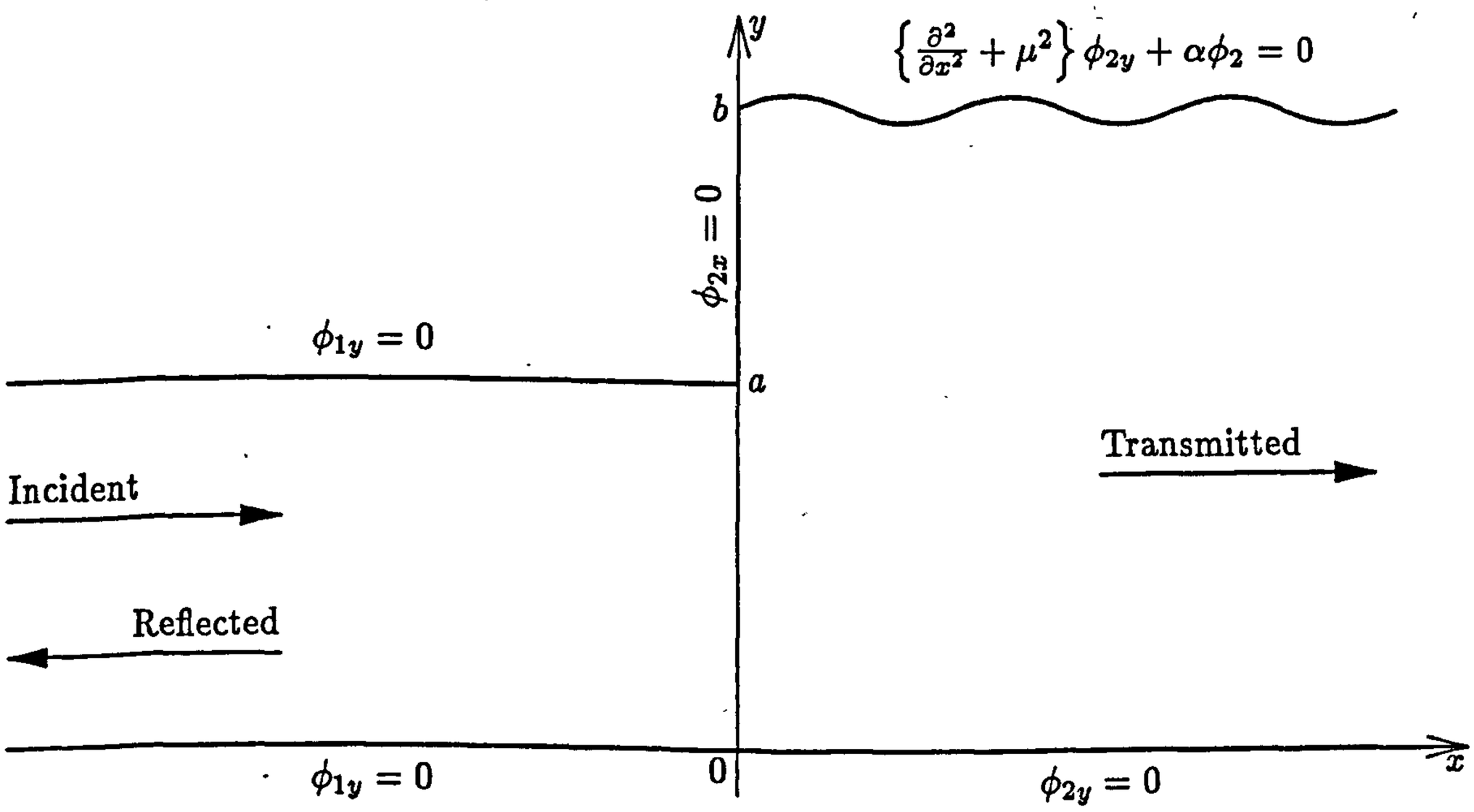

Figure 2.19: Physical configuration for the problem of Section 2.5

problem is described in terms of the fluid velocity potential $\bar{\Phi}(\bar{x}, \bar{y}, \bar{t})$ which satisfies the wave equation. A time harmonic solution is sought and thus the velocity potential may be written in the form

$$\bar{\Phi}(\bar{x}, \bar{y}, \bar{t}) = \bar{\phi}(\bar{x}, \bar{y})e^{-i\omega\bar{t}}, \tag{2.5.1}$$

where $\bar{\phi}(\bar{x}, \bar{y})$ satisfies Helmholtz' Equation, that is

$$\left\{\frac{\partial^2}{\partial \bar{x}^2} + \frac{\partial^2}{\partial \bar{y}^2} + k^2\right\}\bar{\phi}_{tot}(\bar{x}, \bar{y}) = 0. \tag{2.5.2}$$

Once again, the problem is to be non-dimensionalized with respect to a length scale k^{-1} and time scale ω^{-1}, and so the non-dimensionalised boundary conditions (2.1.7) to (2.1.9) still hold. The surface $\bar{y} = \bar{b}, \bar{x} > 0$ consists of a membrane for which the equation of motion is

$$\frac{\partial^2 \bar{H}}{\partial \bar{x}^2} - \frac{1}{c_m^2}\frac{\partial^2 \bar{H}}{\partial \bar{t}^2} = \frac{1}{T}[\bar{P}]_-^+ \tag{2.5.3}$$

where $\bar{H}(\bar{x}, \bar{y}, \bar{t})$ is the membrane displacement, $\bar{P}(\bar{x}, \bar{y}, \bar{t})$ is the fluid pressure (and so $[\bar{P}]_-^+$ is the pressure difference between the internal and external regions across the membrane surface) and $c_m = (T/\rho_m)^{1/2}$ is the *in vacuo* sound speed of waves on the membrane. Equation (2.5.3) must be non-dimensionalised using the same basis as for the rest of the problem. However, there are some properties of $\bar{H}$ and $\bar{P}$ that need to be noted. With the chosen forcing, both these quantities have harmonic time dependence, thus

$$\bar{P}(\bar{x}, \bar{y}, \bar{t}) = \bar{p}(\bar{x}, \bar{y})e^{-i\omega\bar{t}}, \tag{2.5.4}$$

$$\bar{H}(\bar{x}, \bar{y}, \bar{t}) = \bar{h}(\bar{x}, \bar{y})e^{-i\omega\bar{t}}. \tag{2.5.5}$$

where the fluid pressure perturbation, $\bar{P}(\bar{x}, \bar{y}, \bar{t})$ as derived in Crighton *et al* (1992), is related to the velocity potential by

$$\bar{P}(\bar{x}, \bar{y}, \bar{t}) = -\rho\frac{\partial}{\partial \bar{t}}\bar{\Phi}_{tot} = i\omega\rho\bar{\phi}_{tot}(\bar{x}, \bar{y})e^{-i\omega\bar{t}}, \tag{2.5.6}$$

whilst the membrane displacement is given by

$$\frac{\partial \bar{H}}{\partial \bar{t}} = \frac{\partial}{\partial \bar{y}}\bar{\phi}_{tot}e^{-i\omega\bar{t}}. \tag{2.5.7}$$

The membrane boundary condition can be expressed in terms of the velocity potential by substituting (2.5.6) and (2.5.7) into (2.5.3), thus gaining

$$\frac{\partial^2}{\partial \bar{x}^2}\frac{\partial}{\partial \bar{y}}\bar{\phi}_{tot} + \frac{\omega^2}{c_m^2}\frac{\partial}{\partial \bar{y}}\bar{\phi}_{tot} = \frac{\rho\omega^2}{T}[\bar{\phi}_{tot}]_{\bar{b}-}^{\bar{b}+}. \tag{2.5.8}$$

Then, given that $\bar{\phi}_{tot}$ is related to ϕ_{tot} by

$$\bar{\phi}_{tot}(\bar{x}, \bar{y}) = \frac{\omega}{k^2}\phi_{tot}(x, y) \tag{2.5.9}$$

and using the non-dimensional properties gained in previous sections, the non-dimensional membrane boundary condition is given by

$$\left\{\frac{\partial^2}{\partial x^2} + \mu^2\right\}\frac{\partial}{\partial y}\phi_{tot} + \alpha\phi_{tot} = 0, \qquad y = b, \tag{2.5.10}$$

where $\alpha = \omega^2\rho/Tk^3$ is the fluid loading parameter and $\mu^2 = c^2/c_m^2$ is the non-dimensional *in vacuo* membrane wave number. Note that, since the region outside the duct is *in vacuo*, then

$$[\phi_{tot}]_-^+ = -\phi_{tot}(x, b^-), \tag{2.5.11}$$

The non-dimensionalised boundary-value problem can now be described in full. The governing equation is Helmholtz' Equation, that is

$$\nabla^2\phi + \phi = 0. \tag{2.5.12}$$

The duct has different height on either side of the vertical line $x = 0$, so this line is taken as the matching interface and the non-dimensional acoustic field is expressed in terms of two potentials, $\phi_1(x, y)$ for $x < 0$ and $\phi_2(x, y)$ for $x > 0$. Thus,

$$\phi_{tot} = \begin{cases} \phi_1, & x < 0 \\ \phi_2, & x > 0 \end{cases}. \tag{2.5.13}$$

The boundary conditions imposed on $\phi_1(x, y)$ are

$$\frac{\partial\phi_1}{\partial y} = 0, \qquad y = 0, \tag{2.5.14}$$

$$\frac{\partial\phi_1}{\partial y} = 0, \qquad y = a \tag{2.5.15}$$

whilst those on $\phi_2(x, y)$ are

$$\frac{\partial\phi_2}{\partial y} = 0, \qquad y = 0, \tag{2.5.16}$$

$$\left\{\frac{\partial^2}{\partial x^2} + \mu^2\right\}\phi_{2y} + \alpha\phi_2 \,. = 0, \qquad y = b. \tag{2.5.17}$$

The fluid pressure and normal velocity are continuous across the matching interface and these conditions are expressed in terms of the fluid velocity potential by

$$\phi_1 = \phi_2, \qquad x = 0, \qquad 0 \le y \le a \tag{2.5.18}$$

and

$$\frac{\partial\phi_2}{\partial x} = \begin{cases} \frac{\partial\phi_1}{\partial x}, & 0 \le y \le a, \quad x = 0 \\ 0, & a < y \le b, \quad x = 0 \end{cases}. \tag{2.5.19}$$

Unlike the problems of sections 2.1 and 2.4, an edge condition must be imposed at the point where the membrane meets the rigid vertical surface, that is, at the point $(0, b)$. The edge condition specifies the behaviour of the membrane at the corner. Here, either

$$\phi_{2y}(0, b) = 0 \tag{2.5.20}$$

or alternatively

$$\phi_{2xy}(0, b) = 0. \tag{2.5.21}$$

The first of these two conditions implies behaviour similar to that of a hinge, allowing variation in gradient of the membrane at the point where it meets the rigid surface but no variation in displacement. The second of these conditions implies zero membrane gradient but variable displacement, so allowing the membrane edge to slide up and down against the rigid vertical surface.

The form of the duct to the left of the matching interface is identical to that of the previous two problems and the incident field is also the same. Thus, by the same method (separation of variables and application of boundary conditions), ϕ_1 will be of the same form as it has been in the previous two problems, that being

$$\phi_1 = e^{ix} + \frac{A_0}{2}e^{-ix} + \sum_{n=1}^{\infty} A_n \cos\left(\frac{n\pi y}{a}\right) e^{-i\eta_n x} \tag{2.5.22}$$

where $\eta_n = (1 - \frac{n^2\pi^2}{a^2})^{1/2}$ and the term for $n = 0$ is taken outside of the infinite sum and the expression for ϕ_1 is in the form of a standard Fourier cosine series.

The potential, ϕ_2 is made up of purely transmitted waves and so using separation of variables as in Section 2.1, where $\nu_n = (\gamma_n^2 + 1)^{1/2}$ and $\gamma_n, n = 0, 1, 2, \ldots, \infty$ are the roots of the dispersion relation obtained from (2.5.17), that is

$$(\gamma_n^2 + 1 - \mu^2)\gamma_n \sinh(\gamma_n b) - \alpha \cosh(\gamma_n b) = 0. \tag{2.5.23}$$

It follows that

$$\phi_2 = \sum_{n=0}^{\infty} B_n \cosh(\gamma_n y) e^{i\nu_n x} \tag{2.5.24}$$

where the coefficients, B_n are the complex amplitudes of each duct mode.

The only difference between the above analysis and that of Section 2.4 is the dispersion relationship. The expressions found for ϕ_1 and ϕ_2 take the same form as previous with γ_n replacing q_n. It would seem natural, therefore, to follow the method of Section 2.4 further. The next step is again to apply the conditions at the matching interface to the expressions for ϕ_1 and ϕ_2. Continuity of fluid pressure is expressed by (2.5.18) and thus

$$\frac{2 + A_0}{2} + \sum_{\ell=1}^{\infty} A_\ell \cos\left(\frac{\ell\pi y}{a}\right) = \sum_{m=0}^{\infty} B_m \cosh(\gamma_m y), \quad 0 \le y \le a. \tag{2.5.25}$$

The left hand side of this expression is in the form of a Fourier cosine series, whilst the right hand side is not (again, analagous to the method in Section 2.4). Hence the coefficients $A_\ell, \ell = 0, 1, 2, \ldots, \infty$ can be found using standard Fourier analysis, to be

$$\begin{aligned} 2 + A_0 &= \frac{2}{a}\sum_{m=0}^{\infty} B_m \int_0^a \cosh(\gamma_m y)dy \\ &= \frac{2}{a}\sum_{m=0}^{\infty} \frac{B_m \sinh(\gamma_m y)}{\gamma_m} \end{aligned} \tag{2.5.26}$$

and, for $\ell = 1, 2, 3, \ldots$

$$\begin{aligned} A_\ell &= \frac{2}{a}\sum_{m=0}^{\infty} B_m \int_0^a \cosh(\gamma_m y)\cos\left(\frac{\ell\pi y}{a}\right)dy \\ &= \frac{2}{a}\sum_{m=0}^{\infty} B_m R_{\ell m} \end{aligned} \tag{2.5.27}$$

where

$$\begin{aligned} R_{\ell m} &= \int_0^a \cosh(\gamma_m y)\cos\left(\frac{\ell\pi y}{a}\right)dy \\ &= \frac{(-1)^\ell \gamma_m \sinh(\gamma_m a)}{\gamma_m^2 + \frac{\ell^2\pi^2}{a^2}}. \end{aligned} \tag{2.5.28}$$

Combining these two expressions gives the single equation:

$$A_\ell = -2\delta_{0\ell} + \frac{2}{a}\sum_{m=0}^{\infty} B_m R_{\ell m}, \quad \ell = 0,1,2,\ldots,\infty \tag{2.5.29}$$

where $\delta_{\ell m}$ is the Kronecker delta.

Still following the method used in Section 2.4, the expressions for ϕ_1 and ϕ_2, that is (2.5.22) and (2.5.24), are substituted into the matching condition which prescribes that normal velocity is continuous, and so

$$\sum_{n=0}^{\infty} B_n \nu_n \cosh(\gamma_n y) = \begin{cases} \dfrac{2-A_0}{2} - \displaystyle\sum_{\ell=1}^{\infty} A_\ell \eta_\ell \cos\left(\frac{\ell\pi y}{a}\right), & 0 \le y \le a \\ 0, & a < y \le b \end{cases}. \tag{2.5.30}$$

The series on the left hand side side of this equation is not a standard Fourier series, and so the usual Fourier techniques cannot be applied to isolate $B_n, n = 0,1,2,\ldots$. In the previous case, the Sturm Liouville theory was applicable and so a similar approach is considered here as well. Multiplying through by $\cosh(\gamma_m y)$ and integrating from 0 to b gives

$$\sum_{n=0}^{\infty} B_n \nu_n I = \frac{2-A_0}{2}\int_0^a \cosh(\gamma_m y)dy - \sum_{\ell=1}^{\infty} A_\ell \eta_\ell \int_0^a \cos\left(\frac{\ell\pi y}{a}\right)\cosh(\gamma_m y)dy \tag{2.5.31}$$

where

$$I = \int_0^b \cosh(\gamma_n y)\cosh(\gamma_m y)dy. \tag{2.5.32}$$

The integral, I, on the left hand side of (2.5.31) is easily evaluated to obtain

$$I = \begin{cases} \dfrac{\gamma_m \sinh(\gamma_m b)\cosh(\gamma_n b) - \gamma_n \sinh(\gamma_n b)\cosh(\gamma_m b)}{\gamma_m^2 - \gamma_n^2}, & m \neq n \\ \dfrac{\sinh(2q_n b) + 2q_n b}{4q_n} = C_n, & n = m \end{cases}. \tag{2.5.33}$$

As for the Sturm Liouville problem of Section 2.4 the dispersion relation can be used to rearrange the above expression for $m \neq n$. In this case, following the steps of Section 2.4 it is found that

$$\begin{aligned} \gamma_m \sinh(\gamma_m b)\cosh(\gamma_n b) \; & -\gamma_n \sinh(\gamma_n b)\cosh(\gamma_m b) \\ &= \frac{\nu_m^2\gamma_m \sinh(\gamma_m b)\cosh(\gamma_n b) - \nu_n^2\gamma_n \sinh(\gamma_n b)\cosh(\gamma_m b)}{\mu^2} \\ &\neq 0. \end{aligned} \tag{2.5.34}$$

Clearly the eigenfunctions $\cosh(\gamma_n y)$ and $\cosh(\gamma_m y)$ are not orthogonal in the usual sense, and so the eigen-subsystem cannot be described as Sturm Liouville in nature.

The difference here is the second-order boundary condition. It is well known that edge conditions must be applied at the junction between any two boundaries where at least one of the boundaries is described by a high-order condition. The number of edge conditions required depends upon the degree of the highest derivative in the boundary condition. For a second-order boundary condition, as mentioned above, one edge condition is required. Clearly, the Sturm-Liouville orthogonality relation (2.3.22) leaves no scope to apply such a condition. An original orthogonality condition must be derived.

The analysis and subsequent conclusion that the Sturm Liouville theory does not apply here is not unexpected. The methods used to solve the hard/hard, hard/impedance and hard/soft problems are standard eigenfunction matching procedures, of which many examples exist. Peat (1991) uses eigenmode matching techniques extensively to find numerical solutions to acoustic impedance problems involving a geometry of three ducts, either positioned as inlets or outlets, whilst Dalrymple and Martin (1996) use an eigenfunction solution gained by the employment of Fourier transforms to examine the behaviour of ocean surface waves incident on an inlet. These approaches are limited however in that the ducts considered can still only be bounded by surfaces of Dirichlet, Neumann or Robin's type. This is borne out if (2.5.17) is compared with the boundary condition, (2.3.9) in Section 2.3. It is clear that that (2.5.17) does not comply with the necessary conditions prescribed in Section 2.3 that are the minimum requirements to generate a Sturm-Liouville (and thus solvable) system for this particular type of problem. To solve the problem described in this section, a new orthogonality relation is required.

2.6 Derivation of a new orthogonality relation

The failure of the Sturm-Liouville method for solution of the problem in Section 2.5 raises the question of why the similar system in Section 2.4 can be solved and yet this one cannot. The only difference between the two is the upper boundary condition of the duct to the right of the matching interface, $x = 0, 0 \leq y \leq b$. The solution of the problems thus far has relied on the ability to obtain a Sturm-Liouville series for the eigenfunctions and eigenvalues associated with each duct. In Section 2.1, Fourier series are used, which are in fact special forms of Sturm-Liouville series. When considering the problem in Section 2.4, the duct on the right of the matching interface no longer yields a simple Fourier series and so a Sturm-Liouville series is sought instead. The fact that one is found should come as little surprise when the necessary conditions for Sturm-Liouville analysis to be viable, are considered. From Section 2.3, it was seen that for a Sturm-Liouville series to be obtained, the boundary-value problem must be of the form

$$(rY')' + (s + \lambda t)Y = 0, \quad a \leq y \leq b, \tag{2.6.1}$$

$$a_1 Y(a) + a_2 Y'(a) = 0,, \tag{2.6.2}$$

$$b_1 Y(b) + b_2 Y'(b) = 0,. \tag{2.6.3}$$

For the boundary-value problem in Section 2.4, the duct to the right of the matching interface meets all three of these conditions. In this specific case $r(y) = 1$, $s(y) = 1$ and $t(y) = 0$ whilst for the boundary conditions, $a_1 = 0$ and $a_2 = 1$ on a surface located at $y = 0$ for the first, and $b_1 = \alpha$ and $b_2 = \beta$ at $y = b$ in the second. The conclusion of Section 2.3 was that if all conditions are met, a Sturm-Liouville series can be found, and in Section 2.4 this can be seen to be true. Given that $Y_n = \cosh(q_n y)$ then the orthogonality relation given in (2.3.16) is easily seen to be

$$\int_0^b \cosh(q_m y)\cosh(q_n y)dy = 0, \qquad m \neq n. \tag{2.6.4}$$

The problem occurs in Section 2.5 as a result of the high-order of the membrane boundary condition. When ϕ_2 is substituted into the membrane condition the result, expressed in the notation used in Section 2.3, is

$$Y'''(b) + (1-\mu^2)Y'(b) - \alpha Y(b) = 0. \tag{2.6.5}$$

This third order derivative that is included in the condition that would correspond to (2.6.3) violates one of the necessary conditions required for a Sturm-Liouville series to be formed and hence, the method fails for the boundary-value problem attempted in Section 2.5.

To make the problem in Section 2.5 viable for solution, an orthogonality relation for the infinite set of eigenfunctions

$$Y_n(y) = \cosh(\gamma_n y), \quad n = 0, 1, 2, \ldots, \quad 0 \leq y \leq b \tag{2.6.6}$$

where γ_n are the roots of

$$(\gamma_n^2 + 1 - \mu^2)Y_n'(a) - \alpha Y_n(a) = 0, \tag{2.6.7}$$

must be found. The method used follows a similar pattern to that used in Section 2.3 for the formation of general Sturm-Liouville methods, but the resulting orthogonality condition is both different and original. The orthogonality condition is found by recourse to the unforced model system comprising an infinite two dimensional duct bounded by a rigid surface at $\bar{y} = 0$ and a membrane of similar structure to that in the previous section, of tension T and mass per unit area ρ_m, at $\bar{y} = \bar{a}$, where $(\bar{x}, \bar{y})$ are Cartesian co-ordinates. The interior region, $0 \leq \bar{y} \leq \bar{a}$, $-\infty < \bar{x} < \infty$, contains a compressible fluid of sound speed $c = \omega/k$ and density ρ, while the region exterior to the duct is *in vacuo*.

As in the previous problems, the boundary-value problem is non-dimensionalized with respect to a length scale k^{-1} and time scale ω^{-1}. The governing equation in the dimensional problem is the Helmhotlz equation, which, when non-dimensionalised as described above, becomes

$$\nabla^2\phi + \phi = 0. \tag{2.6.8}$$

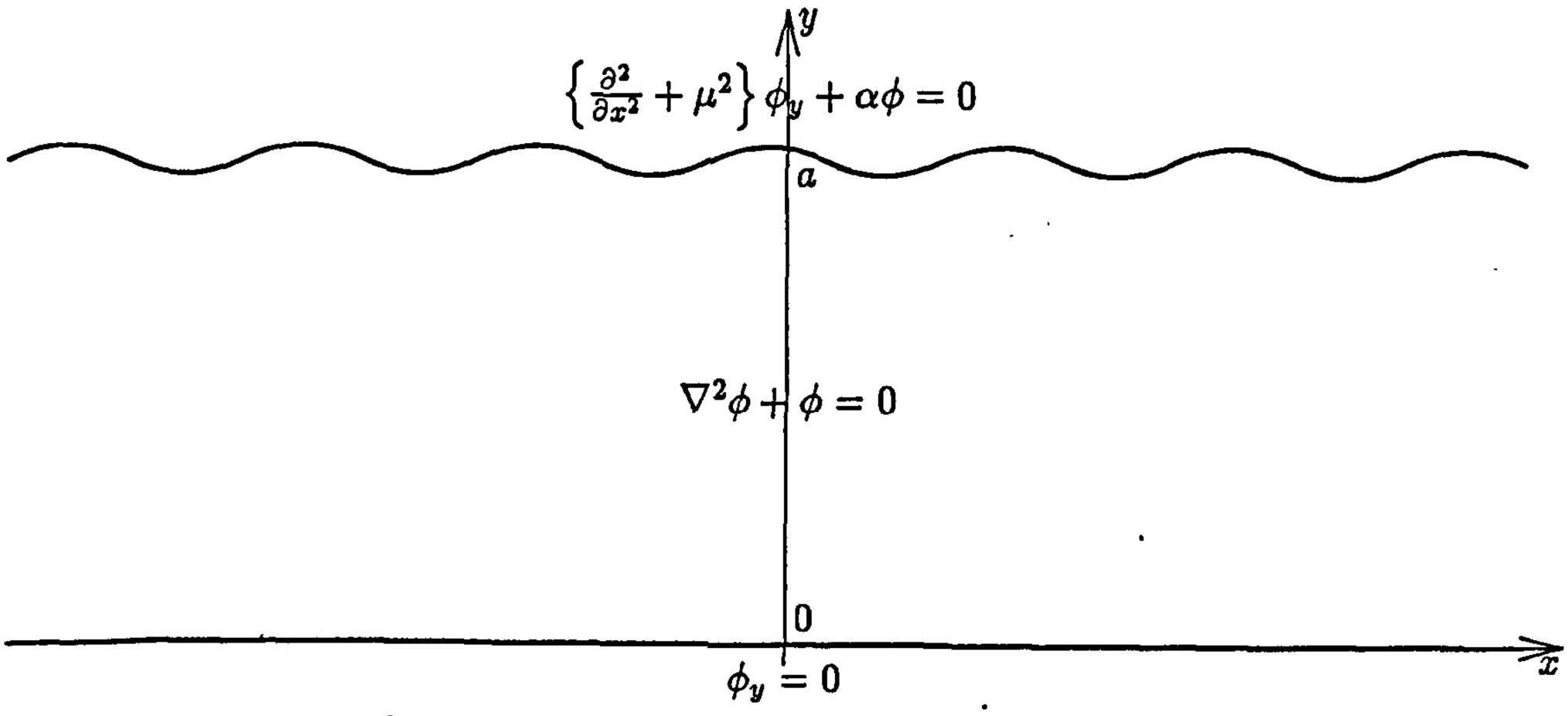

Figure 2.20: Physical configuration of a two dimensional duct, bounded on its upper surface by a membrane

The lower surface of the duct is rigid, and so the boundary consition is given by

$$\frac{\partial\phi}{\partial y}=0, \qquad y=0 \tag{2.6.9}$$

whilst the non-dimensionalised membrane boundary condition, as previously derived in (2.5.3) – (2.5.10), is given by

$$\left\{\frac{\partial^2}{\partial x^2}+\mu^2\right\}\phi_y+\alpha\phi=0, \qquad y=a, \tag{2.6.10}$$

where $\alpha=\omega^2\rho/Tk^3$ is the fluid loading parameter and $\mu^2=c^2/c_m^2$ is the *in vacuo* membrane wave number.

Separable solutions to (2.6.8) that satisfy boundary conditions (2.6.9) and (2.6.10) have the form

$$\phi=\sum_{n=0}^{\infty}\sigma_n Y_n(y)e^{i\nu_n x}, \tag{2.6.11}$$

where the eigenfunctions, $Y_n(y), n=0,1,2,\ldots$, satisfy the system

$$Y_n''(y)-\gamma_n^2 Y_n(y) = 0, \tag{2.6.12}$$

$$(\gamma_n^2+1-\mu^2)Y_n'(a)-\alpha Y_n(a) = 0, \tag{2.6.13}$$

$$Y_n'(0) = 0, \tag{2.6.14}$$

with $\gamma_n=(\nu_n^2-1)^{\frac{1}{2}}$. Here and throughout a prime indicates differentiation with respect to y. To obtain the orthogonality relation, first define function $f_n(y)$ by

$$f_n(y)=(\gamma_n^2+1-\mu^2)Y_n'(y)-\alpha Y_n(y). \tag{2.6.15}$$

Clearly, from (2.6.13) and (2.6.14)

$$\left[f_n(y)Y_m'(y)-f_m(y)Y'_n(y)\right]_0^a=0, \quad m\neq n \tag{2.6.16}$$

which can be rearranged as

$$\left[(\gamma_n^2-\gamma_m^2)Y_n'(y)Y_m'(y)-\alpha(Y_n(y)Y_m'(y)-Y_m(y)Y_n'(y))\right]_0^a=0,\quad m\neq n. \tag{2.6.17}$$

Equation (2.6.17) can be expressed in integral form as

$$(\gamma_n^2-\gamma_m^2)Y_n'(a)Y_m'(a)-\alpha\int_0^a\left[Y_n(y)Y_m''(y)-Y_m(y)Y_n''(y)\right]dy=0,\quad m\neq n. \tag{2.6.18}$$

Applying (2.6.12) to the second gives

$$(\gamma_n^2-\gamma_m^2)Y_n'(a)Y_m'(a)+\alpha(\gamma_n^2-\gamma_m^2)\int_0^a Y_n(y)Y_m(y)dy=0,\quad m\neq n. \tag{2.6.19}$$

It follows that,

$$\alpha\int_0^a Y_n(y)Y_m(y)dy+Y_n'(a)Y_m'(a)=0,\quad m\neq n. \tag{2.6.20}$$

Note, from (2.6.12), that $Y_n(y)$ is actually a function of both γ_n and y. The equivalent expressions $Y_n(y)\equiv Y_n(\gamma_n,y)$ will be used as appropriate in the following steps. For $m=n$, the left hand side of (2.6.17) and (2.6.20) can be equated to obtain

$$\alpha\int_0^a Y_n(y)Y_m(y)dy+Y_n'(a)Y_m'(a)= \tag{2.6.21}$$
$$\left[\lim_{\gamma\to\gamma_n}\frac{\left\{\gamma_n^2Y_n'(y)-\alpha Y_n(y)\right\}Y'(\gamma,y)-\left\{\gamma^2Y'(\gamma,y)-\alpha Y(\gamma,y)\right\}Y_n'(y)}{\gamma_n^2-\gamma^2}\right]_0^a.$$

This limit may be evaluated using L'Hôpital's Rule. The derivative of the numerator with respect to γ is

$$\left[\gamma_n^2Y_n'(y)-\alpha Y_n(y)\right]\frac{d}{d\gamma}Y'(\gamma,y)-Y_n'(y)\left[2\gamma Y'(\gamma,y)+\gamma^2\frac{d}{d\gamma}Y'(\gamma,y)-\alpha\frac{d}{d\gamma}Y(\gamma,y)\right], \tag{2.6.22}$$

whilst that of the denominator is simply 2γ. On evaluating (2.6.22) at the limits specified in (2.6.21) and dividing by 2γ it is found that

$$\left[\lim_{\gamma\to\gamma_n}\frac{\left\{\gamma_n^2Y_n'(y)-\alpha Y_n(y)\right\}Y'(\gamma,y)-\left\{\gamma^2Y'(\gamma,y)-\alpha Y(\gamma,y)\right\}Y_n'(y)}{\gamma_n^2-\gamma^2}\right]_0^a$$
$$=\frac{Y_n'(a)}{2\gamma_n}\frac{d}{d\gamma}K(s)\big|_{\gamma=\gamma_n} \tag{2.6.23}$$

where $K(s)$ is the dispersion function given by

$$K(s)=(\gamma^2+1-\mu^2)Y'(\gamma,a)-\alpha Y(\gamma,a),\quad \gamma=(s^2-1)^{\frac{1}{2}}. \tag{2.6.24}$$

This is consistent with (2.6.13) which states that $K(\nu_n)=0$.

It follows from (2.6.20), (2.6.21) and (2.6.23) that the orthogonality relation for the eigen problem specified by (2.6.12)–(2.6.14) is

$$\alpha\int_0^a Y_m(y)Y_n(y)dy+Y_m'(a)Y_n'(a)=\delta_{mn}C_n \tag{2.6.25}$$

where

$$C_n = \frac{Y_n'(a)}{2\gamma_n}\frac{d}{d\gamma}K(s)\rfloor_{\gamma=\gamma_n} \tag{2.6.26}$$

and δ_{mn} is the usual Kronecker delta. Note the extra term, $Y_m'(a)Y_n'(a)$ on the left hand side. It is this which enables an edge condition to be applied at the edge of the membrane.

The orthogonality relation, (2.6.25), may be written as an inner product of eigenfunctions

$$(Y_m, Y_n) = \delta_{mn}C_n. \tag{2.6.27}$$

This definition may be extended to functions that are sufficiently differentiable over the interval $0 \leq y \leq a$ and have the form

$$g(y) = \sum_{n=0}^{\infty} b_n Y_n(y) \tag{2.6.28}$$

to obtain

$$(g, Y_m) = \alpha \int_0^a g(y)Y_m(y)\,dy + g'(a)Y_m'(a) = b_m C_m. \tag{2.6.29}$$

Expression (2.6.25), in a slightly different form, has been discussed by Warren & Lawrie (1999), and a generalised form of this orthogonality relation can be found in Abrahams & Lawrie (1999). It is this result together with the inner product representation (2.6.29) that enables the boundary-value problem of Section 2.5 to be completed.

The derivation of specialised orthogonality relations to solve non-Sturm-Liouville boundary-value problems is not uncommon. Indeed, such orthogonality conditions are found in many fields of applied mathematics: McIsaac (1991) considers orthoganality relations applicable to electromagnetic fields in waveguides of a specific type; Folk & Herczynski (1986) and Herczynski & Folk (1989) derive orthogonality conditions by which the coeffiecients in the eigenfunction expansions for vibration within an end-loaded elastodynamic slab are found; and Rao & Rao (1988) examine the flexure of rectangular plates, using an orthogonality condition specific to the eigenfunctions found using refined plate theories. In all these examples, the eigen-sub-systems are not Sturm-Liouville, however, specialised orthogonality conditions can be found.

Chapter 3

Reflection and transmission at the junction of a rigid duct with a duct of different height, bounded on its upper surface by a membrane

In section 2.5, a boundary-value problem was specified and an attempt made to solve it using methods taken from Fourier Series analysis and Sturm-Liouville theory. It was seen that the attempted solution method was inappropriate. The reason for this failure is that the above techniques utilise a simple orthogonality relationship which the eigenfunctions for the problem in 2.5 do not satisfy. A different approach to this problem is required.

That different approach was found in the form of (2.6.29), an orthogonality condition that is borne directly from the dispersion relation associated with a duct of similar form to that found to the right of the matching interface in the problem in section 2.5. In this section, that orthogonality condition will be applied to the problem in section 2.5 and a system of equations, similar to that found in sections 2.1 and 2.4 will be found and used to gain a solution for the problem. The results that this yields will be compared with the results from two special cases. Firstly, the case where $a = b$ (a and b being the heights of the two ducts as indicated in figure 3.1) for which the problem can be solved using the Wiener-Hopf technique. Secondly, by selecting the values of α and μ (α being the fluid loading parameter and μ is the non-dimensional *in vacuo* membrane wave number) appropriately the membrane boundary condition can be made to mimic the behaviour of a Dirichlet (soft) boundary condition and so the solution can be compared with that obtained for the hard/soft problem in section 2.4.

...

3.1 Solution of the problem

In section 2.5 the problem was specified and non-dimensionalised, and so at this point the non-dimensionalised boundary-value problem is simply re-stated. The governing equation is Helmholtz' Equation, that is

$$\nabla^2\phi + \phi = 0. \tag{3.1.1}$$

The vertical line $x = 0$ is taken as the matching interface and the acoustic field is expressed in terms of two potentials, $\phi_1(x,y)$ for $x < 0$ and $\phi_2(x,y)$ for $x > 0$. Thus,

$$\phi_{tot} = \begin{cases} \phi_1, & x < 0 \\ \phi_2, & x > 0 \end{cases}. \tag{3.1.2}$$

The duct lying in the region $x < 0, 0 \leq y \leq a$ has rigid boundaries, so the conditions imposed on $\phi_1(x,y)$ are

$$\frac{\partial\phi_1}{\partial y} = 0, \qquad y = 0, \tag{3.1.3}$$

$$\frac{\partial\phi_1}{\partial y} = 0, \qquad y = a. \tag{3.1.4}$$

The upper surface of the duct lying in $x > 0, 0 \leq y \leq b$ comprises a membrane, the non-dimensionalised boundary condition for which was derived in (2.5.3) – (2.5.10), whilst the lower surfaces is rigid, hence for $\phi_2(x,y)$

$$\frac{\partial\phi_2}{\partial y} = 0, \qquad y = 0, \tag{3.1.5}$$

$$\left\{\frac{\partial^2}{\partial x^2} + \mu^2\right\}\phi_{2y} + \alpha\phi_2 = 0, \qquad y = b. \tag{3.1.6}$$

The fluid pressure and normal velocity are continuous across the matching interface and these conditions are expressed in terms of the fluid velocity potential by

$$\phi_1 = \phi_2, \qquad x = 0, \qquad 0 \leq y \leq a \tag{3.1.7}$$

and

$$\frac{\partial\phi_2}{\partial x} = \begin{cases} \frac{\partial\phi_1}{\partial x}, & 0 \leq y \leq a, \quad x = 0, \\ 0, & a < y \leq b, \quad x = 0. \end{cases} \tag{3.1.8}$$

The two possible edge conditions will be considered here. As mentioned in section 2.5, these are

$$\phi_{2y}(0,b) = 0 \tag{3.1.9}$$

or alternatively

$$\phi_{2xy}(0,b) = 0. \tag{3.1.10}$$

As in previous problems, eigenfunction expansions for ϕ_1 and ϕ_2 are required. These are found in (2.5.22) to (2.5.24) and are re-stated here as

$$\phi_1 = e^{ix} + \frac{A_0 e^{-ix}}{2} + \sum_{n=1}^{\infty} A_n \cos\left(\frac{n\pi y}{a}\right) e^{-i\eta_n x} \tag{3.1.11}$$

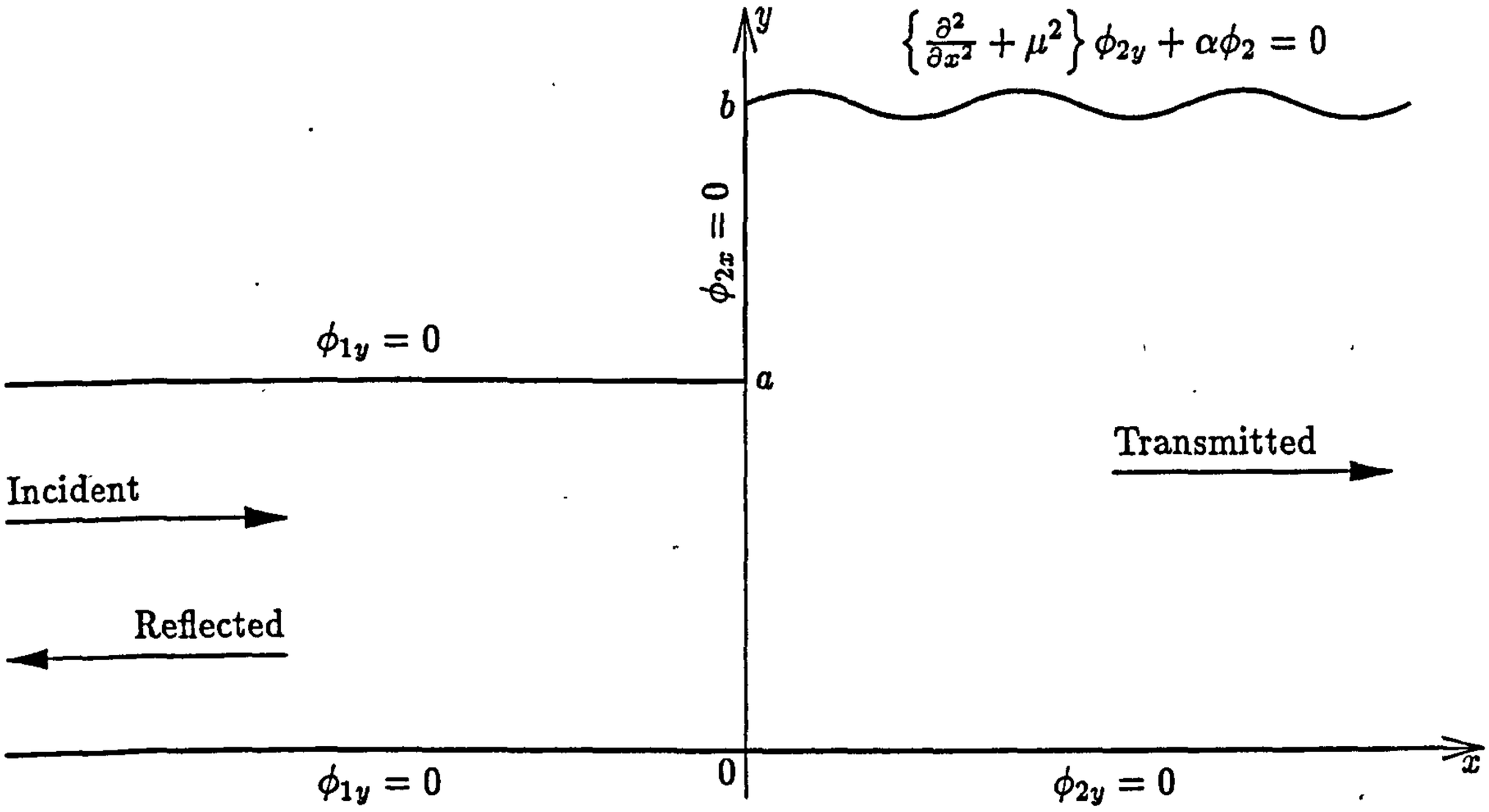

Figure 3.1: Physical configuration for the problem of section 3.1

where $\eta_n = (1-\frac{n^2\pi^2}{a^2})^{1/2}$ and

$$\phi_2 = \sum_{n=0}^{\infty} B_n \cosh(\gamma_n y) e^{i\nu_n x} \tag{3.1.12}$$

in which $\nu_n = (\gamma_n^2+1)^{1/2}$ and $\gamma_n, n = 0,1,2,\ldots,\infty$ are the roots of the dispersion relation

$$(\gamma_n^2+1-\mu^2)\gamma_n \sinh(\gamma_n b) - \alpha\cosh(\gamma_n b) = 0. \tag{3.1.13}$$

The expression for ϕ_1 is a Fourier cosine series and so the method for finding $A_\ell, \ell = 0,1,2,\ldots,\infty$ is the same as in sections 2.1 and 2.4. On applying the matching condition that enforces continuity of fluid pressure at the interface $x = 0, 0 \le y \le a$ to (3.1.11) and (3.1.12), it is found that

$$\frac{2+A_0}{2} + \sum_{\ell=1}^{\infty} A_\ell \cosh\left(\frac{\ell\pi y}{a}\right) = \sum_{m=0}^{\infty} B_m \cosh(\gamma_m y), \quad 0 \le y \le a. \tag{3.1.14}$$

It follows that

$$A_\ell = -2\delta_{0\ell} + \frac{2}{a}\sum_{m=0}^{\infty} B_m R_{\ell m}, \quad \ell = 0,1,2,\ldots,\infty \tag{3.1.15}$$

where

$$\begin{aligned} R_{\ell m} &= \int_0^a \cosh(\gamma_m y)\cos\left(\frac{\ell\pi y}{a}\right) dy \\ &= \frac{(-1)^\ell \gamma_m \sinh(\gamma_m a)}{\gamma_m^2 + \frac{l^2\pi^2}{a^2}}. \end{aligned} \tag{3.1.16}$$

and $\delta_{\ell m}$ is the usual Kronecker delta.

Up to this point the method is directly analogous to that of sections 2.1 and 2.4. However, at this point, as demonstrated in section 2.5 a different approach is required and is supplied by the new orthogonality relation derived in section 2.6. On substituting (3.1.11) and (3.1.12) into the condition for continuity of normal velocity, it is found that

$$\sum_{n=0}^{\infty} B_n \nu_n \cosh(\gamma_n y) = \begin{cases} \dfrac{2-A_0}{2} - \displaystyle\sum_{\ell=1}^{\infty} A_\ell \eta_\ell \cos\left(\dfrac{\ell \pi y}{a}\right), & 0 \le y \le a \\ 0, & a < y \le b \end{cases} \tag{3.1.17}$$

which, using the notation of section 2.6, can be rewritten as

$$g(y) = \sum_{n=0}^{\infty} B_n \nu_n Y_n = \begin{cases} \dfrac{2-A_0}{2} - \displaystyle\sum_{\ell=1}^{\infty} A_\ell \eta_\ell \cos\left(\dfrac{\ell \pi y}{a}\right), & 0 \le y \le a \\ 0, & a < y \le b \end{cases} \tag{3.1.18}$$

where $Y_n = \cosh(\gamma_n y)$. On multiplying this by αY_m and integrating over the range $0 \le y \le b$, it is found that

$$\alpha \int_0^b g(y) Y_m dy = \alpha \int_0^a \left[\frac{2-A_0}{2} - \sum_{\ell=1}^{\infty} A_\ell \eta_\ell \cos\left(\frac{\ell \pi y}{a}\right)\right] Y_m dy. \tag{3.1.19}$$

Expression (2.6.29) is now used, that is

$$\alpha \int_0^b g(y) Y_m(y)\, dy + g'(b) Y_m'(b) = B_m \nu_m C_m, \tag{3.1.20}$$

which can be rearranged to yield

$$\begin{aligned} \alpha \int_0^a g(y) Y_m(y)\, dy &= B_m \nu_m C_m - g'(b) Y_m'(b) \\ &= B_m \nu_m C_m - E Y_m'(b), \end{aligned} \tag{3.1.21}$$

where it can be seen by comparing (3.1.12) with (3.1.18) that

$$E = -i\phi_{2xy}(0,b) = \sum_{m=0}^{\infty} B_m \nu_m Y_m'(b) \tag{3.1.22}$$

and

$$\begin{aligned} C_m &= \frac{Y_m'(b)}{2\gamma_m} \frac{d}{d\gamma} K(s)\big]_{\gamma=\gamma_m} \\ &= \frac{\alpha b}{2} + \left(\gamma_m^2 + \frac{\nu_m^2 - \mu^2}{2}\right) \sinh^2(\gamma_m b). \end{aligned} \tag{3.1.23}$$

For computational purposes it is more convenient to use the coefficient C_n^* defined by $C_m = \alpha C_m^*$ which is obtained from (3.1.23) by using (3.1.13), thus

$$C_m^* = \frac{1}{2}\left[b + \frac{(2\gamma_m + \nu_m^2 - \mu^2)\sinh(2\gamma_m b)}{2\gamma_m(\nu_m^2 - \mu^2)}\right]. \tag{3.1.24}$$

The left hand side of (3.1.21) can be replaced with the right hand side of (3.1.19) and it is then found, after rearrangement, that

$$\begin{aligned} B_n &= \frac{EY_n'(b)}{\nu_n C_n} + \frac{1}{\nu_n C_n^*}\int_0^a \left[\frac{2-A_0}{2} - \sum_{\ell=1}^{\infty} A_\ell \eta_\ell \cos\left(\frac{\ell\pi y}{a}\right)\right] Y_n dy \\ &= \frac{EY_n'(b)}{\nu_n C_n} + \frac{1}{\nu_n C_n^*}\left[\left\{\frac{2-A_0}{2}\right\} R_{0n} - \sum_{\ell=1}^{\infty} A_\ell \eta_\ell R_{\ell n}\right]. \end{aligned} \tag{3.1.25}$$

Once again, an expression for $A_\ell, \ell = 0,1,2,\ldots,\infty$ in terms of a infinite sum of $B_m, m = 0,1,2,\ldots$ have been found and vice versa and so, an infinite system of equations in only one set of coefficients can be formed. As in previous cases, here a system for the coefficients $B_n, n = 0,1,2,\ldots,\infty$ is formed and from that A_ℓ can be found. So on eliminating $A_\ell, \ell = 0,1,2,\ldots,\infty$ between (3.1.15) and (3.1.25), it transpires that

$$B_n = \frac{\gamma_n \sinh(\gamma_n b)E}{\nu_n C_n} + \frac{1}{\nu_n C_n^*}\left[2R_{0n} - \frac{R_{0n}}{a}\sum_{m=0}^{\infty} B_m R_{0m} - \frac{2}{a}\sum_{\ell=1}^{\infty}\sum_{m=0}^{\infty} B_m \eta_\ell R_{\ell m} R_{\ell n}\right]. \tag{3.1.26}$$

For most ranges of parameters, this system is sufficiently convergent to provide results of high accuracy even for a truncation of only a few terms. This reflects the fact that the behaviour at the corner $(0,b)$ is not singular. However, in the case where $a = b$, the resulting truncated matrix is diagonally dominant with diagonal elements that are constant and thus, non-convergent, which makes computation of a complete solution using the system described by (3.1.26) impossible. To remove this undesirable behaviour from the solution matrix, the behaviour of the terms on the diagonal must be considered. As $m \to \infty$ then $\gamma_m \to \frac{im\pi}{b}$, and for the case where $\ell = m$, the expression $R_{\ell m}$ as given in (3.1.16) takes on the form

$$R_{\ell\ell} \to \frac{(-1)^\ell \sin\left(\frac{\ell\pi a}{b}\right) a^2 b}{l\pi(b^2-a^2)}, \qquad l \to \infty. \tag{3.1.27}$$

For the case where $a = b$, L'Hopital's rule is applied to give,

$$R_{\ell\ell} \to \frac{a}{2}, \qquad \ell \to \infty, \quad b \to a. \tag{3.1.28}$$

To improve the convergence of the diagonal terms in the system of (3.1.26), for this special case, the diagonal terms must be removed. To complete this, first define

$$S_{\ell m} = R_{\ell m} - \frac{\delta_{\ell m} a}{2}, \quad \ell, m = 0,1,2,\ldots. \tag{3.1.29}$$

Hence, (3.1.15) can be rewritten as

$$A_\ell = -2\delta_{0\ell} + B_\ell + \frac{2}{a}\sum_{m=0}^{\infty} B_m S_{\ell m}, \quad \ell = 0,1,2,\ldots,\infty \tag{3.1.30}$$

and (3.1.25) becomes

$$B_n = \frac{EY_n'(b)}{\nu_n C_n} + \frac{1}{\nu_n C_n^*}\left[\left\{\frac{2-A_0}{2}\right\} R_{0n} - \frac{aA_n\eta_n}{2} - \sum_{\ell=1}^{\infty} A_\ell \eta_\ell S_{\ell n}\right], n = 0,1,2,\ldots. \tag{3.1.31}$$

At this point, some caution is required. In the case where $n = 0$, (3.1.31) must be considered carefully since the term $\frac{aA_n\eta_n}{2}$ is gained by drawing through a term from a sum from $\ell = 1$ to ∞ and so (3.1.30) cannot be used to find B_0. As a result, for the case where $n = 0$ alone, (3.1.30) is applied to (3.1.25) to give

$$B_0 = \frac{EY_0'(b)}{\nu_0 C_0} + \frac{1}{\nu_0 C_0^*}\left[R_{00} - \frac{R_{00}}{2}\left\{-2 + B_0 + \frac{2}{a}\sum_{m=0}^{\infty} B_m S_{0m}\right\} - \frac{2}{a}\sum_{\ell=1}^{\infty}\sum_{m=0}^{\infty}\eta_\ell B_m R_{\ell 0} R_{\ell m}\right]. \tag{3.1.32}$$

The above expression may be rearranged as

$$B_0\left[\frac{2\nu_0 C_0^* + R_{00}}{2\nu_0 C_0^*}\right] = \frac{EY_0'(b)}{\nu_0 C_0} + \frac{2R_{00}}{\nu_0 C_0^*} - \frac{R_{00}}{a\nu_0 C_0^*}\sum_{m=0}^{\infty} B_m S_{0m} - \frac{2}{a\nu_0 C_0^*}\sum_{\ell=1}^{\infty}\sum_{m=0}^{\infty}\eta_\ell B_m R_{\ell 0} R_{\ell m} \tag{3.1.33}$$

and so

$$B_0 = \frac{\dfrac{2EY_0'(b)}{\alpha} + 4R_{00} - \dfrac{2R_{00}}{a}\displaystyle\sum_{m=0}^{\infty} B_m S_{0m} - \dfrac{4}{a}\displaystyle\sum_{\ell=1}^{\infty}\sum_{m=0}^{\infty}\eta_\ell B_m R_{\ell 0} R_{\ell m}}{2\nu_0 C_0^* + R_{00}}. \tag{3.1.34}$$

For the cases where $n = 1, 2, 3, \ldots$, (3.1.30) is substituted into (3.1.31) and results in

$$\begin{aligned} B_n \;=\; & \frac{EY_n'(b)}{\nu_n C_n} + \frac{R_{0n}}{\nu_n C_n^*} - \frac{R_{0n}}{2\nu_n C_n^*}\left[-2 + B_0 + \frac{2}{a}\sum_{m=0}^{\infty} B_m S_{0m}\right] \\ & - \frac{a\eta_n}{2\nu_n C_n^*}\left[B_n + \frac{2}{a}\sum_{m=0}^{\infty} B_m S_{nm}\right] - \frac{1}{\nu_n C_n^*}\sum_{\ell=1}^{\infty}\eta_\ell s_{\ell n}\left[B_\ell + \frac{2}{a}\sum_{m=0}^{\infty} B_m S_{\ell m}\right], \\ & \qquad n = 1, 2, 3, \ldots. \end{aligned} \tag{3.1.35}$$

The coefficient B_n is easily isolated to obtain

$$\begin{aligned} B_n\left[\frac{2\nu_n C_n^* + \eta_n a}{2\nu_n C_n^*}\right] \;=\; & \frac{EY_n'(b)}{\nu_n C_n} + \frac{1}{\nu_n C_n^*}\left[2R_{0n} - \frac{R_{0n}B_0}{2} - \frac{R_{0n}}{2}\sum_{m=0}^{\infty} B_m S_{0m}\right. \\ & \left. - \frac{\eta_n a}{2}\sum_{m=0}^{\infty} B_m S_{nm} - \sum_{\ell=1}^{\infty}\eta_\ell S_{\ell n} B_\ell - \sum_{\ell=1}^{\infty}\sum_{m=0}^{\infty}\eta_\ell B_m S_{\ell m} S_{\ell n}\right], \\ & \qquad n = 1, 2, 3, \ldots \end{aligned} \tag{3.1.36}$$

and hence

$$\begin{aligned} B_n \;=\; & \left[\frac{2EY_n'(b)}{\alpha} + 4R_{0n} - R_{0n}B_0 - \frac{2R_{0n}}{a}\sum_{m=0}^{\infty} B_m S_{0m} - 2\eta_n\sum_{m=0}^{\infty} B_m S_{nm}\right. \\ & \left. -2\sum_{\ell=1}^{\infty}\eta_\ell B_\ell S_{\ell n} - \frac{4}{a}\sum_{\ell=1}^{\infty}\sum_{m=0}^{\infty}\eta_\ell B_m S_{\ell m} S_{\ell n}\right](2\nu_n C_n^* + \eta_n a), \quad n = 1, 2, 3, \quad \ldots. \end{aligned} \tag{3.1.37}$$

The system described by (3.1.34) and (3.1.37) for $B_n, n = 0, 1, 2, \ldots$ is suitably convergent but as yet incomplete as the value of E is not specified. However, as stated previously, there must be an edge condition imposed at the point where the membrane meets the vertical

rigid surface. The two possible edge conditions, (3.1.9) and (3.1.10), will be considered in turn.

To enforce the first edge condition, $\phi_{2y}(0,b)=0$, consider first the form of ϕ_2 given in (3.1.12). Differentiating this with respect to y and evaluating at the point $(0,b)$ gives

$$\phi_{2y}(0,b)=\sum_{n=0}^{\infty}\gamma_n B_n \sinh(\gamma_n b)=0. \tag{3.1.38}$$

On substituting for B_n via (3.1.26) it is seen that

$$\begin{aligned}0 \;=\; \sum_{n=0}^{\infty}\frac{\gamma_n\sinh(\gamma_n b)}{\nu_n C_n}\Bigg[&\gamma_n\sinh(\gamma_n b)E+\alpha\Bigg\{2R_{0n}-\frac{R_{0n}}{a}\sum_{m=0}^{\infty}B_m R_{0m}\\ &-\frac{2}{a}\sum_{\ell=1}^{\infty}\sum_{m=0}^{\infty}B_m\eta_\ell R_{\ell m}R_{\ell n}\Bigg\}\Bigg]\end{aligned} \tag{3.1.39}$$

which maybe rearranged to obtain

$$E=-\frac{\displaystyle\sum_{n=0}^{\infty}\frac{\alpha\gamma_n\sinh(\gamma_n b)}{\nu_n C_n}\left[2R_{0n}-\frac{R_{0n}}{a}\sum_{m=0}^{\infty}B_m R_{0m}-\frac{2}{a}\sum_{l=1}^{\infty}\sum_{m=0}^{\infty}B_m\eta_l R_{lm}R_{ln}\right]}{\displaystyle\sum_{j=0}^{\infty}\frac{\gamma_j^2\sinh^2(\gamma_j b)}{\nu_j C_j}}. \tag{3.1.40}$$

The imposition of the second edge condition, $\phi_{2xy}(0,b)=0$ is much more straight forward. From (3.1.12)

$$\phi_{2xy}(0,b)=i\sum_{n=0}^{\infty}\nu_n\gamma_n B_n\sinh(\gamma_n b)=0, \tag{3.1.41}$$

however, in (3.1.22), it is stated that $E=-i\phi_{2xy}$ and so it follows directly that

$$E=0. \tag{3.1.42}$$

So, in contrast to section 2.5 where Sturm-Liouville treatment of this problem failed, here a viable system of equations has been found. To check that the results of this system are accurate, some comparison problems are required. One such problem is the problem where the upper boundary of the duct to the right of the matching interface consists of a surface with a Dirichlet boundary condition. This problem was discussed at the end of section 2.4 and results for that problem were given. Later in this chapter these will be compared with results for the heavy fluid loading case of this example, that is where $\alpha\gg 1$ and μ is of moderate value. Under these conditions, the dispersion relation, given in (3.1.14) is approximated by

$$\alpha\cosh(\gamma_n b)=0 \tag{3.1.43}$$

which is the same form as that for a Dirichlet boundary condition. A further comparison problem is investigated in the next section, where the case where $a=b$ is solved using the Wiener-Hopf technique.

The *Mathematica* code for the system found in this section is given in Appendix B.1.

3.2 The Wiener-Hopf technique for the case $a = b$

In the case where $a = b$ the problem solved in section 3.1 is amenable to solution by the Wiener-Hopf technique. The technique involves dividing the complex plane into two halves, overlapping in a strip of analyticity. In this strip, $\epsilon_- < \Im(s) < \epsilon_+$, some known function $K(s)$, the Wiener-Hopf kernel is regular and non-zero. This function is decomposed into a product defined by

$$K(s) = K_+(s)K_-(s) \tag{3.2.1}$$

where $K_+(s)$ is regular and non-zero in $\Im(s) > \epsilon_-$ and $K_-(s)$ is regular and non-zero in $\Im(s) < \epsilon_+$. Note, that in order to obtain a strip of the form $\epsilon_- < \Im(s) < \epsilon_+$ it is often necessary to introduce a small, positive imaginary part to the wavenumber, k. In what follows below, this is assumed. Usually, it is also necessary to decompose a forcing term into a sum of the form

$$F(s) = F_+(s) + F_-(s). \tag{3.2.2}$$

These factorizations, together with the Wiener-Hopf process, enable one to recast an expression of the form

$$K(s)\Phi_+(s) + \Phi_-(s) + F(s) = 0 \tag{3.2.3}$$

into a form whereby explicit expressions for $\Phi_\pm(s)$ can be obtained. The method is explained in detail below, although a more comprehensive discussion of the Wiener-Hopf technique can be found in Noble (1958), and many specific examples of its applications to problems in structural acoustics can be found, for example Cannell (1975), Brazier-Smith (1987) and Lawrie (1986, 1987).

Apart from the fact that $a = b$ the duct is constructed in the same way as that in section 3.1 and so the non-dimensionalised boundary-value problem has governing equation

$$\nabla^2\phi + \phi = 0, \tag{3.2.4}$$

where $\phi(x, y)$ is the time independent scattered potential and the total field is given by

$$\phi^{tot} = \phi(x, y) + e^{ix}. \tag{3.2.5}$$

The boundary conditions are now

$$\frac{\partial\phi}{\partial y} = 0, \quad y = 0, \quad -\infty < x < \infty, \tag{3.2.6}$$

$$\frac{\partial\phi}{\partial y} = 0, \quad y = a, \quad x < 0, \tag{3.2.7}$$

$$\left\{\frac{\partial^2}{\partial x^2} + \mu^2\right\}\phi_y + \alpha\phi = -\alpha e^{ix}, \quad y = a, \quad x > 0. \tag{3.2.8}$$

As in section 3.1, one of two possible edge conditions must be applied at the point $y = a, x = 0$. The choice is either

$$\phi_y(0^+, a) = 0 \tag{3.2.9}$$

or

$$\phi_{xy}(0^+, a) = 0 \tag{3.2.10}$$

where the superscript '+' indicates that these edge conditions are to be applied on the edge to the right of the line $x = 0$, see figure 3.2.

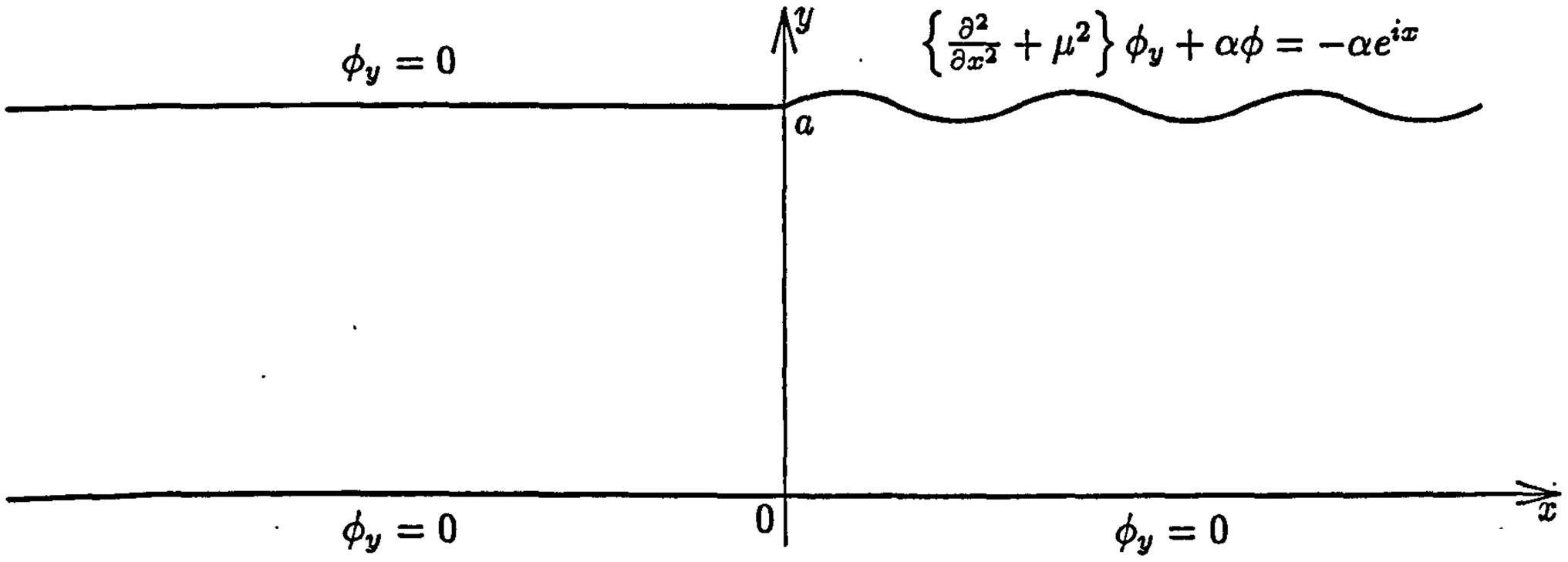

Figure 3.2: Physical configuration for the problem of section 3.2

On taking the full-range Fourier transform of the governing equation, it is found that

$$\Phi_{yy} - \gamma^2\Phi = 0 \tag{3.2.11}$$

where $\Phi(s, y)$ is the Fourier transform of $\phi(x, y)$ and $\gamma = (s^2 - 1)^{\frac{1}{2}}$, and so

$$\Phi(s, y) = A(s)\cosh(\gamma y) + B(s)\sinh(\gamma y). \tag{3.2.12}$$

The Fourier transform of boundary condition (3.2.6), is

$$\Phi_y(s, 0) = 0 \tag{3.2.13}$$

which implies that $B(s) = 0$ in (3.2.12). Hence

$$\Phi(s, y) = A(s)\cosh(\gamma y). \tag{3.2.14}$$

The full-range Fourier transform can be defined as the sum of half-range transforms, viz

$$\begin{aligned}\Phi(s, y) &= \int_{-\infty}^{0} \phi(x, y)e^{isx}dx + \int_{0}^{\infty} \phi(x, y)e^{isx}dx \\ &= \Phi_-(s, y) + \Phi_+(s, y).\end{aligned} \tag{3.2.15}$$

Hence, on applying the lower half-range transform to the boundary condition on the upper surface of the duct for $x < 0$, it is found that

$$\Phi_{y-}(s, a) = 0. \tag{3.2.16}$$

Now, on differentiating (3.2.14) with respect to y,

$$\Phi_y(s, a) = \Phi_{y-}(s, a) + \Phi_{y+}(s, a) = A(s)\gamma\sinh(\gamma a) \tag{3.2.17}$$

and so, using (3.2.16), it is clear that

$$A(s) = \frac{\Phi_{y+}(s,a)}{\gamma \sinh(\gamma a)}. \tag{3.2.18}$$

It follows that

$$\Phi(s,y) = \Phi_{y+}(s,a)\frac{\cosh(\gamma y)}{\gamma \sinh(\gamma a)} \tag{3.2.19}$$

which can be recast as

$$\Phi_+(s,a) = \Phi_{y+}(s,a)\frac{\cosh(\gamma a)}{\gamma \sinh(\gamma a)} - \Phi_-(s,a). \tag{3.2.20}$$

Now, on taking the upper half-range Fourier transform of boundary condition, (3.2.8), it is seen that

$$\int_0^\infty \phi_{yxx} e^{isx} dx + \mu^2 \Phi_{y+}(s,a) + \alpha \Phi_+(s,a) = -\int_0^\infty \alpha e^{ix(1+s)} dx \tag{3.2.21}$$

which can be integrated to obtain

$$p(s) - (s^2 - \mu^2)\Phi_{y+}(s,a) + \alpha \Phi_+(s,a) = -\frac{i\alpha}{1+s} \tag{3.2.22}$$

where

$$p(s) = -\phi_{yx}(0,a) + is\phi_y(0,a). \tag{3.2.23}$$

It is also worthy of note that the right hand side of (3.2.22) contains a singularity in the lower half-plane, at $s = -1$. This will be of significance later in the method. On eliminating $\Phi_+(s,a)$ between (3.2.22) and (3.2.20), the Wiener-Hopf equation is obtained, namely

$$K(s)\Phi_{y+}(s,a) + \alpha \Phi_-(s,a) - p(s) - \frac{i\alpha}{1+s} = 0 \tag{3.2.24}$$

where the kernel, $K(s)$, is defined as

$$K(s) = s^2 - \mu^2 - \frac{\alpha \cosh(\gamma a)}{\gamma \sinh(\gamma a)}. \tag{3.2.25}$$

Equation (3.2.24) is now in the form prescribed by (3.2.3) and is valid only in the strip of analyticity (see figure 3.3).

As mentioned above, a product factorization may be defined for $K(s)$ such that

$$K(s) = K_+(s)K_-(s) \tag{3.2.26}$$

where

$$K_+(-s) = K_-(s). \tag{3.2.27}$$

This factorization is performed later in the section, but for now it is only necessary to know that it can be done. The aim is to rearrange (3.2.24) so that all functions that are regular and non-zero in the region $\epsilon > \epsilon_-$ are on the left hand side of the expression and

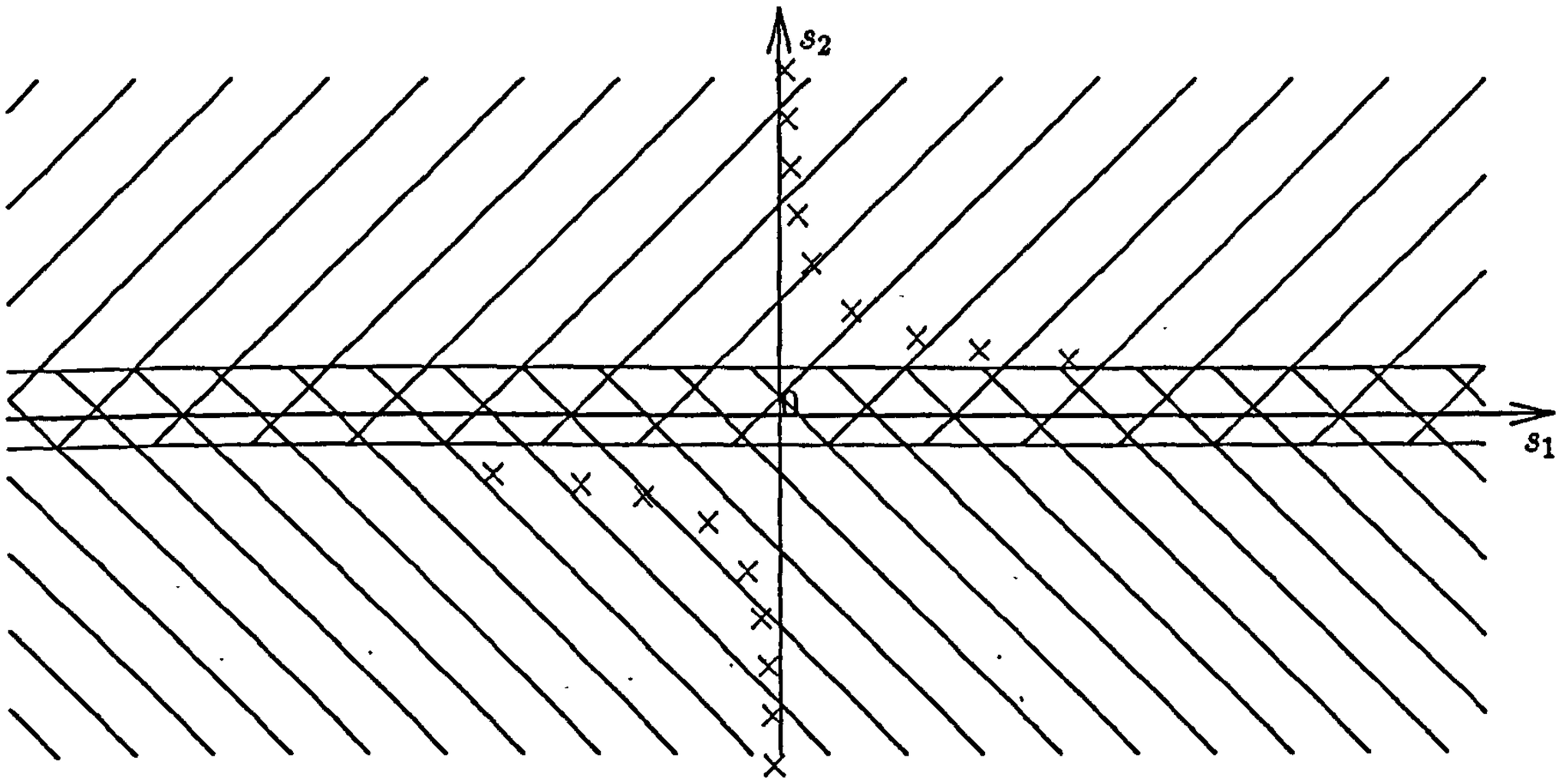

Figure 3.3: The complex s-plane

those that are regular and non-zero in the region $\epsilon < \epsilon_+$ are on the right. On dividing (3.2.24) throughout by $K_-(s)$ it is found that

$$K_+(s)\Phi_{y+}(s,a) = \frac{p(s)}{K_-(s)} + \frac{i\alpha}{K_-(s)(1+s)} - \frac{\alpha\Phi_-(s,a)}{K_-(s)}. \tag{3.2.28}$$

There remains only one problem with this expression which occurs in the second term on the right hand side. This does not completely fulfill the criteria set out above, because $1/(1+s)$ has a singularity at $s=-1$ and is, therefore, not regular in the region $\epsilon < \epsilon_+$. However, this can be overcome by performing a sum split on the term in question, that is

$$\frac{i\alpha}{K_-(s)(1+s)} = \frac{i\alpha}{(1+s)}\left[\frac{1}{K_-(s)} - \frac{1}{K_+(1)}\right] + \frac{i\alpha}{K_+(1)(1+s)}. \tag{3.2.29}$$

On substituting this into (3.2.28) it is found that

$$K_+(s)\Phi_{y+}(s,a) - \frac{i\alpha}{K_+(1)(1+s)} = \frac{p(s)}{K_-(s)} + \frac{i\alpha}{(1+s)}\left[\frac{1}{K_-(s)} - \frac{1}{K_+(1)}\right] - \frac{\alpha\Phi_-(s,a)}{K_-(s)}. \tag{3.2.30}$$

As mentioned above, this expression is valid only in the strip of analyticity, $\epsilon_- < \epsilon < \epsilon_+$. However, analytic continuation can now be used to extend the definition of both sides of (3.2.30) beyond the strip. It is easily shown that

$$K_\pm(s) = O(s), \quad |s| \to \infty, \tag{3.2.31}$$

$$p(s) = O(s), \quad |s| \to \infty, \tag{3.2.32}$$

and also that

$$\Phi_{y+}(s,a) = O(s^{-\beta}), \quad |s| \to \infty, \quad 0 \le \beta < 1, \tag{3.2.33}$$

implying that $\phi_y(x,a)$ has, at worst, an integrable singularity. It follows that the left hand side of (3.2.30) is of order $s^{1-\beta}, s \to \infty$ in the strip whilst the right hand side is of order

1. Thus, appealing to Liouville's theorem, it is apparent that both sides must be equal to some constant. Later in this section, an expression for $K_+(s)$ is found, given in (3.2.85). This is later expanded in (3.2.95) from which it is easy to see that

$$K_+(s) \sim -is, \qquad s \to \infty. \tag{3.2.34}$$

Thus, when this is considered in relation to (3.2.28), it can be seen that this constant is $\phi_y(0,a)$ and so,

$$K_+(s)\Phi_{y+}(s,a) - \frac{i\alpha}{K_+(1)(1+s)} = -\phi_y(0,a) \tag{3.2.35}$$

from which it is seen that

$$\Phi_{y+}(s,a) = \frac{i\alpha}{K_+(1)K_+(s)(1+s)} - \frac{\phi_y(0,a)}{K_+(s)}. \tag{3.2.36}$$

It remains to evaluate $\phi_y(0,a)$ by application of an edge condition. The two possible choices, as detailed in (3.2.9) and (3.2.10) are taken in turn.

Case(i): $\phi_y(0,a) = 0$

In the case where $\phi_y(0,a) = 0$, it is easily seen that (3.2.36) becomes

$$\Phi_{y+}(s,a) = \frac{i\alpha}{K_+(1)K_+(s)(1+s)} \tag{3.2.37}$$

and it follows from (3.2.19) that

$$\Phi(s,y) = \frac{i\alpha\cosh(\gamma y)}{K_+(1)K_+(s)(1+s)\gamma\sinh(\gamma a)}. \tag{3.2.38}$$

Hence,

$$\phi(x,y) = \frac{1}{2\pi}\int_{-\infty}^{\infty} \frac{i\alpha\cosh(\gamma y)e^{-isx}}{K_+(1)K_+(s)(1+s)\gamma\sinh(\gamma a)}ds. \tag{3.2.39}$$

Case(ii): $\phi_{yx}(0,a) = 0$

On comparing (3.2.33) and (3.2.36), it is clear that $\beta = 1$ and so

$$\Phi_{y+}(s,a) = \int_0^{\infty} \phi_y(x,a)e^{isx}dx. \tag{3.2.40}$$

The form of $\Phi_{y+}(s,a)$ as $s \to \infty$ can be obtained by replacing $\phi_y(x,a)$ by its MacLaurin expansion. Hence, on evaluating the first two terms it is found that

$$\Phi_{y+}(s,a) \approx \frac{i}{s}\phi_y(0,a) - \frac{1}{s^2}\phi_{yx}(0,a) + \ldots, |s| \to \infty. \tag{3.2.41}$$

Now, to complete the expression for $\Phi_{y+}(s,a)$ as given in (3.2.35), $\phi_y(0,a)$ must be evaluated, and to accomplish this the right hand side must be expanded in powers of s so that a comparison with (3.2.41) can be made. For this purpose $K_+(s)$ is expressed as

$$K_+(s) \sim is\left(1 + \frac{\kappa}{s}\right) + \ldots \tag{3.2.42}$$

where κ is the constant term in the asymptotic expansion of $K_+(s)$ and will be calculated later in the section. So, using this in (3.2.36), it is found that

$$\Phi_{y+}(s,a) \sim \frac{\alpha\left(1+\frac{\kappa}{s}\right)^{-1}\left(1+\frac{1}{s}\right)^{-1}}{K_+(1)s^2} + \frac{i\phi_y(0,a)\left(1+\frac{\kappa}{s}\right)^{-1}}{s} + \ldots. \tag{3.2.43}$$

This can be expanded using the binomial expansion to give

$$\begin{aligned}\Phi_{y+}(s,a) \sim\ & \frac{\alpha}{K_+(1)s^2}\left(1-\frac{\kappa}{s}+\frac{\kappa^2}{s^2}+\ldots\right)\left(1-\frac{1}{s}+\frac{1}{s^2}+\ldots\right) \\ & +\frac{i\phi_y(0,a)}{s}\left(1-\frac{\kappa}{s}+\frac{\kappa^2}{s^2}+\ldots\right),\end{aligned} \tag{3.2.44}$$

which can be rearranged as

$$\Phi_{y+}(s,a) \sim \frac{i\phi_y(0,a)}{s} + \frac{1}{s^2}\left\{\frac{\alpha}{K_+(1)} - i\kappa\phi_y(0,a)\right\} + O\left(\frac{1}{s^3}\right). \tag{3.2.45}$$

On comparing this with (3.2.41) it is clear, since $\phi_{yx}(0,a)=0$, that

$$\phi_y(0,a) = -\frac{i\alpha}{K_+(1)\kappa}. \tag{3.2.46}$$

Hence,

$$\Phi_{y+}(s,a) = \frac{i\alpha}{K_+(s)K_+(1)}\left[\frac{1}{1+s}+\frac{1}{\kappa}\right], \tag{3.2.47}$$

and from (3.2.19)

$$\Phi(s,y) = \frac{i\alpha\cosh(\gamma y)}{K_+(s)K_+(1)\gamma\sinh(\gamma y)}\left[\frac{1}{1+s}+\frac{1}{\kappa}\right]. \tag{3.2.48}$$

By combining this with the result from the application of the previous edge condition, it follows that

$$\phi(x,y) = \frac{1}{2\pi}\int_{-\infty}^{\infty}\frac{i\alpha\cosh(\gamma y)e^{-isx}}{K_+(s)K_+(1)\gamma\sinh(\gamma a)}\left\{\frac{1}{1+s}+D\right\}ds. \tag{3.2.49}$$

where

$$D = \begin{cases} 0, & \phi_y(0,a)=0 \\ \frac{1}{\kappa}, & \phi_{yx}(0,a)=0 \end{cases}. \tag{3.2.50}$$

Expressions for $\phi(x,y)$, valid for the two edge conditions, $\phi_y(0,a)=0$ and $\phi_{yx}(0,a)=0$, have been found. To find analytic expressions for specific reflected and transmitted modes, $\phi(x,y)$ must be evaluated using residue calculus. Here, it is only the fundamental reflected and transmitted modes which are of interest. The relevent pole for the fundamental reflected pole is at $s=1$. Since $x<0$, the contour of integration is closed in the upper half-plane and so

$$\begin{aligned}\rho(\phi,1) &= \lim_{s\to 1}\left[\frac{-(s-1)\alpha\cosh(\gamma y)e^{-isx}}{K_+(1)K_+(s)\gamma\sinh(\gamma a)}\left\{\frac{1}{1+s}+D\right\}\right] \\ &= \frac{-\alpha e^{-ix}E}{4a[K_+(1)]^2} \\ &= R_0 e^{-ix}\end{aligned} \tag{3.2.51}$$

where $\rho(\phi, 1)$ is used to denote the residue of ϕ at $s = 1$ and

$$E = \begin{cases} 1, & \phi_y(0,a) = 0 \\ \frac{2+\kappa}{\kappa}, & \phi_{yx}(0,a) = 0 \end{cases} . \tag{3.2.52}$$

Thus,

$$|R_0| = \frac{\alpha E}{4a[K_+(1)]^2}. \tag{3.2.53}$$

For the fundamental transmitted mode, T_0, a similar process is employed. The relevant pole is now $s = -\nu_0$. Now, $x > 0$ so the contour of integration is closed in the lower half-plane. Note that there is also an additional pole at $s = -1$ which will be captured, corresponding to the forcing wave. This is the same pole that was noted in (3.2.22). With this pole included it should be further noted that the forcing wave is removed from the final value of $|T_0|$. Thus

$$\begin{aligned} \rho(\phi, -\nu_0) &= \lim_{s \to -\nu_0} \left[\frac{-(s+\nu_0)\alpha \cosh(\gamma y) e^{-isx}}{K_+(1)K_+(s)\gamma \sinh(\gamma a)} \left\{ \frac{1}{1+s} + D \right\} \right] \\ &= \frac{-\alpha e^{i\nu_0 x} K_-(-\nu_0) \cosh(\gamma_0 a) F}{4aK_+(1)K'(-\nu_0)(1-\nu_0)\gamma_0 \sinh(\gamma_0 a)} \\ &= T_0 e^{i\nu_0 x} \end{aligned} \tag{3.2.54}$$

where

$$F = \begin{cases} 1, & \phi_y(0,a) = 0 \\ \frac{\kappa+1-\nu_0}{\kappa}, & \phi_{yx}(0,a) = 0 \end{cases} . \tag{3.2.55}$$

Thus

$$|T_0| = \frac{\alpha K_-(-\nu_0) \cosh(\gamma_0 a) F}{4aK_+(1)K'(-\nu_0)(1-\nu_0)\gamma_0 \sinh(\gamma_0 a)}. \tag{3.2.56}$$

3.2.1 Factorisation of the Wiener-Hopf kernel and determination of κ

In order to evaluate expressions (3.2.53) and (3.2.56) for R_0 and T_0 respectively, it is necessary to specify $K_+(s)$ and κ. First consider $K(s)$, that is

$$K(s) = s^2 - \mu^2 - \frac{\alpha \cosh(\gamma a)}{\gamma \sinh(\gamma a)}, \tag{3.2.57}$$

where, as previously, $\gamma = (s^2 - 1)^{\frac{1}{2}}$. This may be rewritten as

$$K(s) = \frac{f(s)}{\gamma \sinh(\gamma a)} \tag{3.2.58}$$

where

$$f(s) = (s^2 - \mu^2)\gamma \sinh(\gamma a) - \alpha \cosh(\gamma a). \tag{3.2.59}$$

Now, $f(s)$ has no poles, but does have an infinite number of zeros located at $s = \pm\nu_n, n = 0, 1, 2, \ldots$. Furthermore, $f(s)$ is an even function of s and hence, can be written in an infinite product representation of the form

$$f(s) = f(0) e^{\frac{s f'(0)}{f(0)}} \prod_{n=0}^{\infty} \left(1 - \frac{s^2}{\nu_n^2} \right), \tag{3.2.60}$$

(see Titchmarsh 1960). By choosing to set $\gamma(0) = -i$ then, from (3.2.59),

$$f(0) = \mu^2 \sin(a) - \alpha \cos(a). \tag{3.2.61}$$

Also,

$$f'(s) = 2s\gamma \sinh(\gamma a) + (s^2 - \mu^2)\left\{\frac{s}{\gamma}\sinh(\gamma a) + sa\cosh(\gamma a)\right\} - \frac{\alpha s a}{\gamma}\sinh(\gamma a) \tag{3.2.62}$$

so that $f'(0) = 0$. Thus, it follows that

$$f(s) = \left\{\mu^2 \sin(a) - \alpha\cos(a)\right\} \prod_{n=0}^{\infty}\left(1 - \frac{s^2}{\nu_n^2}\right). \tag{3.2.63}$$

Now consider $f(s)$ as a function of γ, say $F(\gamma)$, then

$$F(\gamma) = (\gamma^2 + 1 - \mu^2)\gamma \sinh(\gamma a) - \alpha \cosh(\gamma a). \tag{3.2.64}$$

$F(\gamma)$ has zeroes defined by $\gamma = \pm\gamma_n, \gamma_n = (\nu_n^2 - 1)^{\frac{1}{2}}, n = 0, 1, 2, \ldots$. Further, $F(0) = -\alpha$ and

$$F'(\gamma) = 2\gamma^2 \sinh(\gamma a) + (\gamma^2 + 1 - \mu^2)\left[\sinh(\gamma a) + \gamma a \cosh(\gamma a)\right] - \alpha a \sinh(\gamma a) \tag{3.2.65}$$

which implies that $F'(0) = 0$. So $F(\gamma)$ has the infinite product form

$$F(\gamma) = -\alpha \prod_{n=0}^{\infty}\left(1 - \frac{\gamma^2}{\gamma_n^2}\right). \tag{3.2.66}$$

However, using (3.2.59), it is seen that

$$f(0) = F(-i) = \mu^2 \sin(a) - \alpha\cos(a) = -\alpha \prod_{n=0}^{\infty}\left(1 + \frac{1}{\gamma_n^2}\right). \tag{3.2.67}$$

On substituting this into (3.2.63), it is found that

$$\begin{aligned} f(s) &= -\alpha \prod_{n=0}^{\infty}\left(1 + \frac{1}{\gamma_n^2}\right)\left(1 - \frac{s^2}{\nu_n^2}\right) \\ &= -\alpha \prod_{n=0}^{\infty}\left(1 + \frac{1}{\gamma_n^2} - \frac{s^2}{\gamma_n^2}\right) \end{aligned} \tag{3.2.68}$$

which can be factorised to give

$$f(s) = -\alpha \prod_{n=0}^{\infty}\left\{\left(1 + \frac{1}{\gamma_n^2}\right)^{\frac{1}{2}} - \frac{s}{\gamma_n}\right\}\left\{\left(1 + \frac{1}{\gamma_n^2}\right)^{\frac{1}{2}} + \frac{s}{\gamma_n}\right\}, \tag{3.2.69}$$

where the term on the far right has zeroes at $s = -\nu_n, n = 0, 1, 2, \ldots$ and that to its left has zeroes at $s = \nu_n, n = 0, 1, 2, \ldots$.

Now consider the denominator of (3.2.58), that is

$$\gamma \sinh(\gamma a) = (s^2 - 1)g(s) \tag{3.2.70}$$

where

$$g(s) = \frac{\sinh(\gamma a)}{\gamma}. \tag{3.2.71}$$

Note that $g(0) = \sin(a)$ and that

$$g'(s) = \frac{sa\cosh(\gamma a)}{\gamma^2} - \frac{s\sinh(\gamma a)}{\gamma^3} \tag{3.2.72}$$

which implies that $g'(0) = 0$. Also, $g(s)$ has zeroes when $(s^2-1)^{\frac{1}{2}}a = in\pi$, hence $g(s)$ has the infinite product representation

$$g(s) = \sin(a)\prod_{n=1}^{\infty}\left\{1 - \frac{s^2}{1-\frac{n^2\pi^2}{a^2}}\right\}. \tag{3.2.73}$$

The standard infinite product representation of $\sin(a)$, as given in Abramowitz and Stegun (1964), which is

$$\sin(a) = a\prod_{n=1}^{\infty}\left(1 - \frac{a^2}{n^2\pi^2}\right) \tag{3.2.74}$$

can now be used to obtain

$$\begin{aligned}\gamma\sinh(\gamma a) &= a(s^2-1)\prod_{n=1}^{\infty}\left(1-\frac{a^2}{n^2\pi^2}\right)\left\{1 - \frac{s^2}{\left(1-\frac{a^2}{n^2\pi^2}\right)}\right\} \\ &= a(s^2-1)\prod_{n=1}^{\infty}\left\{\left(1-\frac{a^2}{n^2\pi^2}\right) + \frac{a^2s^2}{n^2\pi^2}\right\}.\end{aligned} \tag{3.2.75}$$

It follows then, from (3.2.58), (3.2.69) and (3.2.75) that

$$K(s) = \frac{\alpha\left(1+\frac{1}{\gamma_0^2}-\frac{s^2}{\gamma_0^2}\right)}{a(1-s^2)}\prod_{n=1}^{\infty}\frac{\left\{\left(1+\frac{1}{\gamma_n^2}\right)^{\frac{1}{2}} - \frac{s}{\gamma_n}\right\}\left\{\left(1+\frac{1}{\gamma_n^2}\right)^{\frac{1}{2}} + \frac{s}{\gamma_n}\right\}}{\left\{\left(1-\frac{a^2}{n^2\pi^2}\right)^{\frac{1}{2}} + \frac{ias}{n\pi}\right\}\left\{\left(1-\frac{a^2}{n^2\pi^2}\right)^{\frac{1}{2}} - \frac{ias}{n\pi}\right\}}. \tag{3.2.76}$$

This may be rearranged as

$$K(s) = \frac{\alpha(\nu_0^2-s^2)}{a(\nu_0^2-1)(1-s^2)}\prod_{n=1}^{\infty}\frac{\left\{\frac{\nu_n}{\gamma_n} - \frac{s}{\gamma_n}\right\}\left\{\frac{\nu_n}{\gamma_n} + \frac{s}{\gamma_n}\right\}}{\left\{\left(1-\frac{a^2}{n^2\pi^2}\right)^{\frac{1}{2}} + \frac{ias}{n\pi}\right\}\left\{\left(1-\frac{a^2}{n^2\pi^2}\right)^{\frac{1}{2}} - \frac{ias}{n\pi}\right\}}, \tag{3.2.77}$$

which is now in a form that can be factorised by inspection. Hence

$$K_{\pm}(s) = \left\{\frac{\alpha}{a(\nu_0^2-1)}\right\}^{\frac{1}{2}}\frac{(\nu_0 \pm s)e^{\mp\chi(s)}}{1\pm s}\prod_{n=1}^{\infty}\frac{\left\{\frac{\nu_n}{\gamma_n} \pm \frac{s}{\gamma_n}\right\}e^{\pm\sigma(s,n)}}{\left\{\left(1-\frac{a^2}{n^2\pi^2}\right)^{\frac{1}{2}} \mp \frac{ias}{n\pi}\right\}} \tag{3.2.78}$$

where $\chi(s)$ is chosen to ensure that $K_{\pm}(s)$ is of algebraic growth as $s \to \infty$, and $\sigma(s,n)$ is chosen to improve the convergence of the infinite product. Also, since $\sigma(s,n)$ is artificially added into the infinite product $\chi(s)$ must cancel the terms of $\sigma(s,n)$.

In order to determine $\sigma(s,n)$ it is necessary to consider the behaviour of the terms of the product as $n \to \infty$. This requires knowledge of the roots of $K(s)$ as $n \to \infty$. It can be seen that

$$\nu_n \sim \frac{i\pi n}{a}, \qquad n \gg 1 \tag{3.2.79}$$

for all α, but the order of the next term is unclear for general α – at worst it will be $O(1)$. Also

$$\begin{aligned} \gamma_n &= (\nu_n^2 - 1)^{\frac{1}{2}} \\ &= \nu_n \left(1 - \frac{1}{\nu_n^2}\right)^{\frac{1}{2}} \\ &\sim \nu_n - \frac{1}{2\nu_n} + \ldots. \end{aligned} \tag{3.2.80}$$

Now consider the terms of the product form of $K_+(s)$. Expanding these in powers of n gives

$$\begin{aligned} &\frac{\nu_n}{\gamma_n}\left\{1 + \frac{s}{\nu_n}\right\}\left\{\left(1 - \frac{a^2}{n^2\pi^2}\right)^{\frac{1}{2}} - \frac{ias}{n\pi}\right\}^{-1} \\ &\qquad \sim \left\{1 + \frac{1}{2\nu_n^2} + O\left(\frac{1}{\nu_n^4}\right)\right\}\left\{1 + \frac{s}{\nu_n}\right\}\left\{1 + \frac{ias}{n\pi} - \frac{a^2}{2n^2\pi^2} - \frac{a^2s^2}{n^2\pi^2}O\left(\frac{1}{n^3}\right)\right\} \\ &\qquad \sim 1 + \frac{s}{\nu_n} + \frac{1}{2\nu_n^2} + \frac{ias}{n\pi} + \frac{ias^2}{n\pi\nu_n} + \frac{a^2}{2n^2\pi^2} - \frac{a^2s^2}{n^2\pi^2} + O\left(\frac{1}{n^3}\right) \\ &\qquad \sim 1 + \frac{s}{\nu_n} + \frac{ias}{n\pi} + O\left(\frac{1}{n^2}\right). \end{aligned} \tag{3.2.81}$$

Thus, using the assumption made in (3.2.79), it is clear that the product part of $K_+(s)$ converges like $\frac{1}{n^2}$. Hence, the choice

$$\sigma(s,n) \sim -\frac{s}{\nu_n} - \frac{ias}{n\pi} \tag{3.2.82}$$

results in the product converging like $\frac{1}{n^3}$.

The growth of the product part of $K_+(s)$ is already algebraic as $s \to \infty$. Hence, no adjustment is needed for this, but $\chi(s)$ must still be chosen to cancel with the terms now included to improve the convergence within the infinite product. Thus

$$e^{-\chi(s)} = \prod_{n=1}^{\infty} e^{\frac{s}{\nu_n} + \frac{ias}{n\pi}} \tag{3.2.83}$$

which implies that

$$\chi(s) = -s\sum_{n=1}^{\infty} \frac{ia}{n\pi} + \frac{1}{\nu_n}. \tag{3.2.84}$$

It follows directly that

$$K_{\pm}(s) = \left\{\frac{\alpha}{a(\nu_0^2 - 1)}\right\}^{\frac{1}{2}} \frac{(\nu_0 \pm s)e^{\pm s\sum_{n=1}^{\infty}\frac{ia}{n\pi} + \frac{1}{\nu_n}}}{1 \pm s} \prod_{n=1}^{\infty} \frac{\left\{\frac{\nu_n}{\gamma_n} \pm \frac{s}{\gamma_n}\right\} e^{\mp\left(\frac{s}{\nu_n} + \frac{ias}{n\pi}\right)}}{\left\{\left(1 - \frac{a^2}{n^2\pi^2}\right)^{\frac{1}{2}} \mp \frac{ias}{n\pi}\right\}}. \tag{3.2.85}$$

Now to complete the evaluation of $\phi(x,y)$, all that is required is an expression for κ, the constant term in the expansion of $K_+(s)$. As stated in (3.2.42), $K_+(s)$ can be expressed as

$$K_+(s) \sim is\left(1+\frac{\kappa}{s}\right)+\ldots. \tag{3.2.86}$$

By taking logarithms of $K(s)$ and integrating such that the contour of integration lies below any singularities it is found that

$$\ln\left[K_+(s)\right] = \frac{1}{2\pi i}\int_{-\infty}^{\infty}\ln\left[K(\zeta)\right]\frac{d\zeta}{\zeta-s}. \tag{3.2.87}$$

Thus, substituting in for $K(s)$ from (3.2.25) gives

$$\ln\left[K_+(s)\right] = \frac{1}{2\pi i}\int_{-\infty}^{\infty}\ln\left[\zeta^2-\mu^2-\frac{\alpha\cosh(\gamma a)}{\gamma\sinh(\gamma a)}\right]\frac{d\zeta}{\zeta-s}. \tag{3.2.88}$$

This expression can be rearranged as

$$\ln\left[K_+(s)\right] = \frac{1}{2\pi i}\int_{-\infty}^{\infty}\ln(\zeta^2-\mu^2)\frac{d\zeta}{\zeta-s}+\frac{1}{2\pi i}\int_{-\infty}^{\infty}\ln\left[1-\frac{\alpha\cosh(\gamma a)}{(\zeta^2-\mu^2)\gamma\sinh(\gamma a)}\right]\frac{d\zeta}{\zeta-s}. \tag{3.2.89}$$

Now consider the first integral alone. Let

$$f(s) = f_+(s)f_-(s) = s^2-\mu^2 \tag{3.2.90}$$

where $f_+(-s) = f_-(s)$. When this condition is enforced on $f_\pm(s)$ it is found that $f_+(s) = (s+\mu)e^{\frac{i\pi}{2}}$ and so, using this in (3.2.89) gives

$$\ln\left[K_+(s)\right] = \ln\left[(s+\mu)e^{\frac{i\pi}{2}}\right]+\frac{1}{2\pi i}\int_{-\infty}^{\infty}\ln\left[1-\frac{\alpha\cosh(\gamma a)}{(\zeta^2-\mu^2)\gamma\sinh(\gamma a)}\right]\frac{d\zeta}{\zeta-s}. \tag{3.2.91}$$

Consider now the second integral in (3.2.89); it can be seen that

$$\begin{aligned}
&\int_{-\infty}^{\infty}\ln\left[1-\frac{\alpha\cosh(\gamma a)}{(\zeta^2-\mu^2)\gamma\sinh(\gamma a)}\right]\frac{d\zeta}{\zeta-s}\\
&\quad= \int_{0}^{\infty}\ln\left[1-\frac{\alpha\cosh(\gamma a)}{(\zeta^2-\mu^2)\gamma\sinh(\gamma a)}\right]\frac{d\zeta}{\zeta-s}\\
&\qquad+\int_{\infty}^{0}\ln\left[1-\frac{\alpha\cosh(\gamma a)}{(\zeta^2-\mu^2)\gamma\sinh(\gamma a)}\right]\frac{d\zeta}{\zeta+s}\\
&\quad= \int_{0}^{\infty}\ln\left[1-\frac{\alpha\cosh(\gamma a)}{(\zeta^2-\mu^2)\gamma\sinh(\gamma a)}\right]\left[\frac{1}{\zeta-s}-\frac{1}{\zeta+s}\right]d\zeta\\
&\quad= 2s\int_{0}^{\infty}\ln\left[1-\frac{\alpha\cosh(\gamma a)}{(\zeta^2-\mu^2)\gamma\sinh(\gamma a)}\right]\frac{d\zeta}{\zeta^2-s^2}.
\end{aligned} \tag{3.2.92}$$

So substituting this into (3.2.91) gives

$$\ln\left[K_+(s)\right] = \ln\left[(s+\mu)e^{\frac{i\pi}{2}}\right]+\frac{1}{s\pi i}\int_{0}^{\infty}\ln\left[1-\frac{\alpha\cosh(\gamma a)}{(\zeta^2-\mu^2)\gamma\sinh(\gamma a)}\right]\left(1-\frac{\zeta^2}{s^2}\right)^{-1}d\zeta. \tag{3.2.93}$$

Now, breaking the range of integration at the point R, where $1 \ll R \ll |s|$, and expanding $\left(1-\frac{\zeta^2}{s^2}\right)^{-1}$ binomially, (3.2.93) becomes

$$\ln\left[K_+(s)\right] = \ln\left[(s+\mu)e^{\frac{i\pi}{2}}\right] + \frac{1}{s\pi i}\int_0^R \ln\left[1-\frac{\alpha\cosh(\gamma a)}{(\zeta^2-\mu^2)\gamma\sinh(\gamma a)}\right]\left(1+\frac{\zeta^2}{s^2}+\ldots\right)d\zeta$$
$$+\frac{1}{s\pi i}\int_R^\infty \ln\left[1-\frac{\alpha}{\zeta^3}\right]\left(1-\frac{\zeta^2}{s^2}\right)^{-1}d\zeta. \qquad (3.2.94)$$

Then, as $R\to\infty$, the last integral in (3.2.94) tends to zero and so

$$K_+(s) = (s+\mu)e^{\frac{i\pi}{2}}e^{-\frac{\Lambda}{s\pi i}}$$
$$= (s+\mu)e^{\frac{i\pi}{2}}\left\{1-\frac{\Lambda}{s\pi i}+\ldots\right\} \qquad (3.2.95)$$

where

$$\Lambda = \int_0^\infty \ln\left[1-\frac{\alpha\cosh(\gamma a)}{(\zeta^2-\mu^2)\gamma\sinh(\gamma a)}\right]d\zeta. \qquad (3.2.96)$$

Thus, when multiplied out this becomes

$$K_+(s) = is\left[1+\frac{\mu-\frac{\Lambda}{\pi i}}{s}+O\left(\frac{1}{s^2}\right)\right], \qquad (3.2.97)$$

and when this is compared with (3.2.86) it is clear that

$$\kappa = \mu+\frac{i}{\pi}\int_0^\infty \ln\left[1-\frac{\alpha\cosh(\gamma a)}{(\zeta^2-\mu^2)\gamma\sinh(\gamma a)}\right]d\zeta. \qquad (3.2.98)$$

Hence, the expressions for R_0 and T_0 can now be evaluated using *Mathematica* (the code for this is found in Appendix B.2) and the results gained can be compared with those gained for the solution found in section 3.1 in the case where $a=b$.

3.3 Results

Figures 3.4 and 3.5 show the modulus of the fundamental reflected and transmitted modes plotted against α for fixed $a=b=1.6$, $\mu=2.2$ and for the edge condition $\phi_{xy}(0,b)=0$. There are two limiting cases displayed here. In the case where $\alpha \ll 1$ the membrane behaves very much like a rigid surface, and in the case where $\alpha \gg 1$ the membrane is behaving more like a soft boundary. The solid line in figure 3.4 represents the value for $|A_0|/2$ given from solving the system of equations found in section 3.1. The dots are the value of $|R_0|$ found using the solution of the same problem by means of the Wiener-Hopf technique as described in section 3.2. It can be seen that $|R_0|$ has a value of almost zero for $\alpha \ll 1$ which is not surprising since the membrane surface is behaving like a rigid surface and there is no change in height in the duct. Thus the incident field passes straight through with the duct having no affect, and so no reflected field is seen.

The results shown are obviously very good, with little difference evident between the two sets of figures. Figure 3.5 compares $|B_0|-1$ (found in section 3.1) with $|T_0|$ (found

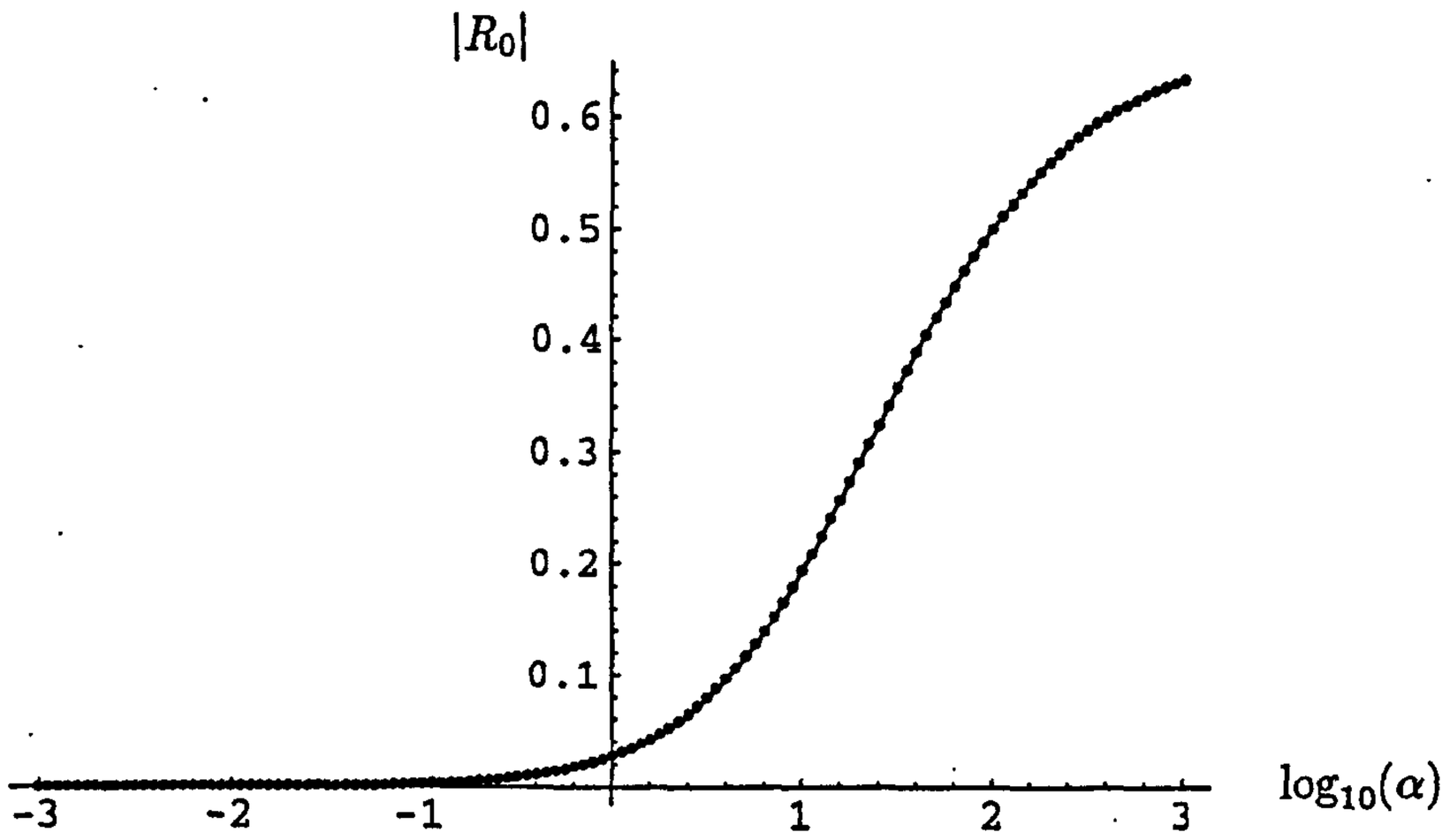

Figure 3.4: Comparison of the modulus of the coefficient for the fundamental reflected mode for the hard/membrane problem with edge condition $\phi_{yx}(0,b) = 0$, $a = b = 1.6$ and $\mu = 2.2$. The eigenfunction expansion results are the solid line and the Wiener-Hopf results are the dots.

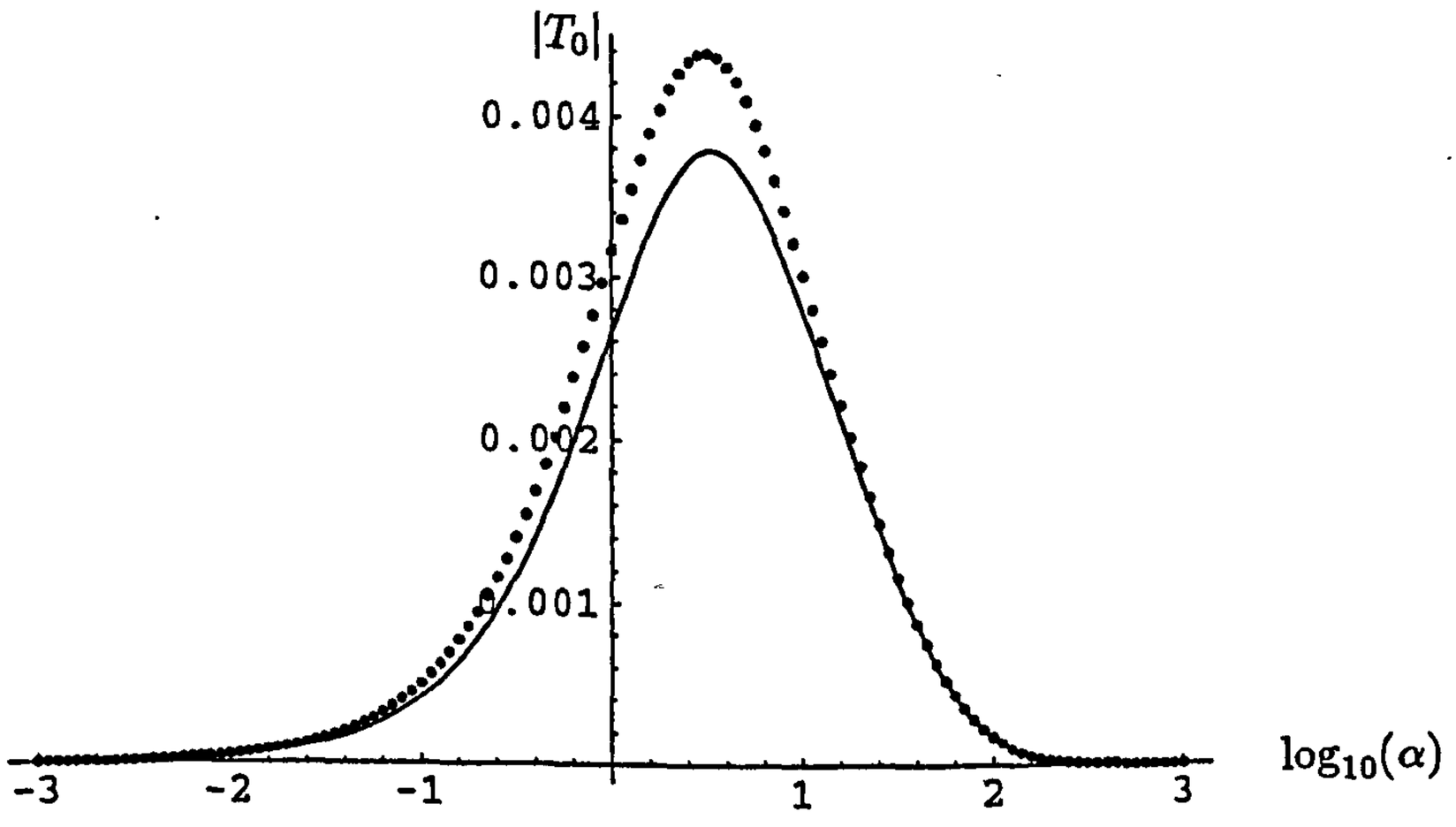

Figure 3.5: Comparison of the modulus of the coefficient for the fundamental transmitted mode for the hard/membrane problem with edge condition $\phi_{yx}(0,b) = 0$, $a = b = 1.6$ and $\mu = 2.2$. The eigenfunction expansion results are the solid line and the Wiener-Hopf results are the dots.

in section 3.2). $|B_0 - 1|$ is used because, as mentioned at the end of section 3.2, the effect of the forcing wave is removed from the expression for $|T_0|$ given in (3.2.54). At first sight this graph appears to be less accurate, but attention should be drawn to the scale on the $|T_0|$ axis. This scale is very fine and so exaggerates any small inaccuracy that may be

evident in the results. Some level of inaccuracy can be expected since the solutions for both the method used in section 3.1 and that for the Wiener-Hopf technique, have been truncated to some degree for the purpose of computation. The accuracy of each set of results could be enhanced by taking further terms in the systems computed, but this is not always possible due to computational time involved in gaining solutions.

When the value of $\alpha \ll 1$ (and so the membrane is behaving much like a hard surface), $|T_0|$ can be seen to be close to zero. In previous results it has been see that in such cases where no change in height is coupled with a purely rigid duct, the fundamental transmitted mode has been equal to 1. However, it is noted again that, for these results, the forcing wave is removed from consideration. Since it is the forcing wave that passes straight through such a duct as this, with no affect on its behaviour, the purely transmitted field can be expected, and indeed is seen, to be zero. Figures 3.6 and 3.7 show the results as described for the previous two graphs, except here the edge condition $\phi_y(0, b)$ is used.

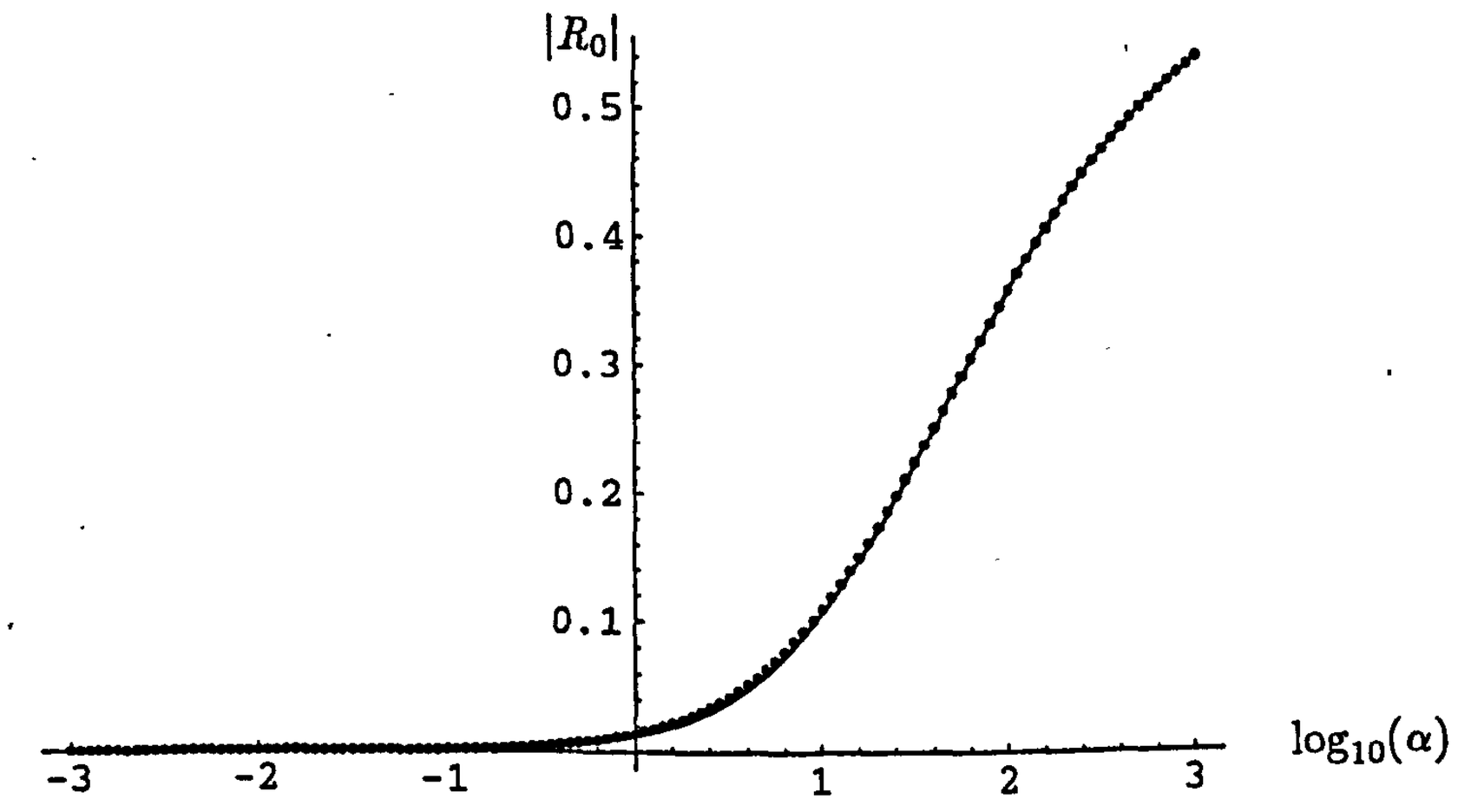

Figure 3.6: Comparison of the modulus of the coefficient for the fundamental reflected mode for the hard/membrane problem with edge condition $\phi_y(0, b) = 0$, $a = b = 1.6$ and $\mu = 2.2$. The eigenfunction expansion results are the solid line and the Wiener-Hopf results are the dots.

Whilst the shapes of the graphs are a little different, the same high level of correlation between the results two sets of results is maintained. The next four graphs (figures 3.8 – 3.11) are for cases where the membrane condition has been made to mimic the behaviour of a Dirichlet condition. To do this α must be very large (in the case here, $\alpha = 5000000$, but it can be taken much higher if necessary to get the correct behaviour) and μ must be relatively small in comparison, ideally $O(1)$. By imposing these conditions, results for the Hard/Membrane case can be compared with those from the Hard/Soft case. The results shown in figures 2.15 – 2.18 are used here to draw a comparison with results found using

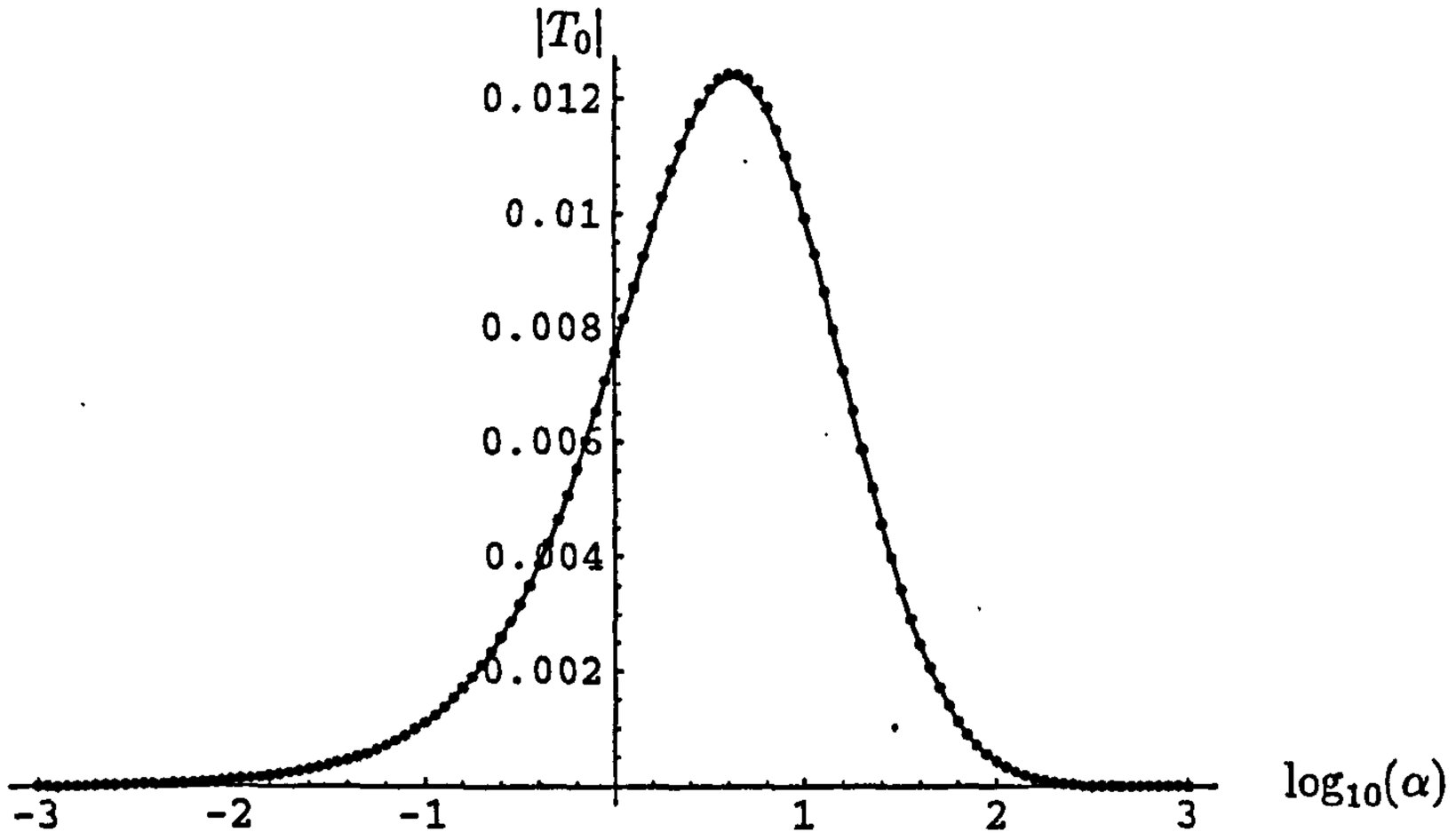

Figure 3.7: Comparison of the modulus of the coefficient for the fundamental transmitted mode for the hard/membrane problem with edge condition $\phi_y(0,b) = 0$, $a = b = 1.6$ and $\mu = 2.2$. The eigenfunction expansion results are the solid line and the Wiener-Hopf results are the dots.

the parameters specified above. All four graphs show excellent agreement between the

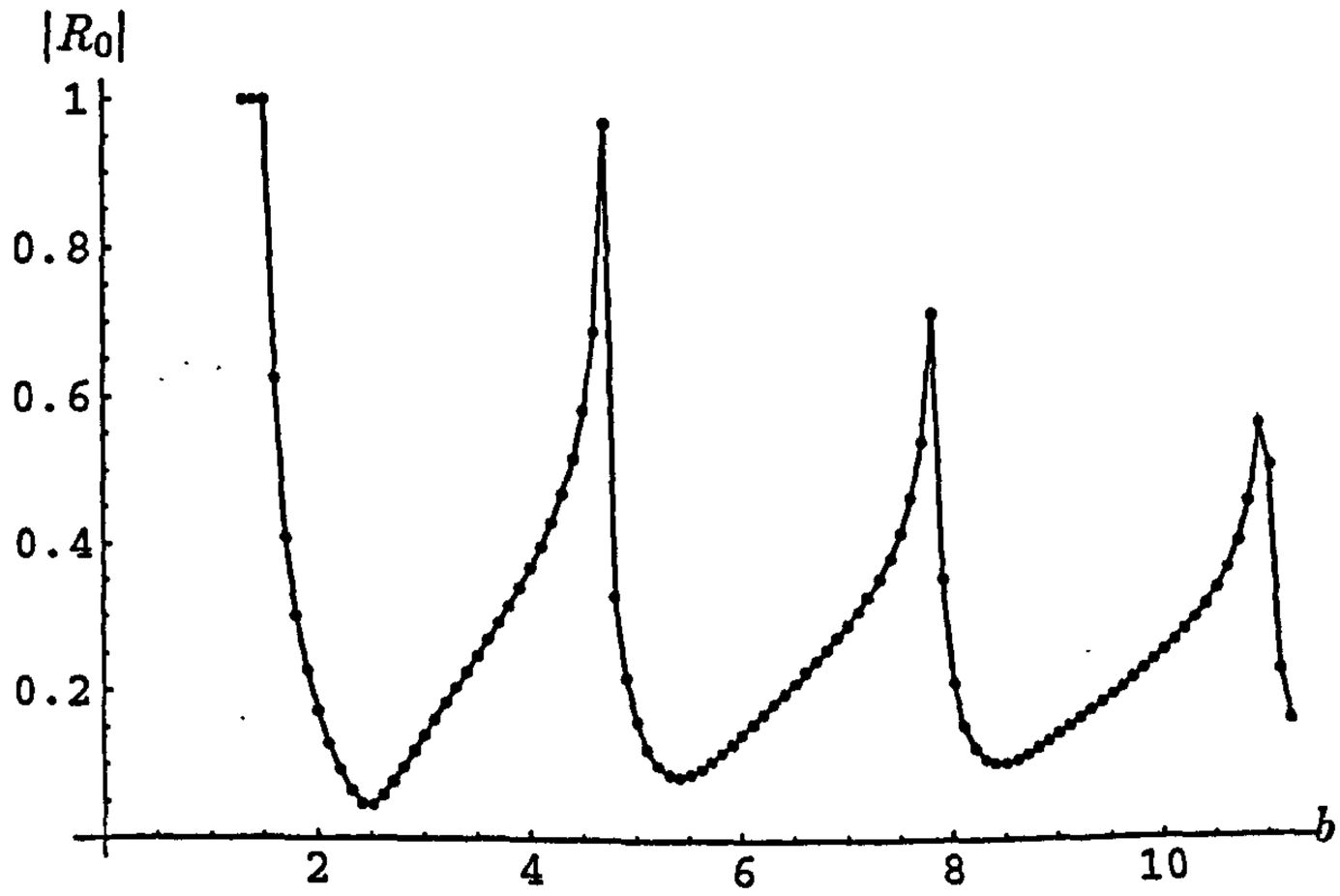

Figure 3.8: Comparison of the modulus of the coefficient for the fundamental reflected mode with $a = 1.211$, $\alpha = 5000000$ and $\mu = 2.2$. The hard/membrane eigenfunction expansion results are the solid line and the hard/soft results (from section 2.6) are the dots.

two sets of results.

As a final set of results, two general cases are considered. The two graphs, figures 3.12

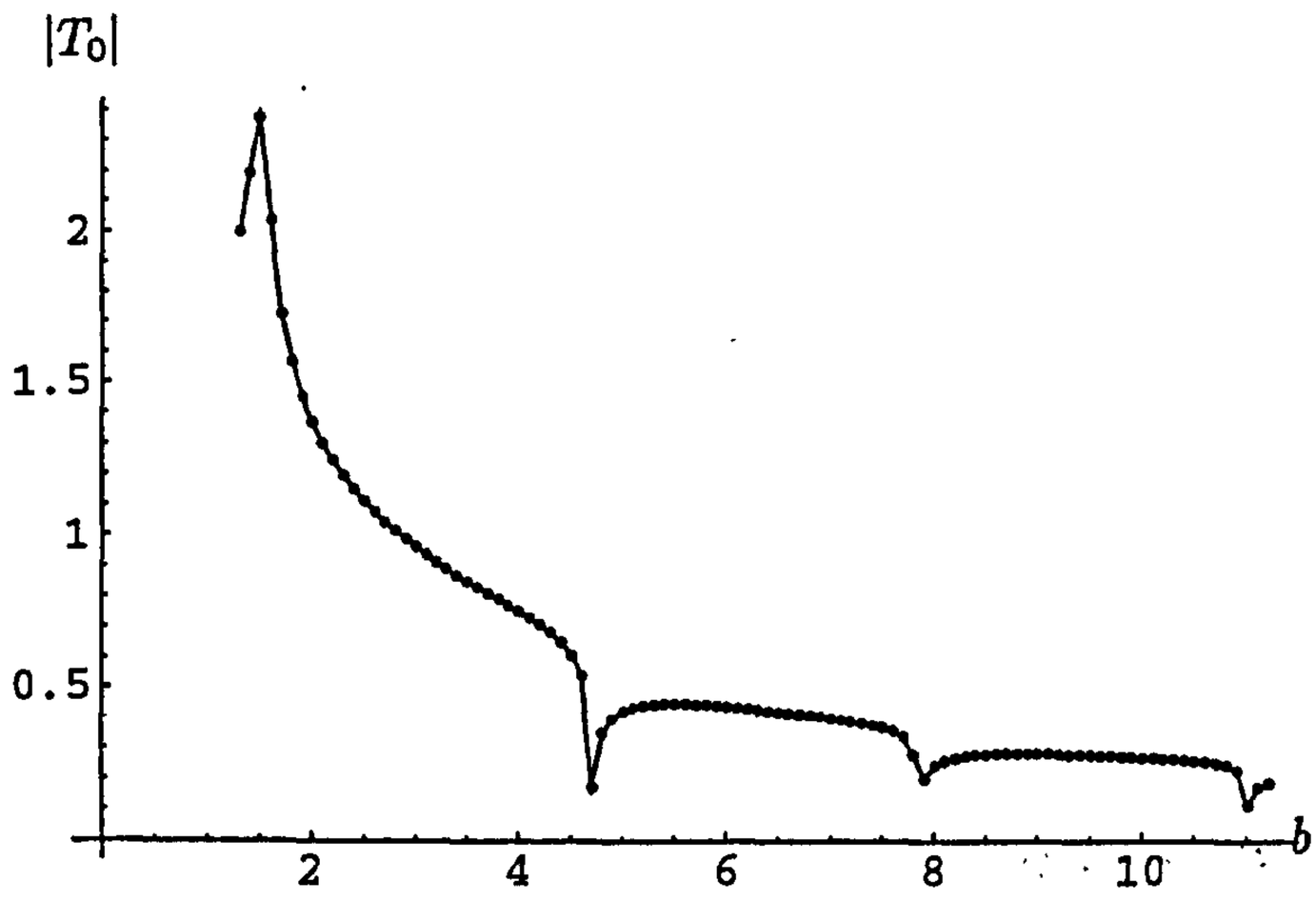

Figure 3.9: Comparison of the modulus of the coefficient for the fundamental transmitted mode with $a = 1.211$, $\alpha = 5000000$ and $\mu = 2.2$. The hard/membrane eigenfunction expansion results are the solid line and the hard/soft results (from section 2.6) are the dots.

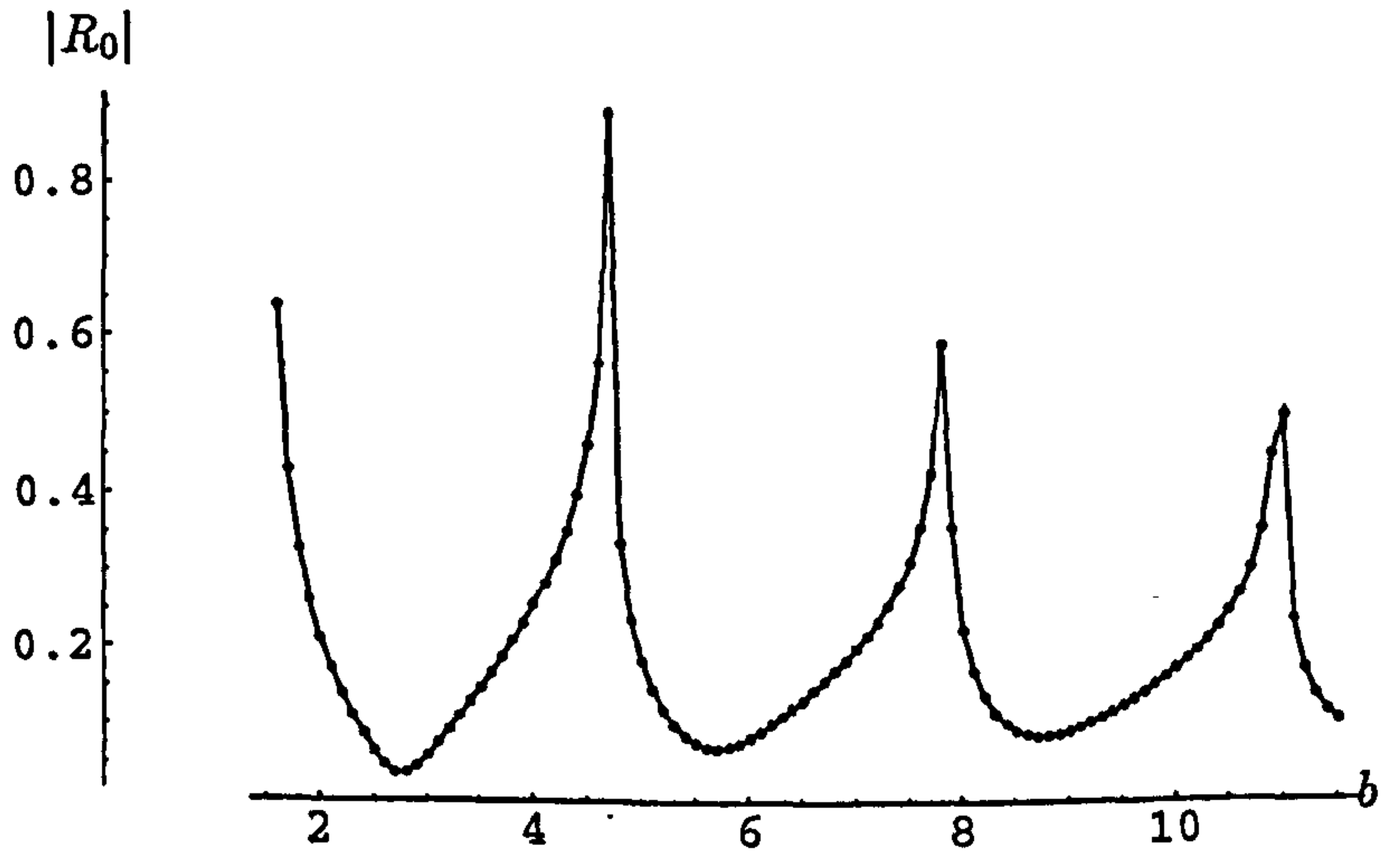

Figure 3.10: Comparison of the modulus of the coefficient for the fundamental reflected mode with $a = 1.51$, $\alpha = 5000000$ and $\mu = 2.2$. The hard/membrane eigenfunction expansion results are the solid line and the hard/soft results (from section 2.6) are the dots.

and 3.13 are both for the case where $a = 1.51$, $\alpha = 50$ and $\mu = 2.2$. In figure 3.12 the edge condition $\phi_{yx}(0, b) = 0$ is applied whereas in figure 3.13, $\phi_y(0, b) = 0$ is used. These results will be used later as a comparison for results gained in chapter 4.

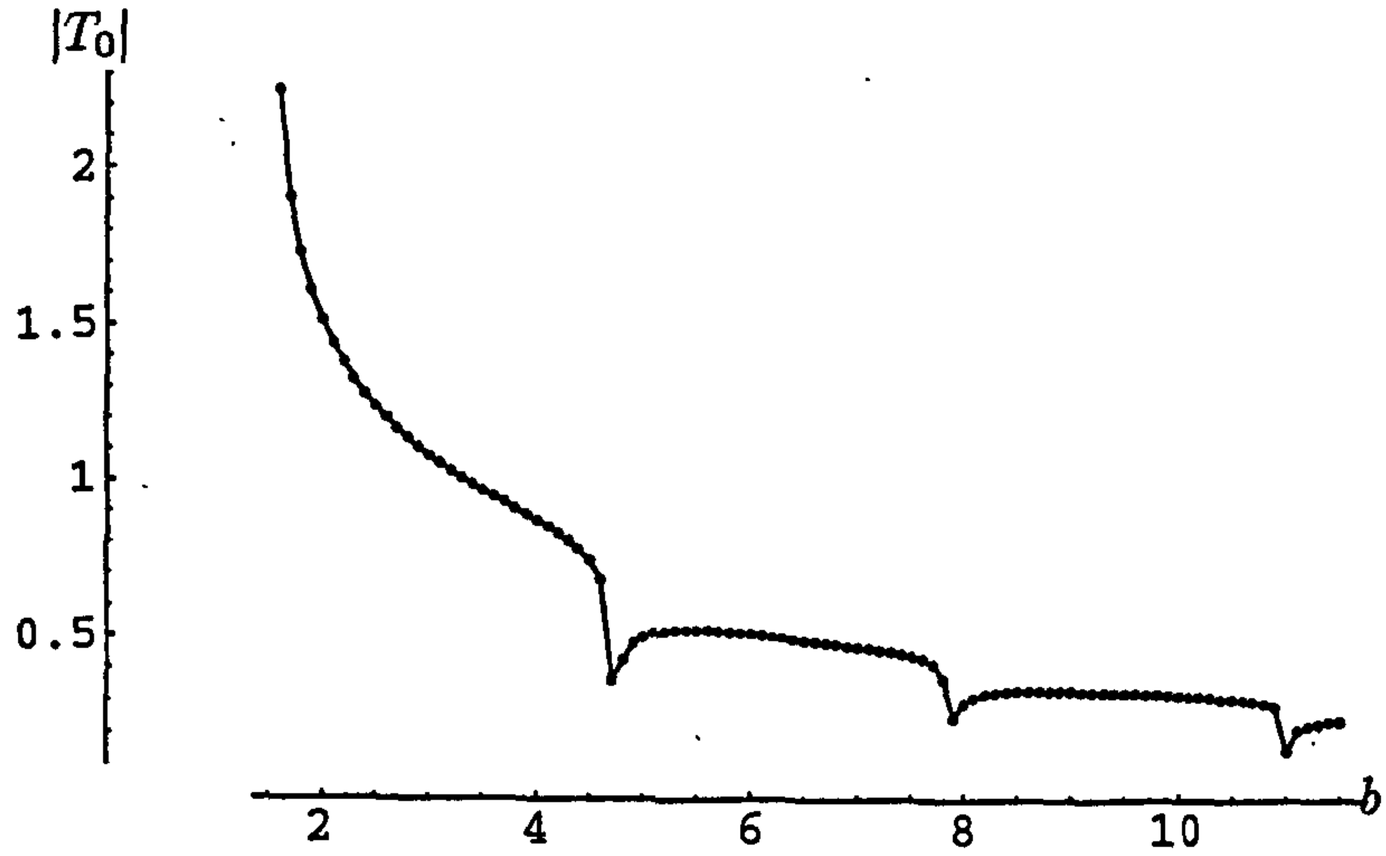

Figure 3.11: Comparison of the modulus of the coefficient for the fundamental reflected mode with $a = 1.51$, $\alpha = 5000000$ and $\mu = 2.2$. The hard/membrane eigenfunction expansion results are the solid line and the hard/soft results (from section 2.6) are the dots.

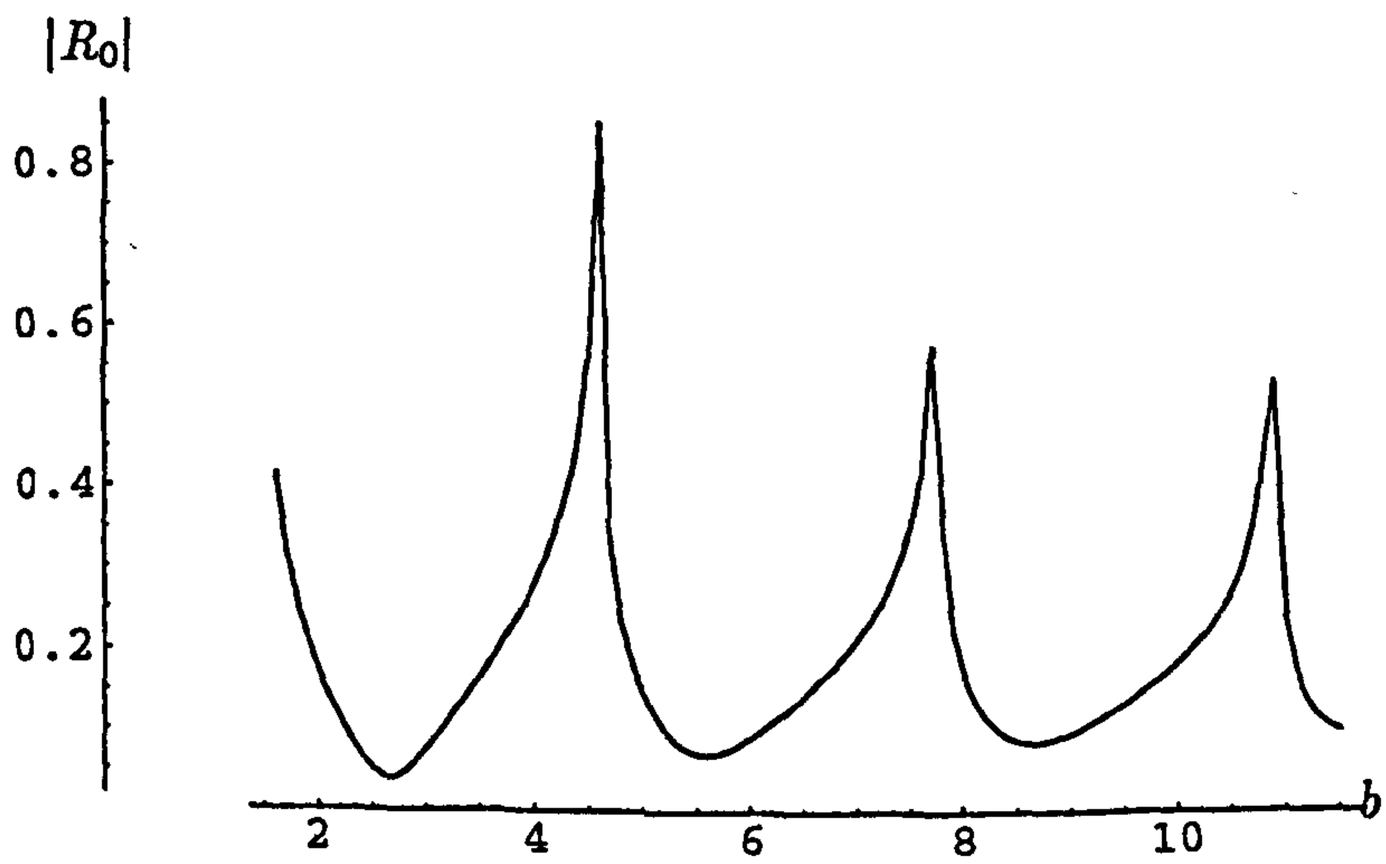

Figure 3.12: Plot of the modulus of the coefficient for the fundamental reflected mode for the hard/membrane problem with edge condition $\phi_{yx}(0,b) = 0$, $a = 1.51$, $\alpha = 50$ and $\mu = 2.2$.

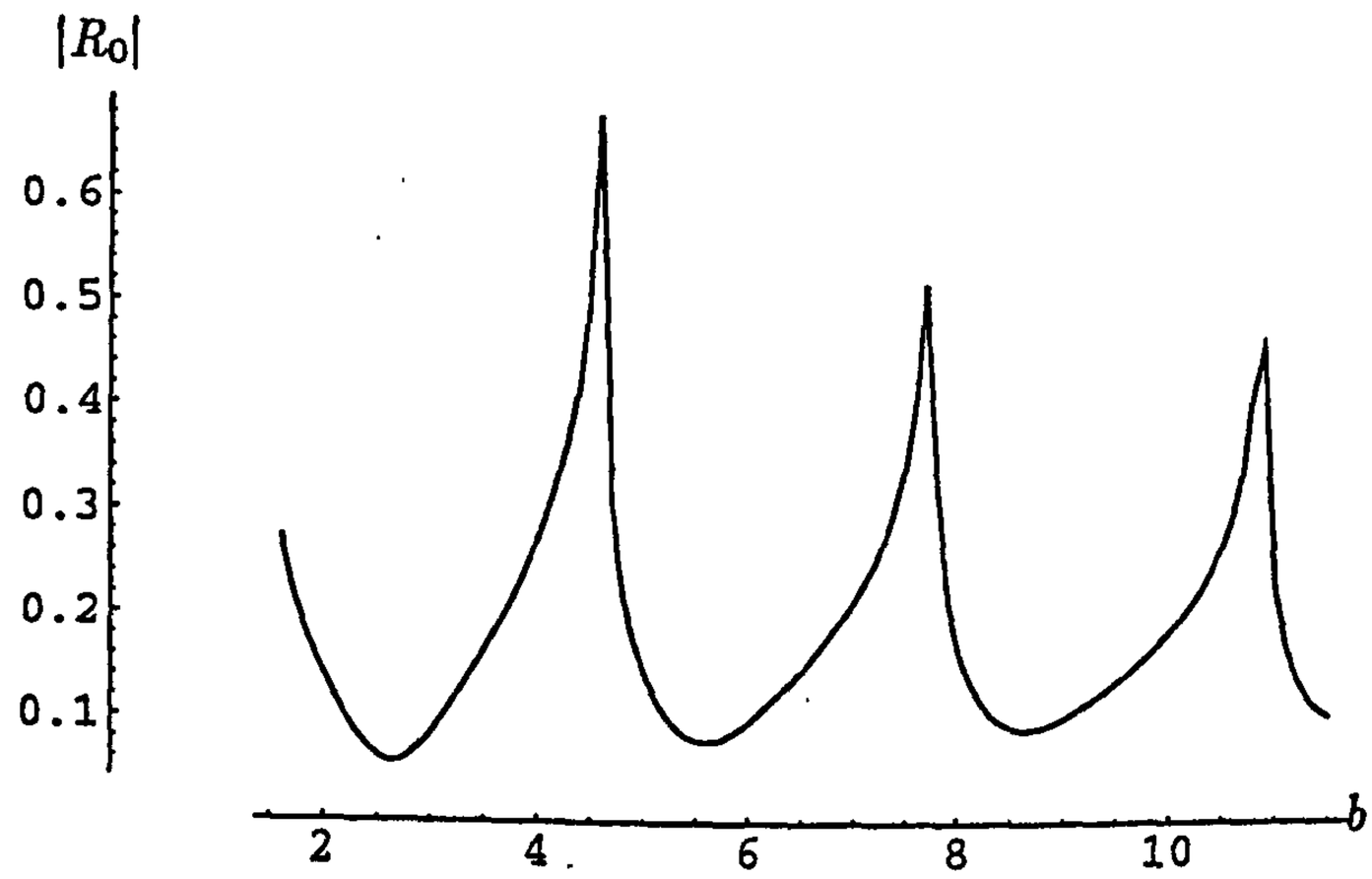

Figure 3.13: Plot of the modulus of the coefficient for the fundamental reflected mode for the hard/membrane problem with edge condition $\phi_y(0,b) = 0$, $a = 1.51$, $\alpha = 50$ and $\mu = 2.2$.

Chapter 4

Refection and transmission at the junction of two membrane bounded ducts of different height

Whilst the problem in Chapter 3 was of considerable interest, not least because it can be solved at all, a problem of greater significance is that comprising two ducts of differring heights, bounded by membranes. The most general case is considered, whereby the material properties of the membranes differ in the two duct regions $0 < y < a$, $x < 0$ and $0 < y < b$, $x > 0$. In this case, it is no longer appropriate to assume a plane incident wave as the duct along which the incident wave travels is not rigid and so the wave will interact in some way with the membrane surface. Instead, forcing is introduced in the form of a fluid-coupled structural wave which propagates in the positive x-direction along the duct lying in $0 \leq y \leq a$, $x < 0$.

In the solution of the problem, Fourier and/or Sturm Liouville techniques are no longer appropriate for either duct region. The orthogonality condition, derived in section 2.6 and used in section 3.1, must now be applied twice. In addition, the problem here considered has two points where membranes meet rigid surfaces and so two edge conditions must be applied. Whereas in Chapter 3 two distinct solutions were found (corresponding to the application of the two different edge conditions), here there will be four distinct solutions as there are four combinations of edge conditions available.

4.1 Solution of the problem

The problem considered in this section is similar to the previous one, in that the duct in question occupies the region $0 \leq y \leq a$, $x < 0$ and $0 \leq y \leq b$, $x > 0$, where $b > a$, and a rigid vertical barrier, lying along $x = 0$, $a \leq y \leq b$, connects the two semi-infinite regions. As usual the lower surface at $y = 0$ is rigid, however, unlike the previous cases, the upper surfaces, at $y = a$, $x < 0$ and $y = b$, $x > 0$, both comprise membranes but with different material properties. Forcing is introduced in the form of a fluid-coupled structural wave

that propogates in the positive x-direction towards $x = 0$, see figure 4.1.

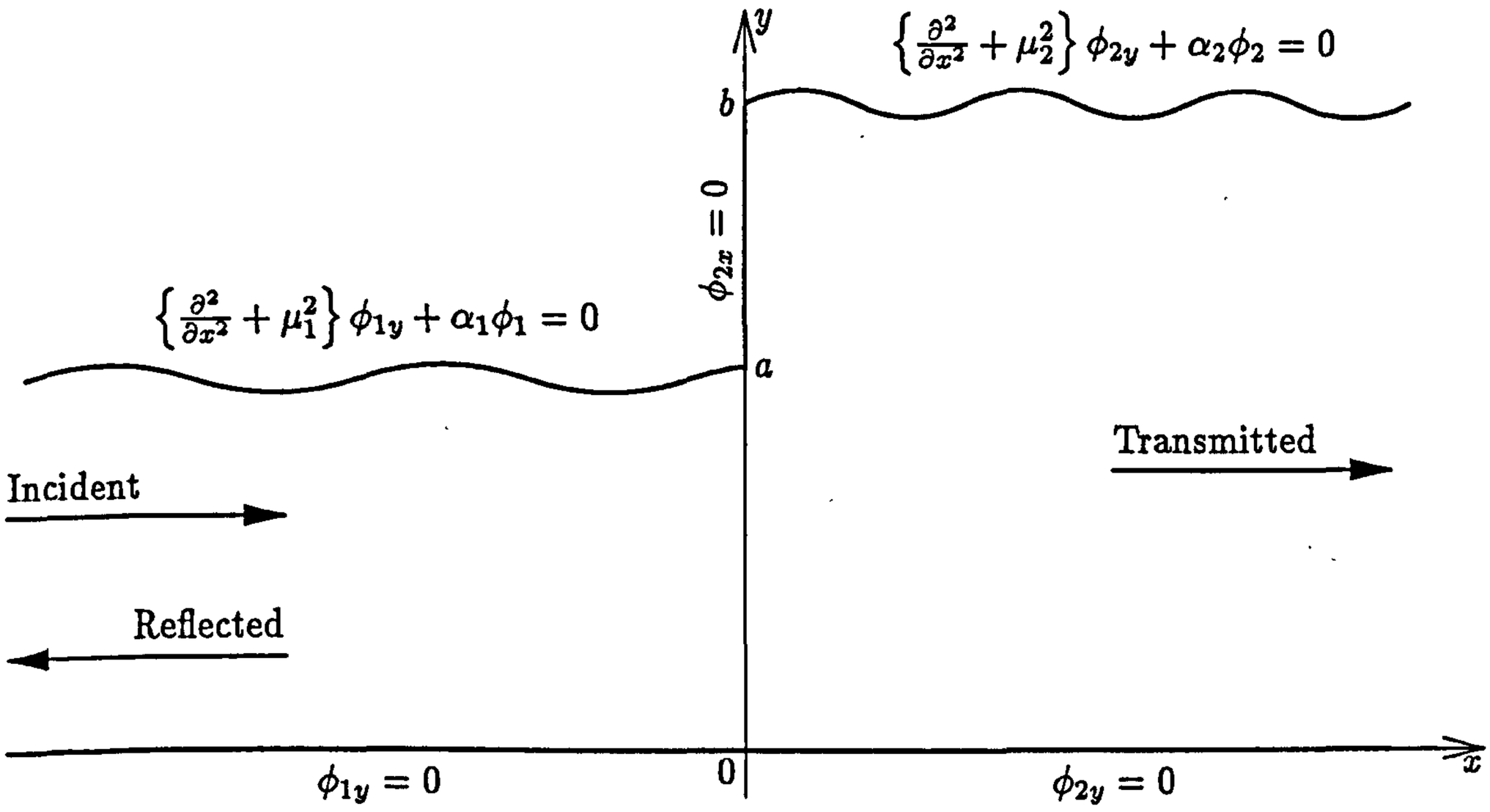

Figure 4.1: Physical configuration for the problem of section 4.1

The non-dimensionalisation of the problem with respect to length parameter k^{-1} and time period ω^{-1}, is conducted in the same manner as in chapters 2 and 3. Again, the non-dimensionalised governing equation is Helmholtz' equation, that is

$$\nabla^2\phi + \phi = 0. \tag{4.1.1}$$

The fluid velocity is in terms of an incident field and two scattered fields by

$$\phi = \begin{cases} \frac{\cosh(\tau_0 y)}{\cosh(\tau_0 a)} e^{i\eta_0 x} + \phi_1, & x < 0 \\ \phi_2, & x > 0 \end{cases}, \tag{4.1.2}$$

where

$$\tau_0 = (\eta_0^2 - 1)^{\frac{1}{2}} \tag{4.1.3}$$

and η_0 is the wavenumber of the fluid-coupled structural wave for the membrane lying along $y = a$, $x < 0$ (see (4.1.14) for further details). For brevity, the boundary conditions are simply stated as

$$\frac{\partial\phi_j}{\partial y} = 0, \qquad j = 1,2\,, \qquad y = 0, \quad -\infty < x < \infty, \tag{4.1.4}$$

$$\left\{\frac{\partial^2}{\partial x^2} + \mu_1^2\right\}\phi_{1y} + \alpha_1\phi_1 = 0, \qquad y = a, \quad x < 0 \tag{4.1.5}$$

$$\left\{\frac{\partial^2}{\partial x^2} + \mu_2^2\right\}\phi_{2y} + \alpha_2\phi_2 = 0, \qquad y = b, \quad x > 0 \tag{4.1.6}$$

where $\alpha_j, j = 1,2$ are the fluid loading parameters of the two membranes and $\mu_j, j = 1,2$ are the non-dimensional *in vacuo* membrane wave numbers. At the matching interface,

continuity of pressure and normal velocity are required, which can be expressed in terms of ϕ_j, $j = 1, 2$ as

$$\phi_2 = \frac{\cosh(\tau_0 y)}{\cosh(\tau_0 a)} + \phi_1, \qquad x = 0, \quad 0 \leq y \leq a, \tag{4.1.7}$$

$$\frac{\partial \phi_2}{\partial x} = \begin{cases} 0, & x = 0, \quad a < y \leq b \\ \frac{\partial \phi_1}{\partial x} + \frac{i\eta_0 \cosh(\tau_0 y)}{\cosh(\tau_0 a)}, & x = 0, \quad 0 \leq y \leq a \end{cases} \tag{4.1.8}$$

In chapter 3, to obtain a unique solution to the problem, an edge condition was imposed at the point where the membrane surface met the rigid vertical surface ($x = 0$, $y = b$). In this case, two such points exist, at $x = 0$, $y = a$ and $x = 0$, $y = b$, and suitable edge conditions must be applied at both. Zero displacement at $(0, a)$ is implied by

$$\tau_0 \tanh(\tau_0 a) + \phi_{1y}(0, a) = 0, \tag{4.1.9}$$

whilst

$$i\eta_0 \tau_0 \tanh(\tau_0 a) + \phi_{1xy}(0, a) = 0, \tag{4.1.10}$$

indicates zero gradient. The corresponding conditions at $(0, b)$ are

$$\phi_{2y}(0, b) = 0 \tag{4.1.11}$$

and

$$\phi_{2xy}(0, b) = 0. \tag{4.1.12}$$

There are four possible combinations of these conditions, each of which yields a different solution, and so each will be considered.

Eigenfunction expansion forms for ϕ_1 and ϕ_2 are found in the usual way, that is by using separation of variables and then applying the boundary conditions relating to the upper and lower surfaces of the relevant ducts. Both the duct to the left and that to the right of the matching interface are bounded below by a rigid surfaces and above by a membrane, so the resulting expressions will be analogous to (3.1.12). Hence, remembering that ϕ_1 is the reflected field and so comprises modes travelling in the negative x direction,

$$\phi_1 = \sum_{n=0}^{\infty} A_n \cosh(\tau_n y) e^{-i\eta_n x} \tag{4.1.13}$$

where $\tau_n = (\eta_n^2 - 1)^{\frac{1}{2}}$ and $s = \pm\eta_n, n = 0, 1, 2, \ldots$ are the roots of the dispersion relation

$$L_1(s) = (s^2 - \mu_1^2)\gamma \sinh(\gamma a) - \alpha_1 \cosh(\gamma a) = 0, \tag{4.1.14}$$

and $\gamma = (s^2 - 1)^{\frac{1}{2}}$. Similarly, given that ϕ_2 comprises only transmitted waves which travel in the positive x direction,

$$\phi_2 = \sum_{n=0}^{\infty} B_n \cosh(\gamma_n y)\, e^{i\nu_n x} \tag{4.1.15}$$

where $\gamma_n = (\nu_n^2 - 1)^{\frac{1}{2}}$ and $s = \pm\nu_n, n = 0, 1, 2, \ldots$ are the roots of the dispersion relation

$$L_2(s) = (s^2 - \mu_2^2)\gamma \sinh(\gamma b) - \alpha_2 \cosh(\gamma b) = 0. \tag{4.1.16}$$

As in all previous problems, it is the complex amplitudes A_n and B_n of equations (4.1.13) and (4.1.15) that are to be determined, and the first step is to apply the matching conditions, (4.1.7) and (4.1.8). By rearranging (4.1.7) it can be seen that

$$\phi_1(0, y) = -\frac{\cosh(\tau_0 y)}{\cosh(\tau_0 a)} + \phi_2(0, y), \quad 0 \le y \le a. \tag{4.1.17}$$

When the eigenfunction expansions (4.1.13) and (4.1.15) are substituted into this, it is seen that

$$\sum_{\ell=0}^{\infty} A_\ell \cosh(\tau_\ell y) = -\frac{\cosh(\tau_0 y)}{\cosh(\tau_0 a)} + \sum_{m=0}^{\infty} B_m \cosh(\gamma_m y), \quad 0 \le y \le a. \tag{4.1.18}$$

It is convenient to define a function $f(y)$ according to

$$f(y) = -\frac{\cosh(\tau_0 y)}{\cosh(\tau_0 a)} + \sum_{m=0}^{\infty} B_m \cosh(\gamma_m y), \quad 0 \le y \le a. \tag{4.1.19}$$

This may then be multiplied by $\alpha_1 Y_{1n}$, where $Y_{1n} = \cosh(\tau_n y)$, and integrated over the range $0 \le y \le a$ to give

$$\alpha_1 \int_0^a f(y) Y_{1n} dy = \alpha_1 \int_0^a \left[-\frac{\cosh(\tau_0 y)}{\cosh(\tau_0 a)} + \sum_{m=0}^{\infty} B_m \cosh(\gamma_m y) \right] Y_{1n} dy. \tag{4.1.20}$$

It is clear from (4.1.18) that $f(y)$ may be represented as an expansion in terms of the eigenfunctions for the left hand duct, that is

$$f(y) = \sum_{\ell=0}^{\infty} A_\ell Y_{1\ell} \tag{4.1.21}$$

where

$$Y_{1\ell}(y) = \cosh(\tau_\ell y), \qquad \ell = 0, 1, 2, \ldots \tag{4.1.22}$$

and it follows that $f(y)$ satisfies the inner product (2.6.27). That is,

$$(f(y), Y_{1n}) = \alpha_1 \int_0^a f(y) Y_{1n} dy + f'(a) Y'_{1n}(a) = A_n D_n \tag{4.1.23}$$

where, from (4.1.19)

$$\begin{aligned} D_\ell &= \frac{Y'_{1\ell}(a)}{2\tau_\ell} \frac{d}{d\gamma} L(s)\big]_{\gamma=\tau_\ell} \\ &= \frac{\alpha_1}{2} \left[a + \frac{(2\tau_\ell + \eta_\ell^2 - \mu_1^2)\sinh(2\tau_\ell a)}{2\tau_\ell(\eta_\ell^2 - \mu_1^2)} \right]. \end{aligned} \tag{4.1.24}$$

With some simple rearrangement, (4.1.23) becomes

$$\begin{aligned} \alpha_1 \int_0^a f(y) Y_{1\ell} dy &= A_\ell D_\ell - f'(a) Y'_{1\ell}(a) \\ &= A_\ell D_\ell - \left[F - \frac{\tau_0 \sinh(\tau_0 a)}{\cosh(\tau_0 a)} \right] Y'_{1\ell}(a) \end{aligned} \tag{4.1.25}$$

where, from (4.1.15)

$$F = \phi_{2y}(0,a) = \sum_{m=0}^{\infty} \gamma_m B_m \sinh(\gamma_m a). \tag{4.1.26}$$

On comparing the right hand side of (4.1.20) with (4.1.25) it is seen that

$$\begin{aligned} A_\ell &= \frac{Y'_{1\ell}(a)}{D_\ell}\left[F - \frac{\tau_0 \sinh(\tau_0 a)}{\cosh(\tau_0 a)}\right] + \frac{\alpha_1}{D_\ell}\int_0^a \left[-\frac{\cosh(\tau_0 y)}{\cosh(\tau_0 a)} + \sum_{m=0}^{\infty} B_m \cosh(\gamma_m y)\right] Y_{1\ell} dy \\ &= \frac{F\tau_\ell \sinh(\tau_\ell a)}{D_\ell} - \frac{\delta_{0\ell}}{\cosh(\tau_0 a)} + \frac{1}{D^*_\ell}\sum_{m=0}^{\infty} B_m T_{\ell m} \end{aligned} \tag{4.1.27}$$

where

$$\begin{aligned} T_{\ell m} &= \int_0^a \cosh(\tau_\ell y)\cosh(\gamma_m y) dy \\ &= \frac{\tau_\ell \sinh(\tau_\ell a)\cosh(\gamma_m a) - \gamma_m \sinh(\gamma_m a)\cosh(\tau_\ell a)}{\tau_\ell^2 - \gamma_m^2}, \end{aligned} \tag{4.1.28}$$

$D^*_\ell = \frac{D_\ell}{\alpha_1}$ and $\delta_{0\ell}$ is the usual Kronecker delta.

To obtain similar expresions for $B_n, n = 0, 1, 2, \ldots$, the orthogonality relation is applied to the second of the matching conditions, (4.1.8). On substituting (4.1.13) and (4.1.15) into (4.1.8), it is seen that

$$\sum_{n=0}^{\infty} i\nu_n B_n \cosh(\gamma_n y) = \begin{cases} 0, & a < y \le b \\ \dfrac{i\eta_0 \cosh(\tau_0 y)}{\cosh(\tau_0 a)} - \displaystyle\sum_{\ell=0}^{\infty} i\eta_\ell A_\ell \cosh(\tau_\ell y), & 0 \le y \le a \end{cases}. \tag{4.1.29}$$

It is again convenient to define a function, $g(y)$, to be the right hand side of (4.1.29), thus

$$g(y) = \begin{cases} 0, & a < y \le b \\ \dfrac{\eta_0 \cosh(\tau_0 y)}{\cosh(\tau_0 a)} - \displaystyle\sum_{\ell=0}^{\infty} \eta_\ell A_\ell \cosh(\tau_\ell y), & 0 \le y \le a \end{cases}. \tag{4.1.30}$$

This may then be multiplied by $\alpha_2 Y_{2n}$, where $Y_{2n} = \cosh(\gamma_n y)$ and integrated over the range $0 \le y \le b$ to give

$$\alpha_2 \int_0^b g(y) Y_{2n}(y) dy = \alpha_2 \int_0^a \left[\frac{\eta_0 \cosh(\tau_0 y)}{\cosh(\tau_0 a)} - \sum_{\ell=0}^{\infty} \eta_\ell A_\ell \cosh(\tau_\ell y)\right] Y_{2n}(y) dy. \tag{4.1.31}$$

However, $g(y)$ has an eigenfunction expansion representation of the form

$$g(y) = \sum_{n=0}^{\infty} \nu_n B_n Y_{2n} \tag{4.1.32}$$

where

$$Y_{2n}(y) = \cosh(\gamma_n y), \qquad n = 0, 1, 2, \ldots \tag{4.1.33}$$

and thus satisfies the inner product, (2.6.29). Thus,

$$(g(y), Y_{2m}) = \alpha \int_0^b g(y) Y_{2m}(y)\, dy + g'(b) Y'_{2m}(b) = B_m \nu_m C_m, \tag{4.1.34}$$

where, in this case

$$\begin{aligned} C_n &= \frac{Y'_{2n}(a)}{2\gamma_n}\frac{d}{d\gamma}L(s)\rfloor_{\gamma=\gamma_n} \\ &= \frac{\alpha_2}{2}\left[b+\frac{(2\gamma_n+\nu_n^2-\mu_2^2)\sinh(2\gamma_n b)}{2\gamma_n(\nu_n^2-\mu_2^2)}\right]. \end{aligned} \tag{4.1.35}$$

This can be rearranged to give

$$\begin{aligned} \alpha_2\int_0^a g(y)Y_{2m}(y)\,dy &= B_m\nu_m C_m - g'(b)Y'_{2m}(b) \\ &= B_m\nu_m C_m - EY'_{2m}(b), \end{aligned} \tag{4.1.36}$$

where, from (4.1.15)

$$E = -i\phi_{2xy}(0,b) = \sum_{n=0}^{\infty} B_n\nu_n Y'_{2n}(b). \tag{4.1.37}$$

On equating the right hand sides of (4.1.31) and (4.1.37) it is found that

$$\begin{aligned} B_n &= \frac{EY'_{2n}(b)}{\nu_n C_n} + \frac{\alpha_2}{\nu_n C_n}\int_0^a\left[\frac{\eta_0\cosh(\tau_0 y)}{\cosh(\tau_0 a)} - \sum_{\ell=1}^{\infty}A_\ell\eta_\ell\cosh(\tau_\ell y)\right]Y_{2n}dy \\ &= \frac{E\gamma_n\sinh(\gamma_n b)}{\nu_n C_n} + \frac{1}{\nu_n C_n^*}\left[\frac{\eta_0 T_{0n}}{\cosh(\tau_0 a)} - \sum_{\ell=1}^{\infty}A_\ell\eta_\ell T_{\ell n}\right], \end{aligned} \tag{4.1.38}$$

where $C_n^* = \frac{C_n}{\alpha_2}$.

Equations (4.1.27) and (4.1.38) comprise a pair of coupled infinite systems for A_n and B_n, $n = 0, 1, 2, \ldots$. On eliminating A_n between these it is found that

$$B_n = \frac{\gamma_n\sinh(\gamma_n b)E}{\nu_n C_n} + \frac{1}{\nu_n C_n^*}\left[\frac{2\eta_0 T_{0n}}{\cosh(\tau_0 a)} - \sum_{\ell=0}^{\infty}\frac{\eta_\ell T_{\ell n}\tau_\ell\sinh(\tau_\ell a)F}{D_\ell} - \sum_{\ell=0}^{\infty}\sum_{m=0}^{\infty}\frac{\eta_\ell B_m T_{\ell m}T_{\ell n}}{D_\ell^*}\right] \tag{4.1.39}$$

which forms an infinite system purely in terms of B_n. However, before the system can be solved it is necessary to specify the constants E and F. At the edge $x = 0$, $y = a$, either zero displacement, (4.1.9), or zero gradient, (4.1.10) may be applied. In the case of zero displacement

$$\tau_0\tanh(\tau_0 a) + \phi_{1y}(0,a) = 0, \tag{4.1.40}$$

and from (4.1.9) and (4.1.26) it is seen that

$$\tau_0\tanh(\tau_0 a) + \phi_{1y}(0,a) = \phi_{2y}(0,a) = F = 0. \tag{4.1.41}$$

The alternative condition, (4.1.10) states that

$$i\eta_0\tau_0\tanh(\tau_0 a) + \phi_{1xy}(0,a) = 0, \tag{4.1.42}$$

which, using (4.1.13) implies

$$\eta_0\tau_0\tanh(\tau_0 a) - \sum_{\ell=0}^{\infty}\eta_\ell A_\ell\tau_\ell\sinh(\tau_\ell a) = 0. \tag{4.1.43}$$

When the expression for A_ℓ given in (4.1.27) is substituted into this, it is seen that

$$\sum_{\ell=0}^{\infty} \frac{F\eta_\ell \tau_\ell^2 \sinh^2(\tau_\ell a)}{D_\ell} = 2\eta_0\tau_0 \tanh(\tau_0 a) - \sum_{\ell=0}^{\infty}\sum_{m=0}^{\infty} \frac{\eta_\ell \tau_\ell B_m T_{\ell m} \sinh(\tau_\ell a)}{D_\ell^*} \tag{4.1.44}$$

and so solving for F,

$$F = \frac{2\eta_0\tau_0 \tanh(\tau_0 a) - \sum_{\ell=0}^{\infty}\sum_{m=0}^{\infty} \frac{\eta_\ell \tau_\ell B_m T_{\ell m} \sinh(\tau_\ell a)}{D_\ell^*}}{\sum_{j=0}^{\infty} \frac{\eta_j \tau_j^2 \sinh^2(\tau_j a)}{D_j}}. \tag{4.1.45}$$

Now consider the edge at $x = 0, y = b$ and take first the case where condition (4.1.12) is enforced. On using (4.1.37), this is

$$E = -i\phi_{2xy}(0, b) = 0. \tag{4.1.46}$$

Alternatively condition (4.1.11), that is

$$\phi_{2y}(0, b) = 0. \tag{4.1.47}$$

The expression for ϕ_2 given in (4.1.15) may be substituted into this, and results in

$$\sum_{n=0}^{\infty} B_n \gamma_n \sinh(\gamma_n y) = 0. \tag{4.1.48}$$

Now substituting in for B_n from (4.1.39) gives

$$\sum_{n=0}^{\infty} \gamma_n \sinh(\gamma_n y) \left[\frac{\gamma_n \sinh(\gamma_n b) E}{\nu_n C_n} + \frac{1}{\nu_n C_n^*} \left\{ \frac{2\eta_0 T_{0n}}{\cosh(\tau_0 a)} - \sum_{\ell=0}^{\infty} \frac{\eta_\ell T_{\ell n} \tau_\ell \sinh(\tau_\ell a) F}{D_\ell} - \sum_{\ell=0}^{\infty}\sum_{m=0}^{\infty} \frac{\eta_\ell B_m T_{\ell m} T_{\ell n}}{D_\ell^*} \right\} \right] = 0 \tag{4.1.49}$$

which can be rearranged to find an expression for E, that is

$$E = \frac{-\sum_{n=0}^{\infty} \frac{\gamma_n \sinh(\gamma_n b)}{\nu_n C_n^*} \left[\frac{2\eta_0 T_{0n}}{\cosh(\tau_0 a)} - \sum_{\ell=0}^{\infty} \frac{\eta_\ell T_{\ell n} \tau_\ell \sinh(\tau_\ell a) F}{D_\ell} - \sum_{\ell=0}^{\infty}\sum_{m=0}^{\infty} \frac{\eta_\ell B_m T_{\ell m} T_{\ell n}}{D_\ell^*} \right]}{\sum_{j=0}^{\infty} \frac{i\gamma_j^2 \sinh^2(\gamma_j b)}{\nu_j C_j}}. \tag{4.1.50}$$

As mentioned at the start of the problem, these edge conditions form four separate cases which are summarised below;

(i) Zero membrane displacement at both edges:

$$F = 0 \tag{4.1.51}$$

$$E = \frac{-\sum_{n=0}^{\infty} \frac{\gamma_n \sinh(\gamma_n b)}{\nu_n C_n^*} \left[\frac{2\eta_0 T_{0n}}{\cosh(\tau_0 a)} - \sum_{\ell=0}^{\infty} \sum_{m=0}^{\infty} \frac{\eta_\ell B_m T_{\ell m} T_{\ell n}}{D_\ell^*} \right]}{\sum_{j=0}^{\infty} \frac{i\gamma_j^2 \sinh^2(\gamma_j b)}{\nu_j C_j}} \tag{4.1.52}$$

(ii) Zero gradient at $(0, a)$ and zero displacement at $(0, b)$:

$$F = \frac{2\eta_0 \tau_0 \tanh(\tau_0 a) - \sum_{\ell=0}^{\infty} \sum_{m=0}^{\infty} \frac{\eta_\ell \tau_\ell B_m T_{\ell m} \sinh(\tau_\ell a)}{D_\ell^*}}{\sum_{j=0}^{\infty} \frac{\eta_j \tau_j^2 \sinh^2(\tau_j a)}{D_j}} \tag{4.1.53}$$

$$E = \frac{-\sum_{n=0}^{\infty} \frac{\gamma_n \sinh(\gamma_n b)}{\nu_n C_n^*} \left[\frac{2\eta_0 T_{0n}}{\cosh(\tau_0 a)} - \sum_{\ell=0}^{\infty} \frac{\eta_\ell T_{\ell n} \tau_\ell \sinh(\tau_\ell a) F}{D_\ell} - \sum_{\ell=0}^{\infty} \sum_{m=0}^{\infty} \frac{\eta_\ell B_m T_{\ell m} T_{\ell n}}{D_\ell^*} \right]}{\sum_{j=0}^{\infty} \frac{i\gamma_j^2 \sinh^2(\gamma_j b)}{\nu_j C_j}} \tag{4.1.54}$$

(iii) Zero displacement at $(0, a)$ and zero gradient at $(0, b)$:

$$F = 0 \tag{4.1.55}$$

$$E = 0 \tag{4.1.56}$$

(iv) Zero gradient at both edges:

$$F = \frac{2\eta_0 \tau_0 \tanh(\tau_0 a) - \sum_{\ell=0}^{\infty} \sum_{m=0}^{\infty} \frac{\eta_\ell \tau_\ell B_m T_{\ell m} \sinh(\tau_\ell a)}{D_\ell^*}}{\sum_{j=0}^{\infty} \frac{\eta_j \tau_j^2 \sinh^2(\tau_j a)}{D_j}} \tag{4.1.57}$$

$$E = 0 \tag{4.1.58}$$

The above expressions for E and F must be used in conjunction with the equation for B_n given in (4.1.39) to form an infinite system for the solution of this problem. As in previous examples, this system can be truncated and solved numerically using *Mathematica*, the code for which is given in Appendix C.1. The results can then be compared with a variety of special cases, all of which are taken from chapters 2 and 3. For the case where $a = b$, an analytic solution to the problem can be obtained using the Wiener-Hopf technique; this provides further corroboration of the results herein.

4.2 The Wiener-Hopf technique for the case $a = b$

For the case where $a = b$, the problem tackled in this chapter becomes amenable to solution using the Wiener-Hopf technique. The duct is constructed in the same way as that in section 4.1 (see figure 4.2) apart from the fact that $a = b$, and so the non-dimensionalised boundary-value problem has governing equation

$$\Delta^2\phi + \phi = 0 \tag{4.2.1}$$

and the boundary conditions are now

$$\frac{\partial\phi}{\partial y} = 0, \quad y = 0, \quad -\infty < x < \infty, \tag{4.2.2}$$

$$\left\{\frac{\partial^2}{\partial x^2} + \mu_1^2\right\}\phi_y + \alpha_1\phi = 0, \quad y = a, \quad x < 0, \tag{4.2.3}$$

$$\left\{\frac{\partial^2}{\partial x^2} + \mu_2^2\right\}\phi_y + \alpha_2\phi = -\left[(\eta_0^2 - \mu_2^2)\tau_0\tanh(\tau_0 a) - \alpha_2\right]e^{i\eta_0 x}, \quad y = a, \quad x > 0. \tag{4.2.4}$$

where $\phi(x, y)$ is the time-independent scattered potential. The total time-independent fluid velocity potential is thus

$$\phi^{tot}(x, y) = \phi(x, y) + \frac{\cosh(\tau_0 y)e^{i\eta_0 x}}{\cosh(\tau_0 a)}, \tag{4.2.5}$$

where the quantities τ_0 and η_0 are defined later in the text.

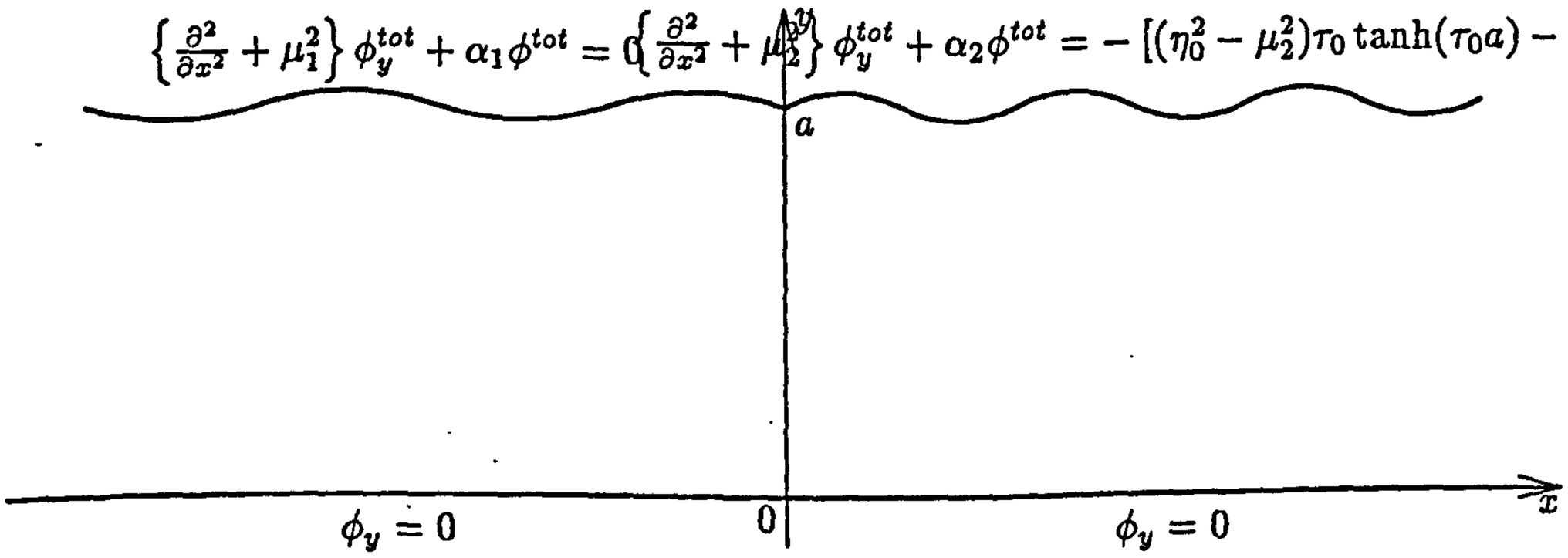

Figure 4.2: Physical configuration for the problem of section 4.2

The conditions that are to be enforced at the edge of the membrane bounding the duct to the left of the line $x = 0$, are zero displacement, $\phi_y^{tot}(0^-, a) = 0$, which is expressed in terms of the scattered potential as

$$\phi_y(0^-, a) = -\tau_0\tanh(\tau_0 a) \tag{4.2.6}$$

or alternatively zero membrane gradient, $\phi_{yx}^{tot}(0^-, a) = 0$, which gives

$$\phi_{xy}(0^-, a) = -i\eta_0\tau_0\tanh(\tau_0 a) \tag{4.2.7}$$

which are equivalent to (4.1.9) and (4.1.10) respectively. Similarly for the edge conditions on the membrane bounding the duct to the right of $x = 0$, the conditions that are equivalent to those given in (4.1.12) and (4.1.11) are

$$\phi_{xy}(0^+, a) = -i\eta_0\tau_0 \tanh(\tau_0 a) \tag{4.2.8}$$

or

$$\phi_y(0^+, a) = -\tau_0 \tanh(\tau_0 a). \tag{4.2.9}$$

On taking the full range Fourier transform of the governing equation

$$\Phi_{yy}(s, y) - \gamma^2 \Phi(s, y) = 0 \tag{4.2.10}$$

where $\Phi(s, y)$ is the Fourier transform of $\phi(x, y)$ and $\gamma = (s^2 - 1)^{\frac{1}{2}}$, and so

$$\Phi(s, y) = A(s)\cosh(\gamma y) + B(s)\sinh(\gamma y). \tag{4.2.11}$$

The Fourier transform of the first of the boundary conditions, (4.2.2), is

$$\Phi_y(s, 0) = 0 \tag{4.2.12}$$

which implies that $B(s) = 0$ and hence

$$\Phi(s, y) = A(s)\cosh(\gamma y). \tag{4.2.13}$$

As in section 3.2, the full range Fourier transform, $\Phi(s, y)$, can be expressed as the sum of two half rang transforms, such that

$$\Phi(s, y) = \Phi_-(s, y) + \Phi_+(s, y) \tag{4.2.14}$$

and so

$$\Phi_-(s, a) + \Phi_+(s, a) = A(s)\cosh(\gamma a). \tag{4.2.15}$$

where $\Phi_\pm(s, a)$ are the upper (+) and lower (−) half range Fourier transforms which are analytic in the overlapping upper and lower halves of the complex plane. Also,

$$\Phi_y(s, a) = \Phi_{y-}(s, a) + \Phi_{y+}(s, a) = A(s)\gamma\sinh(\gamma a). \tag{4.2.16}$$

and so, on differentiating (4.2.14), these two statements may be combined to eliminate $A(s)$. Thus,

$$\Phi_-(s, y) + \Phi_+(s, y) = \{\Phi_{y-}(s, a) + \Phi_{y+}(s, a)\}\frac{\cosh(\gamma y)}{\gamma\sinh(\gamma a)}. \tag{4.2.17}$$

The lower half range Fourier transform is now applied to boundary condition (4.2.3) to obtain

$$\int_{-\infty}^{0} \phi_{yxx} e^{isx} dx + \mu_1^2 \Phi_{y-}(s, a) + \alpha_1 \Phi_-(s, a) = 0. \tag{4.2.18}$$

On integrating by parts, this reduces to

$$p_1(s) - (s^2 - \mu_1^2)\Phi_{y-}(s,a) + \alpha_1\Phi_-(s,a) = 0 \tag{4.2.19}$$

where, using notation $\phi_{yx}(0^-,a) = \phi_{yx}^{0-}$, $\phi_y(0^-,a) = \phi_y^{0-}$, then

$$p_1(s) = \phi_{yx}^{0-} - is\phi_y^{0-}. \tag{4.2.20}$$

Similarly, taking the upper half range Fourier transform of boundary condition (4.2.4) gives

$$\begin{aligned}\int_0^\infty \phi_{yxx}e^{isx}dx &+ \mu_2^2\Phi_{y+}(s,a) + \alpha_2\Phi_+(s,a) \\ &= \frac{1}{i(\eta_0+s)}\left[(\eta_0^2-\mu_2^2)\tau_0\tanh(\tau_0 a) - \alpha_2\right]\left[e^{ix(\eta_0+s)}\right]_0^\infty\end{aligned} \tag{4.2.21}$$

which may be rearranged as

$$p_2(s) - (s^2-\mu_2^2)\Phi_{y+}(s,a) + \alpha_2\Phi_+(s,a) = \frac{iL_2(\eta_0)}{\eta_0+s} \tag{4.2.22}$$

where

$$L_2(\eta_0) = (\eta_0^2-\mu_2^2)\tau_0\tanh(\tau_0 a) - \alpha_2 \tag{4.2.23}$$

and

$$p_2(s) = -\phi_{yx}^{0+} + is\phi_y^{0+} \tag{4.2.24}$$

having let $\phi_{yx}(0^+,a) = \phi_{yx}^{0+}$ and $\phi_y(0^+,a) = \phi_y^{0+}$.

Equation (4.2.17) is now used to eliminate $\Phi_-(s,a)$ from (4.2.19). Thus,

$$p_1(s) - (s^2-\mu_1^2)\Phi_{y-}(s,a) + \alpha_1\left[\{\Phi_{y-}(s,a)+\Phi_{y+}(s,a)\}\frac{\cosh(\gamma a)}{\gamma\sinh(\gamma a)} - \Phi_+(s,a)\right] = 0 \tag{4.2.25}$$

which can be rearranged to give

$$p_1(s) + \left[\frac{\alpha_1\cosh(\gamma a)}{\gamma\sinh(\gamma a)} - (s^2-\mu_1^2)\right]\Phi_{y-}(s,a) + \frac{\alpha_1\cosh(\gamma a)}{\gamma\sinh(\gamma a)}\Phi_{y+}(s,a) - \alpha_1\Phi_+(s,a) = 0. \tag{4.2.26}$$

Now, on eliminating $\Phi_+(s,a)$ using (4.2.22), it is found that

$$\begin{aligned}p_1(s) + \left[\frac{\alpha_1\cosh(\gamma a)}{\gamma\sinh(\gamma a)} - (s^2-\mu_1^2)\right]\Phi_{y-}(s,a) &+ \frac{\alpha_1\cosh(\gamma a)}{\gamma\sinh(\gamma a)}\Phi_{y+}(s,a) \\ - \frac{\alpha_1}{\alpha_2}\left[-p_2(s) + (s^2-\mu_2^2)\Phi_{y+}(s,a) + \frac{iL_2(\eta_0)}{\eta_0+s}\right] &= 0\end{aligned} \tag{4.2.27}$$

which can be expressed as

$$t(s)\gamma\tanh(\gamma a) - \alpha_2 L_1(s)\Phi_{y-}(s,a) - \alpha_1 L_2(s)\Phi_{y+}(s,a) = 0 \tag{4.2.28}$$

where

$$t(s) = \alpha_2 p_1(s) + \alpha_1 p_2(s) - \frac{i\alpha_1 L_2(\eta_0)}{\eta_0+s}, \tag{4.2.29}$$

$$L_1(s) = (s^2-\mu_1^2)\gamma\tanh(\gamma a) - \alpha_1, \tag{4.2.30}$$

$$L_2(s) = (s^2-\mu_2^2)\gamma\tanh(\gamma a) - \alpha_2. \tag{4.2.31}$$

Equation (4.2.28) is the Wiener-Hopf equation for this problem. This contains two unknown functions, $\Phi_{y-}(s,a)$ and $\Phi_{y+}(s,a)$, and is valid only in the strip of overlap between the upper and lower halves of the complex s-plane. On defining a product factorisation for the Wiener-Hopf kernel, $L(s)$, as

$$L(s) = L_+(s)L_-(s) = \frac{L_1(s)}{L_2(s)} = \frac{(s^2-\mu_1^2)\gamma\tanh(\gamma a)-\alpha_1}{(s^2-\mu_2^2)\gamma\tanh(\gamma a)-\alpha_2}, \tag{4.2.32}$$

then (4.2.28) may be rearranged as

$$\frac{t(s)\gamma\tanh(\gamma a)}{L_2(s)L_+(s)} - \frac{\alpha_1\Phi_{y+}(s,a)}{L_+(s)} - \alpha_2\Phi_{y-}(s,a)L_-(s) = 0 \tag{4.2.33}$$

To proceed further with the Wiener-Hopf technique (4.2.33) must be rearranged so that all the '+' functions are on one side and all of the '-' functions are on the other. Equation (4.2.33) is almost of a form where that can be done, but performing a sum split on $\gamma\tanh(\gamma a)$ is tricky. It is easier to perform sum splits on simple poles and so a better way to express $\gamma\tanh(\gamma a)$ is sought. Consider the following pair of equations:

$$\alpha_2 L_1(s) = (\alpha_2 s^2 - \alpha_2\mu_1^2)\gamma\tanh(\gamma a) - \alpha_1\alpha_2, \tag{4.2.34}$$

and

$$\alpha_1 L_2(s) = (\alpha_1 s^2 - \alpha_1\mu_2^2)\gamma\tanh(\gamma a) - \alpha_1\alpha_2. \tag{4.2.35}$$

When (4.2.35) is subtracted from (4.2.34) it is found that

$$\alpha_2 L_1(s) - \alpha_1 L_2(s) = (\alpha_2-\alpha_1)(s^2-\sigma^2)\gamma\tanh(\gamma a) \tag{4.2.36}$$

where

$$\sigma^2 = \frac{\alpha_2\mu_1^2 - \alpha_1\mu_2^2}{\alpha_2-\alpha_1} \tag{4.2.37}$$

and so

$$\gamma\tanh(\gamma a) = \frac{\alpha_2 L_1(s) - \alpha_1 L_2(s)}{(\alpha_2-\alpha_1)(s^2-\sigma^2)}. \tag{4.2.38}$$

Note at this point that σ is undefined for the case where $\alpha_1 = \alpha_2$. It will become clear that σ plays a significant part in the solution of this problem and thus in the expressions that define the reflected and transmitted modes. In subsection 4.2.3, a case where $\alpha_1 = \alpha_2$ is considered, but for now, the analysis shall be continued under the assumption that $\alpha_1 \neq \alpha_2$. Equation (4.2.38) may now be used to rearrange (4.2.33) as

$$\frac{t(s)}{L_2(s)L_+(s)}\left[\frac{\alpha_2 L_1(s) - \alpha_1 L_2(s)}{(\alpha_2-\alpha_1)(s^2-\sigma^2)}\right] - \frac{\alpha_1\Phi_{y+}(s,a)}{L_+(s)} - \alpha_2\Phi_{y-}(s,a)L_-(s) = 0 \tag{4.2.39}$$

from which it follows

$$\frac{t(s)}{(\alpha_2-\alpha_1)(s^2-\sigma^2)}\left[\alpha_2 L_-(s) - \frac{\alpha_1}{L_+(s)}\right] - \frac{\alpha_1\Phi_{y+}(s,a)}{L_+(s)} - \alpha_2\Phi_{y-}(s,a)L_-(s) = 0. \tag{4.2.40}$$

On first attempt at separating (4.2.40) into '+' functions and '-' functions, the expression is rewritten as

$$\frac{t(s)\alpha_2 L_-(s)}{(\alpha_2-\alpha_1)(s^2-\sigma^2)} - \alpha_2\Phi_{y-}(s,a)L_-(s) = \frac{t(s)\alpha_1}{(\alpha_2-\alpha_1)(s^2-\sigma^2)L_+(s)} + \frac{\alpha_1\Phi_{y+}(s,a)}{L_+(s)}. \tag{4.2.41}$$

Equation (4.2.41) is split as prescribed except for some simple poles. To remove these, partial fractions are used to isolate the poles and then simple sum splits are implemented to remove them completely.

Note that

$$\begin{aligned}\frac{t(s)}{s^2-\sigma^2} &= \frac{\alpha_2 p_1(s)-\alpha_1 p_2(s)}{(s-\sigma)(s+\sigma)} - \frac{i\alpha_1 L_2(\eta_0)}{(s-\sigma)(s+\sigma)(s+\eta_0)} \\ &= \frac{\alpha_2(\phi^{0-}_{yx}-is\phi^{0-}_y)-\alpha_1(-\phi^{0+}_{yx}+is\phi^{0+}_y)}{(s-\sigma)(s+\sigma)} - \frac{i\alpha_1 L_2(\eta_0)}{(s-\sigma)(s+\sigma)(s+\eta_0)}.\end{aligned} \tag{4.2.42}$$

This can be expressed in terms of partial fractions as

$$\frac{t(s)}{s^2-\sigma^2} = \frac{U}{s+\sigma} + \frac{V}{s-\sigma} + \frac{W}{s+\eta_0} \tag{4.2.43}$$

where

$$U = \frac{1}{2\sigma}\left[\alpha_1(\phi^{0+}_{yx}+i\sigma\phi^{0+}_y)+\alpha_2(-\phi^{0-}_{yx}-i\sigma\phi^{0-}_y)-W(\eta_0+\sigma)\right], \tag{4.2.44}$$

$$V = \frac{1}{2\sigma}\left[\alpha_1(-\phi^{0+}_{yx}+i\sigma\phi^{0+}_y)+\alpha_2(\phi^{0-}_{yx}-i\sigma\phi^{0-}_y)+W(\eta_0-\sigma)\right], \tag{4.2.45}$$

$$W = -\frac{i\alpha_1 L_2(\eta_0)}{(\eta_0^2-\sigma^2)}. \tag{4.2.46}$$

So, (4.2.41) can be written as

$$\begin{aligned}&\frac{1}{\alpha_2-\alpha_1}\left[\frac{\alpha_2 L_-(s)U}{s+\sigma}+\frac{\alpha_2 L_-(s)V}{s-\sigma}+\frac{\alpha_2 L_-(s)W}{s+\eta_0}\right] - \alpha_2\Phi_{y-}(s,a)L_-(s) \\ &\quad = \frac{1}{\alpha_2-\alpha_1}\left[\frac{\alpha_1 U}{L_+(s)(s+\sigma)}+\frac{\alpha_1 V}{L_+(s)(s-\sigma)}+\frac{\alpha_1 W}{L_+(s)(s+\eta_0)}\right]+\frac{\alpha_1\Phi_{y+}(s,a)}{L_+(s)}.\end{aligned} \tag{4.2.47}$$

Apart from isolated simple poles, equation (4.2.47) is now such that the left hand side comprises minus functions whilst the right hand side contains only plus functions. The offending simple poles are easily subtracted out, for example:

$$\frac{\alpha_2 L_-(s)U}{s+\sigma} = \frac{\alpha_2 U}{s+\sigma}[L_-(s)-L_+(\sigma)] + \frac{\alpha_2 L_+(\sigma)U}{s+\sigma}. \tag{4.2.48}$$

There are three such singularities to be removed, after which it is found that

$$\begin{aligned}&\frac{1}{\alpha_2-\alpha_1}\left[\frac{\alpha_2 U}{s+\sigma}\{L_-(s)-L_+(\sigma)\}+\frac{\alpha_2 W}{s+\eta_0}\{L_-(s)-L_+(\eta_0)\}\right. \\ &\qquad \left.+\frac{\alpha_2 L_-(s)V}{s-\sigma}-\frac{\alpha_1 V}{L_+(\sigma)(s-\sigma)}\right]-\alpha_2\Phi_{y-}(s,a)L_-(s) \\ &= \frac{1}{\alpha_2-\alpha_1}\left[\frac{\alpha_1 U}{L_+(s)(s+\sigma)}-\frac{\alpha_2 L_+(\sigma)U}{s+\sigma}+\frac{\alpha_1 W}{L_+(s)(s+\eta_0)}-\frac{\alpha_2 L_+(\sigma)W}{s+\eta_0}\right. \\ &\qquad \left.+\frac{\alpha_1 V}{(s-\sigma)}\left\{\frac{1}{L_+(s)}-\frac{1}{L_+(\sigma)}\right\}\right]+\frac{\alpha_1\Phi_{y+}(s,a)}{L_+(s)} \equiv E(s)\end{aligned} \tag{4.2.49}$$

where $E(s)$ is an entire function and forms the analytic continuation of either side of (4.2.49) into the whole of the complex s-plane. It is easily shown that

$$L_{\pm}(s) = O(1), \qquad |s| \to \infty, \tag{4.2.50}$$

$$\Phi_{y-}(s,a) = O\left(\frac{1}{s^{\beta+1}}\right), \qquad |s| \to \infty, \tag{4.2.51}$$

$$\Phi_{y+}(s,a) = O\left(\frac{1}{s^{\beta+1}}\right), \qquad |s| \to \infty, \tag{4.2.52}$$

where $0 \leq \beta < 1$. Then, on appealing to Liouville's theorem it is clear that $E(s) = 0$. Hence,

$$\Phi_{y-}(s,a) = \frac{1}{\alpha_2-\alpha_1}\left[\frac{U}{s+\sigma}\left\{1-\frac{L_+(\sigma)}{L_-(s)}\right\}+\frac{W}{s+\eta_0}\left\{1-\frac{L_+(\eta_0)}{L_-(s)}\right\}+\frac{V}{s-\sigma}\left\{1-\frac{\alpha_1}{\alpha_2 L_+(\sigma)L_-(s)}\right\}\right]. \tag{4.2.53}$$

and

$$\Phi_{y+}(s,a) = \frac{1}{\alpha_2-\alpha_1}\left[\frac{U}{s+\sigma}\left\{\frac{\alpha_2 L_+(\sigma)L_+(s)}{\alpha_1}-1\right\}+\frac{W}{s+\eta_0}\left\{\frac{\alpha_2 L_+(\eta_0)L_+(s)}{\alpha_1}-1\right\}+\frac{V}{s-\sigma}\left\{\frac{L_+(s)}{L_+(\sigma)}-1\right\}\right]. \tag{4.2.54}$$

It is easily shown from (4.2.36) that

$$\frac{\alpha_1}{\alpha_2 L_+(\sigma)} = L_-(\sigma), \tag{4.2.55}$$

and it follows that

$$\begin{aligned}\Phi_y(s,a) &= \Phi_{y+}(s,a)+\Phi_{y-}(s,a)\\ &= \frac{L_+(s)}{\alpha_2-\alpha_1}\left[\frac{UL_+(\sigma)}{s+\sigma}+\frac{VL_-(\sigma)}{s-\sigma}+\frac{WL_+(\eta_0)}{s+\eta_0}\right]\left[\frac{\alpha_2}{\alpha_1}-\frac{1}{L(s)}\right].\end{aligned} \tag{4.2.56}$$

However, from (4.2.17) it can be seen that

$$\begin{aligned}\Phi(s,y) &= \frac{\Phi_y(s,a)\coth(\gamma y)}{\gamma\sinh(\gamma a)}\\ &= \frac{L_+(s)}{(\alpha_2-\alpha_1)}\left[\frac{UL_+(\sigma)}{s+\sigma}+\frac{VL_-(\sigma)}{s-\sigma}+\frac{WL_+(\eta_0)}{s+\eta_0}\right]\left[\frac{\alpha_2}{\alpha_1}-\frac{1}{L(s)}\right]\frac{\cosh(\gamma y)}{\gamma\sinh(\gamma a)},\end{aligned} \tag{4.2.57}$$

and so

$$\begin{aligned}\phi(x,y) &= \frac{1}{2\pi}\int_{-\infty}^{\infty}\Phi(s,y)e^{-isx}ds\\ &= \frac{1}{2\pi(\alpha_2-\alpha_1)}\int_{-\infty}^{\infty}L_+(s)\left[\frac{UL_+(\sigma)}{s+\sigma}+\frac{VL_-(\sigma)}{s-\sigma}+\frac{WL_+(\eta_0)}{s+\eta_0}\right]\times\\ &\qquad\left[\frac{\alpha_2}{\alpha_1}-\frac{1}{L(s)}\right]\frac{\cosh(\gamma y)}{\gamma\sinh(\gamma a)}e^{-isx}ds.\end{aligned} \tag{4.2.58}$$

When (4.2.44) and (4.2.45) are substituted into this, the result is

$$\begin{aligned}\phi(x,y) &= \frac{1}{2\pi(\alpha_2-\alpha_1)}\int_{-\infty}^{\infty} L_+(s)\left[\frac{\alpha_2}{\alpha_1}-\frac{1}{L(s)}\right]\times \\ &\left[\frac{L_+(\sigma)}{2\sigma(s+\sigma)}\left[\alpha_1(\phi_{yx}^{0+}+i\sigma\phi_y^{0+})+\alpha_2(-\phi_{yx}^{0-}-i\sigma\phi_y^{0-})-W(\eta_0+\sigma)\right]\right. \\ &\left.+\frac{L_-(\sigma)}{2\sigma(s-\sigma)}\left[\alpha_1(-\phi_{yx}^{0+}+i\sigma\phi_y^{0+})+\alpha_2(\phi_{yx}^{0-}-i\sigma\phi_y^{0-})+W(\eta_0-\sigma)\right]\right. \\ &\left.+\frac{WL_+(\eta_0)}{s+\eta_0}\right]\frac{\cosh(\gamma y)}{\gamma\sinh(\gamma a)}e^{-isx}ds. \qquad (4.2.59)\end{aligned}$$

Of interest here are the amplitudes of reflected and transmitted fluid-coupled structural modes on the membrane surface, $y = a$. For the reflected mode, $x < 0$ so the contour of integration is closed in the upper half-plane and the relevant pole is that at $s = \eta_0$. Hence,

$$\begin{aligned}\rho(\phi,\eta_0) &= \frac{iL_+(\eta_0)L_2(\eta_0)\cosh(\tau_0 a)e^{-i\eta_0 x}}{L_1'(\eta_0)(\alpha_2-\alpha_1)\tau_0\sinh(\tau_0 a)}\left[\frac{WL_+(\eta_0)}{2\eta_0}\right. \\ &+\frac{L_+(\sigma)}{2\sigma(\eta_0+\sigma)}\left[\alpha_1(\phi_{yx}^{0+}+i\sigma\phi_y^{0+})+\alpha_2(-\phi_{yx}^{0-}-i\sigma\phi_y^{0-})-W(\eta_0+\sigma)\right] \\ &\left.+\frac{L_-(\sigma)}{2\sigma(\eta_0-\sigma)}\left[\alpha_1(-\phi_{yx}^{0+}+i\sigma\phi_y^{0+})+\alpha_2(\phi_{yx}^{0-}-i\sigma\phi_y^{0-})+W(\eta_0-\sigma)\right]\right] \qquad (4.2.60)\end{aligned}$$

is the residue contribution to $\phi(x,y)$ from the pole at $s = \eta_0$. Note that

$$L_1'(s) = s\tanh(\gamma a)\left[\frac{s^2-\mu_1^2}{\gamma}+2\gamma\right]+\frac{sa(s^2-\mu_1^2)}{\cosh^2(\gamma a)} \qquad (4.2.61)$$

is the derivative of $L_1(s)$ with respect to s. On putting $s = \eta_0$ in (4.2.38) it is seen that

$$-\tau_0\tanh(\tau_0 a) = \frac{\alpha_1 L_2(\eta_0)}{(\alpha_2-\alpha_1)(\eta_0^2-\sigma^2)} = \frac{iW}{\alpha_2-\alpha_1}. \qquad (4.2.62)$$

and so

$$\frac{1}{\tau_0\tanh(\tau_0 a)(\alpha_2-\alpha_1)} = \frac{i}{W} \qquad (4.2.63)$$

Thus, (4.2.60) becomes

$$\begin{aligned}\rho(\phi,\eta_0) &= \frac{-L_+(\eta_0)L_2(\eta_0)e^{-i\eta_0 x}}{L_1'(\eta_0)W}\left[\frac{WL_+(\eta_0)}{2\eta_0}\right. \\ &+\frac{L_+(\sigma)}{2\sigma(\eta_0+\sigma)}\left[\alpha_1(\phi_{yx}^{0+}+i\sigma\phi_y^{0+})+\alpha_2(-\phi_{yx}^{0-}-i\sigma\phi_y^{0-})-W(\eta_0+\sigma)\right] \\ &\left.+\frac{L_-(\sigma)}{2\sigma(\eta_0-\sigma)}\left[\alpha_1(-\phi_{yx}^{0+}+i\sigma\phi_y^{0+})+\alpha_2(\phi_{yx}^{0-}-i\sigma\phi_y^{0-})+W(\eta_0-\sigma)\right]\right] \\ &= R_0 e^{-i\eta_0 x} \qquad (4.2.64)\end{aligned}$$

where R_0 is the complex amplitude of the reflected mode on the membrane surface. With further rearrangement, the expression for R_0 becomes

$$R_0 = \frac{-L_+(\eta_0)L_2(\eta_0)}{L_1'(\eta_0)W}\left[\frac{WL_+(\eta_0)}{2\eta_0}+\frac{1}{2\sigma(\eta_0^2-\sigma^2)}\{G(\eta_0 P-\sigma Q)+H(\eta_0 Q-\sigma P)\}\right], \qquad (4.2.65)$$

where

$$G = \alpha_1\phi_{yx}^{0+} - \alpha_2\phi_{yx}^{0-} - W\eta_0, \tag{4.2.66}$$

$$H = i\sigma\alpha_1\phi_y^{0+} - i\sigma\alpha_2\phi_y^{0-} - W\sigma, \tag{4.2.67}$$

and

$$P = L_+(\sigma) - L_-(\sigma), \tag{4.2.68}$$

$$Q = L_+(\sigma) + L_-(\sigma). \tag{4.2.69}$$

For the fundamental transmitted mode, the pole of significance is that at $s = -\nu_0$. In this case the contour of integration is closed in the lower half-plane and so following similar steps to those for the reflected coefficient and putting $y = a$ it is seen that the residue from the pole at $s = -\nu_0$ is

$$\begin{aligned}\rho(\phi, -\nu_0) = &\left[\frac{L_+(\sigma)}{2\sigma(\sigma-\nu_0)}\left[\alpha_1(\phi_{yx}^{0+} + i\sigma\phi_y^{0+}) + \alpha_2(-\phi_{yx}^{0-} - i\sigma\phi_y^{0-}) - W(\eta_0+\sigma)\right]\right.\\ &+\frac{L_-(\sigma)}{2\sigma(\sigma+\nu_0)}\left[\alpha_1(\phi_{yx}^{0+} - i\sigma\phi_y^{0+}) + \alpha_2(-\phi_{yx}^{0-} + i\sigma\phi_y^{0-}) - W(\eta_0-\sigma)\right]\\ &\left.+\frac{WL_+(\eta_0)}{\eta_0-\nu_0}\right]\frac{i\alpha_2 L_1(\nu_0)\cosh(\gamma_0 a)}{L_2'(\nu_0)L_+(\nu_0)\alpha_1(\alpha_2-\alpha_1)\gamma_0\sinh(\gamma_0 a)}e^{i\nu_0 x}\\ = &\; T_0 e^{i\nu_0 x}\end{aligned} \tag{4.2.70}$$

where T_0 is the complex amplitude of the reflected mode on the membrane surface and

$$L_2'(s) = s\tanh(\gamma a)\left[\frac{s^2-\mu_2^2}{\gamma} + 2\gamma\right] + \frac{sa(s^2-\mu_2^2)}{\cosh^2(\gamma a)}. \tag{4.2.71}$$

is the derivative of $L_2(s)$ with respect to s. After replacing $\frac{i}{\alpha_2-\alpha_1}$ using (4.2.63) and rearranging, T_0 can be re-expressed as

$$\begin{aligned}T_0 = &\frac{\alpha_2 L_1(\nu_0)\tau_0\tanh(\tau_0 a)}{\alpha_1 W L_2'(\nu_0)L_+(\nu_0)\gamma_0\tanh(\gamma_0 a)}\left[\frac{WL_+(\eta_0)}{\eta_0-\nu_0}\right.\\ &\left.+\frac{1}{2\sigma(\sigma^2-\eta_0^2)}\{G(\sigma Q+\eta_0 P) + H(\sigma P+\eta_0 Q)\}\right].\end{aligned} \tag{4.2.72}$$

4.2.1 Determination of ϕ_y^{0+}, ϕ_y^{0-}, ϕ_{yx}^{0+} and ϕ_{yx}^{0-}

The above analysis has resulted in expressions for R_0 and T_0 (the complex amplitudes of the reflected and transmitted structural modes) in terms of the, as yet unknown, constants ϕ_y^{0+}, ϕ_y^{0-}, ϕ_{yx}^{0+} and ϕ_{yx}^{0-}. These are contained solely in G and H, so once expressions are found for the four unknowns they need only to be substituted into G and H to find the reflected and transmitted modes. Of course, to accomplish this the four unknowns must be determined. Application of the edge conditions will specify two of them, whilst the remaining pair are deduced by considering the large $|s|$ behaviour of $\Phi_\pm(s,a)$. It should

be recalled that the fluid velocity potential has at worst an integrable singularity, from which it follows that

$$\Phi_{y+}(s,y)+\int_0^\infty \frac{\tau_0\sinh(\tau_0 y)}{\cosh(\tau_0 a)}e^{ix(\eta_0+s)}dx = O\left(\frac{1}{s^\beta}\right), \quad 0\le\beta<1, \quad |s|\to\infty, \quad (4.2.73)$$

which, considering the integral on the left hand side, implies that

$$\Phi_{y+}(s,a) = O\left(\frac{1}{s}\right), \quad |s|\to\infty, \quad (4.2.74)$$

and similarly

$$\Phi_{y-}(s,a) = O\left(\frac{1}{s}\right), \quad |s|\to\infty. \quad (4.2.75)$$

Note that this is consistant with (4.2.54) and (4.2.53) respectively.

Now consider again (4.2.19), that is

$$p_1(s)-(s^2-\mu_1^2)\Phi_{y-}(s,a)+\alpha_1\Phi_-(s,a)=0. \quad (4.2.76)$$

On replacing $p_1(s)$ using (4.2.20) and $\Phi_{y-}(s,a)$ with the expression given in (4.2.54), this can be rearranged to give an expression for $\Phi_-(s,a)$. That is

$$\begin{aligned}\Phi_-(s,a) \;=\; & -\frac{\phi_{yx}^{0-}}{\alpha_1}+\frac{is\phi_y^{0-}}{\alpha_1}+\frac{1}{\alpha_1(\alpha_2-\alpha_1)}\left[\frac{U(s^2-\mu_1^2)}{s+\sigma}-\frac{UL_+(\sigma)(s^2-\mu_1^2)}{L_-(s)(s+\sigma)}\right.\\ & \left.+\frac{W(s^2-\mu_1^2)}{s+\eta_0}-\frac{WL_+(\eta_0)(s^2-\mu_1^2)}{L_-(s)(s+\eta_0)}+\frac{V(s^2-\mu_1^2)}{s-\sigma}-\frac{\alpha_1 W(s^2-\mu_1^2)}{\alpha_2 L_+(\sigma)L_-(s)(s-\sigma)}\right].\end{aligned} \quad (4.2.77)$$

Now, assuming the form

$$\frac{1}{L_-(s)}\sim 1+\frac{d_1}{s}+\frac{d_2}{s^2}+\dots \quad (4.2.78)$$

where $d_1, d_2, \dots$ are unknown but constant, (4.2.77) can be expanded in powers of s. It is found that

$$\begin{aligned}\Phi_-(s,a) \;\sim\; & -\frac{\phi_{yx}^{0-}}{\alpha_1}+\frac{is\phi_y^{0-}}{\alpha_1}+\frac{1}{\alpha_1(\alpha_2-\alpha_1)}\left[U\left\{s-\sigma+\frac{1}{s}(\sigma^2-\mu_1^2)\right\}\right.\\ & +V\left\{s+\sigma+\frac{1}{s}(\sigma^2-\mu_1^2)\right\}+W\left\{s-\eta_0+\frac{1}{s}(\eta_0^2-\mu_1^2)\right\}\\ & -UL_+(\sigma)\left\{s+(d_1-\sigma)+\frac{1}{s}(\sigma^2-\mu_1^2-\sigma d_1+d_2)\right\}\\ & -VL_+(\sigma)\left\{s+(d_1+\sigma)+\frac{1}{s}(\sigma^2-\mu_1^2+\sigma d_1+d_2)\right\}\\ & \left.-WL_+(\eta_0)\left\{s+(d_1-\eta_0)+\frac{1}{s}(\eta_0^2-\mu_1^2-\eta_0 d_1+d_2)\right\}\right]+O\left(\frac{1}{s^2}\right).\end{aligned} \quad (4.2.79)$$

Hence,

$$\Phi_-\sim c_0 s+c_1+\frac{c_2}{s}+\dots \quad (4.2.80)$$

where

$$c_0 = \left[\frac{i\phi_y^{0-}}{\alpha_1} + \frac{1}{\alpha_1(\alpha_2-\alpha_1)}\left\{U+V+W-UL_+(\sigma)-WL_+(\eta_0)-\frac{\alpha_1 V}{\alpha_2 L_+(\sigma)}\right\}\right] \tag{4.2.81}$$

$$c_1 = \frac{\phi_{yx}^{0-}}{\alpha_1} + \frac{1}{\alpha_1(\alpha_2-\alpha_1)}\{-U\sigma+V\sigma-W\eta_0-UL_+(\sigma)(d_1-\sigma) -WL_+(\eta_0)(d_1-\eta_0)-\frac{\alpha_1 V(d_1+\sigma)}{\alpha_2 L_+(\sigma)}\} \tag{4.2.82}$$

and it is in fact not necessary to calculate c_2 for the purposes of this analysis. However, it is known that $\Phi_- \sim O\left(\frac{1}{s}\right)$, which implies that $c_0 = c_1 = 0$. Thus, from (4.2.81)

$$0 = i(\alpha_2-\alpha_1)\phi_y^{0-} + U + V + W - UL_+(\sigma) - WL_+(\eta_0) - \frac{\alpha_1 V}{\alpha_2 L_+(\sigma)}. \tag{4.2.83}$$

On replacing U and V with their expanded forms as given in (4.2.44) and (4.2.45), it is found that

$$\begin{aligned} 0 &= i(\alpha_2-\alpha_1)\phi_y^{0-} + R[1-L_+(\eta_0)] \\ &\quad + \frac{1}{2\sigma}\left[\alpha_1(\phi_{yx}^{0+}+i\sigma\phi_y^{0+}) + \alpha_2(-\phi_{yx}^{0-}-i\sigma\phi_y^{0-}) - W(\eta_0+\sigma)\right][1-L_+(\sigma)] \\ &\quad + \frac{1}{2\sigma}\left[\alpha_1(-\phi_{yx}^{0+}+i\sigma\phi_y^{0+}) + \alpha_2(\phi_{yx}^{0-}-i\sigma\phi_y^{0-}) + W(\eta_0-\sigma)\right]\left[1-\frac{\alpha_1}{\alpha_2 L_+(\sigma)}\right]. \end{aligned} \tag{4.2.84}$$

On using (4.2.55) this may be rearranged as

$$\begin{aligned} 0 &= \frac{\alpha_1\phi_{yx}^{0+}}{2\sigma}[L_-(\sigma)-L_+(\sigma)] + \frac{i\alpha_1\phi_y^{0+}}{2}[-L_+(\sigma)-L_-(\sigma)+2] \\ &\quad \frac{\alpha_2\phi_{yx}^{0-}}{2\sigma}[L_+(\sigma)-L_-(\sigma)] + \frac{i\alpha_2\phi_y^{0-}}{2}\left[L_+(\sigma)+L_-(\sigma)-\frac{2\alpha_1}{\alpha_2}\right] \\ &\quad \frac{W}{2\sigma}[\eta_0\{L_+(\sigma)-L_-(\sigma)\} + \sigma\{L_+(\sigma)+L_-(\sigma)\} - 2\sigma L_+(\eta_0)], \end{aligned} \tag{4.2.85}$$

and, using (4.2.68) and (4.2.69), it follows that

$$\begin{aligned} \left(-\alpha_1\phi_{yx}^{0+}+\alpha_2\phi_{yx}^{0-}\right)P + i\sigma\left[\alpha_1\phi_y^{0+}(2-Q) + \alpha_2\phi_y^{0-}\left(Q-\frac{2\alpha_1}{\alpha_2}\right)\right] \\ = R[2\sigma L_+(\eta_0) - \eta_0 P - \sigma Q]. \end{aligned} \tag{4.2.86}$$

Now, on enforcing $c_1 = 0$, equation (4.2.82) becomes

$$\begin{aligned} 0 &= -(\alpha_2-\alpha_1)\phi_{yx}^{0-} - U\sigma + V\sigma - W\eta_0 - UL_+(\sigma)(d_1-\sigma) \\ &\quad -WL_+(\eta_0)(d_1-\eta_0) - \frac{\alpha_1 V(d_1+\sigma)}{\alpha_2 L_+(\sigma)}. \end{aligned} \tag{4.2.87}$$

Upon replacing U and V using (4.2.44) and (4.2.45), this can be expressed in terms of ϕ_{yx}^{0+}, ϕ_{yx}^{0-}, ϕ_y^{0+} and ϕ_y^{0-} as

$$0 = -(\alpha_2-\alpha_1)\phi_{yx}^{0-} - W\eta_0 - WL_+(\eta_0)(d_1-\eta_0)$$

$$\frac{1}{2}\left[\alpha_1(-\phi_{yx}^{0+}+i\sigma\phi_y^{0+})+\alpha_2(\phi_{yx}^{0-}-i\sigma\phi_y^{0-})+W(\eta_0-\sigma)\right.$$
$$\left.-\alpha_1(\phi_{yx}^{0+}+i\sigma\phi_y^{0+})+\alpha_2(\phi_{yx}^{0-}+i\sigma\phi_y^{0-})+W(\eta_0+\sigma)\right]$$
$$-\frac{1}{2\sigma}\left[\alpha_1(\phi_{yx}^{0+}+i\sigma\phi_y^{0+})+\alpha_2(-\phi_{yx}^{0-}-i\sigma\phi_y^{0-})-W(\eta_0+\sigma)\right]L_+(\sigma)(d_1-\sigma)$$
$$-\frac{1}{2\sigma}\left[\alpha_1(-\phi_{yx}^{0+}+i\sigma\phi_y^{0+})+\alpha_2(\phi_{yx}^{0-}-i\sigma\phi_y^{0-})+W(\eta_0-\sigma)\right]L_-(\sigma)(d_1+\sigma) \qquad (4.2.88)$$

which can be rewritten as

$$\begin{aligned}0 \;=\;& \alpha_1\phi_{yx}^{0+}\left[-2\sigma+d_1\{-L_+(\sigma)+L_-(\sigma)\}+\sigma\{L_+(\sigma)+L_-(\sigma)\}\right]\\
&+i\alpha_1\sigma\phi_y^{0+}\left[d_1\{-L_+(\sigma)-L_-(\sigma)\}+\sigma\{L_+(\sigma)-L_-(\sigma)\}\right]\\
&+\alpha_2\phi_{yx}^{0-}\left[\frac{2\sigma\alpha_1}{\alpha_2}+d_1\{L_+(\sigma)-L_-(\sigma)\}+\sigma\{-L_+(\sigma)-L_-(\sigma)\}\right]\\
&+i\alpha_2\sigma\phi_y^{0-}\left[d_1\{L_+(\sigma)+L_-(\sigma)\}+\sigma\{-L_+(\sigma)+L_-(\sigma)\}\right]\\
&+W\left[-2\sigma L_+(\eta_0)(d_1-\eta_0)+\eta_0 d_1\{L_+(\sigma)-L_-(\sigma)\}+\eta_0\sigma\{-L_+(\sigma)-L_-(\sigma)\}\right.\\
&\left.+\sigma d_1\{L_+(\sigma)+L_-(\sigma)\}+\sigma^2\{-L_+(\sigma)+L_-(\sigma)\}\right]. \qquad (4.2.89)\end{aligned}$$

Thus, using (4.2.68) and (4.2.69)

$$\begin{aligned}&\alpha_1\phi_{yx}^{0+}\left[-2\sigma-d_1P+\sigma Q\right]+i\alpha_1\sigma\phi_y^{0+}\left[-d_1Q+\sigma P\right]\\
&+\alpha_2\phi_{yx}^{0-}\left[\frac{2\sigma\alpha_1}{\alpha_2}+d_1P-\sigma Q\right]+i\alpha_2\sigma\phi_y^{0-}\left[d_1Q-\sigma P\right]\\
&\qquad=W\left[2\sigma L_+(\eta_0)(d_1-\eta_0)-P(\eta_0 d_1-\sigma^2)-Q\sigma(d_1-\eta_0)\right]. \qquad (4.2.90)\end{aligned}$$

Hence, a pair of equations in the four variables $\phi_{yx}^{0+}, \phi_y^{0+}, \phi_{yx}^{0-}$ and ϕ_y^{0-} is formed by (4.2.86) and (4.2.90). As expected, an identical system is obtained if the convergence of $\Phi_+(s,a)$ is considered instead of $\Phi_-(s,a)$. The system thus obtained comprises only two equations but contains four unknowns and so is not uniquely solvable as it stands, but the two edge conditions supply further information and enable a simple two by two system to be formed. As seen previously, there are four possible combinations of edge conditions. Each results in a different system for solution and, as in section 4.1, all four cases will be considered.

(i) $\phi_y^{0+} = \phi_y^{0-} = -\tau_0 \tanh(\tau_0 a)$

This pair of edge constraints corresponds to zero displacement on both membranes at $x = 0$, and may be rewritten using (4.2.62) as

$$\phi_y^{0+} = \phi_y^{0-} = \frac{iW}{\alpha_2-\alpha_1}. \qquad (4.2.91)$$

On substituting this into (4.2.86) it is found that

$$\left(-\alpha_1\phi_{yx}^{0+}+\alpha_2\phi_{yx}^{0-}\right)P = W\left[2\sigma L_+(\eta_0)-\eta_0 P\right]. \qquad (4.2.92)$$

Likewise, from (4.2.90)

$$\alpha_1\phi_{yx}^{0+}\left[-2\sigma - d_1P + \sigma Q\right] + \alpha_2\phi_{yx}^{0-}\left[\frac{2\sigma\alpha_1}{\alpha_2} + d_1P - \sigma Q\right] - \sigma W\left[d_1Q - \sigma P\right]$$
$$= W\left[2\sigma L_+(\eta_0)(d_1-\eta_0) - P(\eta_0 d_1 - \sigma^2) - Q\sigma(d_1-\eta_0)\right] \quad (4.2.93)$$

which can be rearranged to give

$$\alpha_1\phi_{yx}^{0+}\left[-2\sigma - d_1P + \sigma Q\right] + \alpha_2\phi_{yx}^{0-}\left[\frac{2\sigma\alpha_1}{\alpha_2} + d_1P - \sigma Q\right]$$
$$= W\left[2\sigma L_+(\eta_0)(d_1-\eta_0) - P\eta_0 d_1 + Q\sigma\eta_0\right]. \quad (4.2.94)$$

Now (4.2.92) and (4.2.94) form a solvable system in the two remaining unknowns, ϕ_{yx}^{0+} and ϕ_{yx}^{0-}, which can be expressed in matrix form as

$$\begin{bmatrix} -P & P \\ -2\sigma - d_1P + \sigma Q & \frac{2\sigma\alpha_1}{\alpha_2} + d_1P - \sigma Q \end{bmatrix}\begin{bmatrix} \alpha_1\phi_{yx}^{0+} \\ \alpha_2\phi_{yx}^{0-} \end{bmatrix}$$
$$= W\begin{bmatrix} 2\sigma L_+(\eta_0) - \eta_0 P \\ 2\sigma L_+(\eta_0)(d_1-\eta_0) - P\eta_0 d_1 + Q\sigma\eta_0 \end{bmatrix}. \quad (4.2.95)$$

It follows that

$$\begin{bmatrix} \alpha_1\phi_{yx}^{0+} \\ \alpha_2\phi_{yx}^{0-} \end{bmatrix} = \frac{\alpha_2 W}{2\sigma P(\alpha_2-\alpha_1)}\begin{bmatrix} \frac{2\sigma\alpha_1}{\alpha_2} + d_1P - \sigma Q & -P \\ 2\sigma + d_1P - \sigma Q & -P \end{bmatrix} \times$$
$$\begin{bmatrix} 2\sigma L_+(\eta_0) - \eta_0 P \\ 2\sigma L_+(\eta_0)(d_1-\eta_0) - P\eta_0 d_1 + Q\sigma\eta_0 \end{bmatrix}. \quad (4.2.96)$$

It is worth taking a moment to consider the situation where the determinant of the matrix in (4.2.95) is equal to 0. If the definition of P as given in (4.2.68) is considered, it is clear that $P \neq 0$ for any value of σ and so, only the case where $\alpha_1 = \alpha_2$ would result in the determinant of the matrix being equal to 0. However, when σ was first defined, it was mentioned that the case where $\alpha_1 = \alpha_2$ would have to be dealt with separately, because of the singularity that occurs in σ at that point. So, the only case where this problem with the determinant occurs is already to be handled separately later.

Now, taking the top line of the matrix solution given in (4.2.96),

$$\alpha_1\phi_{yx}^{0+} = \frac{\alpha_2 W}{2\sigma P(\alpha_2-\alpha_1)}\left[\left\{\frac{2\sigma\alpha_1}{\alpha_2} + d_1P - \sigma Q\right\}\left\{2\sigma L_+(\eta_0) - \eta_0 P\right\}\right.$$
$$\left. - P\left\{2\sigma L_+(\eta_0)(d_1-\eta_0) - P\eta_0 d_1 + Q\sigma\eta_0\right\}\right]. \quad (4.2.97)$$

On multiplying out and noting that

$$-Q = P - 2L_+(\sigma) \quad (4.2.98)$$

this becomes

$$\alpha_1\phi_{yx}^{0+} = \frac{\alpha_2 W}{P(\alpha_2-\alpha_1)}\left[P\eta_0\left\{L_+(\eta_0) - \frac{\alpha_1}{\alpha_2}\right\} + 2\sigma L_+(\eta_0)\left\{\frac{\alpha_1}{\alpha_2} - L_+(\sigma)\right\} + \sigma P L_+(\eta_0)\right]. \quad (4.2.99)$$

Similarly,

$$\alpha_2\phi_{yx}^{0-} = \frac{\alpha_2 W}{2\sigma P(\alpha_2-\alpha_1)}\left[\{2\sigma + d_1 P - \sigma Q\}\{2\sigma L_+(\eta_0) - \eta_0 P\}\right.$$
$$\left. -P\{2\sigma L_+(\eta_0)(d_1-\eta_0) - P\eta_0 d_1 + Q\sigma\eta_0\}\right] \qquad (4.2.100)$$

which, using (4.2.98), can be rearrnged as

$$\alpha_2\phi_{yx}^{0-} = \frac{\alpha_2 W}{P(\alpha_2-\alpha_1)}\left[P\eta_0\{L_+(\eta_0)-1\} + 2\sigma L_+(\eta_0)\{1-L_+(\sigma)\} + \sigma P L_+(\eta_0)\right]. \qquad (4.2.101)$$

It is now possible to write down expressions for G and H given by (4.2.66) and (4.2.67), the expressions being

$$G = \frac{\alpha_2 W}{P(\alpha_2-\alpha_1)}\left[P\eta_0\left(1-\frac{\alpha_1}{\alpha_2}\right) - 2\sigma L_+(\eta_0)\left(1-\frac{\alpha_1}{\alpha_2}\right)\right] - W\eta_0$$
$$= -\frac{2\sigma W L_+(\eta_0)}{P} \qquad (4.2.102)$$

and

$$H = \frac{-\sigma\alpha_1 W}{\alpha_2-\alpha_1} + \frac{\sigma\alpha_2 W}{\alpha_2-\alpha_1} - W\sigma$$
$$= 0. \qquad (4.2.103)$$

When (4.2.102) and (4.2.103) are used in (4.2.65) it is easily found that

$$R_0 = -\frac{[L_+(\eta_0)]^2 L_2(\eta_0)}{L_1'(\eta_0)}\left[\frac{1}{2\eta_0} - \frac{\eta_0}{\eta_0^2-\sigma^2} + \frac{\sigma Q}{(\eta_0^2-\sigma^2)P}\right]. \qquad (4.2.104)$$

Similarly, when (4.2.102) and (4.2.103) are used in (4.2.72) the resultant expression for T_0 is found to be

$$T_0 = \frac{\alpha_2 L_1(\nu_0)L_+(\eta_0)\tau_0\tanh(\tau_0 a)}{\alpha_1 L_2'(\nu_0)L_+(\nu_0)\gamma_0\tanh(\gamma_0 a)}\left[\frac{1}{\eta_0-\nu_0} - \frac{\nu_0}{\sigma^2-\nu_0^2} - \frac{\sigma Q}{(\nu_0^2-\sigma^2)P}\right]. \qquad (4.2.105)$$

(ii) $\phi_y^{0+} = -\tau_0\tanh(\tau_0 a), \phi_{xy}^{0-} = -i\eta_0\tau_0\tanh(\tau_0 a)$

This pair of edge constraints corresponds to zero displacement on the membrane to the right of the point $x=0, y=a$ and zero gradient on the membrane to the left of that point. By using (4.2.62), these conditions can be rewritten as

$$\phi_y^{0+} = \frac{iW}{\alpha_2-\alpha_1} \qquad (4.2.106)$$

and

$$\phi_{xy}^{0-} = \frac{-\eta_0 W}{\alpha_2-\alpha_1}. \qquad (4.2.107)$$

On substituting this into (4.2.86), it is found that

$$-\alpha_1\phi_{yx}^{0+}P + i\sigma\alpha_2\phi_y^{0-}\left(Q-\frac{2\alpha_1}{\alpha_2}\right) = \frac{W}{\alpha_2-\alpha_1}[2\sigma\{(\alpha_2-\alpha_1)L_+(\eta_0)+\alpha_1\}$$
$$+\alpha_1\eta_0 P - \alpha_2\sigma Q]. \qquad (4.2.108)$$

Likewise, from (4.2.90)

$$\begin{aligned}\alpha_1\phi_{yx}^{0+}\left[-2\sigma-d_1P+\sigma Q\right]+i\sigma\alpha_2\phi_y^{0-}\left[d_1Q-\sigma P\right]\\ -\frac{\sigma\alpha_1 W}{\alpha_2-\alpha_1}\left[\sigma P-d_1Q\right]-\frac{\eta_0\alpha_2 W}{\alpha_2-\alpha_1}\left[\frac{2\sigma\alpha_1}{\alpha_2}+d_1P-\sigma Q\right]\\ =W\left[2\sigma L_+(\sigma)(d_1-\eta_0)-P(\eta_0 d_1-\sigma^2)-Q\sigma(d_1-\eta_0)\right]\end{aligned}\tag{4.2.109}$$

which can be rearranged to give

$$\begin{aligned}\alpha_1\phi_{yx}^{0+}\left[-2\sigma-d_1P+\sigma Q\right]+i\sigma\alpha_2\phi_y^{0-}\left[d_1Q-\sigma P\right]\\ =\frac{W}{\alpha_2-\alpha_1}\left[2\sigma\left\{(\alpha_2-\alpha_1)L_+(\sigma)(d_1-\eta_0)+\eta_0\alpha_1\right\}\right.\\ \left.+P\left\{\alpha_2\sigma^2+\alpha_1 d_1\eta_0\right\}-Q\left\{\alpha_1\eta_0\sigma+\alpha_2 d_1\sigma\right\}\right].\end{aligned}\tag{4.2.110}$$

Equations (4.2.108) and (4.2.110) form a complete system in the two remaining unknowns, ϕ_{yx}^{0+} and ϕ_y^{0-}, which can be expressed in matrix form as

$$\begin{bmatrix} -P & Q-\frac{2\alpha_1}{\alpha_2} \\ -2\sigma-d_1P+\sigma Q & d_1Q-\sigma P \end{bmatrix}\begin{bmatrix} \alpha_1\phi_{yx}^{0+} \\ i\sigma\alpha_2\phi_y^{0-} \end{bmatrix}=\frac{W}{\alpha_2-\alpha_1}\begin{bmatrix} C \\ D \end{bmatrix}\tag{4.2.111}$$

where

$$C = 2\sigma\left\{(\alpha_2-\alpha_1)L_+(\eta_0)+\alpha_1\right\}+\alpha_1\eta_0P-\alpha_2\sigma Q,\tag{4.2.112}$$

$$\begin{aligned}D = 2\sigma\left\{(\alpha_2-\alpha_1)L_+(\sigma)(d_1-\eta_0)+\eta_0\alpha_1\right\}+P\left\{\alpha_2\sigma^2+\alpha_1 d_1\eta_0\right\}\\ -Q\left\{\alpha_1\eta_0\sigma+\alpha_2 d_1\sigma\right\}.\end{aligned}\tag{4.2.113}$$

It follows that

$$\begin{bmatrix} \alpha_1\phi_{yx}^{0+} \\ i\sigma\alpha_2\phi_y^{0-} \end{bmatrix}=\frac{W}{(\alpha_2-\alpha_1)\Delta_1}\begin{bmatrix} d_1Q-\sigma P & \frac{2\alpha_1}{\alpha_2}-Q \\ 2\sigma+d_1P-\sigma Q & -P \end{bmatrix}\begin{bmatrix} C \\ D \end{bmatrix}\tag{4.2.114}$$

where the determinant of the matrix, Δ_1, is given by

$$\begin{aligned}\Delta_1 &= -P(d_1Q-\sigma P)-\left(\frac{2\alpha_1}{\alpha_2}-Q\right)(-2\sigma-d_1P+\sigma Q)\\ &= \sigma\left(P^2-Q^2\right)+\frac{2\alpha_1}{\alpha_2}(\sigma Q-d_1P)+2\sigma\left(Q-\frac{2\alpha_1}{\alpha_2}\right).\end{aligned}\tag{4.2.115}$$

Again here, as in case (i), the situation where the denominator of the term multiplying the solution matrix in (4.2.114) is equal to 0 must be considered. The expression given for Δ_1 is easily shown to never be equal to 0, and so again, only the case where $\alpha_1=\alpha_2$ is of interest. As has already been mentioned, at this point σ is undefined and so this particular case requires further investigation anyway. Hence,

$$\begin{aligned}\frac{\Delta_1(\alpha_2-\alpha_1)\alpha_1\phi_{yx}^{0+}}{W} &= (d_1Q-\sigma P)\left[2\sigma\left\{(\alpha_2-\alpha_1)L_+(\eta_0)+\alpha_1\right\}+\alpha_1\eta_0P-\alpha_2\sigma Q\right]\\ &\quad+\left[\frac{2\alpha_1}{\alpha_2}-Q\right]\left[2\sigma\left\{(\alpha_2-\alpha_1)L_+(\sigma)(d_1-\eta_0)+\eta_0\alpha_1\right\}\right.\\ &\quad\left.+P\left\{\alpha_2\sigma^2+\alpha_1 d_1\eta_0\right\}-Q\left\{\alpha_1\eta_0\sigma+\alpha_2 d_1\sigma\right\}\right]\end{aligned}\tag{4.2.116}$$

which can be rearranged to become

$$\alpha_1\phi_{yx}^{0+} = \frac{2\sigma L_+(\eta_0)W}{\Delta_1}\left[\frac{2\alpha_1(d_1-\eta_0)}{\alpha_2} - P\sigma + Q\eta_0\right] - \frac{\alpha_1\eta_0 W}{\alpha_2-\alpha_1}. \tag{4.2.117}$$

Similarly,

$$\begin{aligned}\frac{\Delta_1(\alpha_2-\alpha_1)i\sigma\alpha_2\phi_y^{0-}}{W} &= [2\sigma + d_1P - \sigma Q]\,[2\sigma\{(\alpha_2-\alpha_1)L_+(\eta_0)+\alpha_1\} + \alpha_1\eta_0 P - \alpha_2\sigma Q] \\ &\quad -P\,[2\sigma\{(\alpha_2-\alpha_1)L_+(\sigma)(d_1-\eta_0)+\eta_0\alpha_1\} \\ &\quad +P\left\{\alpha_2\sigma^2+\alpha_1 d_1\eta_0\right\} - Q\{\alpha_1\eta_0\sigma+\alpha_2 d_1\sigma\}\Big]\end{aligned} \tag{4.2.118}$$

which can be rearranged as

$$i\sigma\alpha_2\phi_y^{0-} = \frac{2\sigma L_+(\eta_0)W}{\Delta_1}[2\sigma + P\eta_0 - Q\sigma] - \frac{\alpha_2\sigma W}{\alpha_2-\alpha_1}. \tag{4.2.119}$$

It is now possible to write down expressions for G and H given by (4.2.66) and (4.2.67), these being

$$G = \frac{2\sigma L_+(\eta_0)W}{\Delta_1}\left[\frac{2\alpha_1(d1-\eta_0)}{\alpha_2} - P\sigma + Q\eta_0\right] \tag{4.2.120}$$

and

$$H = -\frac{2\sigma L_+(\eta_0)W}{\Delta_1}[2\sigma + P\eta_0 - Q\sigma]. \tag{4.2.121}$$

When (4.2.120) and (4.2.121) are applied to (4.2.65) the resultant expression for R_0 is

$$\begin{aligned}R_0 &= -\frac{[L_+(\eta_0)]^2 L_2(\eta_0)}{L_1'(\eta_0)}\left[\frac{1}{2\eta_0}\right. \\ &\quad +\frac{1}{\Delta_1(\eta_0^2-\sigma^2)}\left[\left\{\frac{2\alpha_1(d1-\eta_0)}{\alpha_2} - P\sigma + Q\eta_0\right\}\{\eta_0 P - \sigma Q\}\right. \\ &\quad \left.\left. -\{2\sigma + P\eta_0 - Q\sigma\}\{\eta_0 Q - \sigma P\}\right]\right].\end{aligned} \tag{4.2.122}$$

Once simplified, this becomes

$$\begin{aligned}R_0 &= -\frac{[L_+(\eta_0)]^2 L_2(\eta_0)}{L_1'(\eta_0)}\left[\frac{1}{2\eta_0}\right. \\ &\quad \left.+\frac{1}{\Delta_1(\eta_0^2-\sigma^2)}\left\{\frac{2\alpha_1(d1-\eta_0)}{\alpha_2}(\eta_0 P - \sigma Q) + 2\sigma(\sigma P - \eta_0 Q)\right\}\right].\end{aligned} \tag{4.2.123}$$

The transmitted coefficient, T_0, is found in a similar way, by applying (4.2.120) and (4.2.121) to (4.2.72). This gives

$$\begin{aligned}T_0 &= \frac{\alpha_2 L_1(\nu_0)L_+(\eta_0)\tau_0\tanh(\tau_0 a)}{\alpha_1 L_2'(\nu_0)L_+(\nu_0)\gamma_0\tanh(\gamma_0 a)}\left[\frac{1}{\eta_0-\nu_0}\right. \\ &\quad +\frac{1}{\Delta_1(\sigma^2-\nu_0^2)}\left[\left\{\frac{2\alpha_1(d1-\eta_0)}{\alpha_2} - P\sigma + Q\eta_0\right\}\{\sigma Q + \nu_0 P\}\right. \\ &\quad \left.\left. -\{2\sigma + P\eta_0 - Q\sigma\}\{\sigma P + \nu_0 Q\}\right]\right],\end{aligned} \tag{4.2.124}$$

which can be simplified to

$$T_0 = \frac{\alpha_2 L_1(\nu_0) L_+(\eta_0)\tau_0 \tanh(\tau_0 a)}{\alpha_1 L_2'(\nu_0) L_+(\nu_0)\gamma_0 \tanh(\gamma_0 a)} \left[\frac{1}{\eta_0 - \nu_0}\right.$$
$$+\frac{1}{\Delta_1(\sigma^2 - \nu_0^2)} \left\{\frac{2\alpha_1(d1 - \eta_0)}{\alpha_2}(\sigma Q + \nu_0 P)\right.$$
$$\left.\left. - 2\sigma(\sigma P + \nu_0 Q) + \sigma(Q^2 - P^2)(\nu_0 + \eta_0)\right\}\right]. \quad (4.2.125)$$

(iii) $\phi_{xy}^{0+} = -i\eta_0\tau_0 \tanh(\tau_0 a), \phi_y^{0-} = -\tau_0 \tanh(\tau_0 a)$

This pair of edge constraints corresponds to zero gradient on the membrane to the right of the point $x = 0, y = a$ and zero displacement on the membrane to the left of that point. By using (4.2.62), these conditions can be rewritten as

$$\phi_{yx}^{0+} = \frac{-\eta_0 W}{\alpha_2 - \alpha_1} \quad (4.2.126)$$

and

$$\phi_x^{0-} = \frac{iW}{\alpha_2 - \alpha_1}. \quad (4.2.127)$$

On substituting these conditions into (4.2.86) it is found that

$$\alpha_2\phi_{yx}^{0-}P + i\sigma\alpha_1\phi_y^{0+}(2 - Q) = \frac{W}{\alpha_2 - \alpha_1}[2\sigma\{(\alpha_2 - \alpha_1)L_+(\eta_0) - \alpha_1\}$$
$$-\alpha_2\eta_0 P + \alpha_1\sigma Q] \quad (4.2.128)$$

Similarly, from (4.2.90)

$$\alpha_2\phi_{yx}^{0-}\left[\frac{2\sigma\alpha_1}{\alpha_2} + d_1 P - \sigma Q\right] + i\sigma\alpha_1\phi_y^{0+}[\sigma P - d_1 Q]$$
$$-\frac{\alpha_1\eta_0 W}{\alpha_2 - \alpha_1}[-2\sigma - d_1 P + \sigma Q] - \frac{\alpha_2\sigma W}{\alpha_2 - \alpha_1}[d_1 Q - \sigma P]$$
$$= W\left[2\sigma L_+(\sigma)(d_1 - \eta_0) - A(\eta_0 d_1 - \sigma^2) - Q\sigma(d_1 - \eta_0)\right] \quad (4.2.129)$$

which, when rearranged becomes

$$\alpha_2\phi_{yx}^{0-}\left[\frac{2\sigma\alpha_1}{\alpha_2} + d_1 P - \sigma Q\right] + i\sigma\alpha_1\phi_y^{0+}[\sigma P - d_1 Q]$$
$$= \frac{W}{\alpha_2 - \alpha_1}[2\sigma\{(\alpha_2 - \alpha_1)L_+(\sigma)(d_1 - \eta_0) - \eta_0\alpha_1\}$$
$$+P\left\{-\alpha_1\sigma^2 - \alpha_2 d_1\eta_0\right\} + Q\{\alpha_1 d_1\sigma + \alpha_2\eta_0\sigma\}]. \quad (4.2.130)$$

As in previous cases, the two equations, (4.2.128) and (4.2.130), form a complete, and thus solvable system in the two remaining unknowns. This system can be expressed in matrix form as

$$\begin{bmatrix} P & 2 - Q \\ \frac{2\sigma\alpha_1}{\alpha_2} + d_1 P - \sigma Q & \sigma P - d_1 Q \end{bmatrix} \begin{bmatrix} \alpha_2\phi_{yx}^{0-} \\ i\sigma\alpha_1\phi_y^{0+} \end{bmatrix} = \frac{W}{\alpha_2 - \alpha_1}\begin{bmatrix} C \\ D \end{bmatrix} \quad (4.2.131)$$

where

$$C = 2\sigma\{(\alpha_2-\alpha_1)L_+(\eta_0)-\alpha_1\}-\alpha_2\eta_0 P+\alpha_1\sigma Q \tag{4.2.132}$$

$$D = 2\sigma\{(\alpha_2-\alpha_1)L_+(\sigma)(d_1-\eta_0)-\eta_0\alpha_1\}+P\left\{-\alpha_1\sigma^2-\alpha_2 d_1\eta_0\right\}. \\ +Q\{\alpha_1 d_1\sigma+\alpha_2\eta_0\sigma\} \tag{4.2.133}$$

It follows that

$$\begin{bmatrix} \alpha_2\phi_{yx}^{0-} \\ i\sigma\alpha_1\phi_y^{0+} \end{bmatrix} = \frac{W}{\Delta_2(\alpha_2-\alpha_1)}\begin{bmatrix} \sigma P-d_1Q & Q-2 \\ -\frac{2\sigma\alpha_1}{\alpha_2}-d_1P+\sigma Q & P \end{bmatrix}\begin{bmatrix} C \\ D \end{bmatrix} \tag{4.2.134}$$

where the determinant of the original matrix, Δ_2, is given by

$$\Delta_2 = P(\sigma P-d_1Q)-(2-Q)\left(\frac{2\sigma\alpha_1}{\alpha_2}+d_1P-\sigma Q\right) \\ = \sigma\left(P^2-Q^2\right)+2(\sigma Q-d_1P)+\frac{2\sigma\alpha_1}{\alpha_2}(Q-2). \tag{4.2.135}$$

Again, the denominator of the expression multiplying the matrix solution in (4.2.134) must be considered; should this expression ever equal 0, then the solution would be undefined. As in the previous two cases, this only occurs when $\alpha_1=\alpha_2$, which is already being dealt with as a special case, and so the analysis of this case continues, with the assumption that $\alpha_1\neq\alpha_2$ made. The matrix solution to the system gives expressions for both of the two remaining unknowns. Thus,

$$\frac{\alpha_2\phi_{yx}^{0-}\Delta_2(\alpha_2-\alpha_1)}{W} = (\sigma P-d_1Q)\left[2\sigma\{(\alpha_2-\alpha_1)L_+(\eta_0)-\alpha_1\}-\alpha_2\eta_0P+\alpha_1\sigma Q\right] \\ (Q-2)\left[2\sigma\{(\alpha_2-\alpha_1)L_+(\sigma)(d_1-\eta_0)-\eta_0\alpha_1\}\right. \\ \left.+P\left\{-\alpha_1\sigma^2-\alpha_2 d_1\eta_0\right\}+Q\{\alpha_1 d_1\sigma+\alpha_2\eta_0\sigma\}\right] \tag{4.2.136}$$

which, when rearranged, gives

$$\alpha_2\phi_{yx}^{0-} = -\frac{\alpha_2\eta_0 W}{\alpha_2-\alpha_1}+\frac{2\sigma L_+(\eta_0)W}{\Delta_2}[\sigma P-\eta_0 Q-2(d_1-\eta_0)]. \tag{4.2.137}$$

Similarly,

$$\frac{i\sigma\alpha_1\phi_y^{0+}\Delta_2(\alpha_2-\alpha_1)}{W} = \left[-\frac{2\sigma\alpha_1}{\alpha_2}-d_1P+\sigma Q\right]\left[2\sigma\{(\alpha_2-\alpha_1)L_+(\eta_0)-\alpha_1\}-\alpha_2\eta_0P\right. \\ \left.+\alpha_1\sigma Q\right]+P\left[2\sigma\{(\alpha_2-\alpha_1)L_+(\sigma)(d_1-\eta_0)-\eta_0\alpha_1\}\right. \\ \left.+P\left\{-\alpha_1\sigma^2-\alpha_2 d_1\eta_0\right\}+Q\{\alpha_1 d_1\sigma+\alpha_2\eta_0\sigma\}\right] \tag{4.2.138}$$

which can be rearranged to give

$$i\sigma\alpha_1\phi_y^{0+} = -\frac{\alpha_1\sigma W}{\alpha_2-\alpha_1}+\frac{2\sigma L_+(\eta_0)W}{\Delta_2}\left[\sigma Q-\eta_0 P-\frac{2\sigma\alpha_1}{\alpha_2}\right]. \tag{4.2.139}$$

Now expressions for G and H, given as (4.2.66) and (4.2.67) can be written down. These are

$$G = -\frac{2\sigma L_+(\eta_0)W}{\Delta_2}[\sigma P-\eta_0 Q-2(d_1-\eta_0)] \tag{4.2.140}$$

and

$$H = \frac{2\sigma L_+(\eta_0)W}{\Delta_2}\left[\sigma Q - \eta_0 P - \frac{2\sigma\alpha_1}{\alpha_2}\right]. \tag{4.2.141}$$

It is now possible to find an expression for R_0, by applying (4.2.140) and (4.2.141) to (4.2.65) to give

$$\begin{aligned} R_0 \;=\; & -\frac{[L_+(\eta_0)]^2 L_2(\eta_0)}{L_1'(\eta_0)}\left[\frac{1}{2\eta_0}\right. \\ & +\frac{1}{\Delta_2(\eta_0^2-\sigma^2)}\left[\{\sigma P - \eta_0 Q - 2(d_1-\eta_0)\}\{\eta_0 P - \sigma Q\}\right. \\ & \left.\left. -\left\{\sigma Q - \eta_0 P - \frac{2\sigma\alpha_1}{\alpha_2}\right\}\{\eta_0 Q - \sigma P\}\right]\right]. \end{aligned} \tag{4.2.142}$$

After multiplying out, this can be simplified to give

$$\begin{aligned} R_0 \;=\; & -\frac{[L_+(\eta_0)]^2 L_2(\eta_0)}{L_1'(\eta_0)}\left[\frac{1}{2\eta_0}\right. \\ & \left.+\frac{1}{\Delta_2(\eta_0^2-\sigma^2)}\left\{2(d1-\eta_0)(\eta_0 P - \sigma Q) + \frac{2\sigma\alpha_1}{\alpha_2}(\sigma P - \eta_0 Q)\right\}\right]. \end{aligned} \tag{4.2.143}$$

Similarly for T_0, (4.2.140) and (4.2.141) are applied to (4.2.72) to give

$$\begin{aligned} T_0 \;=\; & \frac{\alpha_2 L_1(\nu_0)L_+(\eta_0)\tau_0\tanh(\tau_0 a)}{\alpha_1 L_2'(\nu_0)L_+(\nu_0)\gamma_0\tanh(\gamma_0 a)}\left[\frac{1}{\eta_0-\nu_0}\right. \\ & +\frac{1}{\Delta_1(\sigma^2-\nu_0^2)}\left[\{\sigma P - \eta_0 Q - 2(d_1-\eta_0)\}\{\sigma Q + \nu_0 P\}\right. \\ & \left.\left. -\left\{\sigma Q - \eta_0 P - \frac{2\sigma\alpha_1}{\alpha_2}\right\}\{\sigma P + \nu_0 Q\}\right]\right], \end{aligned} \tag{4.2.144}$$

which simplifies to

$$\begin{aligned} T_0 \;=\; & \frac{\alpha_2 L_1(\nu_0)L_+(\eta_0)\tau_0\tanh(\tau_0 a)}{\alpha_1 L_2'(\nu_0)L_+(\nu_0)\gamma_0\tanh(\gamma_0 a)}\left[\frac{1}{\eta_0-\nu_0}\right. \\ & +\frac{1}{\Delta_1(\sigma^2-\nu_0^2)}\left\{(d1-\eta_0)(\sigma Q + \nu_0 P)\right. \\ & \left.\left. -\frac{2\sigma\alpha_1}{\alpha_2}(\sigma P + \nu_0 Q) + \sigma(Q^2-P^2)(\nu_0+\eta_0)\right\}\right]. \end{aligned} \tag{4.2.145}$$

(iv) $\phi_{xy}^{0+} = \phi_{xy}^{0-} = -i\eta_0\tau_0\tanh(\tau_0 a)$

In this last case, the pair of edge constraints correspond to zero gradient on both membranes at $x = 0$, and may be rewritten as

$$\phi_{xy}^{0+} = \phi_{yx}^{0-} = \frac{-\eta_0 W}{\alpha_2 - \alpha_1}. \tag{4.2.146}$$

When this is substituted into (4.2.86), it is found that

$$i\left[\alpha_1\phi_y^{0+}(2-Q) + \alpha_2\phi_y^{0-}\left(Q - \frac{2\alpha_1}{\alpha_2}\right)\right] = W\left[2L_+(\eta_0) - Q\right], \tag{4.2.147}$$

Likewise, (4.2.90) yields

$$-\frac{\eta_0 W}{\alpha_2-\alpha_1}\left[\alpha_1\{-2\sigma-d_1P+\sigma Q\}+\alpha_2\left\{\frac{2\sigma\alpha_1}{\alpha_2}+d_1P-\sigma Q\right\}\right] +i\sigma\left[\alpha_1\phi_y^{0+}\{\sigma P-d_1Q\}+\alpha_2\phi_y^{0-}\{d_1Q-\sigma P\}\right] = W\left[2\sigma L_+(\eta_0)(d_1-\eta_0)-A(\eta_0 d_1-\sigma^2)-B(d_1\sigma-\eta_0\sigma)\right] \quad (4.2.148)$$

which can be rearranged to give

$$i\left[\alpha_1\phi_y^{0+}\{\sigma P-d_1Q\}+\alpha_2\phi_y^{0-}\{d_1Q-\sigma P\}\right] = W\left[2L_+(\eta_0)(d_1-\eta_0)-P\sigma-Bd_1\right]. \quad (4.2.149)$$

Equations (4.2.147) and (4.2.149) now form a solvable system that can be used to find the two remaining unknowns, ϕ_y^{0+} and ϕ_y^{0-}. The system maybe written in matrix form as

$$\begin{bmatrix} 2-Q & Q-\frac{2\alpha_1}{\alpha_2} \\ \sigma P-d_1Q & d_1Q-\sigma A \end{bmatrix}\begin{bmatrix} i\alpha_1\phi_y^{0+} \\ i\alpha_2\phi_y^{0-} \end{bmatrix} = W\begin{bmatrix} 2L_+(\eta_0)-Q \\ 2L_+(\eta_0)(d_1-\eta_0)-P\sigma-Bd_1 \end{bmatrix}. \quad (4.2.150)$$

It follows that

$$\begin{bmatrix} i\alpha_1\phi_y^{0+} \\ i\alpha_2\phi_y^{0-} \end{bmatrix} = \frac{\alpha_2 W}{2(\alpha_2-\alpha_1)(d_1Q-\sigma P)}\begin{bmatrix} d_1Q-\sigma P & \frac{2\alpha_1}{\alpha_2}-Q \\ d_1Q-\sigma P & 2-Q \end{bmatrix}\times \begin{bmatrix} 2L_+(\eta_0)-Q \\ 2L_+(\eta_0)(d_1-\eta_0)-P\sigma-Bd_1 \end{bmatrix} \quad (4.2.151)$$

The denominator of the multiplying expression in front of the matrix solution in (4.2.151), as in previous cases, is only equal to zero when $\alpha_1=\alpha_2$. This case is already recognised as a special case because of the singularity that occurs in σ at this point, and so analysis continues with the assumption that $\alpha_1\neq\alpha_2$. It is easy to see from (4.2.151) that

$$i\alpha_1\phi_y^{0+} = \frac{\alpha_2 W}{2(\alpha_2-\alpha_1)(d_1Q-\sigma P)}\left[\{d_1Q-\sigma P\}\{2L_+(\eta_0)-Q\} +\left\{\frac{2\alpha_1}{\alpha_2}-Q\right\}\{2L_+(\eta_0)(d_1-\eta_0)-P\sigma-Bd_1\}\right] \quad (4.2.152)$$

and

$$i\alpha_2\phi_y^{0-} = \frac{\alpha_2 W}{2(\alpha_2-\alpha_1)(d_1Q-\sigma P)}\left[\{d_1Q-\sigma P\}\{2L_+(\eta_0)-Q\} +\{2-Q\}\{2L_+(\eta_0)(d_1-\eta_0)-P\sigma-Qd_1\}\right]. \quad (4.2.153)$$

It is now possible to write down forms for G and H given in (4.2.66) and (4.2.67) respectively, that is

$$\begin{aligned} G &= -\frac{\alpha_1\eta_0 W}{\alpha_2-\alpha_1}+\alpha_2\eta_0 W\alpha_2-\alpha_1-W\eta_0 \\ &= 0 \end{aligned} \quad (4.2.154)$$

and

$$\begin{aligned} H &= \frac{\alpha_2\sigma W}{2(\alpha_2-\alpha_1)(d_1Q-\sigma P)}\left\{\frac{2\alpha_1}{\alpha_2}-2\right\}\{2L_+(\eta_0)(d_1-\eta_0) \\ &\qquad -P\sigma-Bd_1\}-W\sigma \\ &= \frac{2\sigma W L_+(\eta_0)(d_1-\eta_0)}{\sigma P-d_1Q}. \end{aligned} \tag{4.2.155}$$

The expressions gained in (4.2.154) and (4.2.155) can be applied to (4.2.65) to give

$$R_0 = -\frac{[L_+(\eta_0)]^2 L_2(\eta_0)}{L_1'(\eta_0)}\left[\frac{1}{2\eta_0}-\frac{(d_1-\eta_0)(Q\eta_0-P\sigma)}{(\eta_0^2-\sigma^2)(Qd_1-P\sigma)}\right]. \tag{4.2.156}$$

Similarly, when (4.2.154) and (4.2.155) are applied to (4.2.65), the resultant expression for T_0 is

$$T_0 = \frac{\alpha_2 L_1(\nu_0)L_+(\eta_0)\tau_0\tanh(\tau_0 a)}{\alpha_1 L_2'(\nu_0)L_+(\nu_0)\gamma_0\tanh(\gamma_0 a)}\left[\frac{1}{\eta_0-\nu_0}-\frac{(d_1-\eta_0)(P\sigma+\nu_0 Q)}{(\nu_0^2-\sigma^2)(P\sigma-d_1Q)}\right]. \tag{4.2.157}$$

4.2.2 Sum split of the Wiener-Hopf kernel and determination of d_1

So, for the four possible combinations of edge conditions, detailed in cases (i) to (iv) above, R_0 and T_0 have distinct forms. However, all these expressions for R_0 and T_0 rely on $L_+(s)$ and $L_-(s)$ and all but one also rely on d_1. Before R_0 and T_0 can be evaluated it will be necessary to construct suitable expressions for these remaining quantities. First, $L_\pm(s)$ will be found. In this case, the Wiener-Hopf kernel is

$$L(s) = \frac{L_1(s)}{L_2(s)} \tag{4.2.158}$$

where

$$L_1(s) = (s^2-\mu_1^2)\gamma\tanh(\gamma a)-\alpha_1, \tag{4.2.159}$$

$$L_2(s) = (s^2-\mu_2^2)\gamma\tanh(\gamma a)-\alpha_2. \tag{4.2.160}$$

Hence, L(s) can be expressed as

$$L(s) = \frac{(s^2-\mu_1^2)\gamma\sinh(\gamma a)-\alpha_1\cosh(\gamma a)}{(s^2-\mu_2^2)\gamma\sinh(\gamma a)-\alpha_2\cosh(\gamma a)}. \tag{4.2.161}$$

However, in section 3.2, a function, $f(s)$ was defined as

$$f(s) = (s^2-\mu^2)\gamma\sinh(\gamma a)-\alpha\cosh(\gamma a). \tag{4.2.162}$$

This was separated to give

$$f(s) = -\alpha\prod_{n=0}^{\infty}\left\{\left(1+\frac{1}{\gamma_n^2}\right)^{\frac{1}{2}}-\frac{s}{\gamma_n}\right\}\left\{\left(1+\frac{1}{\gamma_n^2}\right)^{\frac{1}{2}}+\frac{s}{\gamma_n}\right\}. \tag{4.2.163}$$

Hence, using this infinite product form and applying it to (4.2.161), $L(s)$ can be given as

$$L(s) = \frac{\alpha_1 \prod_{n=0}^{\infty} \left\{ \left(1+\frac{1}{\tau_n^2}\right)^{\frac{1}{2}} - \frac{s}{\tau_n} \right\} \left\{ \left(1+\frac{1}{\tau_n^2}\right)^{\frac{1}{2}} + \frac{s}{\tau_n} \right\}}{\alpha_2 \prod_{n=0}^{\infty} \left\{ \left(1+\frac{1}{\gamma_n^2}\right)^{\frac{1}{2}} - \frac{s}{\gamma_n} \right\} \left\{ \left(1+\frac{1}{\gamma_n^2}\right)^{\frac{1}{2}} + \frac{s}{\gamma_n} \right\}}. \tag{4.2.164}$$

Thus, when separated into plus and minus functions and simplified,

$$L_{\pm}(s) = \left(\frac{\alpha_1}{\alpha_2}\right)^{\frac{1}{2}} \prod_{n=0}^{\infty} \frac{\gamma_n(s \pm \eta_n)}{\tau_n(s \pm \nu_n)}. \tag{4.2.165}$$

The quantity d_1 is analogous to that of κ in subsection 3.2.1 and is, therefore determined using similar analysis. This constant, as defined in terms of $L_-(s)$ by (4.2.78), is

$$\frac{1}{L_-(s)} \sim 1 + \frac{d_1}{s} + \frac{d_2}{s^2} + \dots . \tag{4.2.166}$$

It is also worth noting at this point that a direct implication of (4.2.158) is that

$$L(s) = \frac{L_1(s)}{L_2(s)} = \frac{L_{1+}(s)L_{1-}(s)}{L_{2+}(s)L_{2-}(s)}, \tag{4.2.167}$$

and so

$$\frac{1}{L_-(s)} = \frac{L_{2-}(s)}{L_{1-}(s)} \tag{4.2.168}$$

By following the method dictated by (3.2.87) – (3.2.98), it is clear that

$$\ln\left[\frac{1}{L_-(s)}\right] = \frac{1}{2\pi i} \int_{-\infty}^{\infty} \ln\left[\frac{1}{L(s)}\right] \frac{d\zeta}{\zeta - s}. \tag{4.2.169}$$

Expression (4.2.161) for $L(s)$ as stated can be rearranged as

$$L(s) = \frac{(s^2 - \mu_1^2) - \frac{\alpha_1 \cosh(\gamma a)}{\gamma \sinh(\gamma a)}}{(s^2 - \mu_2^2) - \frac{\alpha_2 \cosh(\gamma a)}{\gamma \sinh(\gamma a)}}. \tag{4.2.170}$$

Hence, from (4.2.169)

$$\ln\left[\frac{1}{L_-(s)}\right] = \frac{1}{2\pi i} \int_{-\infty}^{\infty} \ln\left[\frac{(\zeta^2 - \mu_2^2) - \frac{\alpha_2 \cosh(\gamma a)}{\gamma \sinh(\gamma a)}}{(\zeta^2 - \mu_1^2) - \frac{\alpha_1 \cosh(\gamma a)}{\gamma \sinh(\gamma a)}}\right] \frac{d\zeta}{\zeta - s}. \tag{4.2.171}$$

By using rules of logarithms, it can easily be seen that (4.2.169) can be rearranged to give

$$\begin{aligned} \ln\left[\frac{1}{L_-(s)}\right] = & \frac{1}{2\pi i} \int_{-\infty}^{\infty} \ln\left[(\zeta^2 - \mu_2^2) - \frac{\alpha_2 \cosh(\gamma a)}{\gamma \sinh(\gamma a)}\right] \frac{d\zeta}{\zeta - s} \\ & - \frac{1}{2\pi i} \int_{-\infty}^{\infty} \ln\left[(\zeta^2 - \mu_1^2) - \frac{\alpha_1 \cosh(\gamma a)}{\gamma \sinh(\gamma a)}\right] \frac{d\zeta}{\zeta - s}. \end{aligned} \tag{4.2.172}$$

It is noted that the two expressions on the right hand side of (4.2.172) are equivalent to that in (3.2.88) and so, following the method laid out in (3.2.89) – (3.2.98), $\frac{1}{L_-(s)}$ can be written in the form

$$\frac{1}{L_-(s)} = 1+\frac{1}{s}\left[\mu_1-\mu_2+\frac{i}{\pi}\left\{\int_0^\infty \ln\left[1-\frac{\alpha_1\cosh(\gamma a)}{(\zeta^2-\mu_1^2)\gamma\sinh(\gamma a)}\right]d\zeta - \int_0^\infty \ln\left[1-\frac{\alpha\cosh(\gamma a)}{(\zeta^2-\mu^2)\gamma\sinh(\gamma a)}\right]d\zeta\right\}\right]+\frac{d_2}{s^2}+\ldots. \tag{4.2.173}$$

Thus, referring to (4.2.166)

$$d_1 = \mu_1-\mu_2+\frac{i}{\pi}\left\{\int_0^\infty \ln\left[1-\frac{\alpha_1\cosh(\gamma a)}{(\zeta^2-\mu_1^2)\gamma\sinh(\gamma a)}\right]d\zeta - \int_0^\infty \ln\left[1-\frac{\alpha\cosh(\gamma a)}{(\zeta^2-\mu^2)\gamma\sinh(\gamma a)}\right]d\zeta\right\}. \tag{4.2.174}$$

All of the work carried out on this problem so far is reflected in the *Mathematica* code included in Appendix C.2.

4.2.3 The special case when $\alpha_1 = \alpha_2$

Recall the definition of σ as given in (4.2.38), that is.

$$\sigma = \frac{(\alpha_2\mu_1^2-\alpha_1\mu_2^2)^{\frac{1}{2}}}{(\alpha_2-\alpha_1)^{\frac{1}{2}}}. \tag{4.2.175}$$

When σ was first defined, reference was made to the potential problem caused in the case when $\alpha_1 = \alpha_2$. Here that problem will be addressed.

In the case where $\alpha_1 = \alpha_2$, a singularity occurs in σ. This singularity affects all the expressions found for R_0 and T_0, and so for each pair of edge conditions, the case where $\alpha_1 = \alpha_2$ must considered separately. As an example of the analysis involved, case (i) from subsection 4.2.1 is considered for $\alpha_1 = \alpha_2$.

It is worthwhile noting first, that the expressions for R_0 and T_0 bear striking similarities to each other. Consider the expression I, given as

$$I = K\left[\frac{1}{\eta_0+s}+\frac{s}{\sigma^2-s^2}-\frac{\sigma Q}{(s^2-\sigma^2)P}\right]. \tag{4.2.176}$$

In the case where $s = \eta_0$ and

$$K = -\frac{[L_+(\eta_0)]^2 L_2(\eta_0)}{L_1'(\eta_0)} \tag{4.2.177}$$

then $I = R_0$. However, when $s = -\nu_0$ and

$$K = \frac{\alpha_2 L_1(\nu_0)L_+(\eta_0)\tau_0\tanh(\tau_0 a)}{\alpha_1 L_2'(\nu_0)L_+(\nu_0)\gamma_0\tanh(\gamma_0 a)} \tag{4.2.178}$$

then $I = T_0$. It is convenient to use the common form given in (4.2.176) since K is essentially unaffected if $\alpha_1 = \alpha_2$. Thus, using expression for σ given in (4.2.175), it is easily shown that

$$\frac{s}{\sigma^2-s^2} \to 0, \quad \alpha_1 \to \alpha_2. \tag{4.2.179}$$

Further, $\frac{1}{\eta_0+s}$ is unaffected as $\alpha_1 \to \alpha_2$.

The only term that needs consideration as $\alpha_1 \to \alpha_2$ is the last term of (4.2.176). From (4.2.39) it can be shown that

$$\frac{1}{s^2-\sigma^2} = \frac{\gamma \tanh(\gamma a)(\alpha_2-\alpha_1)}{\alpha_2 L_1(s) - \alpha_1 L_2(s)}, \qquad \gamma = (s^2-1)^{\frac{1}{2}}, \tag{4.2.180}$$

and so

$$\frac{\sigma}{s^2-\sigma^2} = \frac{\gamma \tanh(\gamma a)(\alpha_2-\alpha_1)^{\frac{1}{2}}(\alpha_2\mu_1^2 - \alpha_1\mu_2^2)^{\frac{1}{2}}}{\alpha_2 L_1(s) - \alpha_1 L_2(s)}, \qquad \gamma = (s^2-1)^{\frac{1}{2}}. \tag{4.2.181}$$

From (4.2.68) and (4.2.69), it is clear that

$$\begin{aligned} \frac{Q}{P} &= \frac{L_+(\sigma)+L_-(\sigma)}{L_+(\sigma)-L_-(\sigma)} \\ &= \frac{\alpha_2 L_+^2(\sigma)+\alpha_1}{\alpha_2 L_+^2(\sigma)-\alpha_1} \end{aligned} \tag{4.2.182}$$

Hence, the term in question can be expressed as

$$\frac{\sigma Q}{(s^2-\sigma^2)P} = \frac{\gamma \tanh(\gamma a)(\alpha_2-\alpha_1)^{\frac{1}{2}}(\alpha_2\mu_1^2 - \alpha_1\mu_2^2)^{\frac{1}{2}}(\alpha_2 L_+^2(\sigma)+\alpha_1)}{(\alpha_2 L_1(s) - \alpha_1 L_2(s))(\alpha_2 L_+^2(\sigma)-\alpha_1)}, \qquad \gamma = (s^2-1)^{\frac{1}{2}}. \tag{4.2.183}$$

It follows that

$$\lim_{\alpha_1\to\alpha_2}\left[\frac{\sigma Q}{(s^2-\sigma^2)P}\right] = \frac{\gamma \tanh(\gamma a)(\alpha_2\mu_1^2 - \alpha_1\mu_2^2)^{\frac{1}{2}}(\alpha_2 L_+^2(\sigma)+\alpha_1)}{\alpha_2 L_1(s) - \alpha_1 L_2(s)} \lim_{\alpha_1\to\alpha_2} \frac{(\alpha_2-\alpha_1)^{\frac{1}{2}}}{\alpha_2 L_+^2(\sigma)-\alpha_1}. \tag{4.2.184}$$

It has been stated previously that $L_+(s)$ takes the form

$$L_+(s) = 1 + \frac{d_1}{s} + \ldots \tag{4.2.185}$$

and so it is clear that

$$L_+^2(\sigma) = 1 + \frac{2d_1}{\sigma} + \ldots. \tag{4.2.186}$$

If (4.2.186) is substituted into (4.2.184) then

$$\begin{aligned} \lim_{\alpha_1\to\alpha_2}\left[\frac{\sigma Q}{(s^2-\sigma^2)P}\right] &= \frac{\gamma \tanh(\gamma a)(\alpha_2\mu_1^2 - \alpha_1\mu_2^2)^{\frac{1}{2}}(\alpha_2+\alpha_1)}{\alpha_2 L_1(s) - \alpha_1 L_2(s)} \times \\ &\lim_{\alpha_1\to\alpha_2} \frac{1}{(\alpha_2-\alpha_1)^{\frac{1}{2}} + \frac{2\alpha_2 d_1}{(\alpha_2\mu_1^2-\alpha_1\mu_2^2)^{\frac{1}{2}}}}. \end{aligned} \tag{4.2.187}$$

This leads simply to

$$\frac{\sigma Q}{(s^2-\sigma^2)P} = \frac{\gamma \tanh(\gamma a)(\alpha_2\mu_1^2 - \alpha_1\mu_2^2)(\alpha_2+\alpha_1)}{2\alpha_2 d_1(\alpha_2 L_1(s) - \alpha_1 L_2(s))}. \tag{4.2.188}$$

Thus, bringing together the analysis conducted in this particular case (that being case (i) when $\alpha_1 = \alpha_2$), then

$$R_0 = -\frac{[L_+(\eta_0)]^2 L_2(\eta_0)}{L_1'(\eta_0)}\left[\frac{1}{2\eta_0} - \frac{\tau_0 \tanh(\tau_0 a)(\alpha_2\mu_1^2 - \alpha_1\mu_2^2)(\alpha_2+\alpha_1)}{2\alpha_1\alpha_2 d_1 L_2(\eta_0))}\right] \tag{4.2.189}$$

and

$$T_0 = \frac{\alpha_2 L_1(\nu_0) L_+(\eta_0) \tau_0 \tanh(\tau_0 a)}{\alpha_1 L_2'(\nu_0) L_+(\nu_0) \gamma_0 \tanh(\gamma_0 a)} \left[\frac{1}{\eta_0 - \nu_0} - \frac{\gamma_0 \tanh(\gamma_0 a)(\alpha_2 \mu_1^2 - \alpha_1 \mu_2^2)(\alpha_2 + \alpha_1)}{2\alpha_2^2 d_1 L_1(\eta_0)} \right]. \tag{4.2.190}$$

For Cases (ii), (iii) and (iv) analysis follows in a similar manner to produce appropriate expressions for the situation where $\alpha_1 = \alpha_2$.

4.3 Results

Because of the number of combinations of edge conditions and the infinite range from which α_j and μ_j, $j = 1, 2$, may be selected, an exhaustive set of results is impossible to produce. Therefore, a selection of results is given here. First, for the case $a = b$, results given by the system derived in section 4.1 are compared with those found using the Wiener-Hopf technique as described in section 4.2. Then, by choosing the parameters α_j and μ_j, $j = 1, 2$ in the two boundary conditions appropriately, results given from the system of equations found in section 4.1 can be compared against those found in Chapters 2 and 3.

Figures 4.3 – 4.18 show the graphs of the fundamental reflection and transmitted modes against either α_1 (graphs 4.3 – 4.10) or α_2 (graphs 4.11 – 4.18) for fixed $a = b = 1.5$, $\mu_1 = 1.6$, $\mu_2 = 5$. In each case four curves are shown corresponding to the Wiener-Hopf solution (solid line) and various truncations of (4.1.39). It is noticeable that as the value of α_2 or α_1 increases, the accuracy of the results falls away. This fall off is counteracted to some extent by increasing the number of terms used in the truncation of (4.1.39), but it is still noticeable that accuracy is waining for particularly large values of α_j, $j = 1, 2$, even when 20 terms are used. The reason for this can be seen when τ_ℓ or γ_n are expanded asymptotically. For τ_ℓ, when expanded in terms of ℓ, that being

$$\tau_\ell = \frac{i\ell\pi}{a} + \frac{i\alpha_1 a^2}{\ell^3 \pi} + O\left(\frac{1}{\ell^4}\right), \tag{4.3.1}$$

it is clear that the second term of this expansion becomes large in the case where $\alpha_1 \gg \ell^3$. Thus this term affects the value of τ_ℓ (and in turn η_ℓ) when ℓ is small. This incorrect evaluation of η_ℓ is enough to cause the inaccuracy in the results and also explains why, as n is increased, the accuracy of the results is found to improve. Similar analysis applies to γ_n when $\alpha_2 \gg n^3$ with the result being similarly inaccurate. In all graphs, the edge conditions used are indicated in the captions.

It has already been discussed how, by suitable choice of parameters, a membrane surface can be made to behave in an almost identical way to a soft surface, and now it is desired that a membrane be made to act in the same way as a hard surface. In addition it is necessary to make the incident structural wave behave like the incident plane wave used in section 3. To do this, values of α_1 and μ_1 must both be small. This has the effect

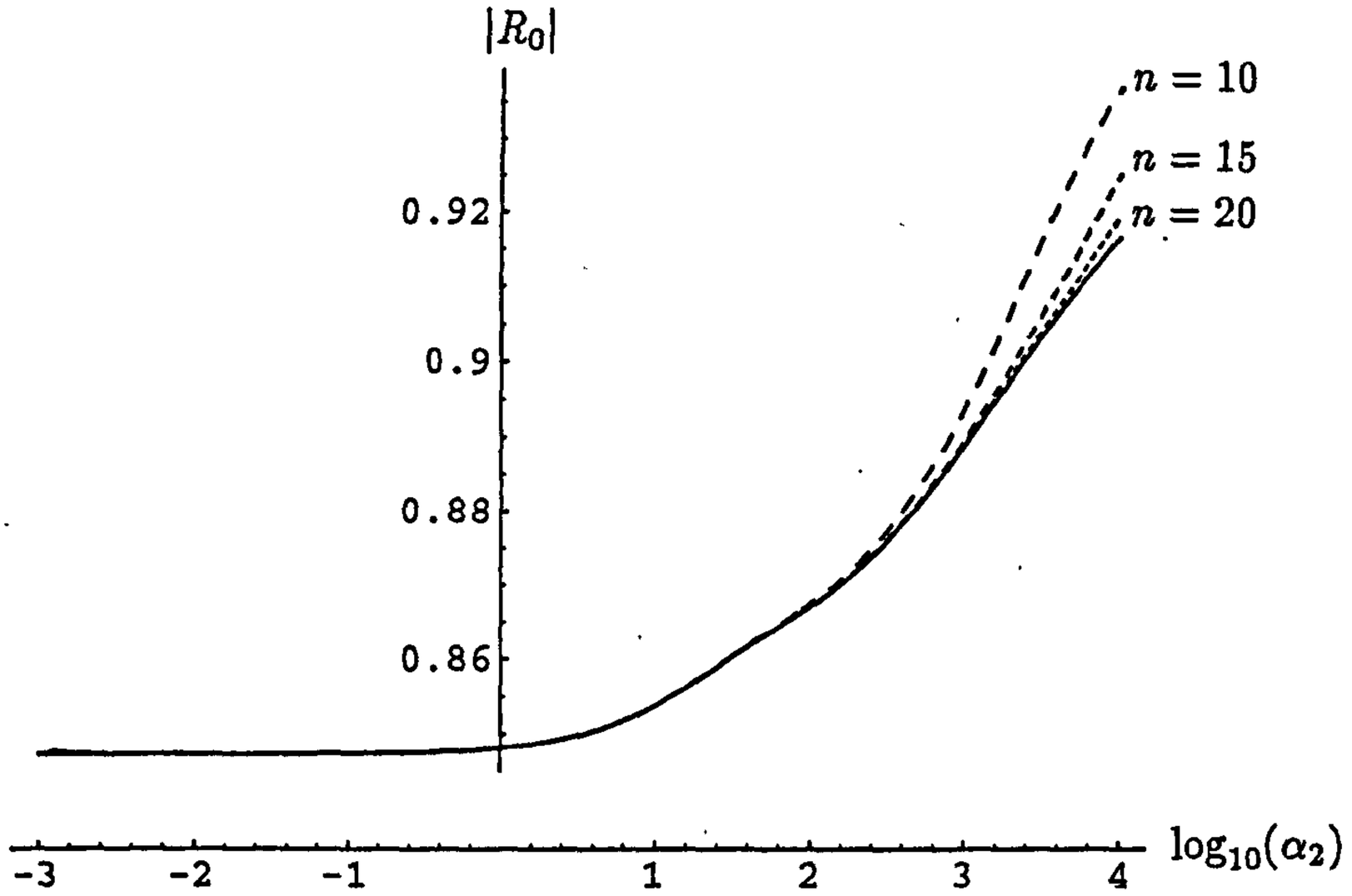

Figure 4.3: Comparison of the modulus of the coefficient for the fundamental reflected mode for the membrane/membrane problem with edge conditions $\phi_{1y}(0,a) = \phi_{2y}(0,b) = 0$ where $a = b = 2.5$, $\alpha_1 = 10$, $\mu_1 = 1.6$ and $\mu_2 = 5$. The eigenfunction expansion are the dotted lines, using the number of terms n for the solution as indicated, whilst the Wiener-Hopf results are the solid line.

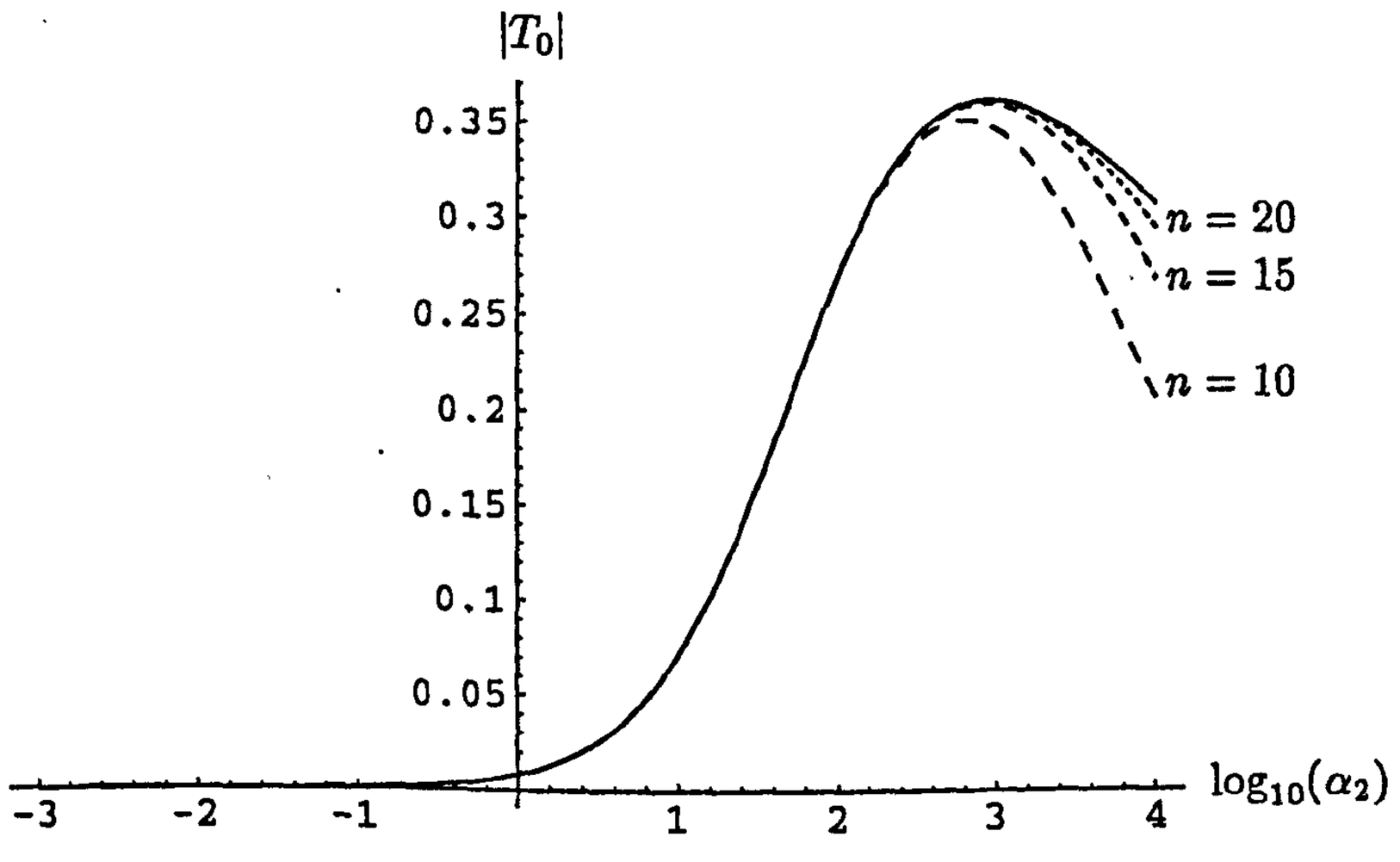

Figure 4.4: Comparison of the modulus of the coefficient for the fundamental transmitted mode for the membrane/membrane problem with edge conditions $\phi_{1y}(0,a) = \phi_{2y}(0,b) = 0$ where $a = b = 2.5$, $\alpha_1 = 10$, $\mu_1 = 1.6$ and $\mu_2 = 5$. The eigenfunction expansion are the dotted lines, using the number of terms n for the solution as indicated, whilst the Wiener-Hopf results are the solid line.

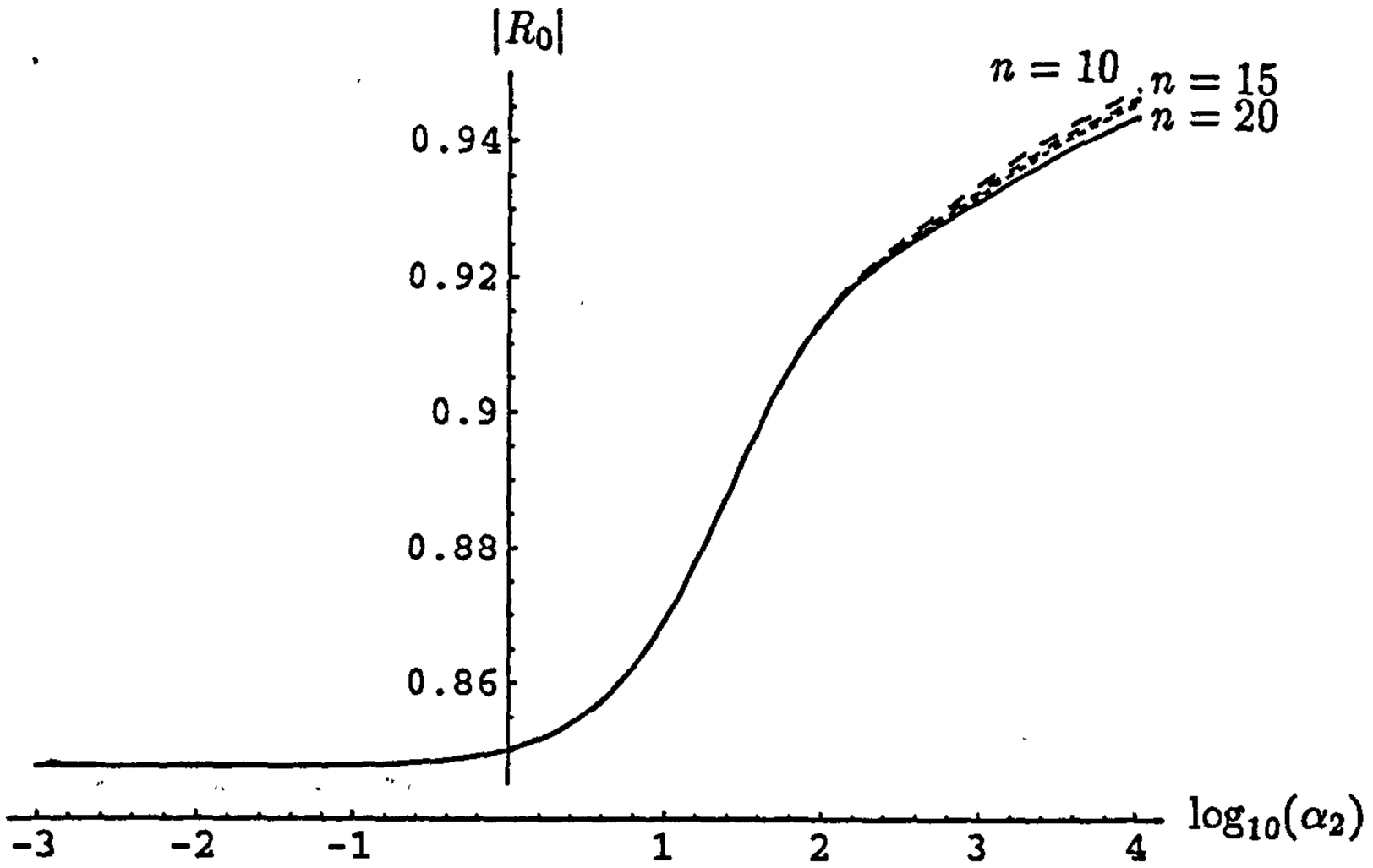

Figure 4.5: Comparison of the modulus of the coefficient for the fundamental reflected mode for the membrane/membrane problem with edge conditions $\phi_{1y}(0,a) = \phi_{2yx}(0,b) = 0$ where $a = b = 2.5$, $\alpha_1 = 10$, $\mu_1 = 1.6$ and $\mu_2 = 5$. The eigenfunction expansion are the dotted lines, using the number of terms n for the solution as indicated, whilst the Wiener-Hopf results are the solid line.

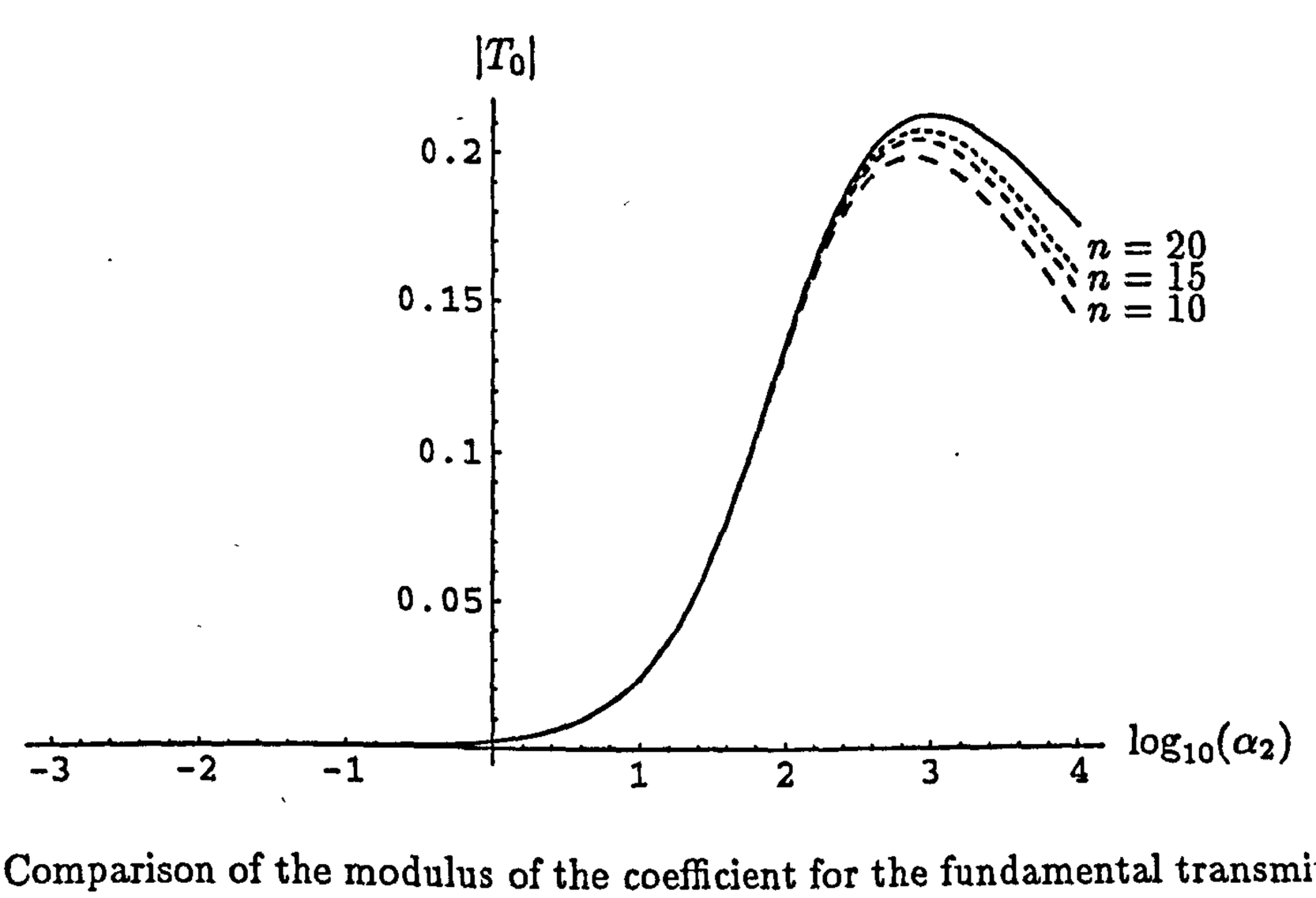

Figure 4.6: Comparison of the modulus of the coefficient for the fundamental transmitted mode for the membrane/membrane problem with edge conditions $\phi_{1y}(0,a) = \phi_{2yx}(0,b) = 0$ where $a = b = 2.5$, $\alpha_1 = 10$, $\mu_1 = 1.6$ and $\mu_2 = 5$. The eigenfunction expansion are the dotted lines, using the number of terms n for the solution as indicated, whilst the Wiener-Hopf results are the solid line.

of forcing η_0 towards 1 and η_1 to tend to 0. With this behaviour in place, it is possible to compare results from the hard/soft and hard/membrane problems, with those gained

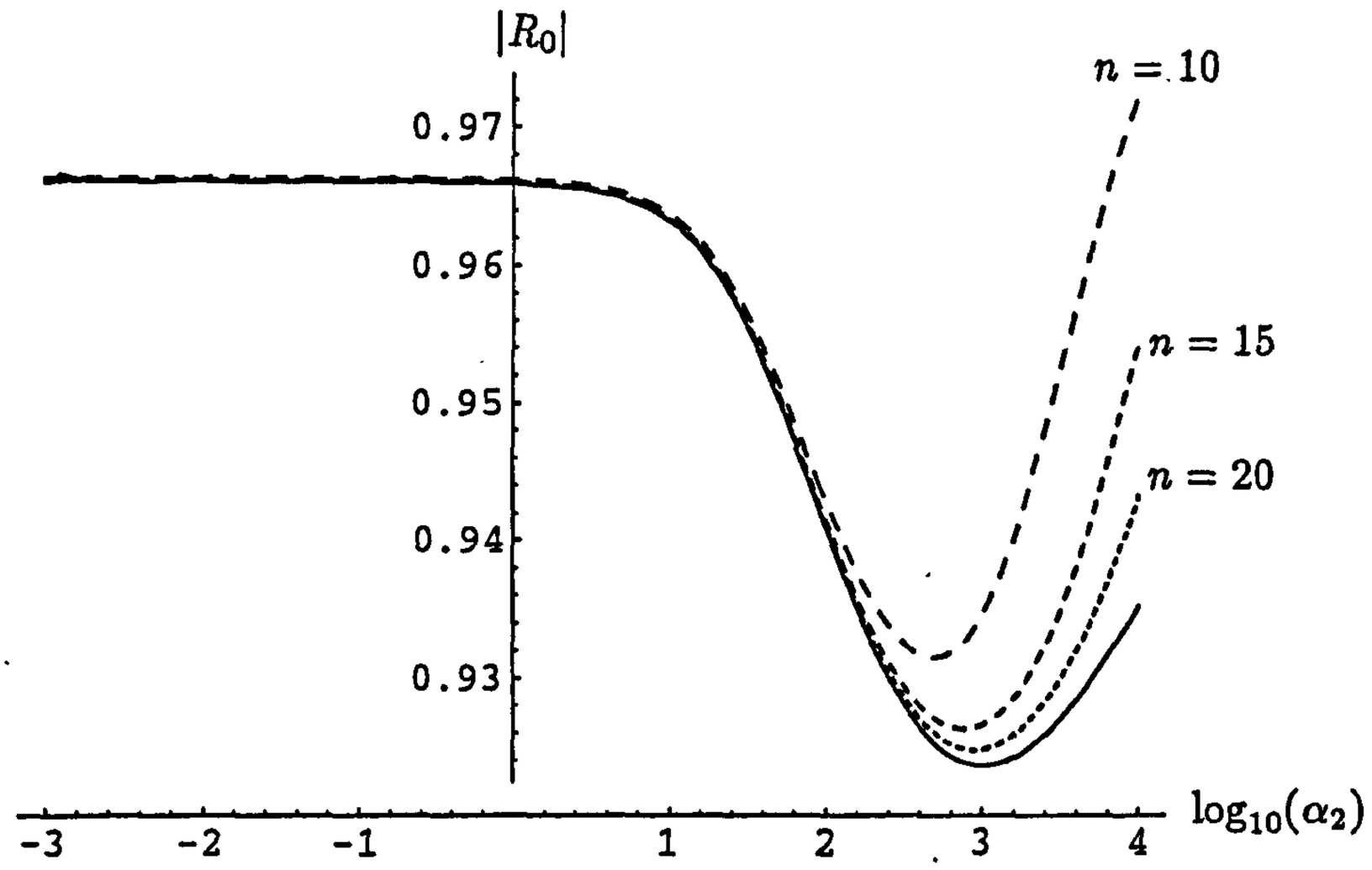

Figure 4.7: Comparison of the modulus of the coefficient for the fundamental reflected mode for the membrane/membrane problem with edge conditions $\phi_{1yx}(0,a) = \phi_{2y}(0,b) = 0$ where $a = b = 2.5$, $\alpha_1 = 10$, $\mu_1 = 1.6$ and $\mu_2 = 5$. The eigenfunction expansion are the dotted lines, using the number of terms n for the solution as indicated, whilst the Wiener-Hopf results are the solid line.

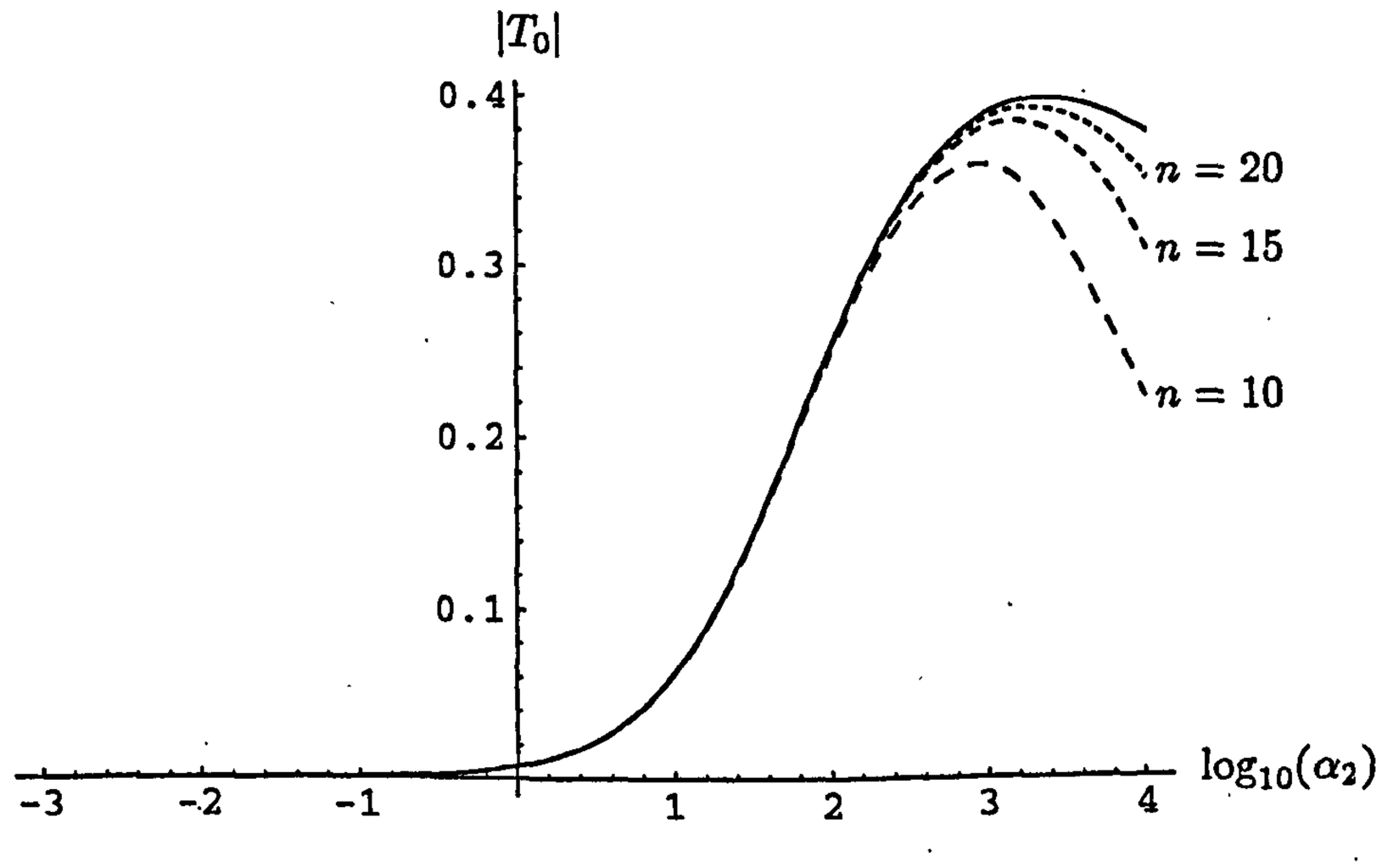

Figure 4.8: Comparison of the modulus of the coefficient for the fundamental transmitted mode for the membrane/membrane problem with edge conditions $\phi_{1yx}(0,a) = \phi_{2y}(0,b) = 0$ where $a = b = 2.5$, $\alpha_1 = 10$, $\mu_1 = 1.6$ and $\mu_2 = 5$. The eigenfunction expansion are the dotted lines, using the number of terms n for the solution as indicated, whilst the Wiener-Hopf results are the solid line.

by using equation (4.1.39). Indeed, in graphs 4.19 – 4.22, it is seen that the correlation is excellent.

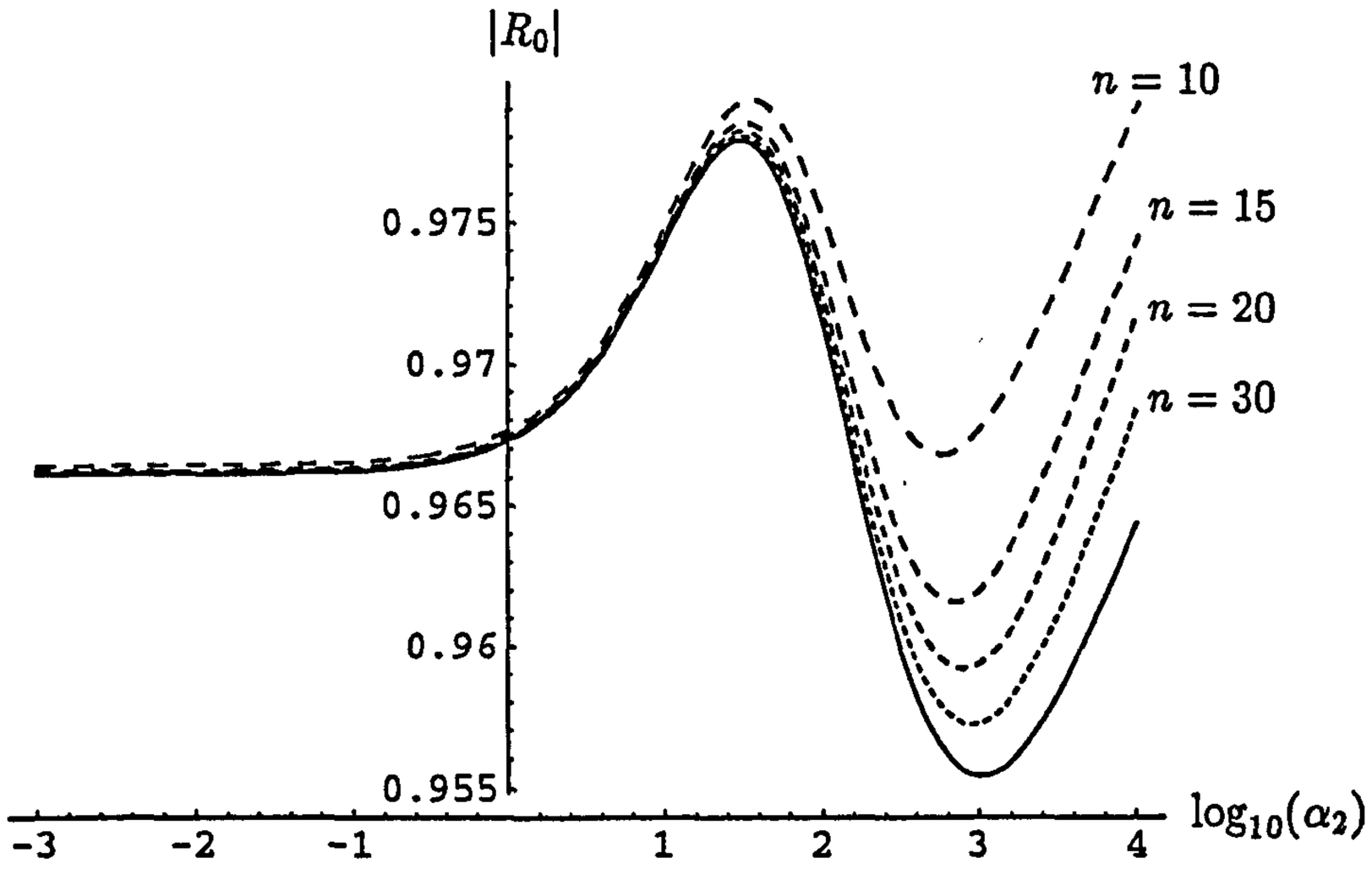

Figure 4.9: Comparison of the modulus of the coefficient for the fundamental reflected mode for the membrane/membrane problem with edge conditions $\phi_{1yx}(0,a) = \phi_{2yx}(0,b) = 0$ where $a = b = 2.5$, $\alpha_1 = 10$, $\mu_1 = 1.6$ and $\mu_2 = 5$. The eigenfunction expansion are the dotted lines, using the number of terms n for the solution as indicated, whilst the Wiener-Hopf results are the solid line.

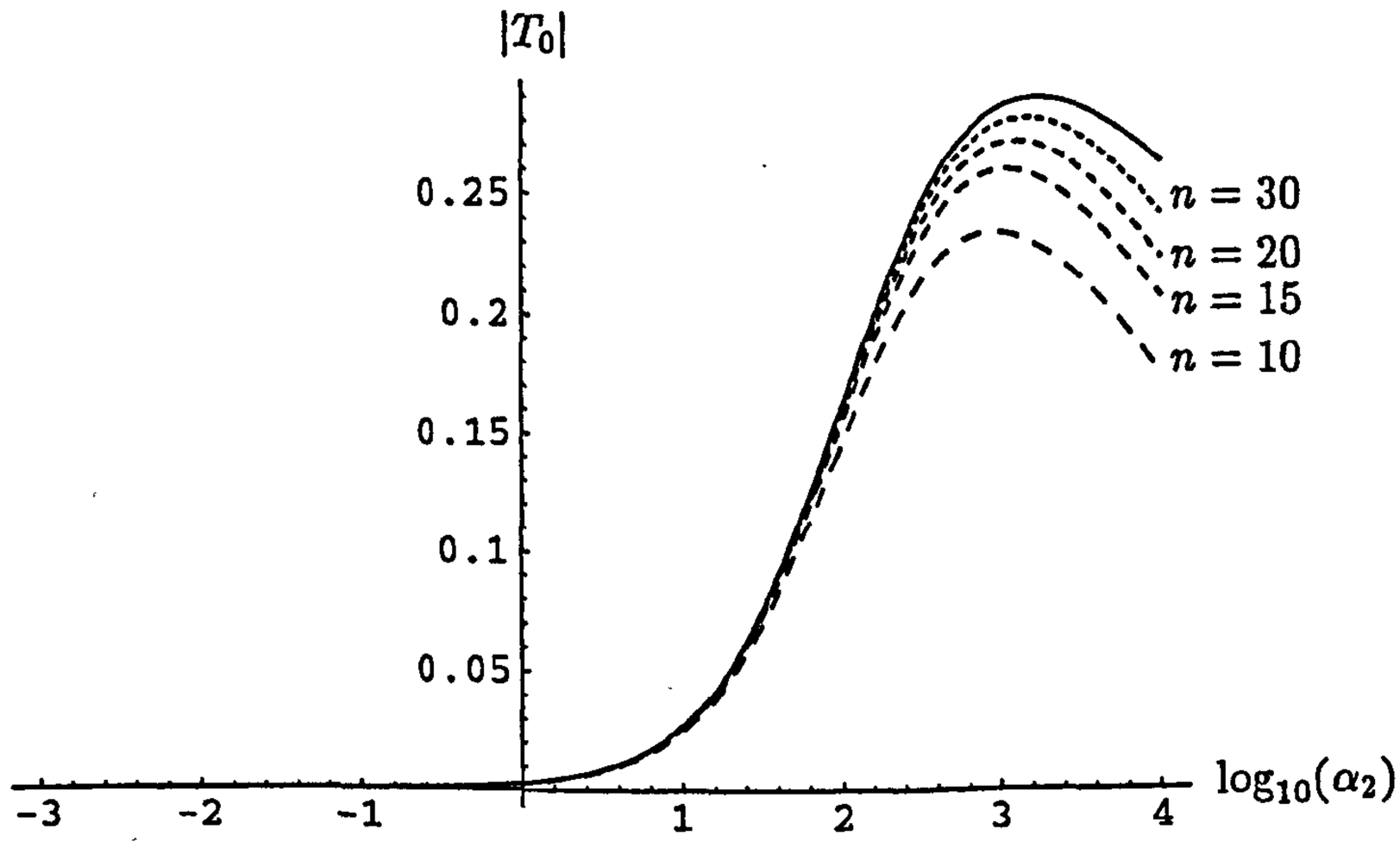

Figure 4.10: Comparison of the modulus of the coefficient for the fundamental transmitted mode for the membrane/membrane problem with edge conditions $\phi_{1yx}(0,a) = \phi_{2yx}(0,b) = 0$ where $a = b = 2.5$, $\alpha_1 = 10$, $\mu_1 = 1.6$ and $\mu_2 = 5$. The eigenfunction expansion are the dotted lines, using the number of terms n for the solution as indicated, whilst the Wiener-Hopf results are the solid line.

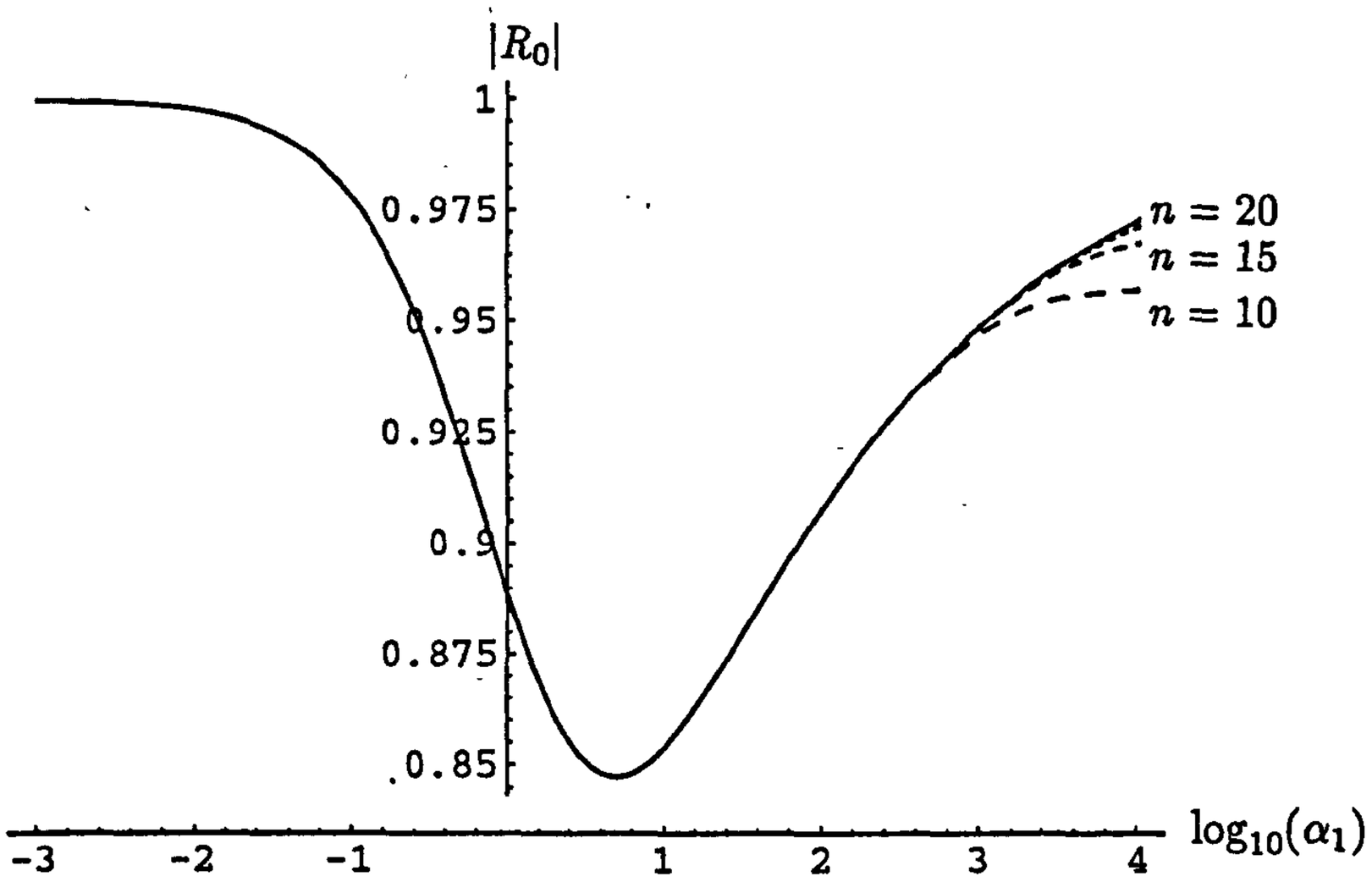

Figure 4.11: Comparison of the modulus of the coefficient for the fundamental reflected mode for the membrane/membrane problem with edge conditions $\phi_{1y}(0,a) = \phi_{2y}(0,b) = 0$ where $a = b = 2.5$, $\alpha_2 = 10$, $\mu_1 = 1.6$ and $\mu_2 = 5$. The eigenfunction expansion are the dotted lines, using the number of terms n for the solution as indicated, whilst the Wiener-Hopf results are the solid line.

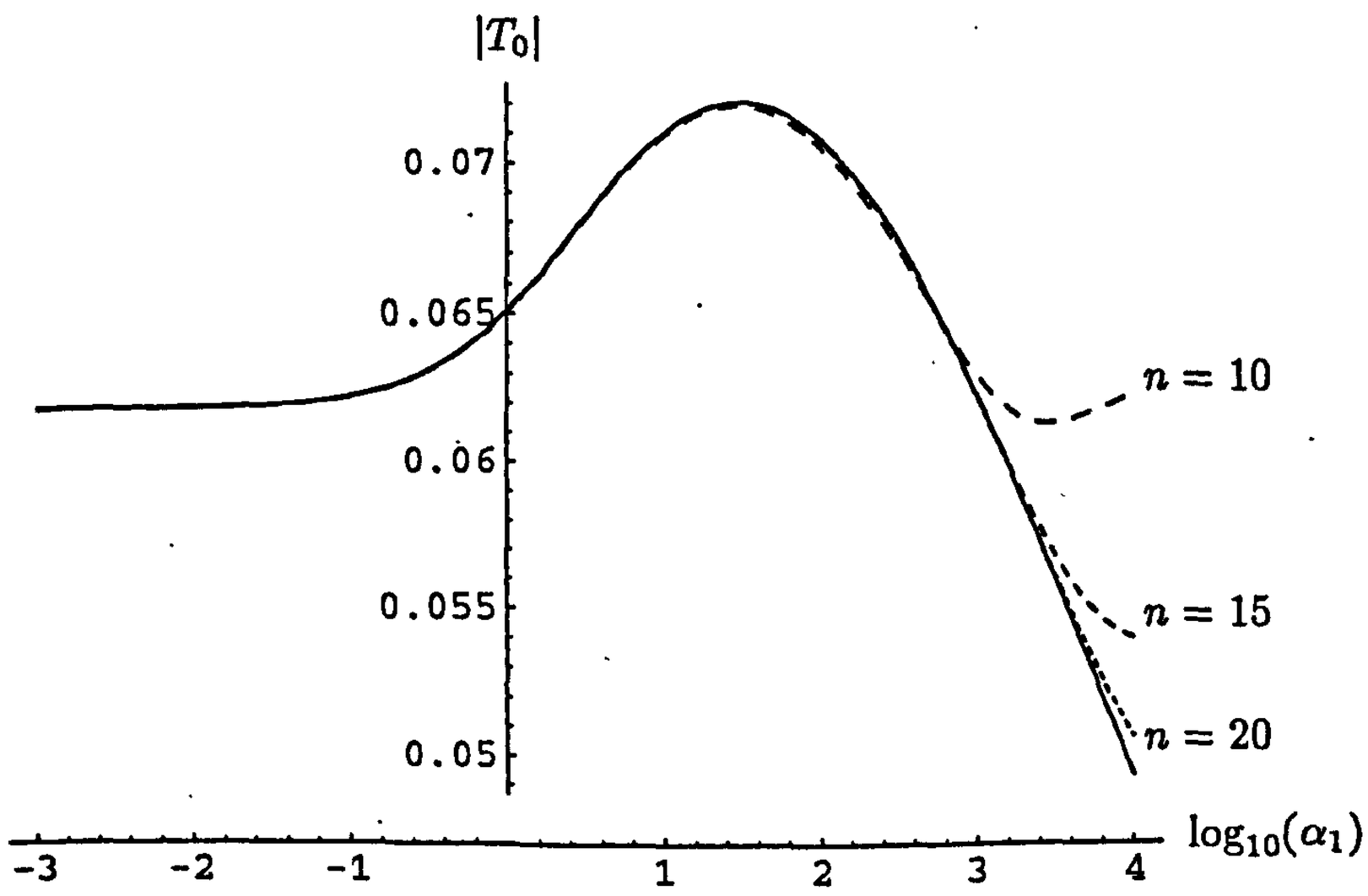

Figure 4.12: Comparison of the modulus of the coefficient for the fundamental transmitted mode for the membrane/membrane problem with edge conditions $\phi_{1y}(0,a) = \phi_{2y}(0,b) = 0$ where $a = b = 2.5$, $\alpha_2 = 10$, $\mu_1 = 1.6$ and $\mu_2 = 5$. The eigenfunction expansion are the dotted lines, using the number of terms n for the solution as indicated, whilst the Wiener-Hopf results are the solid line.

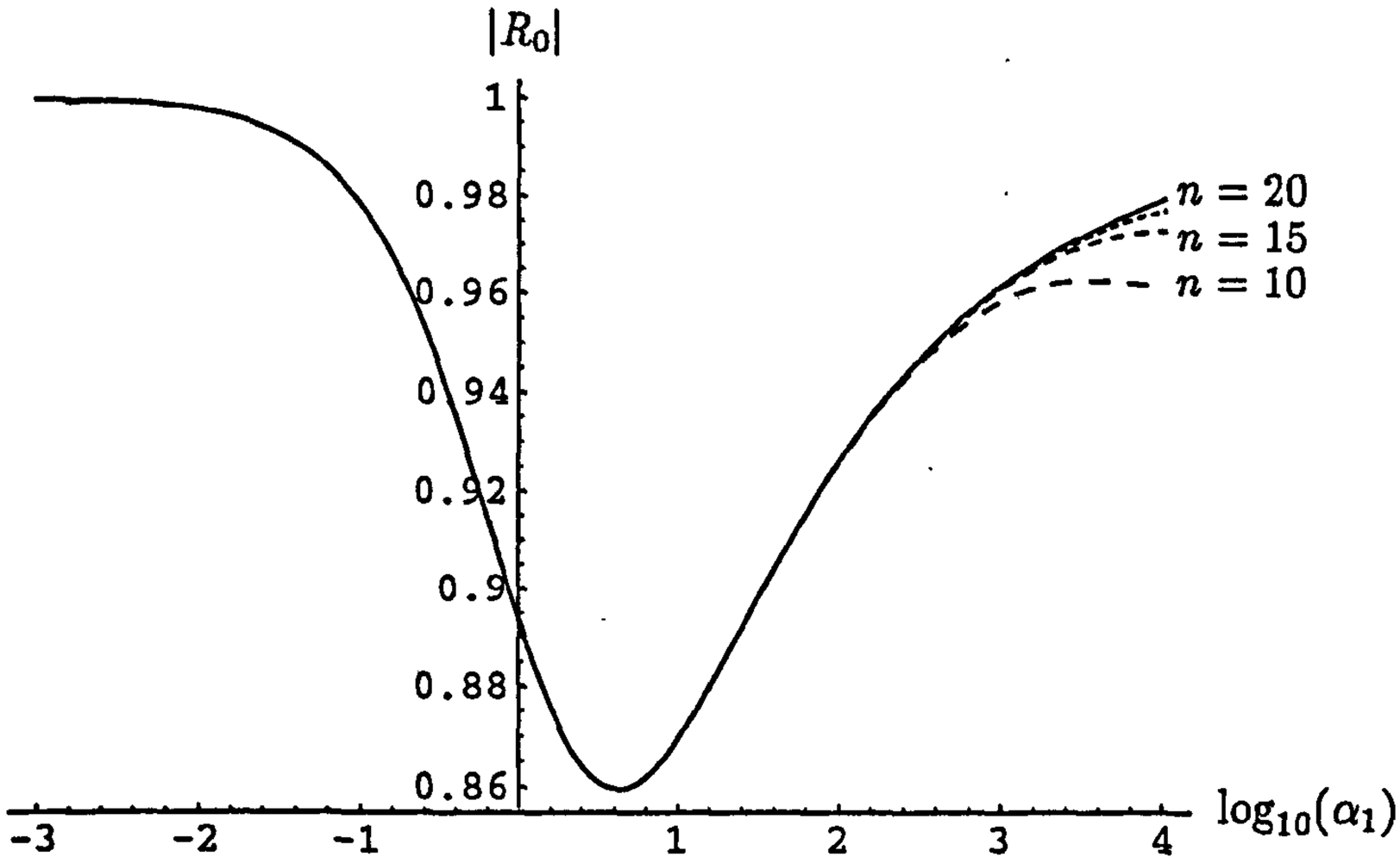

Figure 4.13: Comparison of the modulus of the coefficient for the fundamental reflected mode for the membrane/membrane problem with edge conditions $\phi_{1y}(0,a) = \phi_{2yx}(0,b) = 0$ where $a = b = 2.5$, $\alpha_2 = 10$, $\mu_1 = 1.6$ and $\mu_2 = 5$. The eigenfunction expansion are the dotted lines, using the number of terms n for the solution as indicated, whilst the Wiener-Hopf results are the solid line.

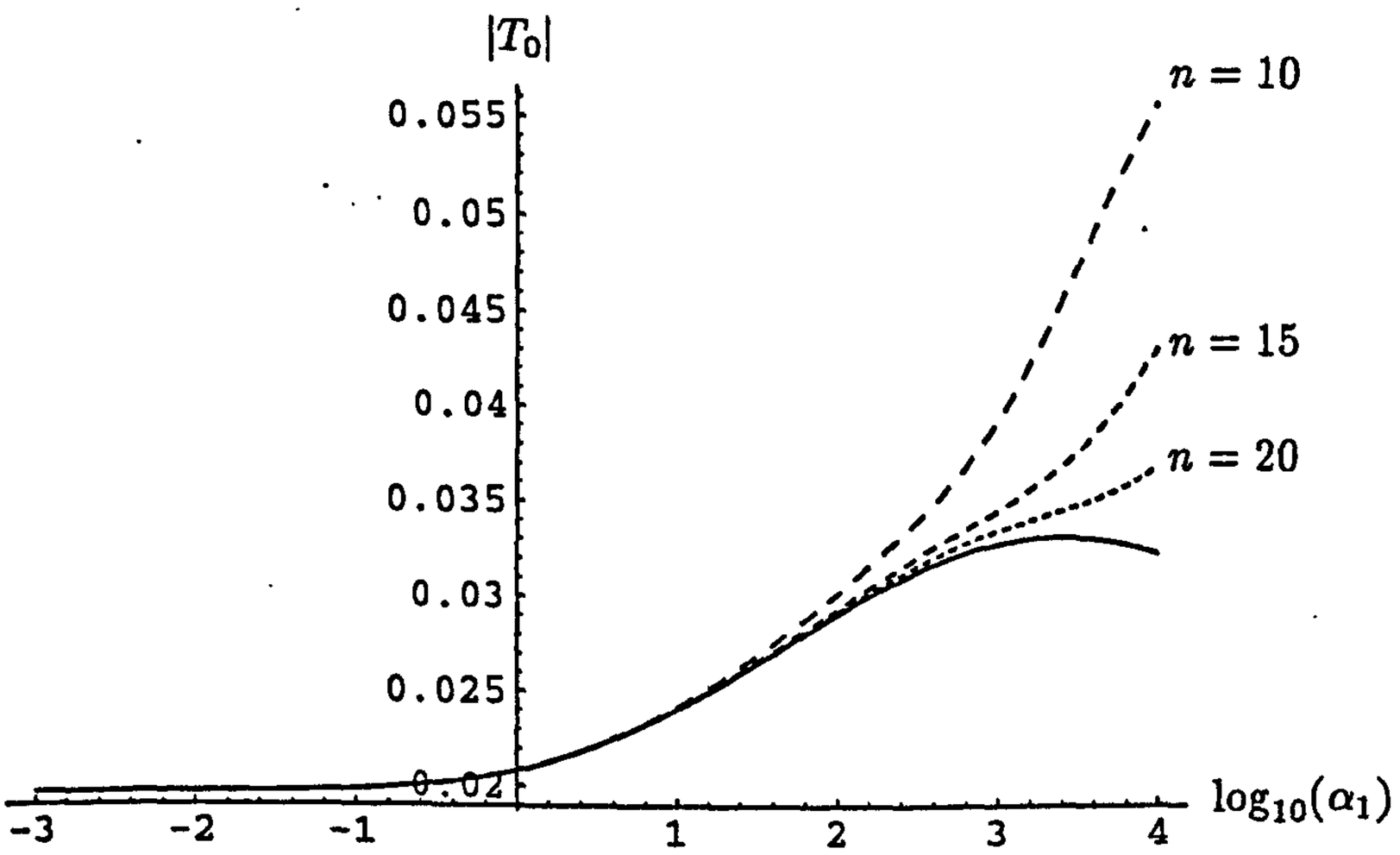

Figure 4.14: Comparison of the modulus of the coefficient for the fundamental transmitted mode for the membrane/membrane problem with edge conditions $\phi_{1y}(0,a) = \phi_{2yx}(0,b) = 0$ where $a = b = 2.5$, $\alpha_2 = 10$, $\mu_1 = 1.6$ and $\mu_2 = 5$. The eigenfunction expansion are the dotted lines, using the number of terms n for the solution as indicated, whilst the Wiener-Hopf results are the solid line.

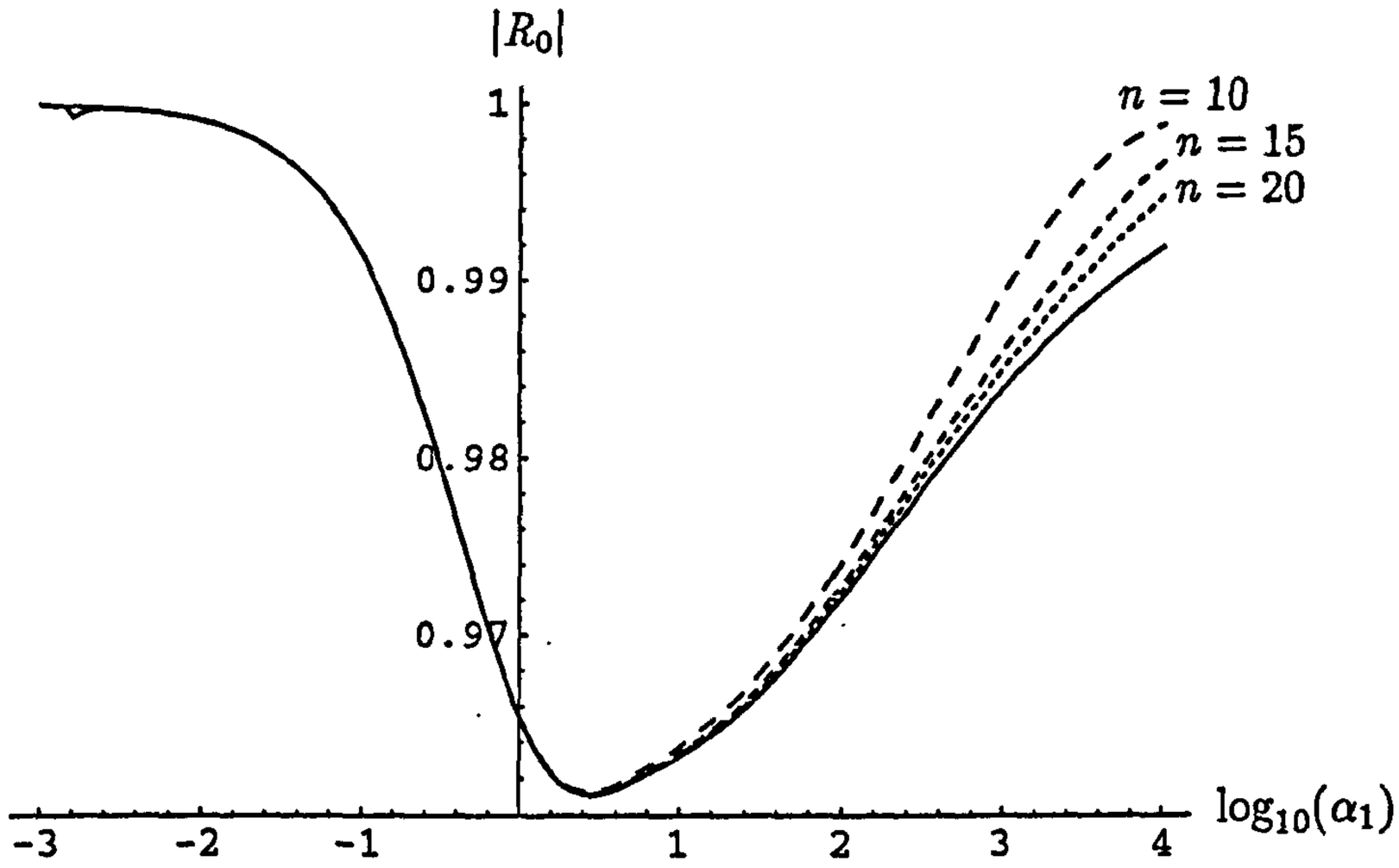

Figure 4.15: Comparison of the modulus of the coefficient for the fundamental reflected mode for the membrane/membrane problem with edge conditions $\phi_{1yx}(0,a) = \phi_{2y}(0,b) = 0$ where $a = b = 2.5$, $\alpha_2 = 10$, $\mu_1 = 1.6$ and $\mu_2 = 5$. The eigenfunction expansion are the dotted lines, using the number of terms n for the solution as indicated, whilst the Wiener-Hopf results are the solid line.

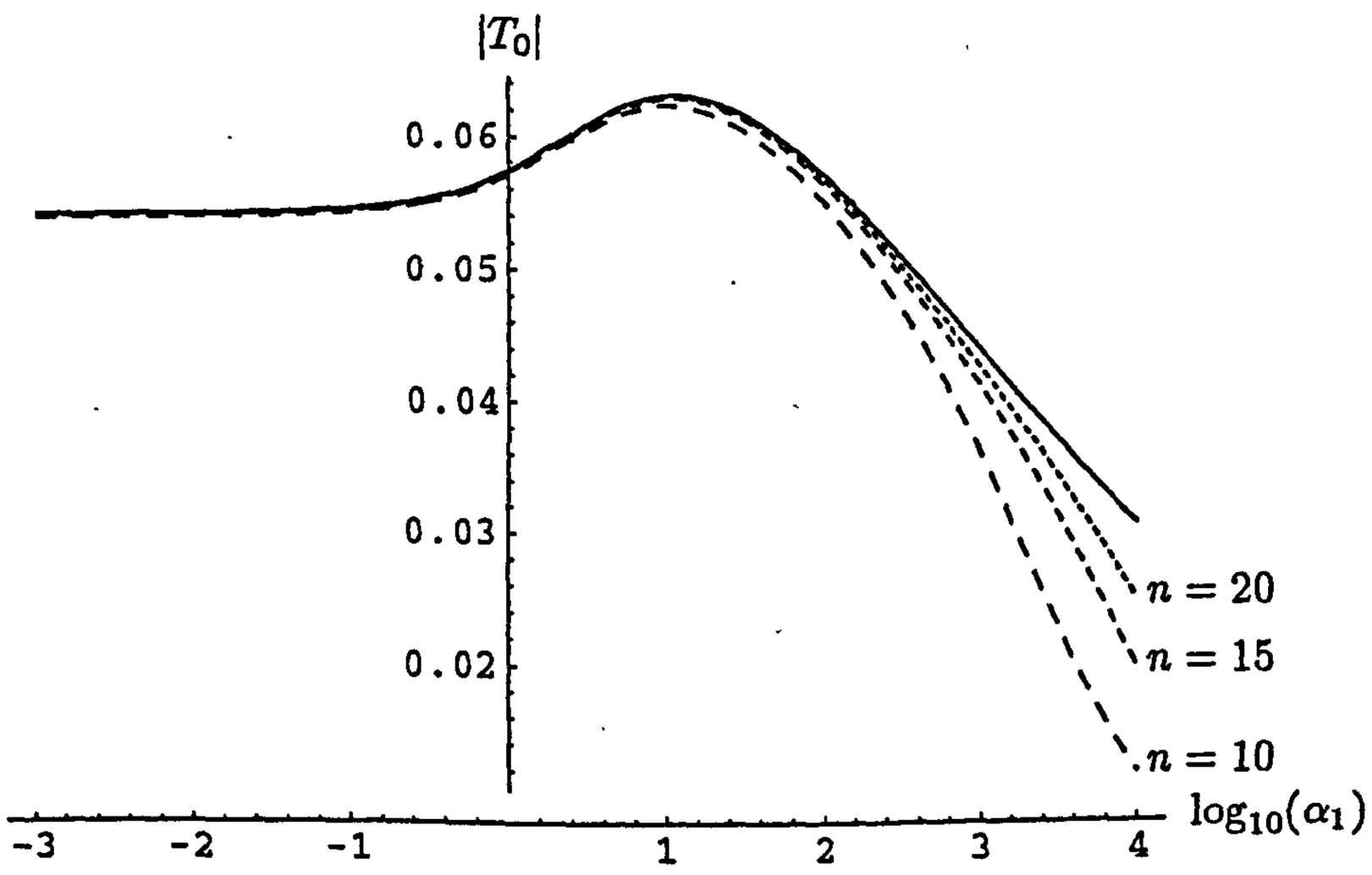

Figure 4.16: Comparison of the modulus of the coefficient for the fundamental transmitted mode for the membrane/membrane problem with edge conditions $\phi_{1yx}(0,a) = \phi_{2y}(0,b) = 0$ where $a = b = 2.5$, $\alpha_2 = 10$, $\mu_1 = 1.6$ and $\mu_2 = 5$. The eigenfunction expansion are the dotted lines, using the number of terms n for the solution as indicated, whilst the Wiener-Hopf results are the solid line.

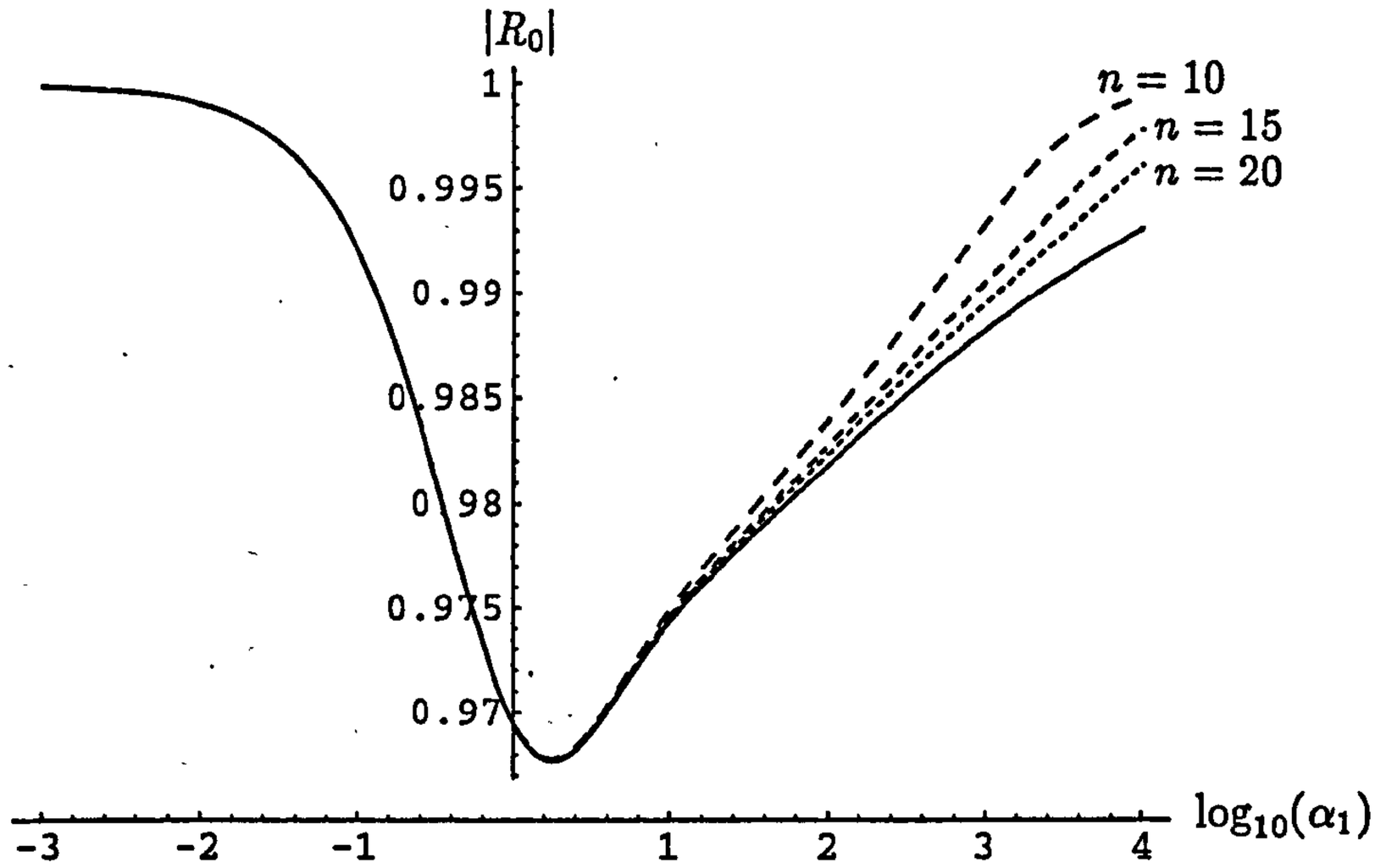

Figure 4.17: Comparison of the modulus of the coefficient for the fundamental reflected mode for the membrane/membrane problem with edge conditions $\phi_{1yx}(0,a) = \phi_{2yx}(0,b) = 0$ where $a = b = 2.5$, $\alpha_2 = 10$, $\mu_1 = 1.6$ and $\mu_2 = 5$. The eigenfunction expansion are the dotted lines, using the number of terms n for the solution as indicated, whilst the Wiener-Hopf results are the solid line.

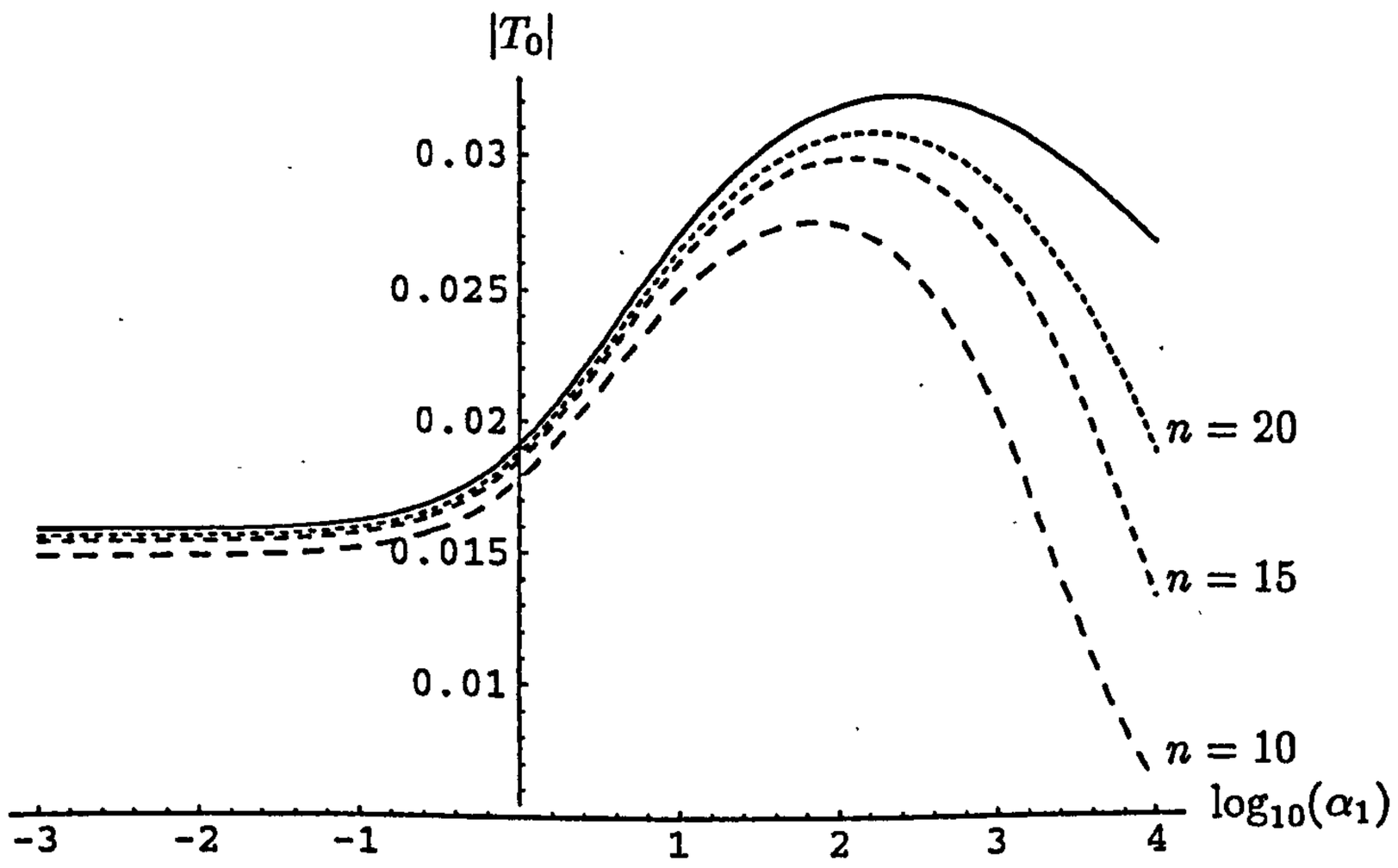

Figure 4.18: Comparison of the modulus of the coefficient for the fundamental transmitted mode for the membrane/membrane problem with edge conditions $\phi_{1yx}(0,a) = \phi_{2yx}(0,b) = 0$ where $a = b = 2.5$, $\alpha_2 = 10$, $\mu_1 = 1.6$ and $\mu_2 = 5$. The eigenfunction expansion are the dotted lines, using the number of terms n for the solution as indicated, whilst the Wiener-Hopf results are the solid line.

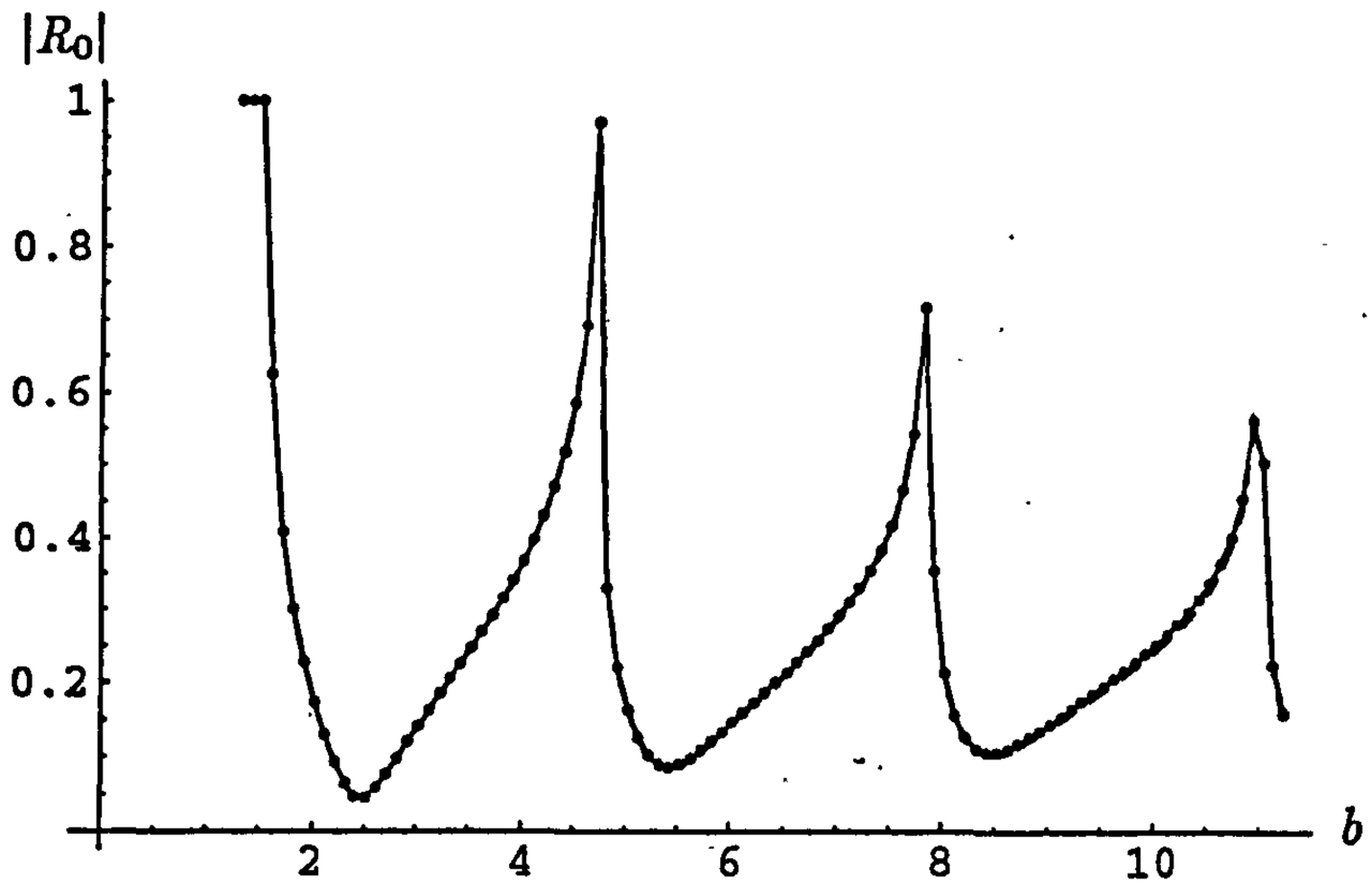

Figure 4.19: Comparison of the modulus of the coefficient for the fundamental reflected mode with $a = 1.211$. The hard/soft problem results (from section 2.4) are shown as solid line, the hard/membrane limiting case results (from section 3.3) are shown as dots and the membrane/membrane limiting case results are shown as a dashed line.

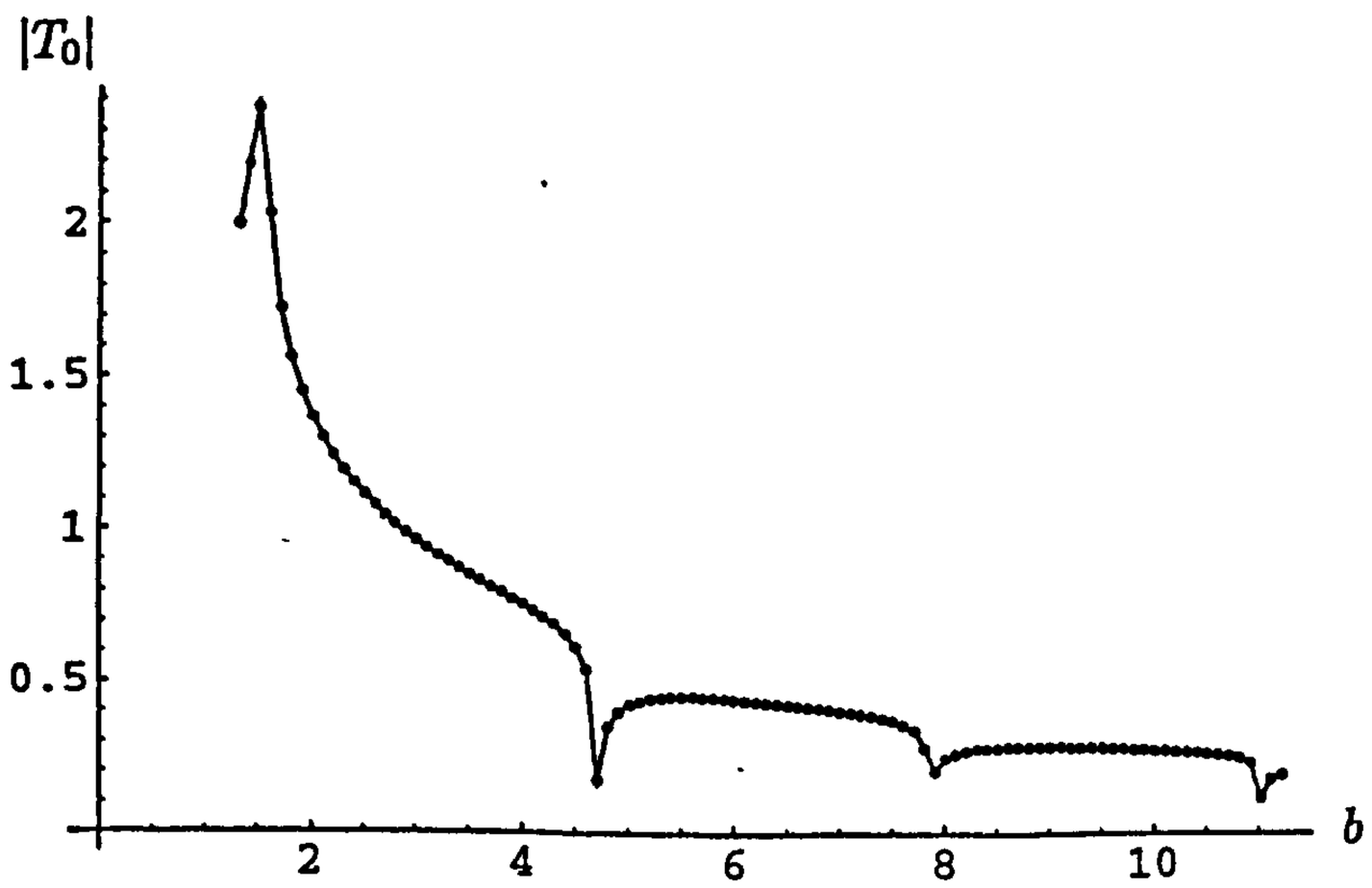

Figure 4.20: Comparison of the modulus of the coefficient for the fundamental transmitted mode with $a = 1.211$. The hard/soft problem results (from section 2.4) are shown as solid line, the hard/membrane limiting case results (from section 3.3) are shown as dots and the membrane/membrane limiting case results are shown as a dashed line.

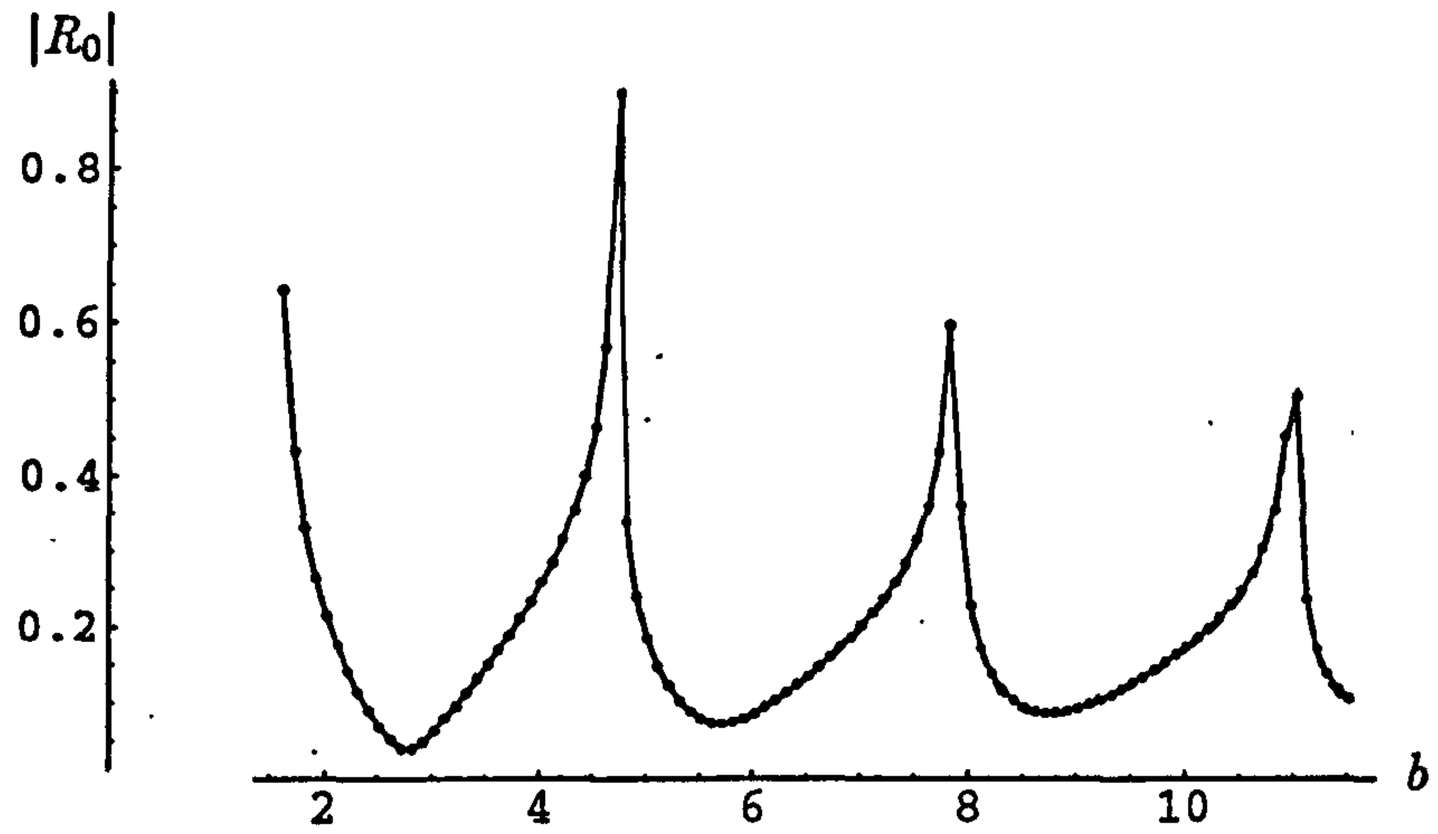

Figure 4.21: Comparison of the modulus of the coefficient for the fundamental reflected mode with $a = 1.51$. The hard/soft problem results (from section 2.4) are shown as solid line, the hard/membrane limiting case results (from section 3.3) are shown as dots and the membrane/membrane limiting case results are shown as a dashed line.

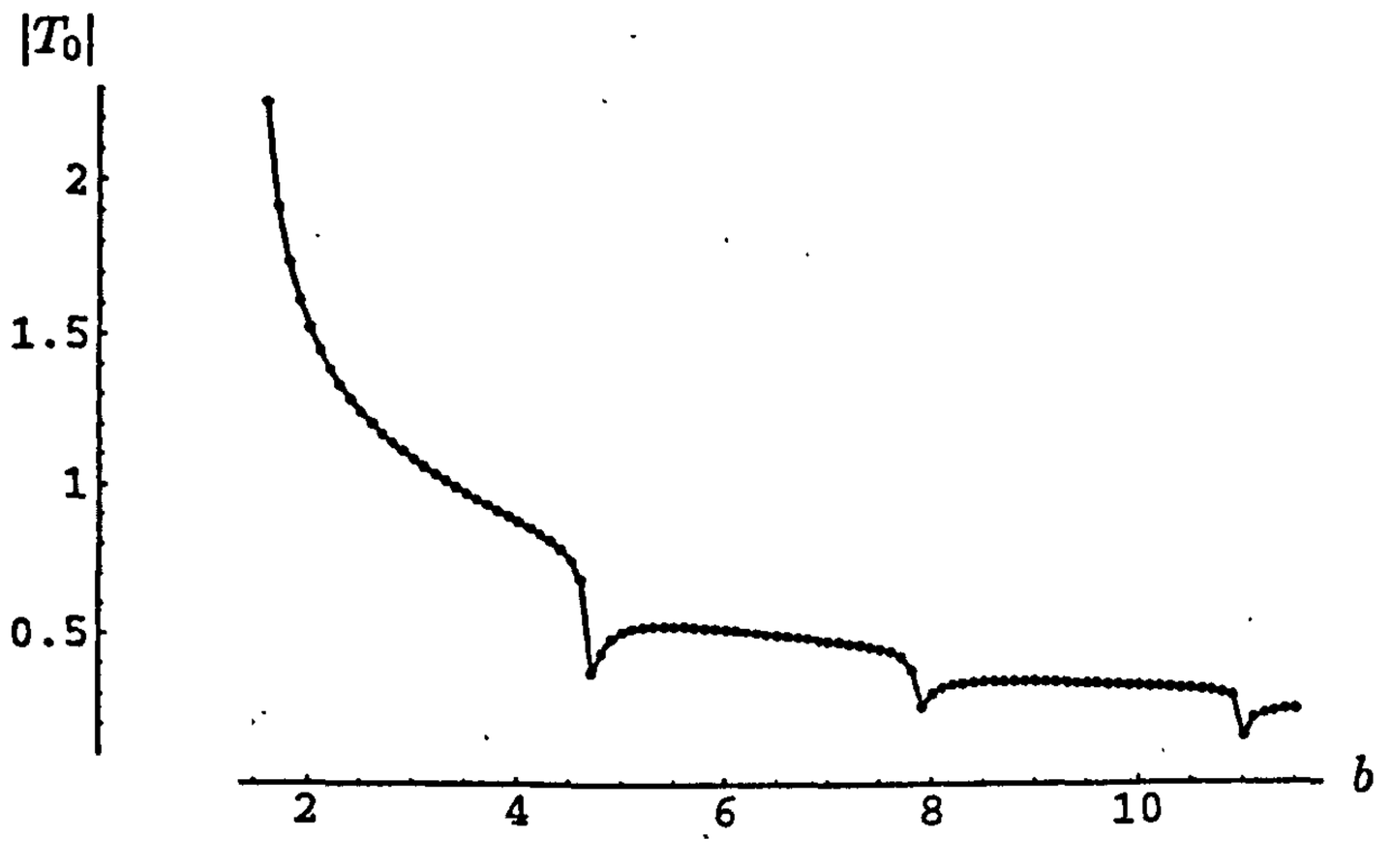

Figure 4.22: Comparison of the modulus of the coefficient for the fundamental transmitted mode with $a = 1.51$. The hard/soft problem results (from section 2.4) are shown as solid line, the hard/membrane limiting case results (from section 3.3) are shown as dots and the membrane/membrane limiting case results are shown as a dashed line.

Similarly, figures 4.23 and 4.24 compare the case where α_1 and μ_1 are selected so that the left hand membrane mimics a rigid surface with the results obtained for the hard/membrane problem (see figures 3.12 and 3.13). Thus in both these graphs $\alpha_1 =$

$\mu_1 = 10^{-11}$, whilst $a = 1.51$, $\mu_2 = 2.2$, $\alpha_2 = 50$ and b varies from 1.51 to 12. Again the agreement between the two sets of results is excellent.

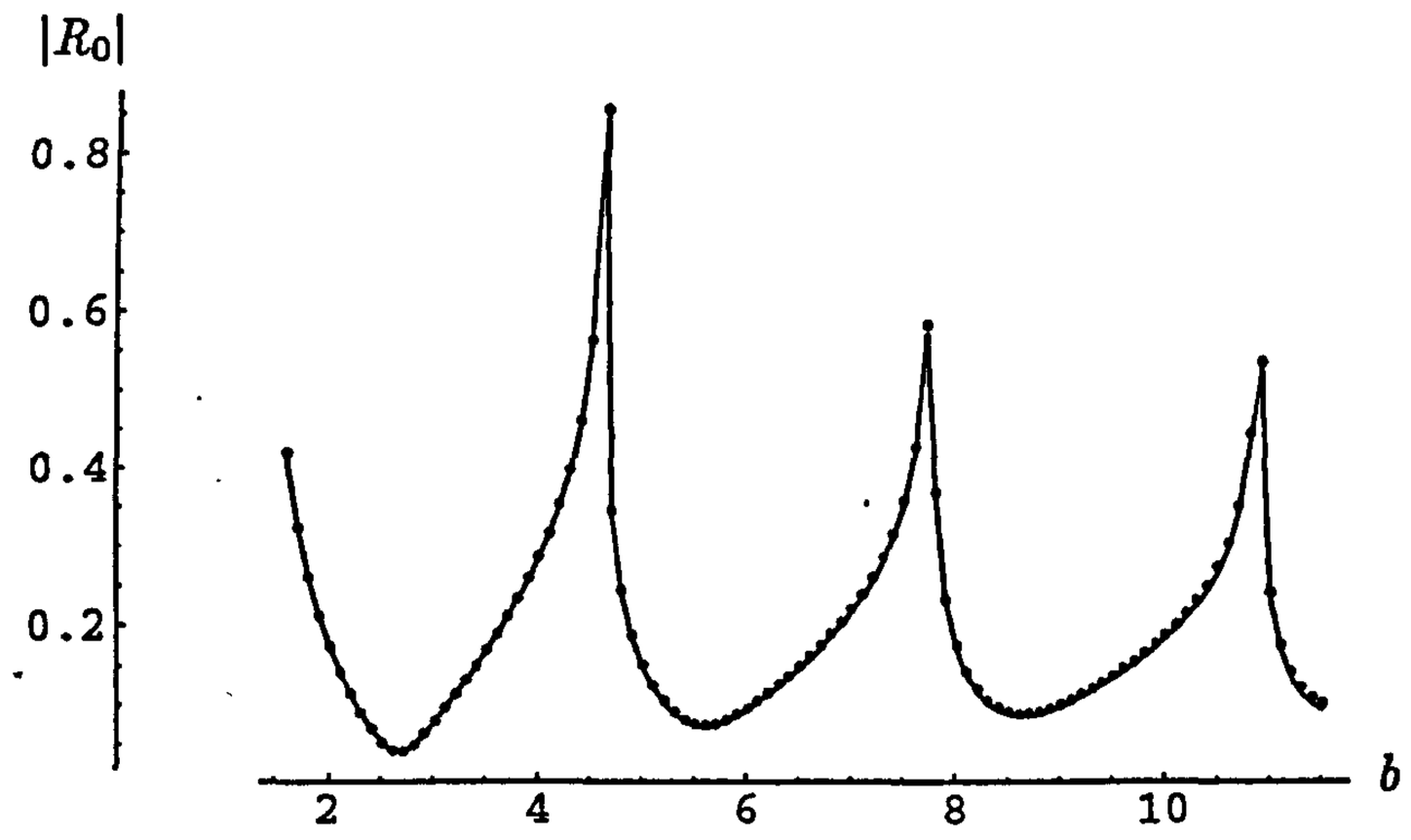

Figure 4.23: Comparison of the modulus of the coefficient for the fundamental reflected mode with edge condition $\phi_{yx}(0,b) = 0$, $a = 1.211$, $\alpha_2 = 50$ and $\mu_2 = 2.2$. The hard/membrane limiting case results (from section 3.3) are shown as dots and the membrane/membrane limiting case results are shown as a solid line.

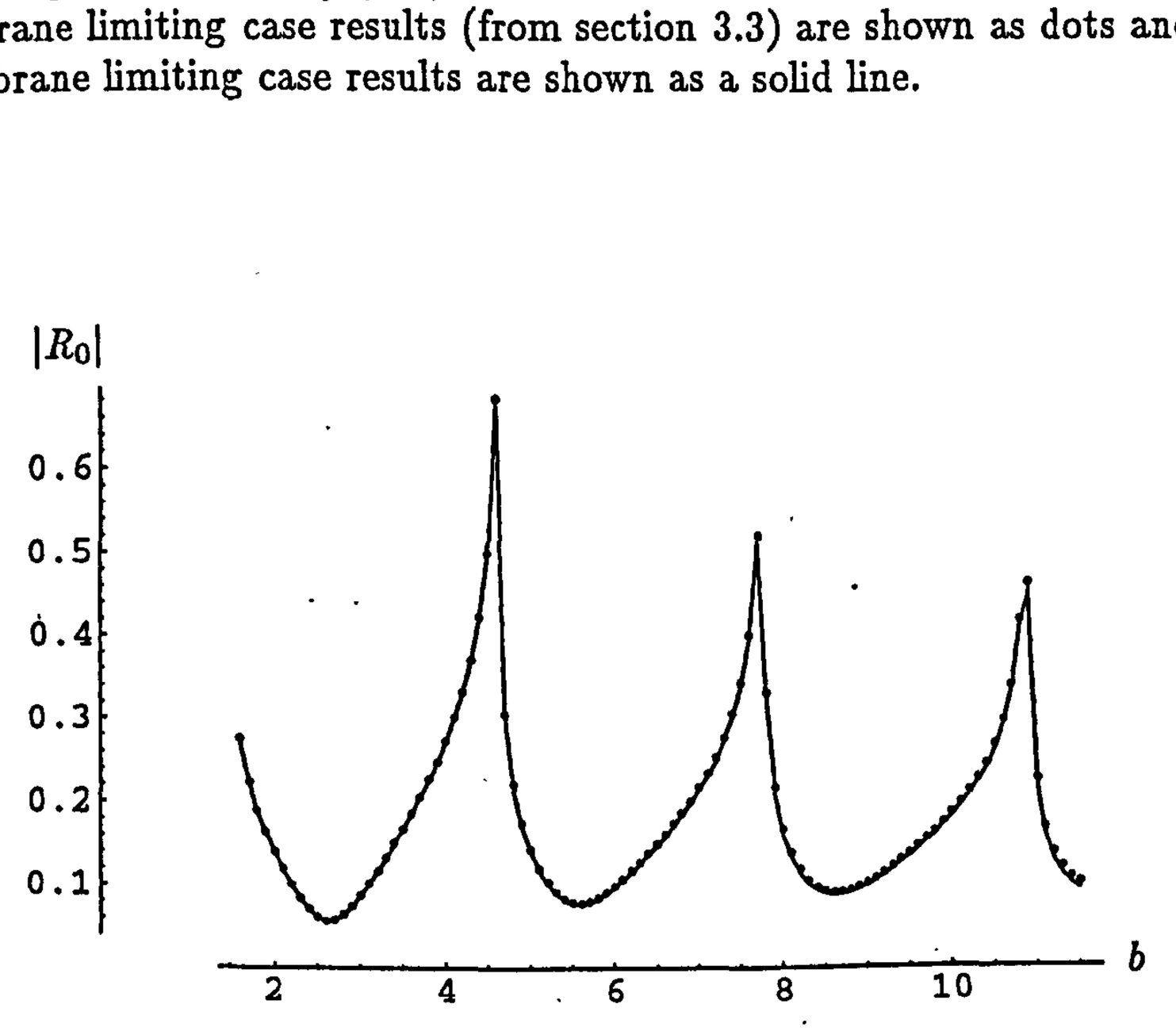

Figure 4.24: Comparison of the modulus of the coefficient for the fundamental reflected mode with edge condition $\phi_y(0,b) = 0$, $a = 1.51$, $\alpha_2 = 50$ and $\mu_2 = 2.2$. The hard/membrane limiting case results (from section 3.3) are shown as dots and the membrane/membrane limiting case results are shown as a solid line.

Clearly, all the results gained in this section show an excellent level of accuracy when

compared with the results gained in previous chapters.

The results can be further extended by applying the physical properties of actually materials to the membranes. Tables of physical constants, such as those found in Kaye & Laby (1986) can be used to evaluate α_j and μ_j, $j = 1, 2$, to give the results applicability to actual problems in engineering.

Chapter 5

Discussion

The problems discussed in this thesis demonstrate how a particular class of problem may be solved by utilizing the orthogonality relation appropriate to the eigen-sub-problem obtained through separation of variables. In section 2.5 it was seen that, for an acoustic duct bounded on its upper surface by a membrane, the standard Sturm-Liouville method failed to yield a solution, and it was later noted that the cause of this failure was because the eigen-system that was generated lacked the flexibility to accommodate the enforcement of an edge condition. For problems involving finite or semi-finite domains, it is inherent in the nature of the membrane boundary condition that an edge condition must be applied, and it is this fact that makes the Strum-Liouville method inappropriate. The key to the success of the method employed in Chapters 3 and 4 was the derivation of a specialised orthogonality relation.

However, in the derivation of the orthogonality condition (as described in section 2.6), much is owed to the lessons learnt from observing the Sturm-Liouville method's derivation in section 2.3. The steps followed to derive the new orthogonality relation are analogous to those followed for the Sturm-Liouville relation. It is only because the dispersion relation differs from one case to the other that the relations themselves differ at all. The derivation of this new orthogonality condition, and its more generalised form (see Abrahams & Lawrie, 1999) enables a whole new class of problems to to be solved in a neat and concise form.

The class of problem that can be solved using this type of orthogonality relation is vast namely the reflection and transmission of plane or fluid-coupled structural waves at a discontinuity in height and/or material property in an otherwise infinite waveguide. It is well known that for cases where there is no change in height such problems can be solved using the Wiener-Hopf technique. However, it should be noted that the classical Wiener-Hopf technique is appropriate only for problems in which the planar boundaries are described by two-part conditions. The modified Wiener-Hopf technique can be applied to problems having three-part boundary conditions but the calculations are cumbersome and require either asymptotic interpretation or numerical evaluation of a pair of coupled

integral equations, see for example, Lawrie (1988). Other extensions of the Wiener-Hopf technique deal with semi-infinite but non-planar geometries. In such cases, the Wiener-Hopf equation assumes a matrix form but exact factorization can be performed in only a small minority of cases and for the vast majority of problems an approximate factorization is necessary, see Lawrie & Abrahams (1994). All such extensions to the Wiener-Hopf technique are inappropriate if the scattering structure has any vertical components and alternative approachs must then be employed such as Jones (1953). In contrast, the eigenfunction expansion method described herein is not limited either to waveguides with planar boundaries or to two-part problems. In principle, the waveguide may undergo several changes in height and material property and, provided the correct orthogonality relation is utilized in each duct region, the solution can still be obtained in a relatively straightforward manner.

The eigenfunction expansion method does, of course, have its limitations. The solution takes the form of an infinite system of algebraic equations which are difficult to interpret asymptotically and must, therefore, be solved numerically. Truncation or iteration are the usual methods by which infinite systems are solved but, in either case, it is necessary that the system converges adequately. It is known (see, for example, Evans & Porter, 1995), that in problems of this class the convergence of the infinite system is inversely proportional to the strength of the corner singularity of the fluid velocity potential. Indeed, this is borne out by the hard/hard problem of section 2.1, for which the system converged very slowly even after the leading order terms were subtracted out of the system and calculated exactly. However, in the membrane/membrane problem the fluid velocity potential is not singular at either corner. This is reflected in the extreme behaviour of the infinite system which, for moderate values of the parameters, gave highly accurate results even for radical truncation when as few as 8 equation were retained (of course more equations are needed if any of the parameters are excessively large or small). A further limitation is the class of problems for which the method is appropriate. Although a vast class, it is characterized by the fact that the propagating medium is contained within the waveguide. The method cannot be applied to problems in which the walls are wave-bearing and there is fluid extending to infinity outside the duct boundaries. For problems of this type the eigenfunctions are not complete, as is evident by the fact that there is always a branch-cut contribution to the far-field even within the duct itself.

A number of alternative approaches and further extensions of this work could be considered. Throughout the work described in this thesis a non-dimensionalisation scheme based on the wavenumber has been used and the height of the two adjoining ducts has been varied to provide a range of results. An equally valid approach would be to non-dimensionalise with respect to the height of one of the ducts, giving results for varying α and μ. Indeed further results could be given by varying the wavenumber which would provide information on the effect of different wave structures passing through a duct of fixed

geometry and material property. It should however be noted that the solutions gained herein can easily be adapted to provide these results as well. By varying the heights of the ducts whilst maintaining a fixed ratio between the heights and varying α and μ in accordance with the factor by which the heights change, the effect is one of varying the wavenumber.

Whilst only two-dimensional problems are considered here, extension to three-dimensional problems is a natural progression. In Lawrie (1986, 1987) the Wiener Hopf method is used to solve axisymmetric three-dimensional problems involving a circular cylinderical duct with discontinuity in material property, that is totally immersed in fluid. A problem similar to this, that is acoustic scattering in a circular cylindrical duct with abrupt change in height and material property (see figure 5.1), can be solved using a suitable orthogonality relation provided the exterior region is *in vacuo*. The orthogonality relation is expected to be a little more complicated than that derived in section 2.6 but should, nevertheless, be relatively straight forward to apply.

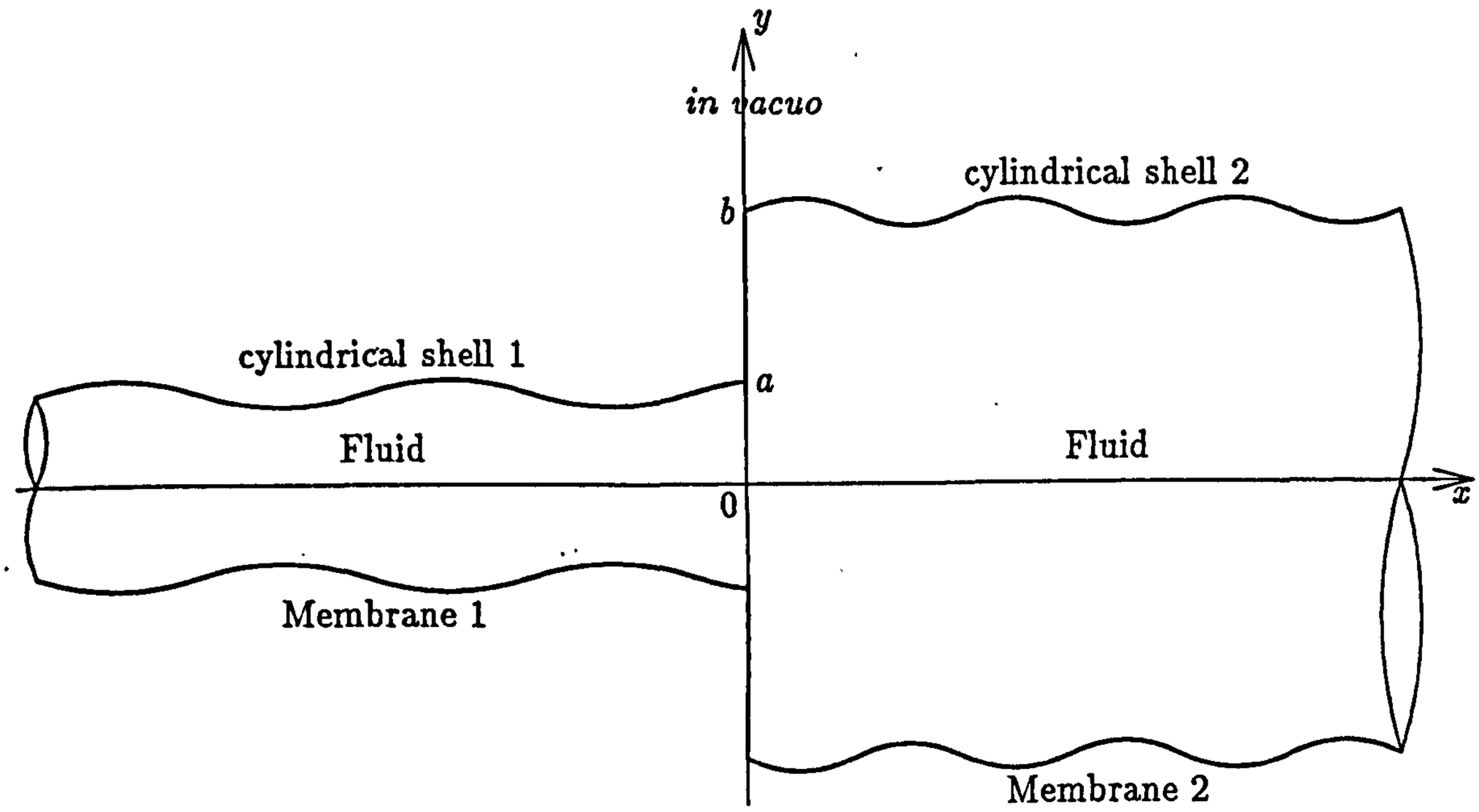

Figure 5.1: Physical configuration for a three-dimensional cylindrical duct problem

This geometry is similar to that of an exhaust pipe silencer and whilst previous work has alluded to such a geometry, the problem represented in figure 5.1 is the closest in both physical structure and material behaviour that has been tackled.

Problems involving three-dimensional rectangular cross-section ducts are also open to solution using orthogonality relations derived in a similar manner to that demonstrated in section 2.6. Such ducts have been considered previously in a number of works, including Kirby & Cummings (1998) and Cummings & Astley (1995), both of which are concerned with the installation of acoustically-absorbent material in air-conditiong ducts to reduce resonance effects at certain frequencies. Air conditioning ducts use silencers to some extent

and it is the geometry associated with the application of a silencer that is considered in both of the above mentioned papers, see figure 5.2. Whilst Cummings & Astley (1995) use an eigenmode method to gain results (that are later compared with experimental readings), Kirby & Cummings (1998) use an alternative finite element method.

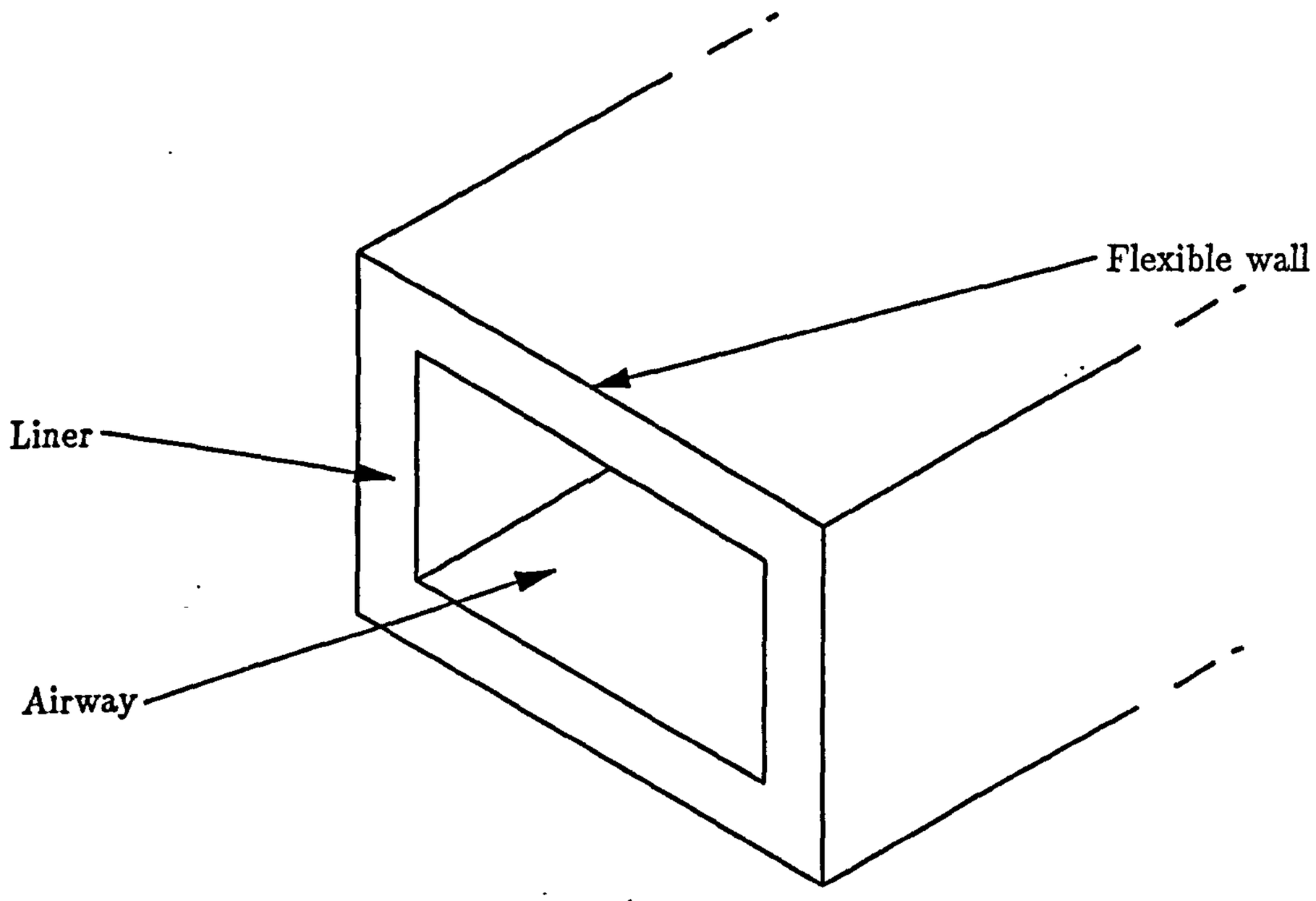

Figure 5.2: Physical configuration for three-dimensional rectangular duct problem considered by Cummings & Astley (1995)

The problems considered by Cummings & Astley (1995) and Kirby & Cummings (1998) are closely related to practical engineering problems involving air-conditioning ducts. The ducts found in such systems are usually completely surrounded by air, but it is common practise to neglect the fluid in the exterior region. Thus, using the methods employed in section 2.6 of this thesis to derive the appropriate orthogonality relation, changes in the geometry of the duct could be considered along with complicated boundary conditions.

In summation, the orthogonality relation that has been derived within this thesis allows the problems considered to be completed in an elegant and compact manner. The problem that is solved in section 4.1 for the case where $a \leq b$ takes noticably less effort both mathematically and computationally, using the eigen-function method, than does the less general case, where $a = b$, which is tackled using the Wiener-Hopf technique. The new technique is borne of simplicity, but ultimately, as shown within, can prove to be a powerful tool.

Appendices

All the problems that are completed in the thesis result in some form of infinite sum. Obviously calculating an infinite sum is impractical (not to mention impossible), but the mathematical solutions that are gained are structured in such a way that high levels of accuracy are gained from systems based on these solutions, that are truncated to just a few terms. Ways of reducing the number of terms required have been discussed throughout and used to improve the convergence of the systems used in the final programmes. These programmes are listed in the appendices and are annotated with reference made to the mathematics completed in the previous chapters.

The text of the programme is written in `verbatim` whilst annotation is in normal text.

Appendix A

Programmes relating to Chapter 2

Detailed in this first appendix are the programmes for evaluating $A_\ell, \ell = 0, 1, 2, \ldots, t$ and $B_n, n = 0, 1, 2, \ldots, t$ (where $t+1$ is the number of terms that the system is truncated to) for the two problems solved in Chapter 2. The two cases from chapter 2 are considered, that being the hard/hard problem in section 2.1, and the hard/impedance problem in section 2.4.

A.1 Programme from section 2.1

The first programme considered is that relating to section 2.1. First the values of a and b are read in, the number of terms that are to be used in the solution is set and the value of r is set as $\frac{a}{b}$.

```
a = 1.51
b = 2.4
terms = 20
r = a/b
```

Then the values of $\eta_\ell, \ell = 0, 1, 2, \ldots, t$ and $\nu_n, n = 0, 1, 2, \ldots, t$ are calculated as specified in (2.1.21) and (2.1.29) respectively.

```
eta = Table[Sqrt[1-((1^2 Pi^2)/(a^2))], {l, 1, terms}]
nu = Table[Sqrt[1-((n^2 Pi^2)/(b^2))], {n, 1, terms}]
```

The function F as detailed in (2.1.52) is input. Note that the function `Polygamma[z]` is a *Mathematica* function and gives the Digamma function as given in (2.1.49) and that `PolyGamma[n, z]` is the nth derivative of that function.

```
f[n_] := If[m == n, (-r Pi^2)/((Sin[r m Pi])^2) +
2 r PolyGamma[1, m r], Pi (Cot[r m Pi] - Cot[r n Pi])/(n - m) +
2 (PolyGamma[r m] - PolyGamma[r n])/(n - m)]
```

The three terms of (2.1.51) that are summed over ℓ and m are clustered together in the function `inner`.

```
inner[n_] := (-4 n^2 r^3/Pi^2)*Sum[((Sin[m Pi r])^2 c[m]/
(nu[[m]]))*((eta[[1]]-(I 1 Pi/a))/
((n^2 r^2 - 1^2)*(m^2 r^2 -1^2)) + (I Pi/(2 a r^2 (n + m)))*
(1/(r n m) + f[n])), {l, 1, terms}, {m, 1, terms}]
```

The remaining term that is summed over just m is given in deqn.

```
deqn[n_] := -(4/Pi^2)*
Sum[((Sin[m Pi r])^2 d[m])/(2 nu[[m]] m^2 r (r+1)),
{m, 1, terms}]
```

The two functions deqn and inner are combined with the simple terms at the beginning of (2.1.51) to give the complete solvable system that (2.1.51) describes. This system is then solved for $D_n, n = 1, 2, 3, \ldots, t$, and the results are placed in an array and sorted to give v.

```
x = Solve[Table[d[n] == 1 - (r-1)/(r+1) + deqn[n] + inner[n],
{n, 1, terms}], Array[d, terms, 1]]
v = Sort[x[[1]]]
```

The values of $A_\ell, \ell = 0, 1, 2, \ldots, t$ are given using the next piece of code which takes in to account the special case when $\ell = 0$ using the definition given in (2.1.41) and calculates all other values using (2.1.42).

```
avals = Table[If[l == 0, (2 (r-1)/(r+1)) + (4/Pi^2 r (r+1))*
Sum[(Sin[m Pi r])^2 d[m]/(m^2 nu[[m]]) /. v[[m]],
{m, 1, terms}], ((4 r (-1)^1)/Pi^2)*
Sum[(Sin[m Pi r])^2 d[m]/(nu[[m]]
*(m^2 r^2 - 1^2)) /. v[[m]], {m, 1, terms}]], {l, 0, terms}]
```

Similarly, the values of $B_n, n = 0, 1, 2, \ldots, t$ are calculated taking the $n = 0$ case as given in (2.1.44) and all others as in (2.1.39).

```
bvals = Table[If[n == 0, -(4 r/(r+1)) -
(4/(Pi^2 (r+1)))*Sum[(Sin[m Pi r])^2 d[m]/
(m^2 nu[[m]]) /. v[[m]], {m, 1, terms}],
2*Sin[n Pi r]*d[n]/(Pi n nu[[n]]) /. v[[n]]], {n, 0, terms}]
```

A.2 Programme from section 2.4

As in the appendix A.1, the programme for the problem tackled in section 2.4 begins with the values of a and b being set, along with the number of terms to be used. Also entered

here are the values for α and β that determine the exact nature of the boundary filling the region $y = b, x > 0$ as is specified in (2.4.5).

```
a = 2.5;
b = 3.8;
alpha = 1;
beta = 1;
terms = 20;
```

The values of $\eta_n, n = 0, 1, 2, \ldots, t$ where $t + 1$ is the number of terms that are to be used, are found. To find the corresponding values for ν_n, and thus $q_n, n = 0, 1, 2, \ldots, t$, a root finder is programmed. It is easy to see that the value of q_n will be arranged such that $0 < q_0 < \frac{i\pi}{2b}$, $\frac{i\pi}{b} < q_1 < \frac{3i\pi}{2b}$ and so on, following the formula $\frac{ni\pi}{b} < q_n < \frac{(2n+1)i\pi}{2b}$. Hence, as an intial estimate of the value of q_n, the set, y, is constructed, comprising the midpoint of these ranges. This value is then used as a starting point for an iterative sequence to find roots of the dispersion relation found when the eigenfunction, $\cosh(qb)$ is applied to (2.4.5). From this the values for ν_n and $q_n, n = 0, 1, 2, \ldots, t$ are found.

```
eta = Table[(1 - n^2 Pi^2/a^2)^0.5, {n, 0, terms}];
y = Table[(4 n + 1) Pi I/(4 b), {n, 0, terms}];
nu = Table[z = FindRoot[beta Cosh[k b] +
alpha k Sinh[k b] == 0, {k, y[[i]]},
MaxIterations -> 1000];
(k^2 + 1)^0.5 /. z, {i, 1, terms+1}];
q = Table[(nu[[n]]^2 - 1)^0.5, {n, 1, terms+1}];
```

The values of $C_n, n = 0, 1, 2, \ldots, t$ are found using the expression given in (2.4.30).

```
c = Table[(Sinh[2 q[[n]] b] + 2 q[[n]] b)/(4 q[[n]]), {n, 1, terms+1}];
```

The function R_{mn} as defined in (2.4.24) is also coded.

```
r[m_, n_] := (-1)^m Sinh[q[[n+1]] a]/
(q[[n+1]] (1 + (m Pi/(a q[[n+1]]))^2));
```

The functions one[n_], two[n_] and three[n_] are coded. These make up the three terms in the brackets of the equation given in (2.4.32).

```
one[n_] := 2 r[0, n];

two[n_] := r[0, n]/a Sum[bvals[m] r[0, m], {m, 0, terms}];

three[n_] := 2/a Sum[eta[[l+1]] bvals[m] r[l, m] r[l, n],
{l, 1, terms}, {m, 0, terms}];
```

These functions are then brought together and divided by $\nu_n C_n$ to give the full expression in (2.4.32), which is defined here as `beqn[n_]`.

```
beqn[n_] := (one[n] - two[n] - three[n])/(nu[[n+1]] c[[n+1]]);
```

The system is then solved and the resulting answers are sorted in `v`. The values found are $B_n, n = 0, 1, 2, \ldots, t$.

```
f = Solve[Table[bvals[n] == beqn[n], {n, 0, terms}],
Array[bvals, terms+1, 0]];
v = Sort[f[[1]]];
```

These are then used in (2.4.22) and (2.4.23) to find the values of $A_\ell, \ell = 0, 1, 2, \ldots, t$.

```
a = Table[If[l==0, -2 + (2/a) Sum[bvals[m] r[0, m] /. v[[m+1]],
{m, 0, terms}], N[(2/a) Sum[b[m] r[l, m] /. v[[m+1]],
{m, 0, terms}]]];
```

Appendix B

Programmes relating to Chapter 3

In this appendix, the programmes for the problems solved in chapter 3 are detailed. The two problems solved were that of a duct with variation in height and a membrane upper surface on the right duct solved in section 3.1, and also the comparison problem without a change in height solved using the Wiener-Hopf technique in section 3.2. A programme for each of these is detailed and annotated.

B.1 Programme for section 3.1

Note that the programme given in this section is that for the special case where $a = b$. The reader will recall that this case is considered because of the diagonal dominance on the resulting matrix solution that is found initially in (3.1.26). It was noted in section 3.1 that by subtracting out the dominant term on the diagonal of the matrix (this accomplished by defining $S_{\ell m}$ in (3.1.29)), the convergence of the system is greatly improved. Since this is the programme used to generate results that are later compared with the Wiener-Hopf problems solutions for the case $a = b$, it is included here. The programme for the solution of the problem considered in section 3.1, for the case where $a \neq b$ is omitted, as it contains little additional functionality to those programmes given in appendix A for the problems considered in sections 2.1 and 2.6. What new *Mathematica* programming techniques are used in that programme are also applied here.

First, the values of the duct heights, a and b are input, along with the value of α and μ, the constants that define the membrane's behaviour, the number of terms that are to be used and the value of ec. The value of ec defines which edge condition is to be used, ec = 0 implying that $\phi_{yx}(0, b) = 0$, ec = 1 implying that $\phi_y(0, b) = 0$.

```
a = 1.6
b = a
alpha = 10
mu = 2.2
terms = 30
ec = 0
```

Define the values for $\eta_l, l = 0, 1, 2, \ldots, t$ as prescribed.

```
eta = Table[(1 - n^2 Pi^2/a^2)^0.5, {n, 0, terms}]
```

To find the values of ν_n and $\gamma_n, n = 0, 1, 2, \ldots, t$ a root finder programme is set up. The six values given by u are the solution to a version of the dispersion relation (3.1.13), considered in the case where ν_n is taken as being very large. For the purpose of the root finder, only the largest positive real solution is required and is set as w. The values found in y are best guesses at the remaining roots, falling between the two extreme cases of $\frac{n\pi i}{b}$ and $\frac{(2n+1)\pi i}{2b}$. The numbers held in u and w are combined in y and rotated once to put them into the correct order, making the large positive real root the first in the list. Taking the values in y as a first estimation, the final command iterates to a root of the actual dispersion relation and outputs the values for ν_n and thus, γ_n are also found.

```
u = NSolve[(x^2 - mu^2)^2 (x^2-1) == alpha^2, x]
w = {x} /. u[[6, 1]]
y = Table[(4 n + 1) Pi I/(4 b), {n, 0, terms-1}]
q = RotateRight[Union[y, w], 1]
nu = Table[z = FindRoot[(k^2 + 1 - mu^2) k*
Sinh[k.b] - alpha Cosh[k b] == 0, {k, q[[i]]},
MaxIterations -> 1000]
(k^2 + 1)^0.5 /. z, {i, 1, terms+1}]
gamma = Table[(nu[[n]]^2 - 1)^0.5, {n, 1, terms+1}]
```

The values for $C_n, n = 0, 1, 2, \ldots, t$, as given in (3.1.23), are found, as well as the values of $C_n^*, n = 0, 1, 2, \ldots, t$, as given by (3.1.24) and here defined as cons. Remember that this form is divided through by α, which in the case where α is large, allows for quicker overall computation of solutions.

```
c = Table[(1/2)*(alpha b +(2 gamma[[n]]^2 + nu[[n]]^2 - mu^2)*
(Sinh[gamma[[n]] b])^2), {n, 1, terms+1}]
cons = Table[(1/2)*
(b + (Sinh[2 gamma[[n]] b]/(2 gamma[[n]] (nu[[n]]^2 - mu^2)))*
(2 gamma[[n]]^2 + nu[[n]]^2 - mu^2)), {n, 1, terms+1}]
```

The function R_{mn} is coded as given in (3.1.16), along with the Dirac delta function and S_{mn} as described in (3.1.29).

```
r[m_, n_] := (-1)^n Sinh[gamma[[m+1]] a]/
(gamma[[m+1]] (1 - (n Pi/(a gamma[[m+1]]))^2))
delta[m_, n_] := If[m==n, 1, 0]
s[m_, n_] := r[m, n] - (a/2) delta[m, n]
```

The next terms create (3.1.37). The expressions given in `one[n_]` through to `five[n_]` make up the expressions with in the square brackets of that equation and these are divided later in the programme by $(2\nu_n C_n^* + \eta_n a)$.

```
one[n_] := 4 r[0, n] - b[0] r[0, n] - (2 r[0, n]/a)*
Sum[b[m] s[0, m], {m, 0, terms}]
```

```
two[n_] := 2 eta[[n+1]] Sum[b[m] s[n, m], {m, 0, terms}]
```

```
three[n_] := 2 Sum[eta[[1+1]] b[1] s[1, n], {1, 1, terms}]
```

```
four[n_] := 4/a Sum[eta[[1+1]] b[m] s[1, m] s[1, n],
{1, 1, terms}, {m,. 0, terms}]
```

```
five[n_] := If[ec == 0, 0, 2 gamma[[n+1]] bvals[terms+1]*
Sinh[gamma[[n+1]] b]/alpha]
```

The next two terms, `six[n_]` and `seven[n_]` go to make up the expression for B_0 given in (3.1.34). Note that the term including E in this expression is exactly the same as that given by `five[0]` and so this term is used later to complete the equation.

```
six[n_] := 4 r[0, n] - (2 r[0, n]/a)*
Sum[b[m] s[0, m], {m, 0, terms}]
```

```
seven[n_] := 4/a Sum[eta[[1+1]] b[m] r[1, m] r[1, n],
{1, 1, terms}, {m, 0, terms}]
```

All the terms created previously are brought together to create the system that is to be solved for $B_n, n = 0, 1, 2, \ldots, t$. The `If` statement in the expression allows for the special case for B_0 to be actioned.

```
beqn[n_] := If[n == 0, (five[0] + six[0] - seven[0])/
(2 nu[[n+1]] cons[[n+1]] + r[0, 0]), (one[n] - two[n] -
three[n] - four[n] + five[n])/(2 nu[[n+1]] cons[[n+1]] +
a eta[[n+1]])]
```

Now, the equations for finding the value of E (here labelled `bvals[terms+1]`) are constructed, first taking the denominator of the fracton given in (3.1.40) ....

```
divide[n_] := Sum[2 gamma[[j+1]]^2 (Sinh[gamma[[j+1]] b])^2/
(2 alpha nu[[j+1]] cons[[j+1]] + a alpha eta[[j+1]]), {j, 0, terms}]
```

and then constructing the remainder of (3.1.40) from the terms that are already used. Here the variable `ec` is applied to determine which of the two possible edge conditions is to be applied and defining the expression for E accordingly.

```
alteqn[n_] := If[ec == 0, 0, Sum[gamma[[1+1]] Sinh[gamma[[1+1]] h]/(2
nu[[1+1]] cons[[1+1]] + a eta[[1+1]])*
(one[1] - two[1] - three[1] - four[1])/divide[1], {1, 0, terms}]]
```

Now combining the two expressions for B_n and E to create a complete system.....

```
toteqn[n_] := If[n == terms+1, alteqn[n], beqn[n]]
```

and solving this system for bvals[n], n= 0,1,2,...,terms+1.

```
f = Solve[Table[bvals[n] == toteqn[n], {n, 0, terms+1}],
Array[bvals, terms+2, 0]]
```

The solution set is sorted into order so that B_0 is first through to E at the end.

```
v = Sort[f[[1]]]
```

Then, apply these values to (3.1.15) to find values for $A_\ell, \ell = 0, 1, 2, \ldots, t$.

```
avals = Table[If[l==0, N[-2 + (2/a) Sum[b[m] r[0, m] /. v[[m+1]],
{m, 0, terms}]], N[(2/a) Sum[b[m] r[1, m] /. v[[m+1]],
{m, 0, terms}]]], {l, 0, terms}]
```

B.2 Programme for section 3.2

Again, for this programme the first step is to input the value of a (rembering that this is a programme for a Weiner Hopf problem and so $a = b$), α, μ and the number of terms required in the infinite product used to gain the solution. Also input here are the function gam[s_] which is used so that γ can be calculated for any value of s and the variable ec which, as in the previous program, determines which edge condition is used, ec = 0 implying that $\phi_{yx}(0, a) = 0$, ec = 1 implying that $\phi_y(0, a) = 0$.

```
a = 1.6
ec = 0
(* Variable ec set equal to 0 has the affect of implying Edge condition
phi_yx = 0, other value of ec imples phi_y = 0 *)
alpha = 5000
mu = 2.2
gam[s_] := (s^2 - 1)^0.5
terms = 200
```

The same algorithm is used to gain the values of ν_n and γ_n as in section B.1.

```
anoughts = Table[alpha = alfs[[t]]
u = NSolve[(x^2 - mu^2)^2 (x^2-1) == alpha^2, x]
```

```
w = {x} /. u[[6, 1]]
y = Table[(4 n + 1) Pi I/(4 a), {n, 0, terms-1}]
q = RotateRight[Union[y, w], 1]
nu = Table[z = FindRoot[(k^2 + 1 - mu^2) k*
Sinh[k a] - alpha Cosh[k a] == 0, {k, q[[i]]},
MaxIterations -> 1000]
(k^2 + 1)^0.5 /. z, {i, 1, terms+1}]
gamma = Table[(nu[[n]]^2 - 1)^(1/2), {n, 1, terms}]
```

The expression for $K_+(s)$ as given in (3.2.85) is defined.

```
kplus[s_] := N[(((alpha/(a (nu[[1]]^2 - 1)))^0.5)*
((nu[[1]] + s)/(1 + s))*
Exp[s Sum[I a/(n Pi) + 1/nu[[n+1]], {n, 1, terms-1}]])*
Product[(((nu[[n+1]] + s)/gamma [[n+1]])/
((1 - a^2/(n^2 Pi^2))^0.5 - I a s/(n Pi)))*
Exp[-s (I a/(n Pi) + 1/nu[[n+1]])], {n, 1, terms-1}]]
kern[x_] := 1 - alpha Coth[gam[x] a]/(gam[x]*
(x^2 - mu^2))
```

Now $K'(s)$ is defined.

```
kdash[s_] := s Tanh[gamma[s] a] ((s^2 - mu^2)/gamma[s] +
2 gamma[s]) + s a (s^2 - mu^2) (Sech[gamma[s] a])^2;
```

Now the form of the variable κ, as given in (3.2.98), is defined. This is described in terms of an integral in the text, where the path of integration lies below any singularities that may occur on the real axis in the complex plane. This is reflected here by the path of integration that is taken.

```
kappa = N[mu + (I/Pi) NIntegrate[Log[kern[x]],
{x, 0, 1 - 10 I, 171 - 10 I, 200, Infinity}]]
```

Finally, R_0 and T_0 are defined as given in (3.2.53) and (3.2.56). The value of ec defines which expression is taken according to the appropriate edge condition.

```
r = If[ec == 0, (alpha/(4 a (Abs[kplus[1]])^2))*(2 + kappa)/kappa,
(alpha/(4 a (Abs[kplus[1]])^2))]
```

```
t = If[ec == 0, alpha kplus[nu[[1]]] Cosh[gamma[[1]] a]
(kappa + 1 - nu[[1]])/(4 a kappa kplus[1] kdash[-nu[[1]]]
(1 - nu[[1]]) gamma[[1]] Sinh[gamma[[1]] a]),
alpha kplus[nu[[1]]] Cosh[gamma[[1]] a]/
(4 a kplus[1] kdash[-nu[[1]]] (1 - nu[[1]])
gamma[[1]] Sinh[gamma[[1]] a])]
```

Appendix C

Programmes relating to Chapter 4

In chapter 4, the problem involving ducts with upper surfaces made up of membranes was considered. First the problem where there is also a variation in the height of the ducts, was completed using the orthogonality condition derived in section 2.6, and then the simpler case where the ducts are of the same height was completed using the Wiener-Hopf technique. In each case a system was yielded that is required to be solved computationally using *Mathematica* and in this appendix, the codes for those programmes are listed.

C.1 Programme for section 4.1

As in previous programmes, first read in the values that specify the systems set up, those being a, b, α_1, μ_1, α_2 and μ_2. The number of terms for the system to be truncated to is set (note that the number is very low for this case) and the edge condition specification variables are also introduced - ec1 defining the condition at $(0^-, a)$ and ec2 defining that at $(0^+, b)$ in such a way that when equal to zero these imply that $\phi_{yx} = 0$ and when equal to one that $\phi_y = 0$. Edge condition variable = 0 implies xy-differential condition, when = 1 implies y-differential condition.

```
a = 1.51
b = 1.73
alf1 = 0.1;
mu1 = 3;
alf2 = 50;
mu2 = 2.2;
ec1 = 0;
ec2 = 0;
terms = 10;
```

For the duct to the left of the matching interface, the roots of the dispersion relation given in (4.1.14), being η_ℓ, are found and thus τ_ℓ are also gained. This piece of code is of a similar form to that used in section B.1.

```
u = NSolve[(x^2 - mu1^2)^2 (x^2-1) == alf1^2, x];
w = {x} /. u[[6, 1]];
y = Table[(4 n + 1) Pi I/(4 a), {n, 0, terms-1}];
q = RotateRight[Union[y, w], 1];
eta= Table[z = FindRoot[(k^2 + 1 - mu1^2) k*
Sinh[k a] - alf1 Cosh[k a] == 0, {k, q[[i]]},
MaxIterations -> 1000];
(k^2 + 1)^0.5 /. z, {i, 1, terms+1}];
tau = Table[(eta[[n]]^2-1)^(1/2), {n, 1, terms+1}];
Clear[u, w, y, q];
```

The same code as used above (with variables relevant to the right hand duct replacing those for the left) is used to gain the values of ν_n and γ_n.

```
u = NSolve[(x^2 - mu2^2)^2 (x^2-1) == alf2^2, x];
w = {x} /. u[[6, 1]];
y = Table[(4 n + 1) Pi I/(4 b), {n, 0, terms-1}];
q = RotateRight[Union[w, y], 1];
nu = Table[z = FindRoot[(k^2 + 1 - mu2^2) k*
Sinh[k b] - alf2 Cosh[k b] == 0, {k, q[[i]]},
MaxIterations -> 1000];
(k^2 + 1)^0.5 /. z, {i, 1, terms+1}];
gamma = Table[(nu[[n]]^2-1)^(1/2), {n, 1, terms+1}];
Clear[u, w, y, q];
```

The values for $D_\ell^*, \ell = 0, 1, 2, \ldots, t$ are set up, taking into account that D_ℓ is as defined in (4.1.24) and that $D_\ell^* = \frac{D_\ell}{\alpha_1}$.

```
d = Table[(1/2)*(a + Sinh[2 tau[[n]] a]*
((eta[[n]]^2 - mu1^2 + 2 tau[[n]]^2)/(2 tau[[n]]*
(eta[[n]]^2 - mu1^2))), {n, 1, terms+1}];
```

Similarly, $C_n^*, n = 0, 1, 2, \ldots, t$ are evaluated from the expression given in (4.1.34) and noting that $C_n^* = \frac{C_n}{\alpha_2}$.

```
c = Table[(1/2)*(b + Sinh[2 gamma[[n]] b]*
((nu[[n]]^2 - mu2^2 + 2 gamma[[n]]^2)/(2 gamma[[n]]*
(nu[[n]]^2 - mu2^2))), {n, 1, terms+1}];
```

The Dirac delta function is constructed and the function $T_{\ell m}$ as defined in (4.1.28) is created.

```
delta[l_, m_] := If[l == m, 1, 0];
t[l_, m_] := (tau[[l+1]] Sinh[tau[[l+1]] a] Cosh[gamma[[m+1]] a] -
```

```
gamma[[m+1]] Sinh[gamma[[m+1]] a] Cosh[tau[[1+1]] a])/
(tau[[1+1]]^2 - gamma[[m+1]]^2);
```

Functions one[n_] through to six[n_] construct the major part of all the functions required to complete the system to find values of $B_n, n = 0, 1, 2, \ldots, t$, E and F.

```
one[n_] := If[ec1 == 1, 0,  (-1)/(nu[[n+1]] c[[n+1]]) Sum[eta[[1+1]]*
t[1, n] tau[[1+1]] Sinh[tau[[1+1]] a] bvals[terms+2]/(d[[1+1]] alf1),
{1, 0, terms}]];

two[n_] := (2 eta[[1]] t[0, n])/
(nu[[n+1]] c[[n+1]] Cosh[tau[[1]] a]);

three[n_] := (-1)/(nu[[n+1]] c[[n+1]]) Sum[eta[[1+1]] bvals[m]*
t[1, n] t[1, m]/(d[[1+1]]), {m, 0, terms}, {1, 0, terms}];

four[n_] := (gamma[[n+1]] Sinh[gamma[[n+1]] b] bvals[terms+1])/
(nu[[n+1]] c[[n+1]] alf2);

five[n_] := 2 eta[[1]] tau[[1]] Tanh[tau[[1]] a];

six[n_] :=  -Sum[eta[[1+1]] tau[[1+1]]*
Sinh[tau[[1+1]] a] bvals[m] t[1, m]/d[[1+1]], {m, 0, terms},
{1, 0, terms}];
```

Thus, taking one[n], two[n], three[n] and four[n] the equation for B_n as given in (4.1.39) is formed.

```
beqn[n_] := one[n] + two[n] + three[n] + four[n];
```

The expression divide1 is the denominator of the function that yields F in (4.1.45).

```
divide1 = Sum[eta[[1+1]] tau[[1+1]]^2 (Sinh[tau[[1+1]] a])^2/
(d[[1+1]] alf1), {1, 0, terms}];
```

Similarly, divide2 is the denominator of (4.1.50) which gives E.

```
divide2 = Sum[I gamma[[j+1]]^2 (Sinh[gamma[[j+1]] b])^2/
(nu[[j+1]] alf2 c[[j+1]]), {j, 0, terms}];
```

The construction of functions five[n] and six[n] is such that, when divided by divide1 as they are in alteqn1[n_], the total expression for F is given as in (4.1.45) and subsequently used in (4.1.53) and (4.1.57). Also taken into consideration here are the occassions when $F = 0$, that being the case when $\phi_y(0, a) = 0$ and thus ec1= 1.

```
alteqn1[n_] := If[ec1 == 0, (five[n] + six[n])/divide1, 0];
```

The options taken into account in `alteqn2[n_]` are rather more complex. If `ec2= 0` this implies that $\phi_{xy}(0,b) = 0$ and thus $E = 0$ also. However, if `ec2= 1` then the expression that gives F depends on the nature of the other edge condition. In this case, when `ec1= 0` the term including F must be included and so the expression for E is as given in (4.1.50) and also in case (ii). If `ec1= 1` then the term including F can be discarded (as it has already been noted that in this case, $F = 0$) and so E is given by (4.1.52).

```
alteqn2[n_] := If[ec2 == 0, 0, If[ec1 == 0, Sum[gamma[[p+1]]*
Sinh[gamma[[p+1]] b](one[p] + two[p] + three[p])/divide2,
{p, 0, terms}], Sum[gamma[[p+1]] Sinh[gamma[[p+1]] b](two[p] +
three[p])/divide2, {p, 0, terms}]]];
```

Finally, the three functions `beqn[n]`, `alteqn1[n]` and `alteqn2[n]` are brought together in a nested `If` statement so that E is given as `bvals[terms+1]` in the solution and F is given as `bvals[terms+2]`

```
toteqn[n_] := If[n == terms+1, alteqn2[n], If[n == terms+2,
alteqn1[n], beqn[n]]];
```

Solve the system and output the solutions into `f`.

```
f = Solve[Table[bvals[n] == toteqn[n], {n, 0, terms+2}],
Array[bvals, terms+3, 0]];
```

Then sort `f` such that B_0 is first through to E and F.

```
v = Sort[f[[1]]];
```

Finally, apply the values gained for $B_n, n = 0,1,2,\ldots,t$ to (4.1.27) to gain values for $A_\ell, \ell = 0,1,2,\ldots,t$.

```
avals = Table[-2 delta[0, l]/(Cosh[tau[[1]] a]) + (tau[[l+1]]*
Sinh[tau[[l+1]] a] bvals[terms+2] /. v[[terms+3]])/
(alf1 d[[l+1]]) + (1/d[[l+1]]) Sum[bvals[m] t[l, m] /. v[[m+1]],
{m, 0, terms}], {l, 0, terms}];
```

C.2 Programme for section 4.2

As for the programme given in C.1 the initial data is read in first, that being the value of A (which in this case is equal to b since this is the Weiner Hopf comparison), α_1, μ_1, α_2 and μ_2. The number of terms to be used is set and the general definition of γ is introduced. The values of `ec1` and `ec2` are read and have the same implications as in the previous program. That is `ec1` defines the condition at $(0^-, a)$ and `ec2` defining that at $(0^+, a)$ in such a way that when equal to zero these imply that $\phi_{yx} = 0$ and when equal to one that $\phi_y = 0$. Edge condition variable = 0 implies xy-differential condition, when = 1 implies y-differential condition.

```
a = 2.3;
alf1 = 1;
mu1 = 3;
alf2 = 50;
mu2 = 2;
ec1 = 1;
ec2 = 1;
terms = 200;
gamma[s_] := (s^2 - 1)^0.5;
```

The values of η_ℓ and $\tau_\ell, \ell = 0,1,2,\ldots,t$ are found using the root finding code employed previously.

```
u = NSolve[(x^2 - mu1^2)^2 (x^2-1) == alf1^2, x];
w = {x} /. u[[6, 1]];
y = Table[(4 n + 1) Pi I/(4 a), {n, 0, terms-1}];
q = RotateRight[Union[y, w], 1];
eta = Table[z = FindRoot[(k^2 + 1 - mu1^2) k*
Sinh[k a] - alf1 Cosh[k a] == 0, {k, q[[i]]},
MaxIterations -> 1000];
(k^2 + 1)^0.5 /. z, {i, 1, terms+1}];
Clear[x, y, q];
```

The values of ν_n and $\gamma_n, n = 0,1,2,\ldots,t$ are find likewise.

```
u = NSolve[(x^2 - mu2^2)^2 (x^2-1) == alf2^2, x];
w = {x} /. u[[6, 1]];
y = Table[(4 n + 1) Pi I/(4 a), {n, 0, terms-1}];
q = RotateRight[Union[y, w], 1];
nu = Table[z = FindRoot[(k^2 + 1 - mu2^2) k*
Sinh[k a] - alf2 Cosh[k a] == 0, {k, q[[i]]},
MaxIterations -> 1000];
(k^2 + 1)^0.5 /. z, {i, 1, terms+1}];
```

The equations for $L_1'(s)$ as given in (4.2.61) and $L_2'(s)$ as given in (4.2.71), and those for $L_1(s)$ and $L_2(s)$ as given in (4.2.30) and (4.2.31) respectively, are coded.

```
l1dash[s_] := s Tanh[gamma[s] a] ((s^2 - mu1^2)/gamma[s] +
2 gamma[s]) + s a (s^2 - mu1^2) (Sech[gamma[s] a])^2;

l2dash[s_] := s Tanh[gamma[s] a] ((s^2 - mu2^2)/gamma[s] +
2 gamma[s]) + s a (s^2 - mu2^2) (Sech[gamma[s] a])^2;
```

```
l1[s_] := (s^2 - mu1^2) gamma[s] Tanh[gamma[s] a] - alf1;

l2[s_] := (s^2 - mu2^2) gamma[s] Tanh[gamma[s] a] - alf2;
```

Hence, the coding of $K(s)$ as given in (4.2.32) is trivial.

```
l[s_] := l1[s]/l2[s];
```

The form of σ as given in (4.2.36) is also coded, using L'Hopital's rule to eliminate singularities in the case where $\alpha_1 = \alpha_2$.

```
sigma = If[alf1 == alf2, (mu1^2 - mu2^2)^0.5,
((alf2 mu1^2 - alf1 mu2^2)/(alf2 - alf1))^0.5];
```

The expressions for $L_+(s)$ and $L_-(s)$ are read in, as detailed in (4.2.165).

```
lplus[s_] := (alf1/alf2)^0.5 Product[gamma[nu[[n]]]*
(s + eta[[n]])/(gamma[eta[[n]]] (s + nu[[n]])), {n, 1, terms}];

lminus[s_] := (alf1/alf2)^0.5 Product[gamma[nu[[n]]]*
(s - eta[[n]])/(gamma[eta[[n]]] (s - nu[[n]])), {n, 1, terms}];
```

```
int1 = NIntegrate[Log[1 - alf1 Coth[gamma[x] a]/
((x^2 - mu1^2) gamma[x])], {x, 0, 3 - 3 I, 150 - 3I, 200}];

int2 = NIntegrate[Log[1 - alf2 Coth[gamma[x] a]/
((x^2 - mu2^2) gamma[x])], {x, 0, 3 - 3 I, 150 - 3I, 200}];

d1 = mu1 - mu2 + (int1 - int2) I/Pi;

det1 = sigma ((lplus[sigma] - lminus[sigma])^2 -
(lplus[sigma] + lminus[sigma])^2 + (2 alf1/alf2)*
(sigma (lplus[sigma] + lminus[sigma]) -
d1 (lplus[sigma] - lminus[sigma])) + 2 sigma*
((lplus[sigma] + lminus[sigma]) - (2 alf1/alf2));

det2 =  sigma ((lplus[sigma] - lminus[sigma])^2 -
(lplus[sigma] + lminus[sigma])^2 + 2*
(sigma (lplus[sigma] + lminus[sigma]) -
d1 (lplus[sigma] - lminus[sigma])) + (2 sigma alf1/
alf2) ((lplus[sigma] + lminus[sigma]) - 2);
```

Finally, a nested `If` statement is used to pick the correct form of R_0 and T_0 according to which ever combination of edge conditions are selected.

```
r = If[ec1 == 0, If[ec2 == 0, -((lplus[eta[[1]]])^2 l2[eta[[1]]]/
l1dash[eta[[1]]])*
(1/(2 eta[[1]]) - ((d1 - eta[[1]])*(lplus[sigma]*
(eta[[1]] - sigma) + lminus[sigma] (eta[[1]] + sigma)))/
((eta[[1]]^2 - sigma^2) (lplus[sigma] (d1 - sigma) +
lminus[sigma] (d1 + sigma)))), -((lplus[eta[[1]]])^2 l2[eta[[1]]]/
l1dash[eta[[1]]]) (1/(2 eta[[1]]) + lplus[sigma]/
(det1 (eta[[1]] + sigma))*(2 alf1 (d1 - eta[[1]])/alf2 - 2 sigma) +
lminus[sigma]/(det1 (eta[[1]] - sigma))*
(- 2 alf1 (d1 - eta[[1]])/alf2 - 2 sigma))],
 If[ec2 == 0, -((lplus[eta[[1]]])^2 l2[eta[[1]]]/l1dash[eta[[1]]])*
(1/(2 eta[[1]]) + lplus[sigma]/(det1 (eta[[1]] + sigma))*
(2 (d1 - eta[[1]]) - 2 sigma alf1/alf2) + lminus[sigma]/
(det1 (eta[[1]] - sigma)) (- 2 (d1 - eta[[1]]) - 2 sigma alf1/alf2)),
-((lplus[eta[[1]]])^2 l2[eta[[1]]]/l1dash[eta[[1]]])*
(-1/(eta[[1]] - sigma) + 2 sigma lplus[sigma]/
((lplus[sigma] - lminus[sigma])*
(eta[[1]]^2 - sigma^2)) + 1/(2 eta[[1]]))]]

t = If[ec1 == 0, If[ec2 == 0, (l1[nu[[1]]] lplus[eta[[1]]]
gamma[eta[[1]]] Tanh[gamma[eta[[1]]] a](nu[[1]]^2 - mu2^2)
/(lplus[nu[[1]]] l2dash[-nu[[1]]] alf1))*(1/(-nu[[1]] +
eta[[1]]) + (d1 - eta[[1]])/(sigma^2 - nu[[1]]^2)*
(lplus[sigma] (sigma + nu[[1]]) - lminus[sigma]
(sigma - nu[[1]]))/(lplus[sigma] (sigma -d1) - lminus[sigma]
(sigma +d1))), alf2 l1[nu[[1]]] lplus[eta[[1]]] gamma[eta[[1]]]
Tanh[gamma[eta[[1]]] a]/(alf1 l2dash[-nu[[1]]] lplus[nu[[1]]]
gamma[nu[[1]]] Tanh[gamma[nu[[1]]] a])*(1/(-nu[[1]] +
eta[[1]]) + 1/(det1 (sigma^2 - nu[[1]]^2))*((2 alf1
(d1 - eta[[1]])/alf2 )*(sigma (lplus[sigma] + lminus[sigma]) +
nu[[1]](lplus[sigma] - lminus[sigma])) - 2 sigma
(nu[[1]] (lplus[sigma] + lminus[sigma]) + sigma(lplus[sigma]
- lminus[sigma])) + sigma ((lplus[sigma] + lminus[sigma])^2
- (lplus[sigma] - lminus[sigma])^2)*(nu[[1]] + eta[[1]]))),
If[ec2 == 0, alf2 l1[nu[[1]]] lplus[eta[[1]]] gamma[eta[[1]]]
Tanh[gamma[eta[[1]]] a]/(alf1 l2dash[-nu[[1]]] lplus[nu[[1]]]
gamma[nu[[1]]] Tanh[gamma[nu[[1]]] a])* (1/(-nu[[1]]
+ eta[[1]]) + 1/(det2 (sigma^2 - nu[[1]]^2))*(sigma
(eta[[1]] + nu[[1]])*((lplus[sigma] + lminus[sigma])^2 -
(lplus[sigma] - lminus[sigma])^2) +  2 (d1 - eta[[1]])*
```

```
(sigma (lplus[sigma] + lminus[sigma]) + nu[[1]](lplus[sigma] -
lminus[sigma])) - (2 sigma alf1/alf2)*(nu[[1]] (lplus[sigma] +
lminus[sigma]) +  sigma(lplus[sigma] - lminus[sigma]))),
(l1[nu[[1]]] lplus[eta[[1]]] gamma[eta[[1]]]
Tanh[gamma[eta[[1]]] a](nu[[1]]^2 - mu2^2)/
(lplus[nu[[1]]] l2dash[-nu[[1]]] alf1))*(-sigma (lplus[sigma] +
lminus[sigma])/((lplus[sigma] - lminus[sigma])
(sigma^2 - nu[[1]]^2)) - nu[[1]]/(sigma^2 - nu[[1]]^2)+
1/(-nu[[1]] + eta[[1]]))]]
```

Finally, the code for the special case when $\alpha_1 = \alpha_2$ that is considered in subsection 4.2.3 is given. The expression found for R_0 as given in (4.2.189) when coded is as follows.

```
rprobcure =  -((lplus[eta[[1]]])^2 l2[eta[[1]]]/
l1dash[eta[[1]]])*(1/(2 eta[[1]]) - (alf2 + alf1)*
(alf2 mu1^2 - alf1 mu2^2) gamma[eta[[1]]]
Tanh[gamma[eta[[1]]] a]/(2 d1 alf1 alf2 l2[eta[[1]]]))
```

Similarly, T_0 as given in (4.2.190) for this particular case is coded as follows.

```
tprobcure = alf2 l1[nu[[1]]] lplus[eta[[1]]]
gamma[eta[[1]]] Tanh[gamma[eta[[1]]] a]/
(alf1 l2dash[-nu[[1]]] lplus[nu[[1]]] gamma[nu[[1]]]
Tanh[gamma[nu[[1]]] a])*((alf2 + alf1)*
((alf2 mu1^2 - alf1 mu2^2) gamma[nu[[1]]]
Tanh[gamma[nu[[1]]] a]/(2 d1 alf2^2 l1[nu[[1]]]))+1/
(-nu[[1]] + eta[[1]]))
```

References

[1] ABRAHAMS, I.D., 1986, Diffraction by a semi-infinite membrane in the presence of a vertical barrier. *J. Sound Vib.* 111(2), 191–207.

[2] ABRAHAMS, I.D., 1987, On the sound field generated by membrane surface waves on a wedge-shaped boundary. *Proc. R. Soc. Lond. A* 411, 239–250.

[3] ABRAHAMS, I.D. & LAWRIE, J.B., 1995. Travelling waves on a membrane: reflection and transmission at a corner of arbitrary angle. I. *Proc. R. Soc. Lond. A* 451, 657–683.

[4] ABRAMOWITZ, M & STEGUN, I.A., 1964. Handbook of Mathematical Functions. *Dover Publications Inc., New York.*

[5] AULD, B.A., 1990. Acoustic Fields and Waves in Solids (Volume II, 2nd Ed.). *Robert E. Krieger Publishing Company.*

[6] BRAZIER-SMITH, P. R., 1987. The acoustic properties of two co-planar half-plane plates. *Proc. R. Soc. Lond. A* 409, 115–139.

[7] CANNELL, P. A., 1975. Edge scattering of aerodynamic sound by a lightly loaded elastic half-plane. *Proc. R. Soc. Lond. A* 347, 213–238.

[8] CANNELL, P. A., 1976. Acoustic edge scatterring by a heavily loaded elastic half-plane. *Proc. R. Soc. Lond. A* 350, 71–89.

[9] CHURCHILL, R.V., & BROWN, J.W., 1982. Fourier Series and Boundary Value Problems. *McGraw-Hill Book Company*

[10] CRIGHTON, D.G., DOWLING, A.P., FFOWCS-WILLIAMS, J.E., HECKL, M. & LEPPINGTON, F.G., 1992. Modern Methods in Analytical Acoustics. *Springer-Verlag.*

[11] CUMMINGS, A & ASTLEY, R.J., 1995. The effects of flanking transmission on sound attenuation in lined ducts. *Journal of Sound and Vibration.* 174, 617–646.

[12] DALRYMPLE, R.A. & MARTIN, P.A., 1996. Water waves incident on an infinitely long rectangular inlet. *Appl. Ocean Res.* 18, 1–11.

[13] EVANS, D.V., 1985. A solution of a class of boundary-value problems with smoothly varying boundary conditions. *Q. Jl Mech appl. Math.* 38, 521–536.

[14] EVANS, D.V. & PORTER, R., 1995. Hydrodynamic characteristics of an oscillating water column device. *Appl. Ocean Res* **17**, 155–164.

[15] FERNYHOUGH, M & EVANS, D.V., 1996. Comparison of a step approximation to an exact solution of acoustic scattering in a uniform-width pipe with nonunifrom wall impedance. *Q. Jl Mech appl. Math.* **49**, 419–437.

[16] FOLK, R.T. & HERCZYNSKI, A., 1986. Solutions of elastodynamic slab problems using a new orthogonality condition. *J. acoust. Soc. Am.* **80**, 1103–1110.

[17] GRANT, A.D. & LAWRIE, J.B., 1999. Acoustic scattering in a duct with elastic plate walls having continuously varying bending characteristics. *Submitted to Q. Jl Mech appl. Math.*

[18] HERCZYNSKI, A. & FOLK, R.T., 1989. Orthogonality condition for the Pochhammer-Chree modes. *Q. Jl Mech appl. Math.* **42**, 523–536.

[19] JONES, D.S., 1953. Diffraction by a thick semi-infinite plate *Proc. R. Soc. Lond. A* **247**, 153–175.

[20] KAYE, G.W.C & LABY, T.H., 1986. Tables of Physical and Chemical Constants (15th Ed.). *Longman Scientific & Technical, UK* .

[21] KELLER, J.B., 1962. Geometric theory of diffraction *J. Optic. Soc. Am.* **52**, 116–130.

[22] KIRBY, R. & CUMMINGS, A., 1998. Structural/acoustic interaction in air-conditioning ducts in the presence of mean flow. *Proc. ISMA* **23**, 677–684.

[23] KORNER, T.W., 1988. Fourier Analysis. *Cambridge University Press.*

[24] LAWRIE, J.B., 1986. Vibrations of a heavily loaded, semi-infinite, cylindrical elastic shell. I. *Proc. R. Soc. Lond. A* **408**, 103–128.

[25] LAWRIE, J.B., 1987. Vibrations of a heavily fluid-loaded, semi-infinite, cylindrical elastic shell. II. *Proc. R. Soc. Lond. A* **415**, 371–387.

[26] LAWRIE, J.B., 1988. Axisymmetric radiation from a finite gap in an infinite, rigid, circular duct. *I.M.A. J. Appl. Math.* **41**, 113–128.

[27] LAWRIE, J.B. & ABRAHAMS, I.D., 1994. Acoustic radiation from two opposed, semi-infinite, co-axial cylindrical waveguides, Part II: separated edges. *Wave Motion* **19**, 83–109.

[28] LAWRIE, J.B. & ABRAHAMS, I.D., 1996. Travelling waves on a membrane: reflection and transmission at a corner of arbitrary angle. II. *Proc. R. Soc. Lond. A* **452**, 1649–1677.

[29] LAWRIE, J.B. & ABRAHAMS, I.D., 1999, An orthogonality condition for a class of problem with high order boundary conditions; applications in sound/structure interaction.. *Q. Jl. Mech appl. Math.* **52**, 161–181

[30] MALHIUZHINETS, G.D., 1958. Excitation, reflection and emission of surface waves from a wedge with given face impedances. *Soviet Phys. Doklady* **3**, 752–755.

[31] MCISAAC, P.R., 1991. Mode orthogonality in reciprocal and nonreciprocal waveguides. *IEEE Transactions on Microwave Theory and Techniques* **39**, 1808–1816.

[32] NOBLE, B, 1958. Methods based on the Weiner-Hopf technique for the solution of partial differential equations. *Pergamon Press.*

[33] NORRIS, A.N. & WICKHAM, G.R., 1995. Acoustic diffraction from the junction of two flat plates. *Proc. R. Soc. Lond A* **451**, 631–655.

[34] OSIPOV, A.V., 1994. General solution for a class of diffraction problems. Letter to *J. Phys. A: Math. Gen.* **27**, L27–L32.

[35] OSIPOV, A.V. & NORRIS, A.N., 1997. Acoustic diffraction by a fluid-loaded membrane corner. *Proc. R. Soc. Lond. A* **435**, 43–64.

[36] PEAT, K.S., 1991. The acoustical impedance at the junction of an extended inlet or outlet duct. *J Sound Vib* **150**, 101–110.

[37] RAO, B.S.R. & RAO, H.S., 1988. Generalised orthogonality relation for the flexure of a rectangular plate using some refined plate theories. *Mech. Struct. & Mach.* **16**, 167–186.

[38] ROSEAU, M., 1976. Asymptotic Wave Theory. *North-Holland, Amsterdam.*

[39] TITCHMARSH, E.C., 1960. The Theory of Functions. *Oxford University Press*, 2nd Ed.

[40] WARREN, D.P. AND LAWRIE, J.B., 1999. Acoustic scatterring in wave-guides of discontinuous geometry and material property. *submitted to Wave Motion.*